MODELING AND ANALYSIS OF DYNAMICS OF MALARIA TRANSMISSION WITH CONTROL MEASURES: IMPORTED CASES

A THESIS SUBMITTED TO THE

CENTRAL DEPARTMENT OF MATHEMATICS

INSTITUTE OF SCIENCE AND TECHNOLOGY

TRIBHUVAN UNIVERSITY

NEPAL

FOR THE AWARD OF

DOCTOR OF PHILOSOPHY

IN MATHEMATICS

BY

RAMESH GAUTAM

August 2024

MODELING AND ANALYSIS OF DYNAMICS OF MALARIA TRANSMISSION WITH CONTROL MEASURES: IMPORTED CASES

A THESIS SUBMITTED TO THE

CENTRAL DEPARTMENT OF MATHEMATICS

INSTITUTE OF SCIENCE AND TECHNOLOGY

TRIBHUVAN UNIVERSITY

NEPAL

FOR THE AWARD OF

DOCTOR OF PHILOSOPHY

IN MATHEMATICS

BY

RAMESH GAUTAM

August 2024

TRIBHUVAN UNIVERSITY

Institute of Science and Technology

DEAN'S OFFICE

Kirtipur, Kathmandu, Nepal

Reference No.:

Institute of Science & Technology Dean's Office Kirtipur 2045

EXAMINERS

The Title of Ph.D. Thesis: " Modeling and Analysis of Dynamics of Malaria Transmission with Control Measures: Imported Cases "

Name of Candidate: Ramesh Gautam

Internal Examiner:

Dr. Ramesh Chandra Timsina
Patan Multiple Campus
Tribhuvan University, NEPAL

External Examiners:

(1) Dr. Samir Shrestha
Kathmandu University
Dhulikhel, NEPAL

(2) Dr. Saroj Kumar Sahani
South Asian University
Delhi, INDIA

(3) Prof. Dr. Xueying Wang
Washington State University
USA

August 30, 2024

(Dr. Surendra Kumar Gautam)
Asst. Dean

DECLARATION

Thesis entitled **"Modeling and Analysis of Dynamics of Malaria Transmission with Control Measures: Imported Cases"** which is being submitted to the Central Department of Mathematics, Institute of Science and Technology (IOST), Tribhuvan University, Nepal for the award of the degree of Doctor of Philosophy (Ph.D.), is a research work carried out by me under the supervision of Prof. Dr. Kedar Nath Uprety, Central Department of Mathematics, Tribhuvan University, Nepal and co-supervised by Prof. Dr. Naveen.K. Vaidya, Department of Mathematics, San Diego State University, CA, USA.

This research is original and has not been submitted earlier in part or full in this or any other form to any university or institute, here or elsewhere, for the award of any degree.

Ramesh Gautam

RECOMMENDATION

This is to recommend that **Ramesh Gautam** has carried out research entitled **"Modeling and Analysis of Dynamics of Malaria Transmission with Control Measures: Imported Cases"** for the award of Doctor of Philosophy (Ph.D.) in **Mathematics** under our supervision. To our knowledge, this work has not been submitted for any other degree.

He has fulfilled all the requirements laid down by the Institute of Science and Technology (IOST), Tribhuvan University, Kirtipur for the submission of the thesis for the award of Ph.D. degree.

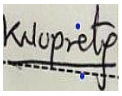

Kedar Nath Uprety, Ph.D.
Supervisor
(Professor)
Central Department of Mathematics
Tribhuvan University
Kirtipur, Kathmandu, Nepal.

Naveen K. Vaidya, Ph.D.
Co-Supervisor
(Professor)
Department of Mathematics
San Diego State University
CA, USA.

August 2024

Phone No. :00977- 14331977

TRIBHUVAN UNIVERSITY

CENTRAL DEPARTMENT OF MATHEMATICS

Institute of Science and Technology

CENTRAL DEPARTMENT OF MATHEMATICS TRIBHUVAN UNIVERSITY KIRTIPUR

KIRTIPUR, KATHMANDU
NEPAL

Ref No.

Date: July 25, 2024

Letter of Approval

On the recommendation of Prof. **Dr. Kedar Nath Uprety,** and **Prof. Dr. Naveen K. Vaidya**, this Ph.D. thesis submitted by **Mr. Ramesh Gautam**, entitled **"Modeling and Analysis of Dynamics of Malaria Transmission with Control Measures: Imported Cases"** is forwarded by Central Department Research Committee (CDRC) to the Dean, IOST, T.U..

Chet Raj Bhatta, PhD
Professor & Head
Central Department of Mathematics
Tribhuvan University,
Kirtipur, Kathmandu

ACKNOWLEDGEMENTS

First and foremost, I wish to extend my profound gratitude to my esteemed supervisor, Prof. Dr. Kedar Nath Uprety, for entrusting me with the opportunity to pursue this doctoral research endeavor. His unwavering confidence in my abilities has been a source of inspiration and a driving force throughout this journey. His continuous guidance, encouragement, insightful comments, and immense knowledge have been invaluable throughout my research. Without his contribution, this thesis would hardly exist. I extend my heartfelt gratitude to my co-supervisor, Prof. Dr. Naveen K. Vaidya, for his invaluable guidance and support. His role, together with that of Professor Uprety, enriched my research journey with diverse perspectives, international exposure, and insightful contributions that have significantly enhanced the depth and quality of this work. Importantly, as a front-line researcher in infectious disease modeling, Prof. Vaidya provided me with the opportunity to broaden my research network and gain institutional support for publication in top-tier journals. I express my sincere thanks to Prof. Chet Raj Bhatta, Head of the Central Department of Mathematics, for his support throughout my research period. I also thankfully acknowledge my colleagues, Dr. Khagendra Adhikari and Dr. Anjana Pokharel, for their collaborative research work. I extend sincere thanks to the University Grant Commission (UGC), Nepal, for the research support grant and PhD fellowship. I am also thankful to the International Mathematical Union for the Graduate Research Assistantship for Developing Countries (GRAID), and the Nepal Mathematical Society (NMS), CIMPA, and IIT Indore for their support. Additionally, I acknowledge the National Science Foundation (NSF) for grants DMS-1951793 and San Diego State University. I appreciate the valuable suggestions from professors and colleagues, and I am also thankful to department staff and the Dean's office for their support. I am forever indebted to my parents, Dam Narayan Gautam and Davi Gautam, and my siblings, Bharat Raj Gautam and Kalpana Ghimire, and for their unconditional sacrifices. My heartfelt love goes to my wife, Rekha Pawan Gautam, for her encouragement and enduring the hardships of our family life. Endless thanks to our children, Aastha and Aadarsha, for making me stronger and more fulfilled. Likewise, I thank all those who wish me success.

Ramesh Gautam
August 2024

सोध सार

नेपालजस्ता न्यून र मध्यम आय भएका देश लगायत धेरै देशले औलो उन्मूलनका लागि धेरै चुनौतीहरूको सामना गरिरहेका छन् । औलोको बोझलाई उल्लेखनीय रूपमा घटाउनमा प्रगति भएता पनि, यी देशहरू अझै पनि औलो प्रसारणको न्यून स्तरसँग संघर्ष गरिरहेका छन् र पूर्ण रूपमा उन्मूलन गर्न गाह्रो भइरहेको छ । औलो जस्ता रोगहरूको गणितीय मोडेलिङले रोगको गतिशीलतामा आवश्यक अन्तरदृष्टि प्रदान गर्दछ । यी अन्तर्दृष्टिहरूले प्रभावकारी रूपमा स्रोतहरू विनियोजन गर्न प्रभावकारी सार्वजनिक स्वास्थ्य रणनीतिहरू विकास गर्न मद्दत गर्दछ, र औलो जस्ता लामोसमयसम्म रहने रोगहरू कम गर्न र उन्मूलन गर्नका लागी प्रमाण-आधारित नीति निर्माण गर्नका लागी सहयोग गर्दछ।

औलो उन्मूलन गर्ने विश्वव्यापी प्रयासमा, मानव गतिशीलता र प्लाज्मोडियम भाइभ्याक्स र ओभेल मलेरियाको पुनरावृत्तिले महत्त्वपूर्ण चुनौतीहरू खडा गरेको छ । यस थीसिसमा, सर्वप्रथम, हामी नेपाल जस्ता न्यून-स्थानीय देशहरूबाट भारत जस्ता उच्च-स्थानीय देशहरूमा आप्रवासी कामदारहरूको सीमापार गतिशीलतालाई एकीकृत गर्दै औलो प्रसारणको गणितीय मोडेल विकास गर्छौं । मोडेलले प्रवासी कामदारहरू विदेशमा कसरी संक्रामक हुन्छन् र औलो लाई आयातित केसहरूको रूपमा आफ्नो देशमा फिर्ता ल्याउँदछ भनेर वर्णन गर्दछ । आठ-आयामी ननलिनयर ननहोमोजीनियस प्रणालीहरूसँगको जटिलताको बावजुद पनि, हामीले तीन औलो मुक्त सन्तुलन र तीन महामारी मापक थ्रेसहोल्डहरू, R_0, R_1, र R_2 प्राप्त गर्न सक्षम भयौं, जसले तिनीहरूको स्थानीय स्थिरता स्थापना गर्दछ । थप रूपमा, हामीले विश्वव्यापी स्थिरता र समान दृढताका लागि प्रमेयहरू स्थापना गरेका छौं । हाम्रो मोडेल सिमुलेशनहरूले देखाउँदछ कि कीटनाशक-उपचारित जालहरू (ITN), भित्री अवशिष्ट स्प्रेइ (IRS), सीमा जाँच र अलगाव (BSI), र माइग्रेसन रिडक्सन (MR), हरूमा MR कम लामखुट्टे टोक्ने दरहरूमा सबैभन्दा प्रभावकारी रणनीति र ITN औलो नियन्त्रण र उन्मूलनको लागि उच्च लामखुट्टेले टोक्ने दरमा सबैभन्दा प्रभावकारी पुष्टी भय।

दोस्रो, हामीले माइग्रेसनले गर्दा महामारी मापक थ्रेसहोल्ड एक भन्दा कम भयर मात्रै औलो मुक्त हुन नसक्ने र थ्रेसहोल्ड मानहरूको लागि बिस्टेबिलिटी प्रदर्शन गर्दै पछाडिको विभाजन घटना निम्त्याउन सक्छ कि भनेर जाँच्नको लागि मोडेलको विस्तृत विभाजन विश्लेषण गरीयको छ । सैद्धान्तिक व्युत्पन्नहरूको साथमा, हामीले गतिशीलताका विभिन्न मोडहरूसँग सम्बन्धित विभिन्न प्रकारका विभाजन रेखाचित्रहरू प्राप्त गर्न MATLAB कोड विकास गर्यौं । हाम्रो पछाडी विभाजन विश्लेषणले स्वदेश र विदेशमा लागू हुनसक्ने नीतिहरु का कारण तीनवटा प्रमुख नतिजाहरू पत्ता लगाएको छ जुन तीन फरक गतिशीलता अवस्थाहरूमा आधारित छ: (क) यदि आप्रवासीहरूको गतिशीलता पूर्ण रूपमा प्रतिबन्धित गर्न सकियो भने, थ्रेसहोल्ड $R_0 < 1$ र रोग-प्रेरित मृत्यु दर केही थ्रेसहोल्ड भन्दा तल झर्दा गृह देश औलो बाट मुक्त हुन्छ । (ख) विदेशमा औलोको संक्रमणबाट पूर्ण सुरक्षाका साथ प्रवासीहरूको आवतजावत जारी छ भने, थ्रेसहोल्ड $R_1 < 1$ र संक्रामक आप्रवासीहरूको गतिशीलता निश्चित थ्रेसहोल्डभन्दा कम भएमा स्वदेश र विदेशमा बस्नेहरू दुवै औलोबाट मुक्त हुन्छन् । यद्यपि, यदि गतिशीलता थ्रेसहोल्ड भन्दा बढी छ भने पछाडि विभाजन हुन्छ र उन्मुलनको लागी थप प्रयास जरुरी पर्दछ । (ग) विदेशमा सुरक्षा बिना आप्रवासीहरूको गतिशीलता भएमा, स्वदेशले स्थानीय नियन्त्रण रणनीतिहरू र केही तहभन्दा तल आप्रवासीहरूको गतिशीलता दर घटाएर मात्र औलोको बोझ कम गर्न सक्छ । तर, विदेश क्षेत्र औलोमुक्त भए मात्रै उन्मूलन सम्भव हुन्छ ।

तेस्रो, हामीले पुन: आवृत्तिमा ढिलाइलाई समावेश गर्दै एक मोडल विकास गर्यौं जसले कम संक्रमण दर भएका देशहरू जस्तै नेपालमा औलो को उन्मूलन कार्यक्रमहरूमा प्लाज्मोडियम विवाक्स र ओभाले मलेरियाका पुन: आवृत्तिहरूको भूमिकालाई सम्बोधन गर्दछ । हाम्रो मोडल विश्लेषणहरू र सिमुलेशनहरूले भविष्यवाणी गर्छन् कि आयातित केसहरूको अभावमा, मलेरियाको प्रारम्भिक पुन: आवृत्ति दर ५०% भन्दा कम र पाँच महिनाभित्र दोस्रो पुन: आवृत्ति १४% भन्दा कम हुने अवस्थामा, २०२५ सम्ममा मलेरिया

उन्मूलन गर्न सकिन्छ । तर, प्रारम्भिक पुन: आवृत्ति दर २८% भन्दा माथि र दोस्रो पुन: आवृत्ति २५% भन्दा माथि हुने अवस्थामा २०२५ सम्ममा मलेरियाको उन्मूलनमा बाधा पुग्नेछ । साथै, महामारी थ्रेसहोल्ड R_0 एक भन्दा माथि पुगेमा हप्फ बिफरकेसनको माध्यमबाट समय-समयमा प्रकोपहरू देखिन्छन् ।

हाम्रो अध्ययनले २०२६ सम्ममा नेपालमा मलेरियाको सफल उन्मूलन सुनिश्चित गर्न दुई प्रमुख नीतिगत सिफारिसहरू गरेको छ: (१) विदेशमा मलेरिया संक्रमणबाट आप्रवासीहरूलाई जोगाउन व्यापक चेतना कार्यक्रम लागू गर्दै, संक्रमण भएका आप्रवासीहरूको गति दरलाई थ्रेसहोल्डभन्दा तल राख्न कडा सीमा स्क्रिनिङ र संक्रमित आप्रवासीहरूको अलगाव गर्न । (२) पुन: आवृत्ति अनुपातलाई एक महत्वपूर्ण स्तरभन्दा तल राख्न व्यापक उपचार विधि र संरचित अनुगमन कार्यक्रमको स्थापना र कार्यान्वयन गर्न ।

कुञ्जी शब्दहरू: मलेरिया मोडेल- क्रस बोर्डर गतिशीलता- नेपाल- अगाडि र पछाडि विभाजन- रिलेप्स- हपफ-विभाजन।

ABSTRACT

Many countries, including low and middle income countries like Nepal, are facing many challenges in pursuing malaria elimination. Despite progress in reducing the malaria burden significantly, these countries still struggle with low levels of malaria transmission, making complete elimination difficult. Mathematical modeling of diseases like malaria provides essential insights into disease dynamics. These insights help develop effective public health strategies for allocating resources efficiently, and support evidence-based policies to reduce endemic diseases like malaria.

In the global effort to eliminate malaria, human mobility and the relapse of *Plasmodium Vivax* and *Plasmodium ovale* malaria pose significant challenges. In this thesis, first, we develop a mathematical model of malaria transmission, integrating the cross-border mobility of migrant workers from low-endemic countries like Nepal to high-endemic countries like India. The model describes how migrant workers become infectious abroad and bring malaria back to their home country as imported cases. Despite complicated features with eight-dimensional nonlinear non-homogeneous systems, we were able to derive three disease-free equilibria and three epidemic thresholds, R_0, R_1, and R_2, which establish their local stability. In addition, we established the theorems for global stability and uniform persistence. Our model simulations show that among insecticide-treated nets (ITN), indoor residual spraying (IRS), border screening and isolation (BSI), and migration reduction (MR), MR is the most effective strategy at low mosquito biting rates, whereas ITN is the most effective at high mosquito biting rates for malaria control and elimination.

Second, we conducted a thorough bifurcation analysis of our model to examine whether migration can cause backward bifurcation phenomena, demonstrating bistability for threshold values less than one. Along with theoretical derivations, we developed MATLAB code to obtain different types of bifurcation diagrams associated with various modes of mobility. Our backward bifurcation analysis revealed three major results considering three different mobility conditions based on policies implemented at home and abroad: (a) If the mobility of migrants is completely restricted, the home country becomes free from malaria when a threshold $R_0 < 1$ and the disease-induced death rate falls below some threshold. (b) If the mobility of migrants continues with complete protection from malaria transmission abroad, then both the home country

and migrants abroad are free from malaria when the threshold $R_1 < 1$, provided the mobility of infectious migrants is below the certain threshold. However, a backward bifurcation occurs if the mobility exceeds the threshold. (c) If there is mobility of migrants without protection abroad, the home country can only reduce the malaria burden with local control strategies and by reducing the mobility rate of migrants below some levels. However, elimination is only possible if the abroad region is free from malaria.

Third, we developed a model incorporating delay in relapses to address the role of Plasmodium vivax and ovale malaria relapses in malaria elimination programs in low-endemic countries like Nepal. Our model analyses and simulations predict that in the absence of imported cases, with less than 50% initial relapse rate of malaria and less than 14% subsequent relapses within five months, malaria can potentially be eliminated by 2025. However, the initial relapse rate above 28% and the subsequent relapses above 25% stand as the obstacle to eliminating malaria by 2025. Also, shortening the relapse interval to two months under an initial relapse rate below 50% enables malaria elimination by 2024, while extending it to six months will cause a delay in elimination beyond 2025. Furthermore, periodic outbreaks are observed via Hopf bifurcation when the reproduction number exceeds unity.
Our study has made two major policy recommendations to ensure the successful elimination of malaria in Nepal by 2026:

(1) Implementing a comprehensive awareness program to protect migrants from malaria transmission abroad, coupled with rigorous border screening and isolation of infectious migrants, to maintain the mobility rate of infectious migrants below the threshold. (2) Establishing and enforcing a comprehensive radical cure treatment protocol, along with a structured follow-up program, to keep relapse proportions below a critical level.

Keywords: *Malaria Model- Cross-Border Mobility- Nepal- Forward and Backward Bifurcations- Relapse- Hopf-Bifurcation.*

LIST OF ACRYNOMS AND ABBREVIATIONS

$\mathbb{R}^6$ $\mathbb{R}^8$	:Six Dimensional Space, Eight Dimensional Space
e.g.	:For Example
et al.	: and others
etc	: and so on
i.e.	:that is
exp, Exp	:exponential
DFE	: Disease-free equilibrium
EE	:Endemic equilibrium
ITN	:Insecticide Treated Net
IRS	:Indoor Residual Spraying
BSI	:Border Screening and Isolation
MR	:Mobility Restriction
ODE	: Ordinary Differential Equation
DDE	: Delay Differential Equation
RDT	:Rapid Digonostic Test
MoHP	:Ministry of Health and Population
GoN	:Government of Nepal
WHO	: World Health Organization
EDCD	: Epidemiology and Diseases Control Division
DoHS	: Department of Health Services
API	: Annual Parasitic Index
CB	: Cross Border
FB	: Forward Bifurcation
BB	:Backward Bifurcation
GS	:Global Stability
WHO	:World Health Organization
DDT	: Dichlorodiphenyltrichloroethane
AIDS	: Acquired Immunodeficiency Syndrome

LIST OF SYMBOLS

S_{hH}	:Susceptible Human Population in Home Country
S_{hM}	:Susceptible Migrants Population in Abroad
I_{hH}	:Infected Human Population in Home Country
I_{hM}	:Infected Migrants Population in Abroad
R_{hH}	:Recovered Human Population in Home Country
R_{hM}	:Recovered Migrants Population in Abroad
N_{hH}	:Total Human Population in Home Country
N_{hA}	:Total Human Population in Abroad
I_{hA}	:Total Human Infectious Human Population in Abroad
S_{vH}	:Susceptible Vector Population in Home Country
S_{vA}	:Susceptible Vector Population in Abroad
I_{vH}	:Infectious Vector Population in Home Country
I_{vA}	:Infectious Vector Population in Abroad
S_h	:Susceptible Human Population
I_p	:Primary Infectious Human Population
I_r	:Infectious Human Population from Relapse
S_v	:Susceptible Vector Population
I_v	:Infectious Vector Population
N_h	:Total Human Population
N_v	:Total Vector Population
R_0, R_1, R_2	:Reproduction numbers for three different cases of mobility patterns
R_0^*, R_1^*	: Backward bifurcation thresholds
E^0, E^{01}, E^{02}	: Disease free equilibrium for three different cases of mobility pattern
ϕ_{ITN}	: Insecticide Treated Nets
ϕ_{IRS}	: Indoor Residual Spraying
ϕ_{BSI}	: Border Spraying and Isolation
ϕ_{MR}	: Mobility Restriction

LIST OF TABLES

Page No.

LIST OF FIGURES

Page No.

TABLE OF CONTENTS

Page No.

CHAPTER 1

1.INTRODUCTION

1.1 Background and Motivation

The Global Malaria Eradication Campaign (1955-1969), launched by WHO in 1955, aimed to eradicate malaria using DDT for indoor spraying and antimalarial drugs. Despite its challenges and discontinuation in 1969, it set the stage for future malaria control efforts Najera et al. (2011). Established in 1998, the Roll Back Malaria (RBM) Partnership coordinates global efforts against malaria, focusing on bed nets, indoor spraying, and improved diagnosis and treatment Worrall et al. (2005). The Global Fund to fight AIDS, Tuberculosis, and Malaria, established in 2002, provides crucial funding for malaria control Kohler and Bowra (2020). The President's Malaria Initiative (PMI), launched by the US in 2005, supports high-burden African countries with prevention and control measures Oxborough (2016). WHO's Global Technical Strategy for Malaria (2016-2030) offers a framework for reducing malaria cases and deaths by 2030 through vector control, case management, and surveillance Organization et al. (2021).

In 2022, 249 million malaria cases were reported in 85 countries, 5 million increase from 2021. The WHO African Region had 233 million cases (94%), with Nigeria, the Democratic Republic of the Congo, Uganda, and Mozambique contributing nearly half of the global total cases. The incidence in this region decreased from 370 per 1,000 population at risk in 2000 to 223 per 1,000 in 2022. In the WHO South-East Asia Region, India accounted for 66% of cases, with 46% of those cases due to P. vivax WHO (2023). Nepal's malaria control efforts began in 1954 with support from USAID. Initially aimed at eradication in 1958, the program shifted to control measures in 1978 due to various challenges.

The Roll Back Malaria Initiative started in 1998, focusing on high-incidence areas. Nepal aims to eliminate malaria by 2025, updating risk classifications for all 77 districts. In 2019, 3.62% of the population was high-risk, 9.79% moderate-risk, 34.52% low-risk, and 52.05% no-risk. The open border policy with India poses public health challenges, including a rise in imported malaria cases compared to indigenous ones Rijal et al. (2019a); Epidemiology and disease control division Nepal (2019). Recently,

the proportion of imported malaria cases has significantly increased compared to indigenous cases, as shown in Figure 1(a) Epidemiology and disease control division Nepal (2019).

Plasmodium vivax poses significant challenges to malaria elimination in Nepal, necessitating targeted interventions for liver hypnozoites, asymptomatic carriers, and sub-microscopic infections. Essential measures include community-based testing, Glucose-6-Phosphate Dehydrogenase (G6PD) testing, and radical cure treatments. Strategic efforts to completely stop P. vivax transmission are crucial and can serve as a model for other regions Epidemiology and disease control division Nepal (2019).

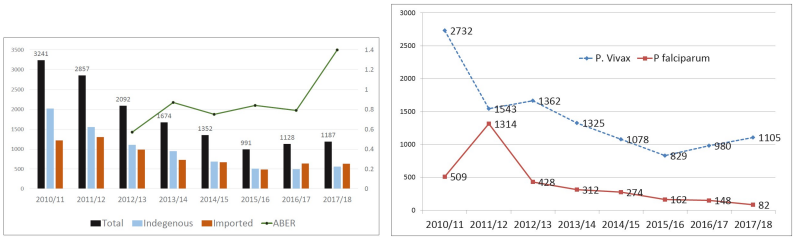

(a) **(b)**

Figure 1: Dominant proportion of imported and *plasmodium vivax* cases over the respective indigenous and *plasmodium falciparum* cases of malaria in Nepal.

.

Global malaria eradication efforts have advanced, but imported cases still challenge malaria-free and elimination-phase countries like Nepal. Travelers from endemic regions introduce malaria, leading to diagnostic delays, high treatment costs, occasional local transmission, and drug-resistant strains. Accurate tracking of international malaria movements is crucial for effective eradication Tattem et al. (2017); Kain et al. (1998). In Europe, countries such as France, Germany, Italy, and the UK have seen increased malaria cases, with underreporting and data variability Muentener et al. (1999). Prompt diagnosis and treatment are vital Askling et al. (2012). In China, almost all malaria cases from 2012 to 2018 were imported, mainly by returning laborers, necessitating targeted prevention strategies Feng et al. (2020); Liu et al. (2014); Zhou et al. (2016).

The trend of malaria cases in Nepal, fluctuating since 1963, peaked in 1985 with over 42,321 cases, marking the highest recorded. Despite malaria elimination efforts starting in 1958, significant decline began only after 1985, with transmission rates decreasing to an annual parasite incidence (API) of 0.08 per 1000 at risk population by 2018 of Health and Population (2019); Dhimal et al. (2014a); Epidemiology and disease

control division Nepal (2019). Nepal aims for zero indigenous malaria by 2022 and national elimination by 2026, but faces challenges due to porous borders with India. While total cases declined 69% from 2009 to 2018, the proportion of imported cases rose from 40% to 58%, predominantly from travelers to malaria-endemic parts of India GoN and Population (2016); Epidemiology and disease control division Nepal (2019). This disparity underscores the persistent challenge of imported and relapse cases, prompting research into effective strategies to achieve Nepal's malaria elimination goals.

1.2 Objectives

The general objectives of this dissertation are twofold: firstly, to develop and analyze a malaria model that integrates cross-border mobility among migrant workers, aimed at tracing the malaria burden in Nepal and proposing effective control strategies. This model will assist policymakers in achieving elimination targets by providing insights into the dynamics of malaria transmission influenced by population movements. Secondly, to examine the relapse behavior of *Plasmodium vivax* and its specific impact on the malaria elimination plan of Nepal and other similar countries. This research aims to enhance understanding of how relapse affects sustained transmission and to propose targeted interventions that support malaria elimination efforts.

Specific Objectives

- To develop and analyze a malaria transmission model incorporating cross-border mobility from a low endemic country (Nepal) to a high endemic country (India).
- To investigate the role of cross-border mobility in the phenomenon of backward bifurcation.
- To develop and analyze a delayed malaria model with relapse, examining the impacts of relapse delays on Nepal's malaria elimination plan by 2026.

1.3 Literature Review

The first known contribution of mathematical modeling in epidemiology is Daniel Bernoulli's work on the inoculation against smallpox in 1760 Bernoulli (1760). Ross,

Halmer, Soper, Kermack and McKendrick all contributed to the application of compartment models to epidemiology between 1900 and 1935 Anderson and May (1991b). Ross (1911) introduced the first deterministic differential equation model of malaria by dividing the human population into susceptible (S_h) and infected (I_h) compartments, with the infected class returning to susceptible class again leading to the SIS structure. The mosquito population also has only two compartments (S_v, I_v), but they do not recover from infection due to their short life span, and thereby follow the SI structure. The malaria parasite spends approximately 10 days inside a mosquito during its life cycle and Macdonald et al. (1950) made extension of Ross model in to (S_h, I_h, S_h) for humans and (S_v, E_v, I_v) structure for mosquito population.

In a natural extension to the Ross and Macdonalds models, Anderson and May (1991b) considered about 21 days latency period of the parasite in humans, and introduced the Exposed (E_h) class in human population and extend the Ross-MacDonald model. They divided the host population into three compartments (S_h, E_h, I_h), along with that in the mosquito population (S_v, E_v, I_v). Therefore, (S_h, E_h, I_h, S_h) model for the human population and (S_v, E_v, I_v) for mosquito population. Malaria burden varies by age and gender. In Africa, most malaria deaths occur in children under 5, while older individuals develop partial immunity through continuous exposure, reducing their risk. Outside Africa, where exposure is less frequent, adults also bear a significant disease burden. David et al. (2010) introduced age and immunity which are the key interrelated factors in malaria transmission.

The importance of incorporation of immunity in malaria models is aptly described by Koella (1991) incorporating immunity into malaria models is important for two reasons. First, the neglect of immunity leads to unrealistic predictions. Incorporating immunity can help to make models more realistic. Secondly, modeling immunity, and in particular the effect of vaccines, can help to predict the outcome of vaccination programs. Forouzannia and Gumel (2014); Anderson (2013b); Filipe et al. (2007); Dietz et al. (1974) have focused on the important aspect by including immunity and age structure of the human community in their malaria models. A malaria transmission model factoring in acquired immunity variation in humans and temperature dependent parameters for mosquitoes was developed in Yang (2000). Analysis using the basic reproduction number (R_0) and derivation of an endemic equilibrium expression emphasized its biological relevance when $R_0 > 1$, highlighting the critical role of immunity and temperature in malaria dynamics.

Parham and Michael (2010), investigated a simple model that permitted valuable and

novel insights by considering the simultaneous effects of rainfall and temperature on mosquito population dynamics, malaria invasion and the impact of seasonality on transmission. Their result identified a temperature window of around $32^oC - 33^oC$ is optimal. Another key result on their finding is that by influencing vector abundance, changes in rainfall patterns in particular strongly govern malaria endemicity, invasion, and extinction. Martens et al. (1995) used a rules-based modeling approach to examine how climate change might affect global malaria transmission. Their model consists of several linked systems: the climate system, the malaria system (divided into a human subsystem and a mosquito subsystem), and the impact system. They used temperature and precipitation as the main climate factors that have a bearing on the malarial transmission potential of the mosquito population.

Hoshen and Morse (2004) formulated dynamic mathematical malaria model comprising both the weather-dependent within-vector stages and the weather-independent within host stages. Similarly, Lou and Zhao (2010) presented a simple mathematical model to investigate the effects of temperature on the ability of Anopheles Maculipennis to transmit Plasmodium Vivax malaria and Chitnis et al. (2008) proposed a malaria model by evaluating the sensitivity indices of the reproductive number, and the endemic equilibrium to model parameters at the baseline values. In their study point out that, the reproductive number and the equilibrium proportions of infectious humans are both most sensitive to the mosquito biting rate in areas of low transmission, while in areas of high transmission the equilibrium proportion of infectious humans is also most sensitive to the human recovery rate. According to their study, controlling the rate of mosquito bites and the human recovery rate is a successful control strategy.

Okosun and Makinde (2011) investigated the possible impact of optimal treatment and control of drug resistance on the transmission of malaria disease by introducing a class of drug resistant individuals into the population. Theoretically, they carried out the stability properties of the model and determine conditions on the parameters for the existence of equilibrium solutions. Rafikov et al. (2009) proposed a mathematical continuous model that considers the generation overlapping and variable environment factors by using optimal control problem strategies. Their model considers interactions between wild and transgenic mosquito populations in a variable environment. Griffin et al. (2010) constructed individual-based simulation model for Plasmodium Falciparum transmission in an African context incorporating the effect of the switch to artemisinin-combination therapy (ACT) and increasing coverage of LLINs. Their findings explored the possibility of available control measures to reduce parasite prevalence to a low

level as laid out in the control phase of the global elimination framework.

The time distribution of sulfadoxine-pyrimethamine protection from malaria studied in Akbari et al. (2012). White et al. (2011) made significant contribution to the literature by conducting a systematic review of the published works on the costs of all malaria control interventions using electronic database. Result of the study identified 78% of fifty-five studies of the costs and forty three studies of the cost-effectiveness of malaria interventions in Sub-Saharan Africa. Economies of scale were observed in the implementation of ITNs, IRS and IPT, with lower unit costs reported in their studies with population level benefit, the median incremental cost effectiveness ratio per disability adjusted life year averted was provided to inform rational resource allocation by donors and domestic health budgets.

Smith et al. (2009) used mathematical models to establish rationally defined endpoints, timelines and criteria for monitoring and evaluation of ITN programs. The model predicts that over the period of 5-10 year endemic control will be stabilized and it is also possible to transform malaria in the short to medium-term through high levels of ITN ownership. Stuckey et al. (2014) introduced Open Malaria stochastic simulation modeling to simulate the impact of case management and malaria control interventions (singly and/or in combination of interventions) in western Kenya compared to the corresponding simulated outputs of a case without interventions. Their results indicate that increased coverage of vector control intervention has a huge impact compared to adding an IST intervention to the current implementation strategy.

One of the important reasons for the failure of strategies to eradicate infectious disease is because of their neglect of the mobility patterns of the host. The importance of the role of human migration is evident in the recent increase in malaria incidence not only in the endemic zones, but also in zones where malaria had been eradicated Martens and Hall (2000); Sandia Mago (1993); Aragon and Espinal (1992); Bailey (1982). Mainly two types of mobility patterns that can spread the infection to newer areas, are considered migration, i.e., when the people move from one region to another with no returns; and visitation, when the people return to their original region after visiting other regions.

The effects of migration and visitation on transmission of malaria were shown in Torres-Sorando and Rodriguez (1997) by modifying the basic Ross model to include space that is fragmented into number of patches. Only humans are assumed to move among the patches and mosquitoes are evenly distributed. Impact of seasonal labor

migration to India on the dynamics of the HIV epidemic in Far-Western Nepal studied in Vaidya and Wu (2011b). This is the main motivation for the development of malaria models incorporating cross-border mobility. With this rich literature, we did not find the mathematical modeling of malaria disease using system of ordinary differential equation incorporating cross-border mobility Nepal and many other countries of world are also in malaria elimination phase but mobility of cross-border workers becoming a problem to achieve their elimination plan. Our study is focused on the mobility of workers from Nepal and its impact on malaria elimination plan.

1.4 Research Outline

In this research, we propose a deterministic model of malaria that integrates cross-border mobility of migrant workers from low to high malaria endemic countries like Nepal and India. Also, it propose a delay malaria model integrating the relapse proportions and relapse delays of Vivax and Ovale malaria. Through these models, we aim to uncover insightful results regarding the humans mobility, and relapse cases and persistence of malaria disease. Furthermore, we investigate the factors contributing malaria persistence and significant challenges to achieving malaria elimination in low-endemic countries like Nepal. The thesis is structured as follows. Chapter 1 covers worldwide malaria eradication programs and their implications in addressing ultimate public health challenges.

Additionally, it describes worldwide impact of imported cases of malaria through human mobility and relapse issue to provide the rationale of the study, research problems. It provides an overview of literature of mathematical models of malaria. The objectives of the study are specifically presented, and the introductory chapter concludes with an outline of the thesis structure. Chapter 2 start with the historical background of malaria disease, its discoveries and the parasite life-cycle. It presents definitions of key terminologies, theorems for stability analysis, persistence theory, backward bifurcation analysis. It also covers details about data fitting and parameter estimation using the principle of the least squares method. These concepts will be essential for understanding the subsequent chapters.

Chapter 3 covers the formulation of the malaria model with cross-border mobility. Model fitting validation and simulations are presented to address the malaria elimination program of Nepal by 2026. Also, it covers stability of disease free equilibria and persistence theory. Chapter 4 delves into backward bifurcation analysis, exploring

various possibilities of the cross-border mobility. Taking two real world scenarios regarding human mobility, we did extensive backward bifurcation analysis to evaluate the impact of mobility parameters and human mosquito parameters in malaria persistence and elimination. Chapter 5 addresses the relapse problem using a system of delay differential equations. It includes extensive equilibria analysis and theory of hopf bifurcation. With wide simulations, it predicts malaria status in Nepal due to impact of relapse proportion and relapse delay to achieve the malaria free condition in absence of imported cases. Chapter 6 serves as a summary and conclusion, presenting insights drawn from the previous chapters. It also outlines future research directions.

CHAPTER 2

2. PRELIMINARIES

This chapter provides fundamentals of infectious disease modeling, focusing specifically on malaria. The chapter commences by explaining history and life cycle of parasite in malaria disease. In addition, it covers fundamental terminologies and subsequently, it delves into methodologies for obtaining various equilibrium solutions of the system. It also describes the next-generation method to derive the pivotal parameter known as the basic reproduction number. Furthermore, the chapter elucidates techniques to study stability analysis of equilibrium, encompassing forward and backward bifurcations as well as Hopf-bifurcation. Finally, it discusses the tools and techniques of data fitting using the principle of the least squares method.

2.1 Background of Malaria Disease

2.1.1 History of Malaria

Malaria has been a significant health concern for humans for thousands of years. Hippocrates, often called the "Father of Medicine," documented the symptoms of malaria as early as the 4th or 5th century BC. The disease continued to affect many throughout history, including notable figures such as Alexander the Great, who is believed to have died from malaria at the age of 32. The term "malaria" was introduced in 1718 by the Italian physician Francisco Torti. Derived from the Italian words "mala aria," meaning "bad air," this name reflected the ancient belief that the disease was caused by the noxious air of swamps Smith (1999); Jones and Brown (2005). Because of the scientific community's research, our understanding of malaria disease dynamics has increased over time.

The discovery of malaria protozoan parasites is attributed to Charles Louis Alphonse Laveran, a French army surgeon, who in 1880 observed the presence of Plasmodium parasites within the blood of malaria patients, pioneering the understanding of the disease's causative agent Laveran (1881). By 1890, scientists identified three species: Camillo Golgi, an Italian physician and Nobel laureate, played a significant role in the discovery of Plasmodium vivax Golgi (1886). Ettore Marchiafava and Angelo Celli,

Italian physicians and researchers, made significant contributions to the identification and characterization of Plasmodium falciparum and Plasmodium malariae Marchiafava and Celli (1885). Subsequently, in 1897, a noteworthy breakthrough was made by William MacCallum, who observed and studied the sexual reproduction of a malaria-like parasite found in birds, specifically Haemoproteus columbae Cox F (2010); MacCallum (1897). In the same year the crucial role of mosquitoes in malaria transmission was unveiled by Sir Ronald Ross, a British medical doctor. Ross's experiments, conducted in India, demonstrated that malaria parasites were transmitted through the bite of infected female mosquitoes of the Anopheles genus, a discovery that earned him the Nobel Prize in Physiology or Medicine in 1902 Ross (1897). In 1922, John Stephens in West Africa discovered a fourth species, Plasmodium ovale. Later in Southeast Asia, clinicians identified Plasmodium knowlesi malaria as the fifth human malaria parasite. These discoveries revolutionized our understanding of malaria and contributed to advancements in its prevention and treatment Antinori et al. (2012); Beier (1998).

2.1.2 Life Cycle of Malaria Parasite

The life cycle of malaria parasites (Plasmodium spices) begins when an infected female Anopheles mosquito injects sporozoites into a human during a blood meal. These sporozoites travel to the liver where they invade hepatocytes and undergo asexual replication (schizony), producing thousands of merozoites for 7-10 days for Disease Control et al. (2018). In the erythrocytic cycle, these merozoites invade and infect red blood cells, developing first into ring-shape tropozoites, then mature and finally schizonts, which release new merozoites upon Red Blood Cell (RBC) rupture, causing clinical symptoms of malaria Cornelio and Seriano (2011). Some merozoites differentiate into sexual forms called gametocytes, which are ingested by another musquito during a subsequent blood meal. In mosquito's midgut, gametocytes mature into gametes, fuse to form zygotes, and develop into motile ookinetes that panetrate the midgut wall, forming oocysts. These oocysts produce sporozoites through replication, and when they brust, sporozoites migrate to the mosquito's salivary glands, ready to infect a new human host perpetuating the cycle Antinori et al. (2012). The parasite spends around 15 days in the mosquito and 15 days in the human liver before a 72-hour period in the blood, with the cycle repeating upon subsequent mosquito bites Cornelio and Seriano (2011).

Understanding the different stages of the malaria parasite's life cycle and its transmission between humans and mosquitoes is crucial for developing effective strategies to

treat, prevent and control of malaria Milner (2018).

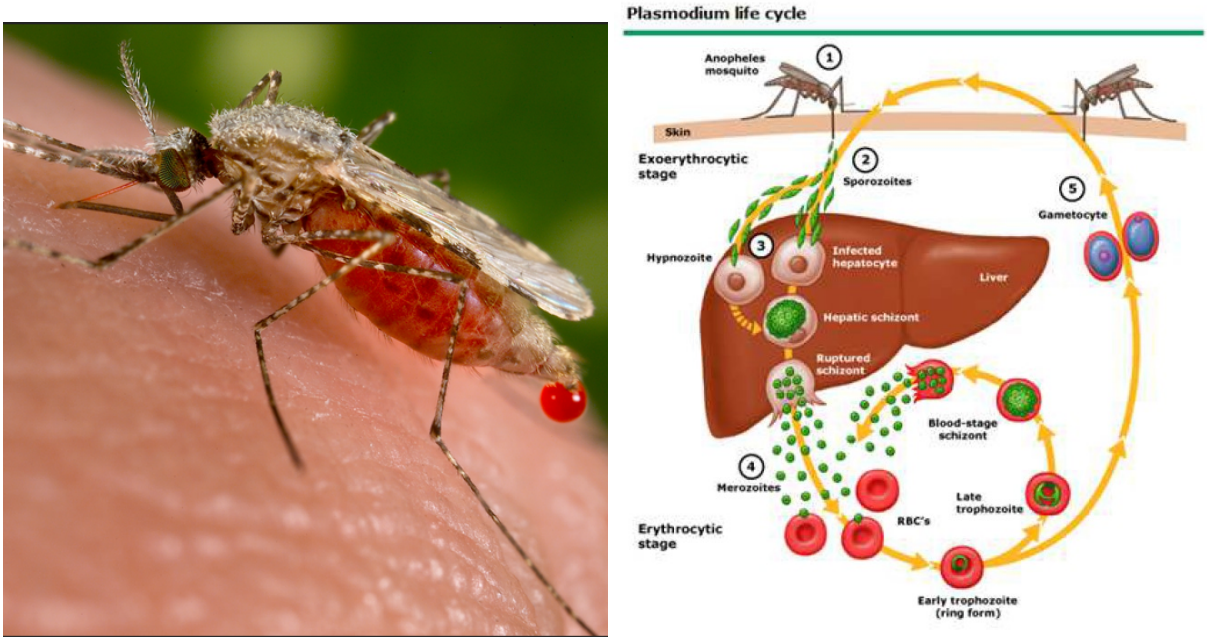

(a) **(b)**

Figure 2: Female Anopheles mosquito (vector of malaria disease) and life-cycle of plasmodium parasite in human.

2.1.3 Diagnosis, Control Tools and Treatment of Malaria

Malaria diagnosis typically occurs during the blood stage of the parasite cycle. Microscopy of blood smears is the "gold standard," detecting 20 to 50 parasites per microliter with skilled technicians, or 100 parasites per microliter more commonly Smith and Brown (2015); Jones and White (2014). This method requires trained personnel, quality control, and appropriate equipment. PCR and qPCR are highly sensitive, detecting 0.05 to 10 parasites per microliter, but require costly equipment and take about three hours to process. Rapid Diagnostic Tests (RDTs) are low-cost tools that generally detect infections at 200 parasites per microliter or more, but may miss lower-level infections, leading to false negatives. Loop-mediated isothermal DNA Amplification (LAMP) shows a sensitivity of 5 parasites per microliter, with a processing time of one hour Smith and Brown (2015); Williams and Johnson (2014); Harris and White (2015). Selecting the appropriate diagnostic tool is crucial, especially in resource-limited settings. However, relying on less sensitive methods like RDTs can leave many infections undetected, contributing to the infectious reservoir.

Malaria control methods include Insecticide-Treated Bed Nets (ITNs), Indoor Residual Spraying (IRS), larviciding, and Mass Drug Administration (MDA), targeting specific areas or groups like infants and pregnant women (Intermittent Preventative Treatment, IPT). Mass Screen and Treat (MSAT) and Mass Fever Treatment (MFT) are other strategies Green and Thompson (2020). The WHO recommends Artemisinin-based combination therapies (ACTs) as the first-line treatment for uncomplicated Plasmodium falciparum malaria. Common ACTs include artemether-lumefantrine, artesunate-amodiaquine, artesunate-mefloquine, and dihydroartemisinin-piperaquine. Chloroquine is used for *Plasmodium vivax, Plasmodium ovale*, and *Plasmodium malariae* infections, with primaquine for preventing relapses. Quinine and atovaquone-proguanil are used for severe malaria and both treatment and prevention, respectively Roberts and Johnson (2016); Miller and Clark (2018).

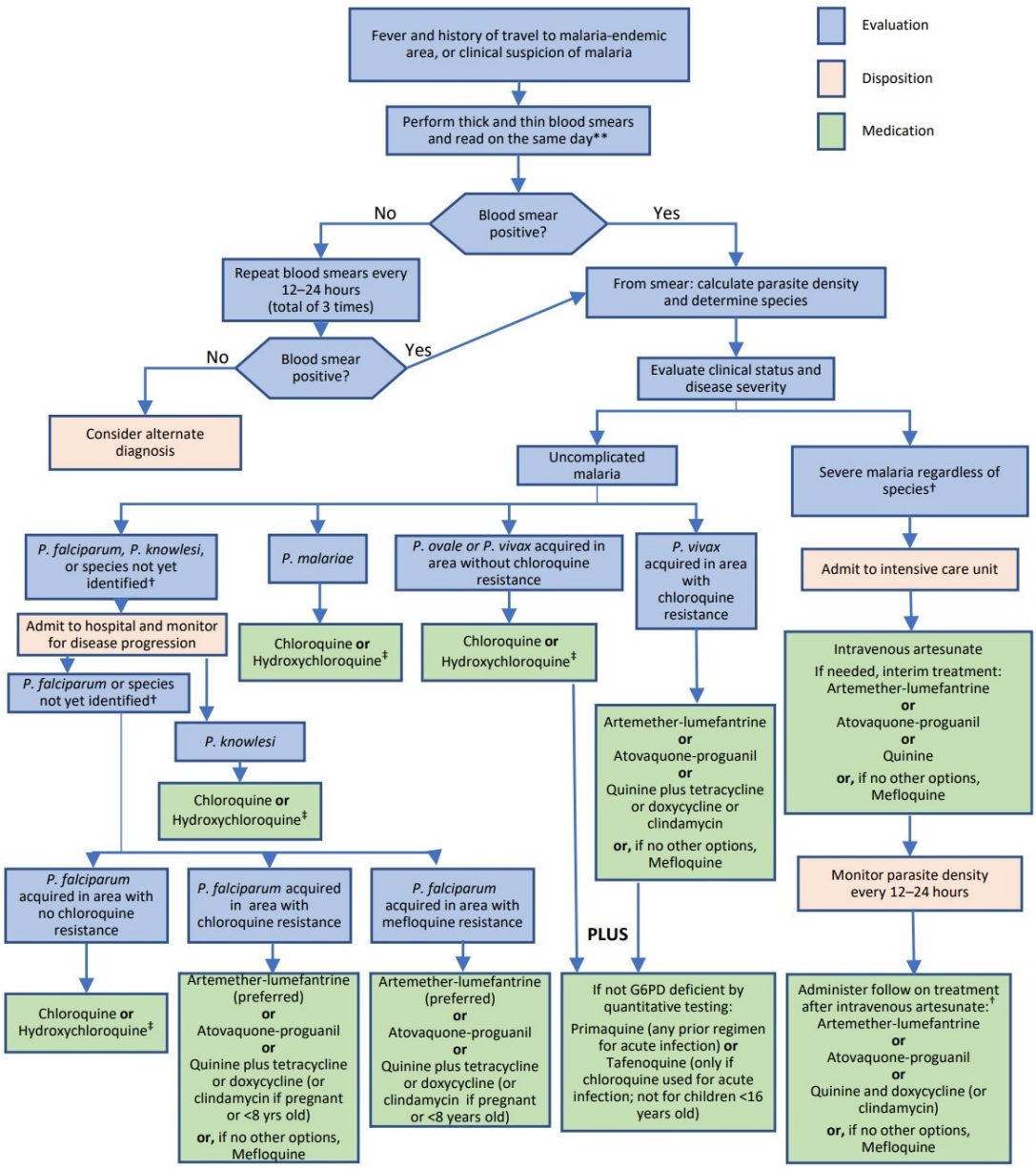

Figure 3: Diagnosis and treatment process of malaria disease.

2.2 Basic Terminologies in the Disease Modeling

2.2.1 Basic Terminologies in Malaria Modeling

Susceptible Human: The class of human individuals who have no immunity to the infectious agent, so might become infected from malaria if bitten by an infectious

female Anopheles mosquito.

Exposed Human: When susceptible humans to malaria disease bitten by infectious female Anopheles mosquito, they are considered exposed. Being exposed does not necessarily mean they will get sick, and usually, these individuals are not capable of spreading the disease to others. In mathematical representations, it is common to simplify by assuming that all exposed individuals will eventually contract the disease, although this may not always be the case in reality.

Infected and Infectious Human: If the malaria parasites establish themselves in an exposed individual, then that individual becomes infected. Infected individuals who can transmit the disease are called infectious. Infected individuals may not be infectious during the entire time of being infected.

Recovered Human: The recovered human population includes individuals who have successfully cleared both the liver-stage and blood-stage malaria parasites from their bodies, indicating an effective immune response and immunity against future malaria infections. In the case of malaria disease, these individuals may lose immunity over time and could be susceptible again.

Latent Human: Individuals in the latent class have previously been infected with the malaria and have successfully cleared parasites in their bloodstream, and they do not exhibit symptoms of malaria. However, the parasite may persist in their liver in a dormant form can reactivate and cause a relapse of the disease at a later time. Latent individuals are not infectious to others unless the dormant parasite is reactivated, leading to a new episode of active infection.

Susceptible Mosquito: Female Anopheles mosquitoes that do not carry malaria parasites but are at risk of acquiring the parasites when they feed on the blood of infectious humans with malaria are called susceptible mosquito.

Exposed Mosquito: When a susceptible mosquito bites an infectious human individual, this bite may transmit malaria disease, and the susceptible mosquito may become exposed. An exposed mosquito may or may not develop the malaria disease.

Infectious Mosquito: Infectious mosquitoes are female Anopheles mosquitoes that have accumulated a sufficient number of malaria parasites in their salivary glands. When these mosquitoes bite susceptible humans, they have the potential to transmit the malaria parasite, thereby exposing these humans to the risk of acquiring the disease.

Disease Induced Mortality: Disease-induced mortality refers to the number of individuals who have died from a specific disease within a defined period, such as a year, divided by the total population.

Latency Period: Latency is the period between exposure to a disease-causing agent, like a virus or bacterium, and the onset of infectiousness.

Incubation Period: The incubation period is the span of time from the initial exposure to an infectious agent to the emergence of the first signs or symptoms of a disease.

Prevalence or Active Number of Cases: Prevalence indicates the total count of individuals with a disease at a particular moment. Occasionally, it is calculated as the number of people with the disease at that time divided by the total population size.

Indigenous Malaria Cases : Any case contracted within the country, with no evidence of a direct link to an imported case.

Imported Malaria Cases : An imported case is one that is due to mosquito-borne transmission and is acquired in another country. The National Malaria Program has standardized the initial classification of 'imported' malaria as a confirmed case of malaria detected within 1 month of return from an endemic area outside the country.

Introduced Malaria Cases : Any case contracted locally, with strong epidemiological evidence linking it directly to a known imported case (first generation from an imported case; i.e., the mosquito was infected by a patient classified as an imported case). In areas where transmission is known to be ongoing, there is limited practical value in classifying cases as introduced.

Cumulative Number of Cases: The total number of individuals affected by a disease from the start to the present or over a specific period.

Incidence or New Cases: Incidence refers to the count of individuals who develop an illness within a set timeframe, such as a year. Occasionally, it is calculated as the number of people falling ill in a specific period divided by the total population. Typically, it is based on clinical cases alone, potentially underreporting the actual incidence as it does not account for subclinical cases.

2.2.2 State of Infectious Diseases

Endemic: An infection is termed endemic in a population when it persists at a consistent baseline level within a specific geographic region, without external introductions. This is seen in diseases like the flu, common cold, and malaria.

Epidemic: This occurs when the number of cases of a disease increases above what is normally expected in that population in that area. It is typically a sudden outbreak that spreads rapidly and affects many individuals.

Outbreak: An outbreak is a sudden surge in new disease cases in a specific area. COVID-19 began as an outbreak in Wuhan, China, in December 2019 when numerous cases of unexplained pneumonia were confirmed.

Annual Parasitic Index (API): The Annual Parasite Index (API) is a public health metric used to assess the prevalence and burden of certain parasitic diseases, particularly malaria. It is commonly used in epidemiology and public health to monitor and evaluate the impact of control measures and interventions aimed at reducing the transmission of parasitic diseases.

The API is calculated as WHO (2019):

$$\text{API} = \frac{\text{Number of new cases of the disease in a year} \times 1000}{\text{Risk population in the year}}$$

.

To introduce SIR-SI human-mosquito malaria model Zhilan and Dominik (2003), we define the following parameters and state variables. Λ_h, Λ_v are the human and mosquito recruitment from birth respectively. S_h, I_h, R_h are susceptible, infectious and recovered human population respectively and S_v, I_v are the susceptible and infectious mosquito populations respectively. μ_h, μ_v are the natural death rates of human and mosquito respectively and γ_h is the human recovery rate. The incidence rate of humans and mosquito are $\frac{\beta_{hv} I_v}{S_h + I_h + R_h}$ and $\frac{\beta_{vh} I_h}{S_h + I_h + R_h}$ respectively.

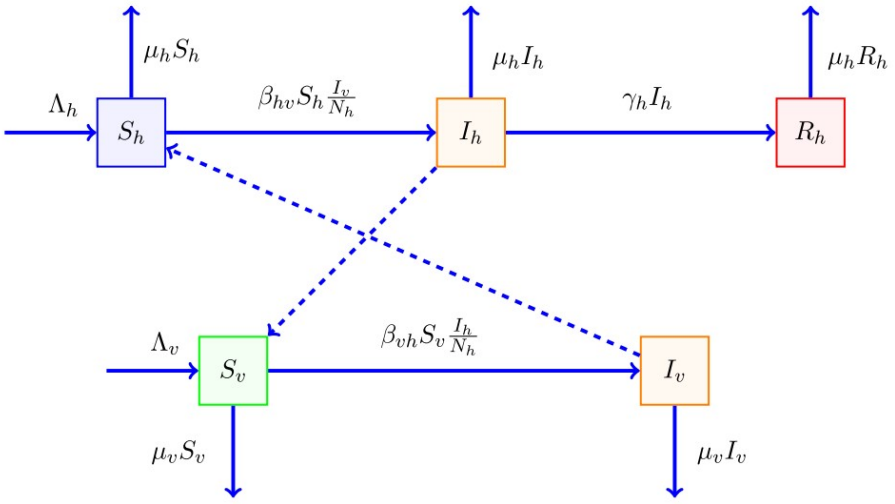

Figure 4: Malaria transmission from infected human to susceptible mosquito and from infected mosquito to susceptible human.

Then the system of equations:

$$\frac{dS_h}{dt} = \Lambda_h - \beta_{hv} \frac{S_h I_v}{S_h + I_h + R_h} - \mu_h S_h, \tag{2.1}$$

$$\frac{dI_h}{dt} = \beta_{hv} \frac{S_h I_v}{S_h + I_h + R_h} - (\gamma_h + \mu_h) I_h, \tag{2.2}$$

$$\frac{dR_h}{dt} = \gamma_h I_h - d_h R_h, \tag{2.3}$$

$$\frac{dS_v}{dt} = \Lambda_v - \beta_{vh} \frac{S_v I_h}{S_h + I_h + R_h} - \mu_v S_v, \tag{2.4}$$

$$\frac{dI_v}{dt} = \beta_{vh} \frac{S_v I_h}{S_h + I_h + R_h} - \mu_v I_v, \tag{2.5}$$

Equilibrium of the System: In a disease model, an equilibrium solution refers to a state where the number of individuals in each compartment (Susceptible, Infectious, etc.) remains relatively constant over time. Equilibrium solutions can provide insights into the long-term behavior of the disease within a population. In this research, we used two types of equilibrium.

Disease-free Equilibrium: A disease-free equilibrium is a state in a population with no exposed, infected and infectious individuals. At the disease-free equilibrium, there are no infected individuals in the population $I_h = 0,\ I_v = 0$. Also, at equilibrium

$\frac{d}{d_t}S_h = 0, \frac{d}{d_t}I_h = 0, \frac{d}{d_t}R_h = 0, \frac{d}{d_t}S_v = 0, \frac{d}{d_t}I_v = 0$. If follows that the disease free equilibrium is $\left(\frac{\Lambda_h}{\mu_h}, 0, 0, \frac{\Lambda_v}{\mu_v}, 0\right)$.

Endemic Equilibrium: An endemic equilibrium is a state where the disease is consistently present at a steady, unchanging level within a population. At the endemic equilibrium $I_h > 0,\ I_v > 0$, together with $\frac{d}{d_t}S_h = 0, \frac{d}{d_t}I_h = 0, \frac{d}{d_t}R_h = 0, \frac{d}{d_t}S_v = 0, \frac{d}{d_t}I_v = 0$.

Density Dependent Contact: In density-dependent contact, the contact rate (biting rate in vector-borne disease like malaria) and hence the transmission of a disease is depend on population density, i.e., the number of individuals per unit area or volume. As population density increases, the chances of contact between individuals also increase, which can lead to higher incidence rate. In this case, if b is average biting rate per mosquito per time and N_h is human population then per time number of bites that can each mosquito made is bN_h and incidence rate in human $\frac{bN_h\alpha_{vh}S_hI_v}{N_h} = b\alpha_{vh}S_hI_v$. In the case of malaria, density dependent is not rational since average mosquito biting rate b is fixed.

Frequency Dependent Contact: In frequency-dependent contact, contact rate (biting rate) and hence disease transmission is vary with frequency of interactions regardless of population density. In this case average biting rate is independent with available human population and the incidence rate of malaria in human is given by $\frac{b\alpha_{vh}S_hI_v}{N_h}$.

2.3 Autonomous and Non-Autonomous Nonlinear Systems in SIR Models

2.3.1 Autonomous System

An autonomous system is one where the system of differential equations does not explicitly depend on time. This means the coefficients in the system are constants or functions of the state variables only, but not directly of time t .

2.3.2 Non-Autonomous System

A non-autonomous system is one where the system of differential equations explicitly depends on time. This means the coefficients or the forcing terms in the system are

functions of time t.

2.3.3 Solution of Linear Homogeneous System

Theorem 2.3.1 *In a linear equation of one-dimension* $\frac{dX}{dt} = AX$*, where* A *is constant then* $X(t) = Ce^{At}$ *is a solution of the system Strang (2016).*

Theorem 2.3.2 *In the linear system of two dimension:* $\frac{dX}{dt} = AX$,$X \in \mathbb{R}^2$ *and* A *is* 2×2 *matrix, if,* $u = v_1 e^{\lambda_1 t}$ *and* $v = v_2 e^{\lambda_2 t}$ *are two independent solutions of homogeneous linear system then their linear combination* $c_1 u + c_2 v$ *is also a solution of the system.*

The sum $\sum_{k=1}^{n} c_k v_k e^{\lambda_k t}$ is the solution in n-dimensional linear system.

Jacobian of a system at equilibrium: In some cases, behavior of nonlinear system can be analyzed from the corresponding linear system. The Jacobian of the system (2.1-2.5) at the equilibrium is

$$J = \begin{pmatrix} \frac{\partial f_1}{\partial S_h} & \frac{\partial f_1}{\partial I_h} & \frac{\partial f_1}{\partial R_h} & \frac{\partial f_1}{\partial S_v} & \frac{\partial f_1}{\partial I_v} \\ \frac{\partial f_2}{\partial S_h} & \frac{\partial f_2}{\partial I_h} & \frac{\partial f_2}{\partial R_h} & \frac{\partial f_2}{\partial S_v} & \frac{\partial f_2}{\partial I_v} \\ \frac{\partial f_3}{\partial S_h} & \frac{\partial f_3}{\partial I_h} & \frac{\partial f_3}{\partial R_h} & \frac{\partial f_3}{\partial S_v} & \frac{\partial f_3}{\partial I_v} \\ \frac{\partial f_4}{\partial S_h} & \frac{\partial f_4}{\partial I_h} & \frac{\partial f_4}{\partial R_h} & \frac{\partial f_4}{\partial S_v} & \frac{\partial f_4}{\partial I_v} \\ \frac{\partial f_5}{\partial S_h} & \frac{\partial f_5}{\partial I_h} & \frac{\partial f_5}{\partial R_h} & \frac{\partial f_5}{\partial S_v} & \frac{\partial f_5}{\partial I_v} \end{pmatrix}$$

at equilibrium, where f_i are right hand side of the system (2.1-2.5) .

Non-hyperbolic and hyperbolic equilibrium: Non-hyperbolic equilibrium point of a dynamical system where the Jacobian matrix has at least one eigenvalue with a real part equal to zero. This contrasts with a hyperbolic equilibrium, where all eigenvalues have non-zero real parts. Non-hyperbolic equilibria are significant because their stability cannot be determined using linearization alone, necessitating more advanced methods like the Central Manifold Theorem Hirsch et al. (2012).

Theorem 2.3.3 (Hartman-Grobman Theorem) *Grobman (1959); Hartman (1960) Consider a system evolving in time with state* $u(t) \in \mathbb{R}^n$ *that satisfies the differential equation* $\frac{du}{dt} = f(u)$ *for some smooth map* $f : \mathbb{R}^n \to \mathbb{R}^n$*. Now suppose the map has a hyperbolic equilibrium state* $u^* \in \mathbb{R}^n$ *i.e.* $f(u^*) = 0$ *and the Jacobian matrix* $A = [\partial f_i / \partial x_j]$ *of* f *at states* u^* *has no eigenvalue with real part equal to zero. Then*

there exists a neighbourhood N of the equilibrium u^* and a homeomorphism $g : N \to \mathbb{R}^n$ such that $g(u^*) = 0$ and such that in the neighbourhood N the flow of $\frac{du}{dt} = f(u)$ is topologically conjugate by the continuous map $U = g(u)$ to the flow of its linearisation $\frac{dU}{dt} = AU$.

Remarks: Real-world problems are often nonlinear, and obtaining exact analytical solutions is generally impractical. The Hartman-Grobman Theorem provides a local characterization of the behavior of dynamical systems near a hyperbolic equilibrium point (no eigenvalue is with real part zero). It states that near such a point, the nonlinear system behaves qualitatively like its linearization.

Basic Reproduction Number (R_0)**:** It is the average number of new infections produced by an infectious individual in his/her infectious period in a completely susceptible population. It is denoted by R_0. Normally given by R_0 = (number of contacts per time) $\times$ (probability of infection in a contact) $\times$ (duration of infectiousness during epidemics). For complicated models that includes seasonality methods or heterogeneity the next generation matrix (NGM) method is used in computing the R_0. In the field of epidemiology, R_0 serves as a critical threshold. When R_0 is greater than one, it indicates the potential for epidemics, while an R_0 less than one suggests the absence of epidemics. The basic reproduction number (R_0) plays a pivotal role in guiding public health interventions and control strategies to prevent and manage disease outbreaks. The reproduction number over the time is called effective reproduction number.

Spectral Radius or Spectral Bound: The spectral radius of a square matrix A is the maximum absolute value of its eigenvalues. It is denoted by $\rho(A)$.

Next Generation Matrix Method for R_0: Here an outline of this method is given, the proof and further details can be found in Van den Driessche and Watmough (2002) and Van den Driessche and Watmough (2008). Let $x = (x_i)^T$, $i = 1, 2, 3, ..., m$ represent vector of disease state variables (exposed and infectious compartments) and $\frac{dx_i}{dt} = F_i(x) - V_i(x), i = 1, 2, ..., m$ is a system of models for the disease compartments. In this splitting, $F_i(x)$ is the rate of appearance of new infections in compartment i, and $V_i(x)$ is the rate of other transitions between compartment i and other infected compartments. It is assumed that both $F_i(x)$ and $V_i(x)$ are in C^2. Then F and V are the Jacobian of $f_i(x)$ and $V_i(x)$ at the disease-free equilibrium x^*. F is entry wise non-negative and V is non-singular M-matrix Berman and Plemmons (1994). The basic reproduction number is the spectral radius of FV^{-1} Anderson and May (1992).

2.4 Stability of Equilibrium

Local stability: A system is locally stable if small perturbations from an equilibrium point lead to trajectories that return to the equilibrium point over time. Mathematically, for a system to be locally stable, all eigenvalues of the Jacobian matrix evaluated at the equilibrium point must have negative real parts. This ensures that any perturbation from the equilibrium decays over time, eventually returning the system to its equilibrium state. Eigenvalues with zero real parts indicate a different kind of behavior, possibly involving sustained oscillations or other complex dynamics, which are not characteristic of local stability.

Asymptotic Stability: A system is asymptotically stable if, in addition to being locally stable, trajectories converge to the equilibrium point as time goes to infinity. This means that the system not only returns to equilibrium after small disturbances but also stays at the equilibrium as time progresses.

Global Stability: A system is globally stable if the desired stability properties hold for all initial conditions in the entire state space, not just in a local neighborhood of the equilibrium point. It requires demonstrating stability over the entire state space. Global stability often involves proving that the system's behavior is stable for all possible initial conditions, which is a stronger condition than local or asymptotic stability.

Theorem 2.4.1 *Martcheva (2015) A necessary and sufficient condition for an equilibrium to be locally asymptotically stable is that all eigenvalues of the Jacobian at the equilibrium have negative real part. i.e., for starting the dynamics with the initial condition near the equilibrium point eventually converge to the equilibrium point. But if the eigenvalue are pure imaginary, then the stability is only local.*

Routh-Hurwitz Criteria: In higher-dimensional models, the Jacobian at the disease-free equilibrium yields a characteristic polynomial of degree three or higher. The reproduction number is derived from the constant term, and its relationship to 1 indicates disease spread direction. To assess stability, the Routh-Hurwitz criterion provides necessary and sufficient conditions for ensuring negative real parts of eigenvalues.

Theorem 2.4.2 *Martcheva (2015) Consider the nth-degree polynomial with real constant coefficients* $P(\lambda) = \lambda^n + a_1\lambda^{n-1} + a_2\lambda^{n-2} + ... + a_n = 0$. *Define n Hurwitz matrices using the coefficients* a_i *of characteristic polynomial:*

$$H_1 = (a_1), H_2 = \begin{bmatrix} a_1 & 1 \\ a_3 & a_2 \end{bmatrix}, H_3 = \begin{bmatrix} a_1 & 1 & 0 \\ a_3 & a_2 & a_1 \\ a_5 & a_4 & a_3 \end{bmatrix} \cdots,$$

$$H_n = \begin{bmatrix} a_1 & 1 & 0 & 0 & ...0 \\ a_3 & a_2 & a_1 & 1 & ...0 \\ a_5 & a_4 & a_3 & a_2 & ...0 \\ ... & ... & ... & ... & ... \\ 0 & 0 & 0 & 0 & ...a_n \end{bmatrix},$$

where $a_j = 0$ if $j > n$. All roots of the polynomial $P(\lambda)$ are negative or have negative real part if and only if the determinants of all Hurwitz matrices are positive i.e., $Det(H_j) > 0, j = 1, 2, 3, ..., n$.

Theorem 2.4.3 *(**Krasovskii-LaSalle Theorem** Martcheva (2015)): Consider the autonomous system $\dot{x} = f(x)$, where x^* is an equilibrium point such that $f(x^*) = 0$. Suppose there exists a continuously differentiable function $V : \mathbb{R}^n \to \mathbb{R}$ that is positive definite, radially unbounded, and satisfies $\dot{V}(x) \leq 0$ for all $t \geq 0$ and all $x \in \mathbb{R}^n$. Define the invariant set $S = \{x \in \mathbb{R}^n \mid \dot{V}(x) = 0\}$. If S contains only the equilibrium x^*, then x^* is globally asymptotically stable. This implies that every solution $x(t)$ of the system $\dot{x} = f(x)$, starting sufficiently close to x^*, converges to x^* as $t \to \infty$.*

2.4.1 Bifurcation

A qualitative change in the behavior of a system due to a change in a parameter is called bifurcation. Here we discuss three types of bifurcations:

1. **Forward Bifurcation:** This is a simple phenomenon where disease becomes endemic in a population when $R_0 > 1$ whereas disease die-out from the population when $R_0 < 1$. i.e., there is simple exchange of stability of disease-free equilibrium and endemic equilibrium below and above 1.

2. **Backward Bifurcation:** This is a complex phenomenon, where even if the reproduction number is below one, multiple endemic equilibria exist. In this case, a bistability phenomenon exists, indicating lower and higher endemic levels.

3. **Hopf Bifurcation:** This is also a complex phenomenon, where endemic equilibria lose their stability at some time when $R_0 > 1$, and periodic oscillations occur, indicating periodic outbreaks Brauer et al. (2008).

Castillo-Chavez and Song Bifurcation Theorem Martcheva (2015)

Theorem 2.4.4 *Consider the following general system of ODEs with a parameter* ϕ *:* $\frac{d\vec{x}}{dt} = \vec{f}(\vec{x}, \phi)$*,* $\vec{f} : \mathbb{R}^n \times \mathbb{R} \to \mathbb{R}^n$*,* $\vec{f} \in C^2(\mathbb{R}^n \times \mathbb{R})$*, where* 0 *is an equilibrium point of the system, that is,* $\vec{f}(0, \phi) \equiv 0$ *for all* ϕ*. Assume the following: A is the linearization matrix of system around the equilibrium* 0 *with* ϕ *evaluated at* 0*. Zero is a simple eigenvalue of A , and other eigenvalues have negative real parts. The matrix A has a nonnegative right eigenvector* $\vec{w}$ *and a left eigenvector* $\vec{v}$ *each corresponding to the zero eigenvalue. Let* f_k *be the kth component of* $\vec{f}$ *and*

$$a = \sum_{m,i,j=1}^{n} v_m u_i u_j \frac{\partial^2 f_m}{\partial x_i \partial x_j}(0,\ 0),\ b = \sum_{m,i=1}^{n} v_m u_i \frac{\partial^2 f_m}{\partial x_i \partial \phi}(0,\ 0), \tag{2.6}$$

where f_m *be the* m^{th} *component of f. If* $a > 0$ *and* $b > 0$*, then a backward bifurcation occurs at* $\phi = 0$*. However, for* $b > 0$ *and* $a \leq 0$ *is the case of forward bifurcation.*

2.5 Data Fitting and Model Validation

In mathematical modeling, especially with ordinary differential equation (ODE) models, accurately estimating unknown parameters is essential for the model to reflect real-world dynamics. MATLAB provides powerful tools to achieve this by combining its ODE solvers with optimization functions. The process involves defining an objective function that measures the difference between the model's predictions and the observed data. Optimization algorithms then adjust the model's parameters to minimize this difference. The result is a set of parameters that make the model closely match the real system's behavior, allowing for accurate predictions and analysis Moler (2004).

Complex-step Derivative approximation technique: We used the complex-step derivative approximation technique described in Rahman et al. (2019) to identify parameters that can be estimated from the available data and to obtain the 95% confidence interval of the estimated parameters. $J(\phi) = \sum_{k=1}^{n} \left(L_{t_k}(\phi) - \bar{L_{t_k}}\right)^2$, L_{t_k} and $\bar{L_{t_k}}$ are the model solution and available data and $\phi = (\phi_1, \phi_2, ..., \phi_m)$ is the set of parameters to be estimated.

In order to derive confidence intervals for the estimated parameters, we compute standard errors for ϕ using a method outlined in Banks et al. (2014); Rahman et al. (2019). For this, we first compute the sensitivity matrix S of the parameters,

$$S = \begin{bmatrix} \frac{\partial L_{t_1}}{\partial \phi_1} & \frac{\partial L_{t_1}}{\partial \phi_2} & \cdots & \frac{\partial L_{t_1}}{\partial \phi_m} \\ \frac{\partial L_{t_2}}{\partial \phi_1} & \frac{\partial L_{t_2}}{\partial \phi_2} & \cdots & \frac{\partial L_{t_2}}{\partial \phi_m} \\ \vdots & \vdots & \ddots & \vdots \\ \frac{\partial L_{t_n}}{\partial \phi_1} & \frac{\partial L_{t_n}}{\partial \phi_2} & \cdots & \frac{\partial L_{t_n}}{\partial \phi_m} \end{bmatrix}.$$

Since we are unable to formulate the closed form of $\frac{\partial L_{t_k}}{\partial \phi_j}$, $j = 1, 2, \ldots, m$, and $k = 1, 2, \ldots, n$ from the model, we use the following complex-step approximation to compute the partial derivatives. We employ a Taylor series expansion of L_{t_k} using a complex step ih, where h is a small positive constant ($h = 10^{-40}$ in our calculations), and i is the imaginary unit. The expansion can be written as:

$$L_{t_k}(\phi_j + ih) \approx L_{t_k}(\phi_j) + ihL'_{t_k}(\phi_j) - \frac{h^2}{2!}L''_{t_k}(\phi_j) + \ldots$$

By isolating the imaginary part of this expression and dividing by h, we arrive at:

$$L'_{t_k}(\phi_j) = \frac{\partial L_{t_k}}{\partial \phi_j} \approx \frac{\mathrm{Im}[L_{t_k}(\phi_j + ih)]}{h} + O(h^2),$$

where $O(h^2)$ represents the terms of second-order and higher. Thus, the partial derivatives can be approximated by:

$$\frac{\partial L_{t_k}}{\partial \phi_j} \approx D_j^h(L_{t_k}) = \frac{\mathrm{Im}[L_{t_k}(\phi_j + ih)]}{h}, \quad \text{for } j = 1, 2, \ldots, m \text{ and } k = 1, 2, \ldots, n.$$

Using these derivatives, we construct an approximation of the sensitivity matrix S, which we denote as $\hat{S}$. The standard deviation for each parameter ϕ_j, for $j = 1, 2, \ldots, m$, is then given by:

$$\sqrt{\left(\sigma^2 \left\{\hat{S}^T \hat{S}\right\}^{-1}\right)_{ii}},$$

where $\sigma^2 \approx \hat{\sigma}^2 = \frac{J(\phi)}{n-m}$, and ϕ represents the estimated parameter values.

2.6 Limitations of Ordinary Differential Equation

Ordinary Differential Equations (ODEs) effectively model the spread of diseases like malaria but assume instantaneous interactions, which can miss key time delays in biological processes. Delay Differential Equations (DDEs) address this by incorporating latency periods, offering a more accurate framework for disease dynamics Keeling and Rohani (2008). In Chapter 5, we will introduce delay differential equation to describe various delays in the malaria transmission process.

2.7 Delay Differential Equation Models of Vector-Borne Diseases

Delay Differential Equations (DDEs) extend ordinary differential equations by incorporating time delays, where the rate of change at a given time depends on both current and past states. The simplest form of a DDE is

$$\dot{x}(t) = F(t, x(t), x(t-\tau_1), x(t-\tau_2), \ldots, x(t-\tau_k)),$$

where τ_j are time delays. $x(t)$ is the state of the system at the current time t. It represents the value of the function x at the present time. DDEs require an initial history function to specify the system's state prior to $t = 0$ and $x(t-\tau_j)$ is the state of the system at a previous time $t-\tau_j$. It represents the value of the function x at a time delayed by τ_j units from the current time t and τ_j is the time delay associated with this term. In modeling vector-borne diseases like malaria, DDEs account for delays such as the incubation periods of the pathogen in both the vector and the host. These delays are crucial as they significantly impact disease dynamics.

Theorem 2.7.1 (Hopf BifurcationMartcheva (2015)) *Consider the delay-differential equation*

$$\dot{x}(t) = F(x(t), x(t-\tau_1), \ldots, x(t-\tau_{n-1}), \mu), \tag{2.7}$$

where μ is a parameter. Assume the following conditions are satisfied:

1. *F is analytic in both x and μ in the neighborhood of (x^*, μ_0) in $\mathbb{R}^n \times \mathbb{R}$.*
2. *$F(x^*, \mu) = 0$ for μ in an open interval around μ_0, and $x(t) = x^*$ is an isolated stationary solution of Eq. (2.7).*
3. *The characteristic equation of Eq. (2.7) has a pair of complex conjugate eigenvalues λ and $\bar{\lambda}$ such that $\lambda(\mu) = b(\mu) + i\omega(\mu)$, where $\omega(\mu_0) = \omega_0 > 0$, $b(\mu_0) = 0$, and $\frac{db}{d\mu}(\mu_0) \neq 0$.*
4. *The other eigenvalues of the characteristic equation have strictly negative real parts.*

Then, the delay-differential equation Eq. (2.7) admits a family of periodic solutions bifurcating from x^*, known as Hopf periodic solutions.

CHAPTER 3

3. MODELING MALARIA TRANSMISSION IN NEPAL: IMPACT OF IMPORTED CASES THROUGH CROSS-BORDER MOBILITY

In this chapter, we develop a novel mathematical model to study how the imported malaria cases through the Nepal-India open-border affect the Nepal government's goal of eliminating malaria by 2026. Mathematical analyses and numerical simulations of our model, validated by malaria case data from Nepal, indicate that eliminating malaria from Nepal is possible if strategies promoting the absence of cross-border mobility, complete protection of transmission abroad, or strict border screening and isolation are implemented. For each strategy, we establish the conditions for the elimination of malaria. We further use our model to identify the control strategies that can help maintain a low endemic level. Our results show that the ideal control strategies should be designed according to the average mosquito biting rates that may depend on the location and season.

3.1 Introduction

In the literature of malaria modeling, the studies Anderson (2013a); Ngwa (2004); Anderson and May (1991a); Jeffrey and Pia (2002); Chiyaka et al. (2009); Hastings (1997); Torres-Sorando and Rodriguez (1997); Koutou et al.; Arik et al. (2017); Ngwa and Shu (2000); H. Juliette et al. (2020) extended the basic Ross-MacDonald-Anderson and May model by incorporating age structure, loss of immunity, the effect of social, economic, and environmental factors, human migration, drug resistance of vector, the impact of bed-nets, multi-groups, and multi patches. Even though some mathematical models Le Menach et al. (2011); Sturrock Hugh et al. (2013); Thomas et al. (2014); Bradley et al. (2015); Isobel et al. (2018) include cross-border mobility, there remains uncertainty on the various aspects of the role of imported cases in vector-borne disease, particularly malaria transmission. Except for some descriptive, analytical, and retrospective studies EDCD (2020); Organization (2018); Dhimal et al. (2014b); Shanker et al. (2019); Smith et al. (2009), none of the previous models focused on the dynamics of indigenous and imported malaria cases in the context of Nepal, which is

in critical condition of achieving the 2026 malaria elimination goal due to cross-border mobility of migrant workers.

Motivated from a previous study Vaidya and Wu (2011a), which addressed the impact of cross-border mobility on HIV-AIDS epidemics in Nepal, we develop a novel transmission dynamics model of malaria by incorporating the imported cases through the cross-border mobility into a basic malaria model. Using the data of malaria cases in Nepal, we estimate the critical parameters of malaria dynamics in Nepal. We thoroughly analyze our model to study the impact of cross-border mobility on disease eradication and threshold dynamics. We further use our model to predict the future trend of imported and indigenous malaria cases and evaluate the different control strategies to achieve the malaria elimination goal by 2026.

3.2 Method

3.2.1 Data Source

In this study, we used the data containing both indigenous and imported malaria cases in Nepal. Since the total cases were not classified as imported and indigenous before 2009, we considered the data only from 2009 to 2019 for our model fitting. The primary data sources related to malaria cases in Nepal are the National Malaria Surveillance Guidelines 2019 published by the Government of Nepal, Ministry of Health and Population Department of Health Services Epidemiology and Disease Control Division (EDCD) of Health and Population (2019); Dhimal et al. (2014b). In addition, we also obtained the data of Annual Parasitic Incidence (API) of India from the Malaria Site India of Health and Family Welfare (2020); National Vector Borne Disease Control Programme (2020).

3.2.2 Model Formulation

To develop a transmission dynamics model of malaria, we divide the total population of the home country into two groups: the population living in the home country (N_{hH}) and the population living abroad as migrant workers (N_{hM}). Each of these groups is further divided into three subgroups: susceptible (S_{hH}), infectious (I_{hH}), and recovered (R_{hH}) in the home country and susceptible (S_{hM}), infectious (I_{hM}), and recovered (R_{hM}) living abroad as migrant workers. Moreover, we consider susceptible and

infectious mosquito populations in the home country (S_{vH}, I_{vH}) and abroad (S_{vA}, I_{vA}). We note that the migrant workers, N_{hM}, are included in the total human population abroad (N_{hA}) and thus the corresponding abroad groups, susceptible (S_{hA}), infectious (I_{hA}), and recovered (R_{hA}) include S_{hM}, I_{hM}, and R_{hM}, respectively.

In our model, malaria transmission occurs from infected mosquitoes to susceptible humans and from infected humans to susceptible mosquitoes through mosquito bites. We assume that b and b' are the per capita biting rates of mosquitoes in the home country and abroad, respectively. α_{vh} and α'_{vh} are the probability in the home country and abroad, respectively, that an infectious mosquito transmit malaria to a susceptible human in a single bite. Similarly, α_{hv} and α'_{hv} are the probability in the home country and abroad, respectively, that the malaria is transmitted from infectious human to a susceptible mosquito in a single infectious bite. For the home country, the total number of bites (per time) from all the infectious mosquitoes is bI_{vH} (infectious bites). Among these bites, the susceptible humans get $\frac{bI_{vH}S_{hH}}{N_{hH}}$ infectious bites. Therefore, the incidence rate of humans (i.e., the new human infections per unit time) is $\frac{b\alpha_{vh}I_{vH}S_{hH}}{N_{hH}}$ Xing et al. (2020); Brauer (2011); Wairimu et al. (2018); Wan and Cui (2009); Chitnis et al. (2008); Xiulei et al. (2020). Similarly, the incidence rate for humans in abroad is $\frac{b'\alpha'_{vh}I_{vA}S_{hA}}{N_{hA}}$. Also, the total number of bites (per time) made by the susceptible mosquitoes in the home country is bS_{vH}. Among these bites, the total number of bites from the infectious humans (infectious bites) is $\frac{bS_{vH}I_{hH}}{N_{hH}}$. Therefore, the incidence rate of mosquitoes (i.e., the new mosquito infections per unit time) is $\frac{b\alpha_{hv}I_{hH}S_{vH}}{N_{hH}}$. Similarly, the incidence rates for mosquitoes in abroad is $\frac{b'\alpha'_{hv}I_{hA}S_{vA}}{N_{hA}}$.

The infectious humans recover with the rate γ_h, and the recovered individuals lose their immunity and move back to the susceptible class at the rate q. Because of the short lifespan of mosquitoes, we do not consider the recovered class for the mosquitoes population. The parameters Λ and d_h represent the recruitment rate and the natural death rate of humans, respectively, while the parameters ϕ and d_v represent the recruitment rate and the death rate of mosquitoes, respectively. We assume that η represents the per capita cross-border mobility rate for susceptible populations (S_{hH}, S_{hM}) and recovered populations (R_{hH}, R_{hM}). Since infected individuals may behave differently in their travels from and to the home country, we take p and θ as the cross-border mobility rate for infectious individuals from and to the home country, respectively. In the model, θI_{hM} and $\frac{b\alpha_{vh}I_{vH}S_{hH}}{N_{hH}}$ represent the imported and indigenous malaria incidence at home country, respectively.

The schematic diagram of our model is presented in Figure 5. The system of ordinary

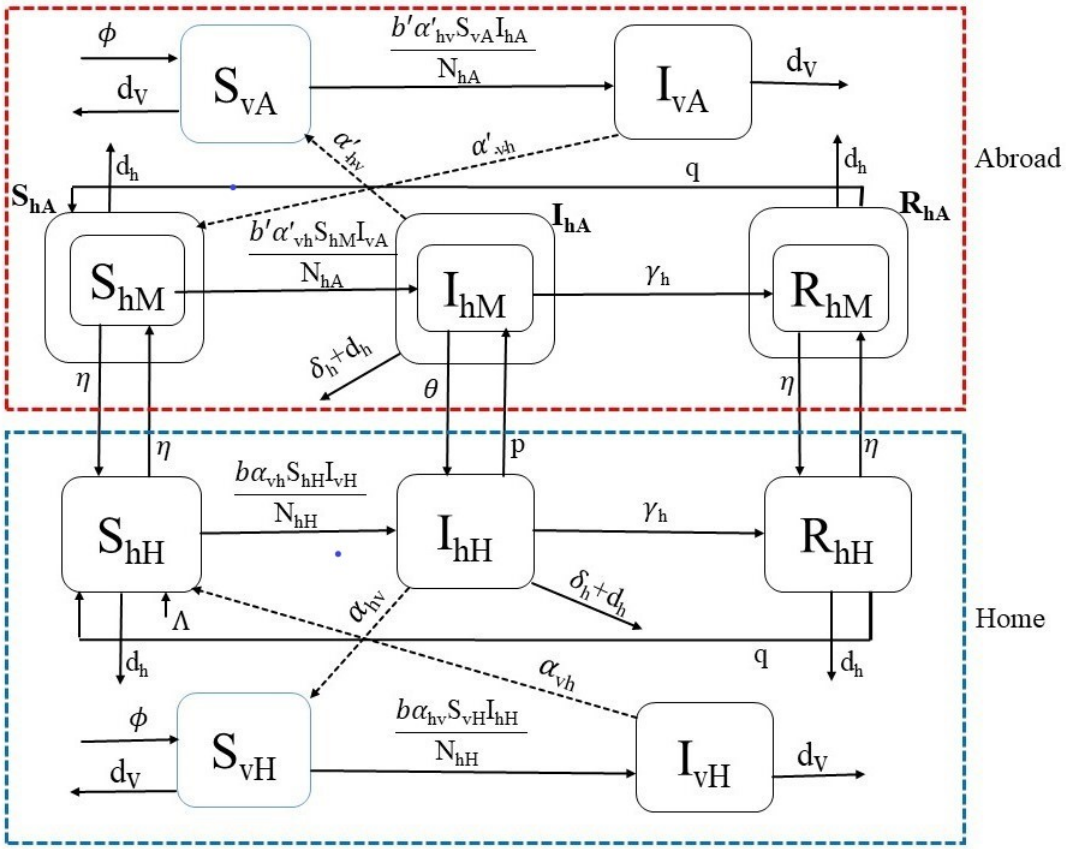

Figure 5: Malaria transmission dynamics with cross-border mobility. The upper SI-SIRS (inside red dashed line) and lower SI-SIRS (inside blue dashed line) represent the dynamics of malaria abroad and in the home country. The solid arrows represent the transfer of populations, and the dotted arrows represent the interaction between the susceptible human and infectious female Anopheles mosquitoes and infectious humans with susceptible female Anopheles mosquitoes. Here, subscripts H, A, and M refer to home, abroad, and migrant, respectively, and the subscript h and v refer to human and vector (mosquito), respectively.

differential equations describing the transmission dynamics of malaria discussed above

is as follows:

$$S'_{hH} = \Lambda + \eta S_{hM} + qR_{hH} - \frac{b\alpha_{vh}I_{vH}}{N_{hH}}S_{hH} - (\eta + d_h)S_{hH}, \tag{3.1}$$

$$I'_{hH} = \frac{b\alpha_{vh}I_{vH}}{N_{hH}}S_{hH} + \theta I_{hM} - (p + d_h + \delta_h + \gamma_h)I_{hH}, \tag{3.2}$$

$$R'_{hH} = \gamma_h I_{hH} + \eta R_{hM} - (\eta + d_h + q)R_{hH}, \tag{3.3}$$

$$S'_{vH} = \phi - \frac{b\alpha_{hv}I_{hH}}{N_{hH}}S_{vH} - d_v S_{vH}, \tag{3.4}$$

$$I'_{vH} = \frac{b\alpha_{hv}I_{hH}}{N_{hH}}S_{vH} - d_v I_{vH}, \tag{3.5}$$

$$S'_{hM} = \eta S_{hH} + qR_{hM} - \frac{b'\alpha'_{vh}I_{vA}}{N_{hA}}S_{hM} - (d_h + \eta)S_{hM}, \tag{3.6}$$

$$I'_{hM} = \frac{b'\alpha'_{vh}I_{vA}}{N_{hA}}S_{hM} + pI_{hH} - (\theta + \delta_h + d_h + \gamma_h)I_{hM}, \tag{3.7}$$

$$R'_{hM} = \gamma_h I_{hM} + \eta R_{hH} - (\eta + d_h + q)R_{hM}, \tag{3.8}$$

$$S'_{vA} = \phi - \frac{b'\alpha'_{hv}I_{hA}}{N_{hA}}S_{vA} - d_v S_{vA}, \tag{3.9}$$

$$I'_{vA} = \frac{b'\alpha'_{hv}I_{hA}}{N_{hA}}S_{vA} - d_v I_{vA}. \tag{3.10}$$

Since the detailed dynamics of malaria abroad makes the model extremely complex and uncertain, we introduce an index $\psi(t)$ called Annual Parasite Incidence (API), for which the data are publicly available. We introduce this index into the model to approximate the incidence rate abroad. Here $\psi(t)$ is defined as the number of positive cases of malaria per population under surveillance, i.e., $\psi(t) = \dfrac{I_{hA}(t)}{N_{hA}(t)}$. The incidence rate of humans in abroad is given by

$$\lambda'_h = \frac{b'\alpha'_{vh}I_{vA}(t)}{N_{hA}(t)} = \frac{b'\alpha'_{vh}I_{vA}(t)}{I_{hA}(t)}\psi(t).$$

Both $b'\alpha'_{vh}I_{vA}(t)$ and $I_{hA}(t)$ are differentiable functions in the interval $(0, T)$, where T is the final time of the disease dynamics considered. Assuming that $I_{hA}(t) \neq 0,\ \forall\, t \in [0, T]$, the mean value theorem of integral calculus allows us to approximate the integral of the continuous function $\dfrac{b'\alpha'_{vh}I_{vA}(t)}{I_{hA}(t)}$ with a constant $\zeta = \dfrac{b'\alpha'_{vh}}{T}\int_0^T \dfrac{I_{vA}(t)}{I_{hA}(t)}dt \approx b'\alpha'_{vh}\dfrac{I_{vA}(t_0)}{I_{hA}(t_0)}$ for some $t_0 \in (0, T)$. Thus, we approximate the incidence rate abroad by $\lambda'_h = \zeta\psi(t)$ and estimate the value of ζ from the data fitting. With this approximation,

the system (3.1-3.10) reduces to the system of the following eight differential equations.

$$S'_{hH} = \Lambda + \eta S_{hM} + qR_{hH} - \frac{b\alpha_{vh}I_{vH}}{N_{hH}}S_{hH} - (\eta + d_h)S_{hH}, \tag{3.11}$$

$$I'_{hH} = \frac{b\alpha_{vh}I_{vH}}{N_{hH}}S_{hH} + \theta I_{hM} - (p + d_h + \delta_h + \gamma_h)I_{hH}, \tag{3.12}$$

$$R'_{hH} = \gamma_h I_{hH} + \eta R_{hM} - (\eta + d_h + q)R_{hH}, \tag{3.13}$$

$$S'_{vH} = \phi - \frac{b\alpha_{hv}I_{hH}}{N_{hH}}S_{vH} - d_v S_{vH}, \tag{3.14}$$

$$I'_{vH} = \frac{b\alpha_{hv}I_{hH}}{N_{hH}}S_{vH} - d_v I_{vH}, \tag{3.15}$$

$$S'_{hM} = \eta S_{hH} + qR_{hM} - \zeta\psi(t)S_{hM} - (d_h + \eta)S_{hM}, \tag{3.16}$$

$$I'_{hM} = \zeta\psi(t)S_{hM} + pI_{hH} - (\theta + \delta_h + d_h + \gamma_h)I_{hM}, \tag{3.17}$$

$$R'_{hM} = \gamma_h I_{hM} + \eta R_{hH} - (\eta + d_h + q)R_{hM}. \tag{3.18}$$

3.3 Results

3.3.1 Estimation of Parameters and Population Size

The population of Nepal was estimated to be 23,151,423 in 2001 Wiki (2001) and 26,494,504 in 2011 Wiki (2011). Taking the average population growth per year from 2001 to 2011, we estimated the population of Nepal in 2009 (the base year of our dynamics, i.e., $t = 0$) to be 25,825,888. About 5.5 million Nepalese, including 1.9 million male workers, were living abroad of Labour and Employment (2020), mostly in India. These migrant workers bring malaria upon their return home, contributing the significant number of imported malaria cases in Nepal GoN and Population (2016). Note that the majority of Nepalese migrants working in India are male Vaidya and Wu (2011a). Therefore, we took $N_{hM}(0) = 1.9$ million. With 5.5 million living abroad, the population inside Nepal is approximately 20,325,888. Since most of the hilly and mountainous regions of Nepal are considered risk free zone of malaria, leaving only about 48% of Nepalese residing in other regions in high, moderate or low risk area Rijal et al. (2019b), we estimated $N_{hH}(0) = 9,756,426$. Moreover, we used the information from the data and divided the total population into different compartments and obtained $S_{hH}(0) = 9,754,000, I_{hH}(0) = 2,000, R_{hH}(0) = 426, S_{hM}(0) = 1,898,300, I_{hM}(0) = 1,400, R_{hM}(0) = 300, S_{vH}(0) = 9,754,176$, and $I_{vH}(0) = 2,250$. About 37.5% of the total migrant workers ($\sim 179,464$) traveled from Nepal to India in 2009 of Labour and Employment (2018). This allows us to estimate per capita annual mobility rate of

migrants from Nepal to India as:

$$\eta = \frac{\text{Number of migrants from Nepal to India}}{\text{Total risk population of malaria in Nepal}} = \frac{179,464}{9,756,426} = 0.0183$$

per human per year.

The Crude Birth Rate (CBR), i.e., the number of live birth per year per 1,000 people, of Nepal for the year 2009 was 23.189 Wiki (2011), which implies the human recruitment rate per year for the population in the risk area is $\Lambda = 48\%$ of $\frac{23.189 \times 25,825,888}{1000} = 287,460$. Since the average life expectancy of Nepalese individuals in 2009 was 67.178 years Rijal et al. (2019a), the natural death rate of humans per year is taken as $d_h = 0.0149$ (per year). The number of deaths due to malaria in the base year TNH (2012) was 6, so we calculated $\delta_h = 0.0017$ per year. The duration of immunity for recovered people varies widely from region to region, and we took the immunity period to be 3 months, i.e., $q = 4$ per year Chitnis et al. (2008). For model fitting, we assumed that all the cases are recorded and that malaria-infected Nepalese do not move to India as workers while sick. Therefore, we took p=0.

The population of female Anopheles mosquitoes has been estimated to be 1-10 times the human population Chitnis et al. (2008); Xiulei et al. (2020); Chamchod and Britton (2011). Thus we took the mosquito population equal to base year human population $9,756,426$. Based on the previous studies Chitnis et al. (2008); Xiulei et al. (2020); Castillo-Chavez and Song (2004); Chamchod and Britton (2011); Abu-Raddad et al. (2006), we took the probability of disease transmission, per bite, from an infectious mosquito to a susceptible human as $\alpha_{vh} = 0.0195$, and from an infectious human to a susceptible mosquito as $\alpha_{hv} = 0.63$. Similarly, the human recovery rate and the mosquito death rate were obtained from previous studies as $\gamma_h = 1.85$ per year and $d_v = 27.9113$ per year Chitnis et al. (2008); Xiulei et al. (2020); Castillo-Chavez and Song (2004); Chamchod and Britton (2011); Abu-Raddad et al. (2006). The remaining parameters, θ, ζ, and b, were estimated from the data fitting.

3.3.2 Model Fitting to the Data

As per the national planning of malaria elimination by 2026, the Government of Nepal introduced the strategic plan in 2014, which includes the distribution of Long Lasting Insecticide Treated Nets (LLINs) and Indoor Residual Spraying (IRS) intended to reduce mosquito bites GoN and Population (2016). Thus in our model fitting, we allow the different biting rates for the period before ($b = b_1$) and after ($b = b_2$) 2014.

The available data are the yearly indigenous malaria incidence, the yearly imported malaria incidence, and the total malaria incidence in Nepal. From the solution of our model, the indigenous, the imported, and the total malaria incidences at time t, denoted by $L(t)$, $I(t)$, and $T(t)$, respectively, can be computed using the following expressions:

$$L(t) = \frac{b\alpha_{vh}S_{hH}I_{vH}}{N_{hH}}, \;\; I(t) = \theta I_{hM}, \; T(t) = L(t) + I(t). \tag{3.19}$$

The model system of differential equations was solved numerically using the fourth-order Runge-Kutta method. Using the solutions, we obtained the best-fit parameters using the nonlinear least-squares regression method that minimizes the following sum of the squared residuals:

$$J(\phi) = \sum_{k=1}^{n} \left[(L(t_k) - \bar{L}(t_k))^2 + (I(t_k) - \bar{I}(t_k))^2 + (T(t_k) - \bar{T}(t_k))^2 \right], \tag{3.20}$$

where $L(t_k)$, $I(t_k)$, $T(t_k)$ and $\bar{L}(t_k)$, $\bar{I}(t_k)$, $\bar{T}(t_k)$ are the model predicted incidences and those given in the available data. In our data fitting, we used the total 30 data points to estimate four parameters $\phi = (\theta, \; \zeta, \; b_1, b_2)$. The ratio of data to the free parameters used in our model, i.e., 7:1 , is well within the recommended range of 5:1 to 10:1 Schunn et al. (2005). Also, three types of data (indigenous, imported, and total) included in fitting provide additional feature of malaria infection. To obtain the confidence limits for the estimated parameters, we computed standard errors from the sensitivity matrix S using the techniques described previously Rahman et al. (2019). Furthermore, we computed the rank of the matrix S^TS and found the matrix to be of the full rank (rank = 4), which ascertain the identifiability of these parameters of the model Hongyu et al. (2011). i.e., the matrix S^TS is square matrix of order 4 with linearly independent columns and hence is invertible. All computations were carried out in MATLAB 2018A (The MathWorks, Inc.). In Figure 6, we present the model prediction, along with the data, of the indigenous, the imported, and the total malaria incidence. The model fits have captured the dynamics pattern of the multiple data well, and the model prediction is also consistent with the cumulative data (Figure 6), thereby validating the model. All estimated parameters, as well as the fixed parameters, are provided in Table 2. As indicated by the data GoN and Population (2016), the model solutions also show the decreasing trend of the malaria cases from 2009, with the indigenous case being more than the imported case until 2014. However, after 2014, the imported case overtook the indigenous case, indicating the alarming situation originating from the imported cases. Our estimates show that

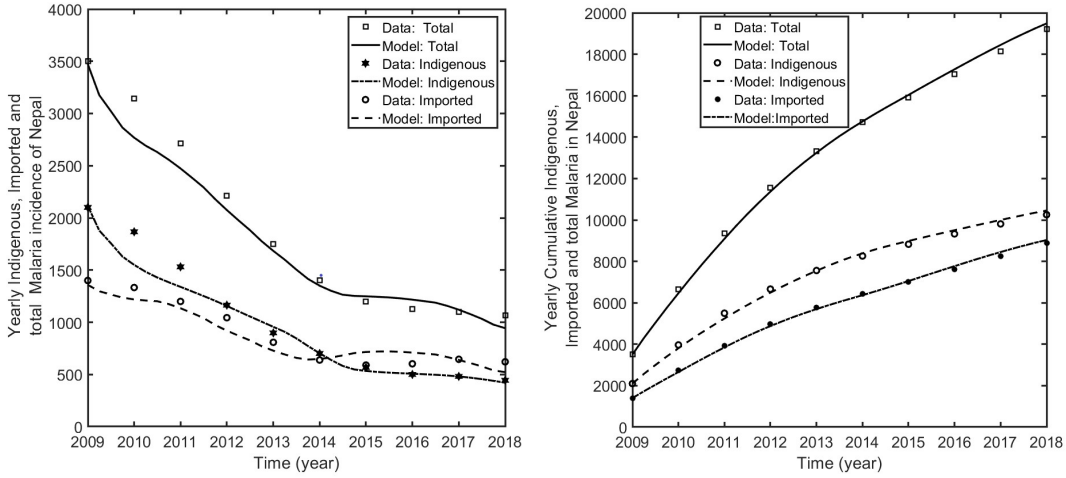

(a) **(b)**

Figure 6: Model fitting to the data. (a) Solution of the fitted model along with the data of indigenous, imported, and total malaria incidences in Nepal, and (b) Model prediction of cumulative indigenous, cumulative imported, and cumulative total cases in Nepal.

Description	State variables	Base Value (References)
Risk humans population in Nepal	$N_{hH}(0)$	9,756,426 (Calculated)
Susceptible humans in Nepal	$S_{hH}(0)$	9,754,000 (Calculated)
Infectious humans in Nepal	$I_{hH}(0)$	2,000 (Assumed)
Recovered humans in Nepal	$R_{hH}(0)$	426(Assumed)
Susceptible Migrants in India	$S_{hM}(0)$	1,898,300 GoN and Population (2016)
Infectious Migrants in India	$I_{hM}(0)$	1,400 (Assumed)
Recovered Migrants in India	$R_{hM}(0)$	300(Assumed)
Susceptible mosquitoes in Nepal	$S_{vH}(0)$	9,754,176(Assumed)
Infectious mosquitoes in Nepal	$I_{vH}(0)$	2,250 (Assumed)

Table 1: Base value of demographic variables of malaria in Nepal

the biting rate of mosquitoes is $b_1 = 48.0$ (95% CI: [38.13, 57.87]) before 2014, and $b_2 = 39.5$ (95% CI: [29.63, 49.37]) after 2014. These estimated values are consistent with the values provided in many previous studies Chitnis et al. (2008); Xiulei et al. (2020). Similarly, we estimated the disease import rate $\theta = 0.98$ (95% CI: [0.42, 1.54]) and the

parameter corresponding to the incidence rate in India $\zeta = 0.00105$ (95% CI: [0.0005, 0.0016]).

Description	Param.	Base value (References)
Probability of malaria transmission from an infectious mosquito (per bite) to a susceptible human	α_{vh}	0.0195 Abu-Raddad et al. (2006)
Probability of malaria transmission from an infectious human to a susceptible mosquito (per bite)	α_{hv}	0.63 Castillo-Chavez and Song (2004)
Humans recruitment rate	Λ	287,460 Number$\times yr^{-1}$ (Calculated)
Per capita recovery rate of humans	γ_h	1.85 yr^{-1}Abu-Raddad et al. (2006)
Per capita natural birth and death rate of mosquitoes	d_v	27.9 yr^{-1} Chamchod and Britton (2011)
Per capita disease induced death rate of humans	δ_h	$0.00171yr^{-1}$(Calculated)
Per capita natural death rate of humans	d_h	$0.0149yr^{-1}$ (Calculated)
Per capita mobility rate of healthy humans	η	$0.0183yr^{-1}$ (Calculated)
Per capita disease import rate of humans	θ	0.98 yr^{-1} Estimated [0.4172, 1.5428]
Per capita disease export rate of humans	p	0 yr^{-1} (Assumed)
Per capita rate of Immunity loss of humans	q	4 yr^{-1} Chitnis et al. (2008)
Parameter related with incidence rate in India	ζ	0.00105 yr^{-1} (Estimated) [0.0005, 0.0016]
Per capita biting rate of mosquitoes at home country up to 2014	b_1	48 yr^{-1}(Estimated) [39.6537, 66.3463]
Per capita biting rate of mosquitoes at home country after 2014	b_2	39.5 yr^{-1}(Estimated) [29.6318, 49.3682]

Table 2: Model parameters of incidence of malaria in Nepal

3.3.3 Model Analysis

Note that our model is non-autonomous due to the presence of time-dependent parameter $\psi(t)$. Since $\psi(t)$ depends on the policy implemented abroad, the time-dependent nature of this parameter remains unknown, and the analysis of this non-

autonomous model is complicated and uncertain. Therefore, for the purpose of analysis, we consider the autonomous form of the model by taking a constant $k = (\zeta/T)\int_0^T \psi(t)dt$ as an approximation to the incidence rate abroad.

3.3.4 Positivity and Boundedness of Solutions

In this section, we show that the solutions of all the state variables are non-negative and bounded in order to demonstrate that the model is well-posed and biologically valid for describing malaria transmission dynamics. The results are presented in the following theorem.

Theorem 3.3.1 *If* $S_{hH}(0) > 0,\ I_{hH}(0) \geq 0,\ R_{hH}(0) \geq 0,\ S_{hM}(0) \geq 0,\ I_{hM}(0) \geq 0,\ R_{hM}(0) \geq 0,\ S_{vH}(0) > 0,\ I_{vH}(0) \geq 0$*, then the solution set* $\{S_{hH}(t),\ I_{hH}(t),\ R_{hH}(t),\ S_{hM}(t),\ I_{hM}(t),\ R_{hM}(t),\ S_{vH}(t),\ I_{vH}(t)\}$ *of the system (3.11 - 3.18) is positive and bounded for all* $t > 0$.

Proof: First we show that if $S_{vH}(0) > 0$ then $S_{vH}(t) > 0$ for all $t > 0$. From the Eq. (3.14), we get $S_{vH}(t) \geq S_{vH}(0)Exp\left[-\int_0^t \left(\frac{b\alpha_{vh}I_{hH}}{N_{hH}} + d_v\right)dt\right] > 0$.

Now we prove that if $S_{hH}(0) > 0$, then $S_{hH}(t) > 0$ for $t > 0$. Suppose if possible $S_{hH}(t) > 0$ for all $t > 0$ is not possible. Then there exists first time point $t = t_s > 0$ such that $S_{hH}(t_s) = 0$. From Eq. (3.11), $S'_{hH}(t)|(t = t_s) = \Lambda + \eta S_{hM}(t_s) + qR_{hH}(t_s)$. We claim that $S_{hM}(t_s), R_{hH}(t_s)$ both can not be negative. If possible, $\min\{S_{hM}(t_s), R_{hH}(t_s)\} = S_{hM}(t_s) < 0$, then there exist $t_m > 0$, $t_m < t_s$ be the first time point such that $S_{hM}(t_m) = 0$. From Eq. (3.16) $S'_{hM}(t)|(t = t_m) = \eta S_{hH}(t_m) + qR_{hM}(t_m)$. Again, we claim that $R_{hM}(t_m)$ can not be negative. If possible, assume that there exists first time point $t_r > 0$, $0 < t_r < t_m$ such that $R_{hM}(t_r) = 0$. Then from Eq. (3.18) $R'_{hM}|(t = t_r) = \gamma_h I_{hM}(t_r) + \eta R_{hH}(t_r)$. Now we claim $I_{hM}(t_r)$ can not be negative. If possible there exist first time point $t_h > 0$, $t_h < t_r$ such that $I_{hM}(t_h) = 0$. Then from Eq. (3.17) $I'_{hM}|(t = t_h) = kS_{hM}(t_h) + PI_{hH}(t_h)$. Again we claim $I_{hH}(t_h)$ can not be negative. If possible, there exist first time point $0 < t_i$, $t_i < t_h$ such that $I_{hH}(t_i) = 0$. From Eq. (3.12), $I'_{hH}|(t = t_i) > 0$ when $I_{vH}(t_i)$ is not negative. If possible there exist first time point $0 < t_k$ with $t_k < t_i$ such that $I_{vH}(t_k) = 0$. It follows from Eq. (3.15) that $I'_{vH}|(t = t_k) > 0$. Then there exist small enough $\zeta > 0$ with $t_k - \zeta < t < t_k$ such that $I_{vH}t) < 0$. Which is contradiction to t_k is the first time point such that $I_{vH}(t_k) = 0$. Thus, going back we must have $S_{hH}(t) > 0$ for all $t > 0$. In this way we can show that $S_{hM} > 0$ and $I_{hH}, I_{hM}, R_{hM} \geq 0$ and $I_{vH} \geq 0$ for

$t \geq 0$. Thus human population are always positive for $t > 0$. Also, adding the system (3.11-3.13) and the system (3.16-3.18), we get $\frac{dN_h(t)}{dt} \leq \Lambda - d_h N_h(t)$, which implies that $\lim_{t\to\infty} N_h(t) \leq \frac{\Lambda}{d_h}$. Again, adding the system (3.14-3.15), we get $\frac{dN_v(t)}{dt} = \phi - d_v N_v(t)$, which implies that $\lim_{t\to\infty} N_v(t) \leq \frac{\phi}{d_v}$. □

Using the above conditions, we derive that for any $\epsilon > 0$, there exists $t_\epsilon > 0$ such that the solution of the system with $t \geq t_\epsilon$ lies in the compact set $\Omega = \Omega_h \times \Omega_v$, where

$$\Omega_h = \left\{ (S_{hH}, I_{hH}, R_{hH}, S_{hM}, I_{hM}, R_{hM}) \in \mathbb{R}^6_+ : N_h \leq \frac{\Lambda}{d_h} + \epsilon \right\}$$

and

$$\Omega_v = \left\{ (S_{vH}, I_{vH}) \in \mathbb{R}^2_+ : N_v \leq \frac{\phi}{d_v} + \epsilon \right\}.$$

3.3.5 Existence of Equilibria

For convenience, we let $S_{hH} = x,\ I_{hH} = y,\ R_{hH} = z,\ S_{hM} = X, I_{hM} = Y,\ R_{hM} = Z,\ S_{vH} = l$, and $I_{vH} = m$, and we take $(x^*, y^*, z^*, l^*, m^*, X^*, Y^*, Z^*)$ to represent the equilibrium point of the system (3.11 -3.18). For simplicity, we assume that also for the infectious compartments, the mobility rate is equal in both ways, from home to abroad and vice versa, i.e., $\theta = p$. Taking,

$$\lambda_h^* = \beta_h \frac{m^*}{N_{hH}^*},\ \lambda_v^* = \beta_v \frac{y^*}{N_{hH}^*},\ \beta_v = b\alpha_{hv},\ \beta_h = b\alpha_{vh}, \tag{3.21}$$

the system (3.11-3.18) provides

$$\begin{aligned} x^* &= \frac{P}{K_1 + K_2\ \lambda_h^*},\ y^* = \frac{Q_1 + Q_2\lambda_h^*}{K_1 + K_2\ \lambda_h^*},\ z^* = \frac{Q_3 + Q_4\lambda_h^*}{K_1 + K_2\ \lambda_h^*}, \\ X^* &= \frac{S_1 + S_2\lambda_h^*}{K_1 + K_2\ \lambda_h^*},\ Y^* = \frac{T_1 + T_2\lambda_h^*}{K_1 + K_2\ \lambda_h^*},\ Z^* = \frac{U_1 + U_2\lambda_h^*}{K_1 + K_2\ \lambda_h^*}, \end{aligned} \tag{3.22}$$

where $P,\ Q_1,\ Q_2,\ Q_3,\ Q_4,\ S_1,\ S_2,\ T_1,\ T_2,\ U_1,\ U_2,\ K_1,\ K_2$ are non-negative constants with the combination of model parameters computed using Wolfram Mathematica. The closed-forms of these expressions are provided in Supplementary Material of Gautam et al. (2022). With some algebraic manipulation, we obtain

$$N_{hH}^* = \frac{P + Q_1 + Q_3 + \lambda_h^*(Q_2 + Q_4)}{K_1 + K_2\ \lambda_h^*}, \lambda_v^* = \frac{\beta_v(Q_1 + Q_2\lambda_h^*)}{P + Q_1 + Q_3 + \lambda_h^*(Q_2 + Q_4)},$$

$$\begin{aligned} m^* &= \frac{\phi\beta_v(Q_1 + Q_2\lambda_h^*)}{d_v\left(\beta_v Q_1 + d_v P + Q_1 d_v + Q_3 d_v + (Q_2 d_v + Q_4 d_v + \beta_v Q_2)\lambda_h^*\right)}, \\ l^* &= \frac{\phi - m^* d_v}{d_v}. \end{aligned} \tag{3.23}$$

Then, from the Eq. (3.21) and Eq. (3.23), we obtain

$$a_0\lambda_h^{*3} + a_1\lambda_h^{*2} + a_2\lambda_h^{*} + a_3 = 0, \tag{3.24}$$

where,

$$\begin{aligned}
a_0 &= Q_2Q_4d_v\beta_v + 2Q_2Q_4d_v^2 + Q_2^2d_v\beta_v + Q_2^2d_v^2 + Q_4^2d_v^2 > 0,\\
a_1 &= PQ_2d_v\beta_v + 2PQ_2d_v^2 + 2PQ_4d_v^2 + Q_2Q_3d_v\beta_v + Q_1Q_4d_v\beta_v + 2Q_2Q_3d_v^2\\
&\quad + 2Q_1Q_4d_v^2 + 2Q_1Q_2d_v\beta_v + 2Q_1Q_2d_v^2 + 2Q_3Q_4d_v^2 - K_2Q_2\phi\beta_h\beta_v,\\
a_2 &= P^2d_v^2 + PQ_1d_v\beta_v + 2PQ_1d_v^2 + 2PQ_3d_v^2 + Q_1Q_3d_v\beta_v + 2Q_1Q_3d_v^2 + Q_1^2d_v\beta_v\\
&\quad + Q_1^2d_v^2 + Q_3^2d_v^2 - K_2Q_1\phi\beta_h\beta_v - K_1Q_2\phi\beta_h\beta_v,\\
a_3 &= -K_1Q_1\phi\beta_h\beta_v \leq 0.
\end{aligned}$$

Since the primary focus of our study is to evaluate the impact of imported cases via cross-border mobility on the local malaria transmission and control, we now analyze the existence of equilibria for four important cases stated based on the mobility and outside transmission parameters $\eta,\ \theta$, and k. The cases we consider are: (I) $\eta = 0,\ \theta = 0,\ k \neq 0$ (absence of cross-border mobility); (II) $\eta \neq 0,\ \theta \neq 0,\ k = 0$ (complete protection of transmission abroad); (III) $\eta \neq 0,\ \theta = 0,\ k \neq 0$ (strict border screening and isolation); and (IV) $\eta \neq 0,\ \theta \neq 0,\ k \neq 0$ (presence of cross-border mobility, no protection, and no border screening or isolation). We now perform equilibria analysis for each of these four cases in the following subsections.

3.3.5.1 Case-I: $\eta = 0,\ \theta = 0,\ k \neq 0$

In this case, $Q_1,\ Q_3,\ S_1,\ T_1,\ U_1$ are zero and $P \neq 0,\ K_1 \neq 0,$ implying that one root of Eq. (3.24) is zero, i.e., $\lambda_h^* = 0$. Then, from Eq. (3.22) and Eq. (3.23), we obtain a disease-free equilibrium point, E_0, given by

$$E_0 = \left(\frac{\Lambda}{d_h},\ 0,\ 0,\ \frac{\phi}{d_v},\ 0,\ 0,\ 0,\ 0\right).$$

We now derive the epidemic threshold index, R_0, corresponding to this disease-free equilibrium point (E_0) by using the second-generation matrix method Van den Driessche and Watmough (2002); Diekmann et al. (1990).

From the system (3.11-3.18), the newly infectious matrix F_i and its Jacobian matrix

$\mathbb{F}$ at the disease-free equilibrium point E_0 are

$$F_i = \begin{pmatrix} \dfrac{\beta_h S_{hH} I_{vH}}{N_{hH}} \\ \dfrac{\beta_v S_{vH} I_{hH}}{N_{hH}} \\ kS_{hM} \end{pmatrix}, \ \mathbb{F} = \begin{pmatrix} 0 & \beta_h & 0 \\ \dfrac{\beta_v \ \phi \ d_h}{\Lambda d_v} & 0 & 0 \\ 0 & 0 & 0 \end{pmatrix}.$$

Again, the transfer matrix V_i and its Jacobian matrix $\mathbb{V}$ at the disease-free equilibrium point,

$$V_i = \begin{pmatrix} (\theta + \delta_h + \gamma_h + d_h) I_{hH} - \theta \ I_{hM} \\ d_v i_{vH} \\ (\theta + \gamma_h + \delta_h + d_h) I_{hA} - \theta \ I_{hH} \end{pmatrix}, \ V = \begin{pmatrix} d_h + \delta_h + \gamma_h & 0 & 0 \\ 0 & d_v & 0 \\ 0 & 0 & \gamma_h + \delta_h + d_h \end{pmatrix}.$$

Here the dominant eigenvalue of $\mathbb{F}\mathbb{V}^{-1}$ gives the following epidemic index.

$$R_0 = \sqrt{\frac{\phi d_h \beta_h \beta_v}{(d_h + \gamma_h + \delta_h) \, \Lambda d_v^2}}.$$

The other possible solutions of Eq.(3.24) and complete bifurcation analysis will discuss later in Chapter 4.

3.3.5.2 Case-II: $\eta \neq 0, \ \theta \neq 0, \ k = 0$

In this case, $Q_1, \ Q_3, \ T_1, \ U_1$ are zero, and $P, \ S_1, \ K_1$ are positive, which shows one of λ_h^* to be zero from the Eq. (3.24). Then from the Eq. (3.22) and Eq. (3.23), we obtain another disease-free equilibrium point, E_{01}, given by

$$E_{01} = \left(\frac{\Lambda \, (d_h + \eta)}{d_h \, (d_h + 2\eta)}, \ 0, \ 0, \ \frac{\phi}{d_v}, \ 0, \ \frac{\eta \Lambda}{2\eta d_h + d_h^2}, \ 0, \ 0 \right).$$

We also obtain the epidemic threshold index, R_1, corresponding to this disease-free equilibrium point, E_{01}, as follows.

From the system (3.11-3.18), the newly infectious matrix F_i and its Jacobian matrix $\mathbb{F}$ at the disease-free equilibrium point E_{01} are

$$F_i = \begin{pmatrix} \dfrac{b\alpha_{vh} S_{hH} I_{vH}}{N_{hH}} \\ \dfrac{b\alpha_{hv} S_{vH} I_{hH}}{N_{hH}} \\ kS_{hM} \end{pmatrix}, \ \mathbb{F} = \begin{pmatrix} 0 & \beta_h & 0 \\ \dfrac{\phi d_h \beta_v \, (d_h + 2\eta)}{\Lambda d_v \, (d_h + \eta)} & 0 & 0 \\ 0 & 0 & 0 \end{pmatrix}.$$

Again, the transfer matrix V_i and its Jacobian matrix $\mathbb{V}$ at the disease-free equilibrium point E_{01} are,

$$V_i = \begin{pmatrix} (\theta + \delta_h + \gamma_h + d_h)I_{hH} - \theta\, I_{hM} \\ \\ d_v i_{vH} \\ \\ (\theta + \gamma_h + \delta_h + d_h)I_{hM} - \theta\, I_{hH} \end{pmatrix}$$

,

$$\mathbb{V} = \begin{pmatrix} d_h + \gamma_h + \delta_h + \theta & 0 & -\theta \\ 0 & d_v & 0 \\ -\theta & 0 & d_h + \gamma_h + \delta_h + \theta \end{pmatrix}.$$

Then the dominant eigenvalue of $\mathbb{F}\mathbb{V}^{-1}$ gives the epidemic index R_1:

$$R_1 = R_0 \sqrt{1 + \frac{(\eta\,(d_h + \gamma_h + \delta_h) - \theta d_h)}{(d_h + \eta)\,(d_h + \gamma_h + \delta_h + 2\theta)}}.$$

Note that the migrant workers presumably travel less while they are infected. This implies $\eta - \theta \geq 0$ and hence $R_1 \geq R_0$ in general. In this case also the complete endemic equilibrium and bifurcation analysis will discuss later in Chapter 4.

3.3.5.3 Case-III: $\eta \neq 0,\ \theta = 0,\ k \neq 0$

In this case, Q_1 is 0, and $K_1,\ P,\ Q_3,\ S_1,\ T_1,\ U_1$ are positive. One root of the Eq. (3.24) is zero, giving a disease-free equilibrium point, E_{02}. However, this disease-free equilibrium condition asserts the absence of the disease only within the home country while allowing the disease among migrants abroad. The expression for E_{02} is given by

$$E_{02} = \left(\frac{P}{K_1},\ 0,\ \frac{Q_3}{K_1},\ \frac{\phi}{d_v},\ 0,\ \frac{S_1}{K_1},\ \frac{T_1}{K_1},\ \frac{U_1}{K_1}\right),$$

and the corresponding epidemic threshold index is From the system (3.11-3.18), the newly infectious matrix F_i and its Jacobian matrix $\mathbb{F}$ at the disease-free equilibrium point E_{02} are

$$F_i = \begin{pmatrix} \dfrac{b\alpha_{vh} S_{hH} I_{vH}}{N_{hH}} \\ \\ \dfrac{b\alpha_{hv} S_{vH} I_{hH}}{N_{hH}} \\ \\ kS_{hM} \end{pmatrix}, \mathbb{F} = \begin{pmatrix} 0 & \dfrac{P\beta_h}{P + Q_3} & 0 \\ \dfrac{K_1 \phi \beta_v}{(P + Q_3) d_v} & 0 & 0 \\ 0 & 0 & 0 \end{pmatrix}$$

Again, the transfer matrix V_i and its Jacobian matrix $\mathbb{V}$ at the disease-free equilibrium point E_{02} are

$$V_i = \begin{pmatrix} (\theta + \delta_h + \gamma_h + d_h)I_{hH} - \theta\ I_{hM} \\ \\ d_v I_{vH} \\ \\ (\theta + \gamma_h + \delta_h + d_h)I_{hM} - \theta\ I_{hH} \end{pmatrix},\ \ \mathbb{V} = \begin{pmatrix} d_h + \gamma_h + \delta_h & 0 & 0 \\ 0 & d_v & 0 \\ 0 & 0 & d_h + \gamma_h + \delta_h \end{pmatrix}.$$

Then the dominant eigenvalue of $\mathbb{F}\mathbb{V}^{-1}$ provides the epidemic index R_2.

$$R_2 = \sqrt{\frac{PK_1\phi\beta_h\beta_v}{(P+Q_3)^2 d_v^2\,(d_h + \gamma_h + \delta_h)}}.$$

Note that $\eta = 0$ implies $R_2 = R_0$ as expected.

3.3.5.4 Case-IV: $\eta \neq 0,\ \theta \neq 0,\ k \neq 0$

In this case, $a_3 \neq 0$ implying $\lambda_h^* \neq 0$ (from Eq. (3.24)) and $m^* \neq 0$ (from Eq. (3.21)). This implies that the disease-free equilibrium point does not exist, indicating that malaria eradication is not possible as long as there is a presence of cross-border mobility, absence of protection abroad, and absence of border screening and isolation.

To analyze possible endemic equilibrium points, we represent $\alpha,\ \beta$, and γ to be the three possible roots of the cubic Eq. (3.24). The product of roots, $\alpha\beta\gamma = -\dfrac{a_3}{a_0}$. Since $a_0 > 0$ and $a_3 < 0$, $\alpha\beta\gamma > 0$. This shows that all three roots can not be negative real numbers. Also, Eq. (3.24) can not have one negative real root and two complex roots because otherwise, two complex roots $\alpha = a + ib,\ \beta = a - ib$ and one negative real root γ provides $\alpha\beta\gamma = (a^2 + b^2)\gamma < 0$, which is not possible here (since here the product of roots must be positive due to $a_0 > 0$ and $a_3 < 0$). Thus, the Eq. (3.24) provides at least one positive value of λ_h^*, and hence the system admits at least one endemic equilibrium point.

To identify whether the system has 1, 2, or 3 endemic equilibrium points, we first transform the Eq. (3.24) in terms of the equilibrium infected humans, y^*, to obtain $F_L(y^*) = F_R(y^*)$, where $F_L(y^*) = -M_2 y^* - M_3$ and $F_R(y^*) = M_0(y^*)^3 + M_1(y^*)^2$. The equilibrium values of y^*, i.e., $y_1^*,\ y_2^*,\ y_3^*$, are then given by the intersection of the curves $F_L(y)$ and $F_R(y)$ (Figure 7). As shown in Figure 7, the slope $-M_2$ of the linear function $F_L(y)$, which can be explained in terms of the infection rate β_h, can help determine the existence of 1, 2, or 3 equilibria. An increase in β_h (i.e., a decrease in the slope of $F_L(y)$) makes the equilibrium point y_1^* and y_3^* move to the

right and y_2^* move to the left, eventually giving $y_1^* = y_2^*$ corresponding to two equilibria $y_1^* = y_2^*$ and y_3^* (Figure 7b). Increasing β_h further, y_1^* and y_2^* disappear, and only one equilibrium point y_3^* exists. Since the equilibrium point y_3^* attains the highest value, we can correspond this situation to the worst-case scenario, i.e., a high endemic level. Similarly, decreasing β_h (i.e., increasing the slope of the linear function $F_L(y)$) causes y_1^* and y_3^* to move to the left and y_2^* to move to the right. At some point, y_2^* and y_3^* coincide with each other, giving only two equilibrium points y_1^* and $y_2^* = y_3^*$. If β_h is decreased further, then y_2^* and y_3^* disappear, leaving only y_1^* as an endemic equilibrium point. Since y_1^* corresponds to the smallest equilibrium point, the case in which the only y_1^* exists can be considered as the endemic condition with the minimum burden. Therefore, increasing the slope $-M_2$ (for example, decreasing β_h), making it less than its threshold value (corresponding to $y_2^* = y_3^*$), can be a vital control strategy to maintain the endemic at a low level. In summary, the parameter a_3, which

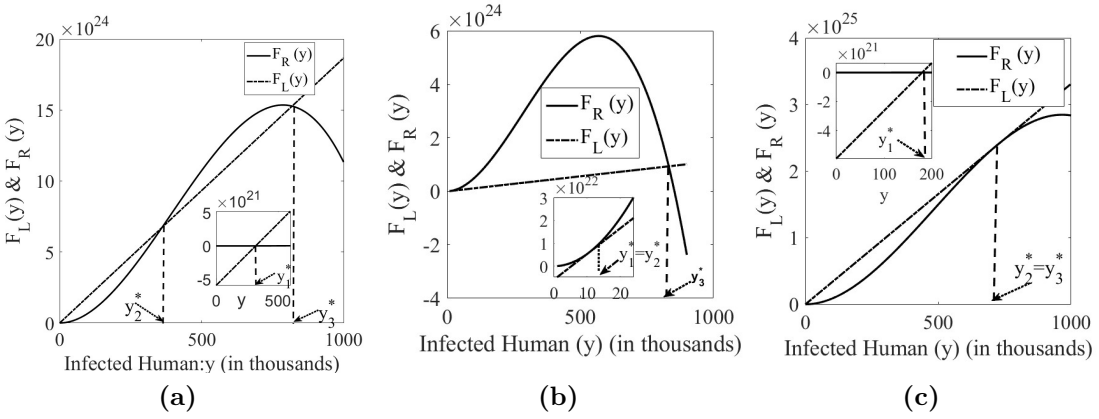

Figure 7: Endemic equilibriums. (a) Graphs of $F_L(y)$ and $F_R(y)$ with possible three intersections corresponding to three endemic equilibrium points. (b) Graphs of $F_L(y)$ and $F_R(y)$ with exactly two endemic equilibrium points $y_1^* = y_2^*$ and y_3^*. Decreasing the slope of $F_L(y)$ further gives only one equilibrium point y_3^* (a high epidemic level). (c) Graphs of $F_L(y)$ and $F_R(y)$ with exactly two endemic equilibrium points y_1^* and $y_2^* = y_3^*$. Increasing the slope of $F_L(y)$ further gives only one equilibrium point y_1^* (a low epidemic level.)

is always non-positive, provides an important threshold for disease-free equilibrium to occur ($a_3 = 0$). As long as $a_3 \neq 0$ (i.e., $a_3 < 0$), there is no DFE, and the system always provides at least one endemic equilibrium. The absence of DFE with at least one endemic equilibrium can be attributable to ongoing infection abroad and the importation of malaria cases through cross-border mobility, making $a_3 \neq 0$. When $a_3 = 0$ (presence of DFE), 1 or 2 endemic equilibrium points exist according to the

sign of other parameters (a_1, a_2), which depend upon the thresholds R_0, R_1, or R_2. Similarly, when $a_3 < 0$ (absence of DFE), 1 to 3 endemic equilibrium points exist according to the sign of other coefficients.

3.3.6 Stability Analysis and Uniform Persistence

In this section, we provide some analytical results related to the stability and uniform persistence of the system, specifically, the local stability of the disease-free equilibrium points and the uniform persistence for Case-I and Case-II. In addition, for Case-III, we provide the local stability of the disease-free equilibrium point that corresponds to the absence of disease within the home country only. We were unable to prove the uniform persistence for Case-III and Case-IV because of the complexity of the model, presumably due to the absence of the overall disease-free equilibrium point in these cases.

3.3.6.1 Case-I: $\eta = 0,\ \theta = 0,\ k \neq 0$

We prove the local stability of the disease-free equilibrium E_0 as stated in the following theorem.

Theorem 3.3.2 *The disease free equilibrium point E_0 of the system of (3.11-3.18) is locally asymptotically stable if $R_0 < 1$, and unstable if $R_0 > 1$.*

Proof: The local stability of E_0 is determined by the following Jacobian matrix of the system (3.11-3.18) evaluated at E_0: $\mathbb{J} = \begin{pmatrix} J_{H,5\times5} & 0_{5\times3} \\ 0_{3\times5} & J_{A,3\times3} \end{pmatrix}$,

where $J_{H,5\times5} = \begin{pmatrix} -d_h & 0 & q & 0 & -\beta_h \\ 0 & -T & 0 & 0 & \beta_h \\ 0 & \gamma_h & -G & 0 & 0 \\ 0 & -\dfrac{\phi d_h \beta_v}{\Lambda} & 0 & -d_v & 0 \\ 0 & \dfrac{\phi d_h \beta_v}{\Lambda} & 0 & 0 & -d_v \end{pmatrix}$, $J_{A,3\times3} = \begin{pmatrix} -H & 0 & q \\ k & -T & 0 \\ 0 & \gamma_h & -G \end{pmatrix}$,

$T = (d_h + \gamma_h + \delta_h)$, $G = (d_h + q)$, and $H = (d_h + k)$. The roots of the characteristic polynomial equation of J_H are

$$\lambda_1 = -d_h,\ \lambda_2 = -d_h + q,\ \lambda_3 = -d_v,$$
$$\lambda_4 = \frac{-\left(d_h + d_v + \gamma_h + \delta_h\right) - \sqrt{\left(d_h + d_v + \gamma_h + \delta_h\right)^2 - 4d_v\left(d_h + \delta_h + \gamma_h\right)\left(1 - R_0^2\right)}}{2},$$
$$\lambda_5 = \frac{-\left(d_h + d_v + \gamma_h + \delta_h\right) + \sqrt{\left(d_h + d_v + \gamma_h + \delta_h\right)^2 - 4d_v\left(d_h + \delta_h + \gamma_h\right)\left(1 - R_0^2\right)}}{2}.$$

The roots, λ, of the characteristic polynomial equation of the matrix J_A are given by

$$\lambda^3 + e_1\lambda^2 + e_2\lambda + e_3 = 0, \text{where}$$
$$e_1 = 3d_h + \gamma_h + \delta_h + k + q,$$
$$e_2 = 2d_h\gamma_h + 2d_h\delta_h + 2kd_h + 2qd_h + 3d_h^2 + k\gamma_h + k\delta_h + q\gamma_h + q\delta_h + kq,$$
$$e_3 = d_h^2\gamma_h + d_h^2\delta_h + kd_h\gamma_h + kd_h\delta_h + kqd_h + kd_h^2 + qd_h\gamma_h + qd_h\delta_h + qd_h^2 + d_h^3 + kq\delta_h.$$
$$e_1e_2 - e_3 = 4d_h\gamma_h\delta_h + 8d_h^2\gamma_h + 2d_h\gamma_h^2 + 8d_h^2\delta_h + 2d_h\delta_h^2 + 2k^2d_h +$$
$$6kd_h\gamma_h + 6kd_h\delta_h + 6kqd_h + 8kd_h^2 + 2q^2d_h + 6qd_h\gamma_h + 6qd_h\delta_h + 8qd_h^2 +$$
$$8d_h^3 + k^2\gamma_h + k^2\delta_h + 2k\gamma_h\delta_h + k\gamma_h^2 + k\delta_h^2 + 3kq\gamma_h + 2kq\delta_h +$$
$$q^2\gamma_h + q^2\delta_h + 2q\gamma_h\delta_h + q\gamma_h^2 + q\delta_h^2 + k^2q + kq^2 > 0.$$

Here, $e_1,\ e_2,\ e_3,\ e_1e_2 - e_3$ are positive. Using Routh Hurwitz criteria, all the eigenvalues of J_A have negative real part. Therefore, all the eigenvalues of J_H are negative when $R_0 < 1$. Thus the disease-free equilibrium point E_0 is locally asymptotically stable if $R_0 < 1$, and unstable if $R_0 > 1$. □

From the eigenvalues of the Jacobian matrix J at E_0, we have the following lemma.

Lemma 3.3.1 *For the Jacobian matrix J, the following statements hold:*

1. $R_0 = 1$ *if and only if* $S(J) = 0$,
2. $R_0 > 1$ *if and only if* $S(J) > 0$,
3. $R_0 < 1$ *if and only if* $S(J) < 0$,

where $S(J) := max\{Re(\lambda) : \lambda$ *is eigenvalue of the jacobian of system at DFE* $E_0\}$.

Here we apply the Krasovkii-LaSalle Theorem Martcheva (2015) to establish the condition for the global stability of the disease-free equilibrium in the home country.

Theorem 3.3.3 *(**Global stability of** E_0) For $\eta = 0,\ \theta = 0$, the disease-free equilibrium E^0 of the system (3.11-3.15) is globally asymptotically stable when $R_0^2 + \dfrac{\delta_h \phi \beta_h \beta_v}{\Lambda(d_h + \delta_h + \gamma_h)d_v^2} < 1$.*

Proof: Let $p = (S_{hH}(t), I_{hH}(t), R_{hH}(t), S_{vH}(t), I_{vH}(t))$, be any solution of the system (3.11-3.15), then $N_{vH}(t) \leq \dfrac{\phi}{d_v}$ and $N'_{hH} = \Lambda - d_h N_{hH} - \delta_h I_{hH} \geq \Lambda - (d_h + \delta_h)N_{hH}$. Then, $N_{hH}(t) \geq \dfrac{\Lambda}{d_h + \delta_h}$.

We construct a Lyapunov function, $V\left(I_{hH}, I_{vH}\right) = \dfrac{d_v}{\beta_h} I_{hH} + I_{vH}$.

Then, taking derivative with respect to t, we obtain

$$\begin{aligned}
V' &= \frac{d_v}{\beta_h} I'_{hH} + I'_{vH} \\
&= \frac{d_v I_{vH} S_{hH}}{N_{hH}} - \frac{d_v}{\beta_h}(d_h + \delta_h + \gamma_h) I_{hH} + \frac{\beta_v I_{hH} S_{vH}}{N_{hH}} - d_v I_{vH} \\
&= \left[\frac{\beta_v S_{vH}}{N_{hH}} - \frac{d_v}{\beta_h}(d_h + \delta_h + \gamma_h)\right] I_{hH} - \left[-\frac{d_v S_{hH}}{N_{hH}} + d_v\right] I_{vH} \\
&\leq \left[\frac{\beta_v \dfrac{\phi}{d_v}}{\dfrac{\Lambda}{d_h + \delta_h}} - \frac{d_v}{\beta_h}(d_h + \delta_h + \gamma_h)\right] I_{hH} \text{ (Since } S_{hH}(t) \leq N_{hH}(t)) \\
&= \left[R_0^2 + \frac{\delta_h \phi \beta_h \beta_v}{\Lambda(d_h + \delta_h + \gamma_h)d_v^2} - 1\right] I_{hH}.
\end{aligned}$$

This gives $V' \leq \left[\left(R_0^2 + \dfrac{\delta_h \phi \beta_h \beta_v}{\Lambda(d_h + \delta_h + \gamma_h)d_v^2} - 1\right)\right] I_{hH}$. Therefore, $V' \leq 0$ for all $p \geq 0$ when $R_0^2 + \dfrac{\delta_h \phi \beta_h \beta_v}{\Lambda(d_h + \delta_h + \gamma_h)d_v^2} < 1$.

Let $B = \{p : V' = 0\}$, then $B \subset \{p : I_{hH} = 0\}$. If $C \subset B$ is the largest invariant set of the system (3.11-3.15) and p is any solution of the system in C, then for all $t \in R$, p is defined and bounded. Again $C \subseteq \{p : I_{hH} = 0\}$, thus $I_{hH}(t) \equiv 0$. Moreover, from Eq. (3.13), $R_{hH} \equiv 0$. Also, from Eq. (3.15), $I_{vH} \equiv 0$ and finally, Eq. (3.11) gives $S_{hH} \equiv \dfrac{\Lambda}{d_h}$ and Eq. (3.14) gives $S_{vH} \equiv \dfrac{\phi}{d_v}$. Therefore, $p = (\dfrac{\Lambda}{d_h}, 0, 0, \dfrac{\phi}{d_v}, 0)$ and $C \equiv \{E^0\}$. Applying the Krasovkii-LaSalle theorem Martcheva (2015), the disease-free equilibrium E^0 is globally asymptotically stable and the disease eventually becomes extinct when $R_0^2 + \dfrac{\delta_h \phi \beta_h \beta_v}{\Lambda(d_h + \delta_h + \gamma_h)d_v^2} < 1$. □

We now establish that $R_0 > 1$ can also provide a condition for the uniform persistence of the disease in the home country in the absence of cross-border mobility. Here, we use

the following notations and definitions. It can be proved that the disease persists when $R_0 > 1$ Gautam et al. (2022). We summarize the result showing uniform persistence in Theorem 3.3.4.

Theorem 3.3.4 *(**Uniform persistence**) For $\eta = 0$, $\theta = 0$, the decoupled system (3.11-3.15) is uniformly persistent with respect to $(\Omega_o, \partial\Omega_o)$ for $R_0 > 1$ in the sense that there is a positive constant $\sigma > 0$ such that every solution*

$$(S_{hH}, I_{hH}, R_{hH}, S_{vH}, I_{vH})$$

of (3.11-3.15) with $(S_{hH}(0), I_{hH}(0), R_{hH}(0), S_{vH}(0), I_{vH}(0)) \in \Omega_o$ satisfies

$$\liminf I_{hH} \geq \sigma, \ \liminf I_{vH} \geq \sigma, \tag{3.25}$$

where,

$$\begin{aligned}
&\Omega_o = \{(S_{hH}, I_{hH}, R_{hH}, S_{vH}, I_{vH}) \in \Re^5_+ : I_{hH} > 0 \quad or \quad I_{vH} > 0\},\\
&\partial\Omega_o = \{(S_{hH}, I_{hH}, R_{hH}, S_{vH}, I_{vH}) \in \Re^5_+ : I_{hH} = 0 \quad and \quad I_{vH} = 0\},\\
&\Omega = \Omega_o \cup \partial\Omega_o = \Re^5_+.
\end{aligned}$$

In the absence of cross-border mobility, it is enough to consider only the decoupled system (3.11-3.15). We assume that $\tau(t)P$ is the solution maps generated by the decoupled system (3.11-3.15) with initial value P. We denote $M_\partial = \{P \in \partial\Omega_o : \tau(t)P \in \partial\Omega_o\}$, and $\omega(P) = \{y : \tau(t)P \to y \text{ as } t \to \infty\}$. We first state and prove the following three lemmas.

Lemma 3.3.2 *The sets Ω_o and $\partial\Omega_o$ are positively invariant under the flow induced by the decoupled system (3.11-3.15) of the home country.*

Proof: For any $(S_{hH}(0), I_{hH}(0), R_{hH}(0), S_{vH}(0), I_{vH}(0)) \in \Omega_o$, we have from the first and fourth equations of the system,

$$\begin{aligned}
S_{hH}(t) &= e^{-\int_0^t B(s_1)ds_1}\left[\int_0^t e^{\int_0^{s_2} B(s_1)ds_1} A(s_2)ds_2 + S_{hH}(0)\right],\\
S_{vH}(t) &= e^{-\int_0^t F(s_1)ds_1}\left[\int_0^t e^{\int_0^{s_2} F(s_1)ds_1} \phi\, ds_2 + S_{vH}(0)\right],
\end{aligned}$$

where, $A(t) := \Lambda + qR_{hH} > 0$, $B(t) := \frac{\beta_h I_{vH}}{N_{hH}} + d_h$, and $F(t) := \frac{\beta_v I_{hH}}{N_{hH}} + d_v$. The Jacobian matrix J_0 corresponding to the second and fifth equations of the system is

$$J_0 = \begin{pmatrix} \frac{-\beta_h I_{vH} S_{hH}}{N_{hH}^2} - (\delta_h + d_h + \gamma_h) & \frac{\beta_h S_{hH}}{N_{hH}} \\ \frac{\beta_v S_{vH}}{N_{hH}} \left(1 - \frac{I_{hH}}{N_{hH}}\right) & -d_v \end{pmatrix}.$$

Since J_0 is an irreducible matrix with non negative off diagonal elements then $S(J_0)$ is simple with an associated strongly positive eigenvector Smith and Waltman (1995). Hence the vector $(I_{hH}(t), I_{vH}(t))$ is positive for all $t > 0$. Again from the third equation of the system,

$$R_{hH}(t) = e^{-\int_0^t D(s_1)ds_1} \left[\int_0^t e^{\int_0^{s_2} D(s_1)ds_1} C(s_2)ds_2 + R_{hH}(0) \right]$$

where $C(t) = \gamma_h I_{hH} > 0$ and $D(t) = d_h + q$. $S_{hH}(t), R_{hH}(t), S_{vH}(t) > 0, \forall t > 0$. Hence the sets Ω_o is positively invariant. Since Ω is positively invariant and $\partial\Omega_o$ is relatively closed in Ω_o, it gives $\partial\Omega_o$ is also positively invariant. Thus both Ω_o and $\partial\Omega_o$ are positively invariant under the flow induced by the decoupled system (3.11-3.15). □

Lemma 3.3.3 *Every forward orbit of $\tau(t)$ in $M\partial$ converge to E_0, i.e, E_0 is the fixed point of $\tau(t)$ and acyclic in $M\partial$.*

Proof: Since $P \in M_\partial$, $\tau(t)P \in M_\partial$ for all $t \geq 0$. From the definition of M_∂, $I_{vH}(t) = 0$, $\forall t \geq 0$. Using $I_{vH}(t) = 0$ in Eq. (3.15), it follows that $I_{hH}(t) = 0$ for all $t \geq 0$. Then from the first, third, and fourth equation of the system (3.11-3.15),

$$\frac{dS_{hH}}{dt} + d_h S_{hH} = \Lambda, \ \frac{dR_{hH}}{dt} + (d_h + q)R_{hH} = 0, \ \frac{dS_{vH}}{dt} + d_v S_{vH} = \phi.$$

Solving the first order linear ordinary differential equations, we have $\lim_{t\to\infty} S_{hH}(t) = \frac{\Lambda}{d_h}$, $\lim_{t\to\infty} R_{hH}(t) = 0$, $\lim_{t\to\infty} S_{vH}(t) = \frac{\phi}{d_v}$. It follows that any forward orbit of $\tau(t)$ in M_∂ converges to E_0. □

Lemma 3.3.4 *If $R_0 > 1$, then there exists $\rho > 0$ such that*

$$\lim_{t\to\infty} \ Sup \ \|\tau(t)P - E_0\| \geq \rho, \ \ \forall P \in \Omega_o.$$

i.e., E_0 is uniform weak repeller with $\tau(t)$.

Proof: Suppose, if possible, there exists $P_o \in \Omega_o$, such that $\lim_{t\to\infty}$ Sup $\|\tau(t)P_o - E_0\| < \rho$. Since $\lim_{t\to\infty} N_{hH}(t) \leq \frac{\Lambda}{d_h}$ and $\lim_{t\to\infty} S_{vH}(t) = \frac{\phi}{d_v}$ then there exists $t_2 > 0, \forall t \geq t_2$ and a

sufficiently small positive number ρ_o such that $N_{hH}(t) \leq \frac{\Lambda}{d_h} + \rho_o$ and $S_{hH}(t) \geq \frac{\Lambda}{d_h} - \rho_o$ and $S_{vH}(t) \geq \frac{\phi}{d_v} - \rho_o$. Here, t_2 is essentially a time after which the system stabilizes close to its long-term behavior, within a small margin ρ_0. Before t_2, the system may still be transitioning, but after t_2, the variables $N_{hH}(t)$, $S_{hH}(t)$ and $S_{vH}(t)$ are sufficiently close to their limiting values.

Using these inequalities in the Eq. (3.12) and in Eq. (3.15), we obtain

$$\begin{aligned} I'_{hH} &\geq \beta_h \left(1 - \frac{2\rho_0}{\frac{\Lambda}{d_h} + \rho_0}\right) I_{vH} - (d_h + \delta_h + \gamma_h) I_{hH}, \\ I'_{vH} &\geq \frac{\beta_v \left(\frac{\phi}{d_v} - \rho_o\right)}{\left(\frac{\Lambda}{d_h} + \rho_o\right)} I_{hH} - d_v I_{vH}. \end{aligned}$$

We consider the corresponding auxiliary equations

$$\begin{aligned} I'_{hH} &= \beta_h \left(1 - \frac{2\rho_0}{\frac{\Lambda}{d_h} + \rho_0}\right) I_{vH} - (d_h + \delta_h + \gamma_h) I_{hH}, \\ I'_{vH} &= \frac{\beta_v \left(\frac{\phi}{d_v} - \rho_o\right)}{\left(\frac{\Lambda}{d_h} + \rho_o\right)} I_{hH} - d_v I_{vH}, \forall t \geq t_2. \end{aligned} \tag{3.26}$$

Let J_{ρ_o} be the Jacobian of the system (3.26), then

$$J_{\rho_o} = \begin{pmatrix} -(\delta_h + d_h + \gamma_h) & \beta_h \left(1 - \frac{2\rho_0}{\frac{\Lambda}{d_h} + \rho_0}\right) \\ \frac{\beta_v \left(\frac{\phi}{d_v} - \rho_o\right)}{\left(\frac{\Lambda}{d_h} + \rho_o\right)} & -d_v \end{pmatrix}$$

Since $S(J) > 0$, there exists a sufficiently small $\rho_o > 0$ such that $S(J_{\rho_o}) > 0$. Since J_{ρ_o} is irreducible and has non-negative off-diagonal elements, it follows that $S(J_{\rho_o})$ is a simple and associates with strongly positive eigenvector $\tilde{v} \in \mathbb{R}^2_+$, i.e $(I_{hH}(t), I_{vH}(t)) >> 0 \ \ \forall t \geq t_2$. Then there is a positive number a such that $(I_{hH}(t), I_{vH}(t)) \geq a\tilde{v}$ and hence the solution of the Eq. (3.26) is

$$V(t) := ae^{S(J_{\rho_o})(t-t_2)}\tilde{v} \ \ , \forall\, t \geq t_2$$

with $V(t_2) := a\tilde{v}$. Hence it follows from (Smith and Waltman, 1995, Theorem B.1) that

$$(I_{hH}(t), I_{vH}(t)) \geq ae^{S(J_{\rho_o})(t-t_2)}\tilde{v}, \ \ \forall t \geq t_2.$$

Since $S(J_{\rho_o}) > 0$, then the solution $\lim_{t\to\infty} I_{hH}(t) \to \infty$, $\lim_{t\to\infty} I_{vH}(t) \to \infty$ which is a contradiction, and hence $\lim_{t\to\infty}$ Sup $\|\tau(t)P - E_0\| \geq \rho$, $\forall P \in \Omega_o$. □

We are now ready to state the following theorem, which establishes the condition for malaria persistence in Nepal when cross-border mobility is absent. Now we establish the Theorem 3.3.4.

Proof: Assume that $R_0 > 1$, then it follows from Lemma 3.3.1 that $S(J) > 0$. Let $\tau(t)P$ is the solution maps generated by the decoupled system (3.11-3.15) with initial value $P \in \Omega_o$. Clearly, the system $\{\tau(t)\}_{t\geq 0}$ admits the global attractor in $\Re^5_+$. From the Lemma 3.3.3, E_0 is a fixed point of $\tau(t)$ and acyclic in $M\partial$, every solution in $M\partial$ approaches E_0. Moreover, Lemma 3.3.4 implies that E_0 is an isolated invariant set in Ω and $W^s(E_0) \cap \Omega_o = \phi$. By the acyclicity theorem of uniform persistence for maps Zhao (2001), it follows that $\tau(t)$ is uniformly persistent with respect to $(\Omega_o, \partial\Omega_0)$. Hence there exists $\sigma > 0$ such that $\lim_{t\to\infty}$ Inf $I_{hH} \geq \sigma$, $\lim_{t\to\infty}$ Inf $I_{vH} \geq \sigma$. This completes the proof. □

3.3.6.2 Case-II: $\eta \neq 0,\ \theta \neq 0,\ k = 0$ (Complete Protection of Transmission Abroad)

The local stability of the disease-free equilibrium E_{01}, corresponding to the case when complete protection of transmission is in force outside Nepal, is given by the following theorem.

Theorem 3.3.5 *The disease free equilibrium point E_{01} of the system (3.11-3.18) is locally asymptotically stable if $R_1 < 1$, and unstable if $R_1 > 1$.*

Proof: The Jacobian matrix of the system (3.11-3.18) at E_{01} is $\mathbb{J}_1 = \begin{pmatrix} A^1_{4\times4} & B^1_{4\times4} \\ C^1_{4\times4} & D^1_{4\times4} \end{pmatrix}$, where

$$A^1_{4\times4} = \begin{pmatrix} -D & 0 & q & \eta \\ 0 & -A & 0 & 0 \\ 0 & \gamma_h & -B & 0 \\ \eta & 0 & 0 & -d_h \end{pmatrix},\ B^1_{4\times4} = \begin{pmatrix} 0 & 0 & 0 & -\beta_h \\ \theta & 0 & 0 & \beta_h \\ 0 & \eta & 0 & 0 \\ 0 & q & 0 & 0 \end{pmatrix},$$

$$C^1_{4\times4} = \begin{pmatrix} 0 & \theta & 0 & 0 \\ 0 & 0 & \eta & 0 \\ 0 & -C & 0 & 0 \\ 0 & C & 0 & 0 \end{pmatrix},\ D^1_{4\times4} = \begin{pmatrix} -A & 0 & 0 & 0 \\ \gamma_h & -B & 0 & 0 \\ 0 & 0 & -d_v & 0 \\ 0 & 0 & 0 & -d_v \end{pmatrix},$$

$A = (d_h + \gamma_h + \delta_h + \theta),\ B = (d_h + \eta + q),\ C = \dfrac{\phi d_h \beta_v (d_h + 2\eta)}{\Lambda d_v (d_h + \eta)}$, and $D = (d_h + \eta)$. Let λ be eigenvalues of the matrix J_1, then the characteristic polynomial is

$$P(\lambda) = (d_h + \lambda)(d_v + \lambda)(d_h + 2\eta + \lambda)(d_h + \lambda + q)(d_h + 2\eta + \lambda + q)\, Q(\lambda),$$

where $Q(\lambda) = \lambda^3 + h_1\lambda^2 + h_2\lambda + h_3$,

$$\begin{aligned}
h_1 &= 2d_h + d_v + 2(\gamma_h + \delta_h + \theta), \\
h_2 &= \frac{(2 - R_1^2)(d_v (d_h + \gamma_h + \delta_h)(d_h + \gamma_h + \delta_h + 2\theta))}{d_h + \gamma_h + \delta_h + \theta} + P_1, \\
h_3 &= \left(1 - R_1^2\right) d_v (d_h + \gamma_h + \delta_h)(d_h + \gamma_h + \delta_h + 2\theta), \\
P_1 &= \frac{(\gamma_h + \delta_h)(2\theta^2 + \gamma_h(2\delta_h + 3\theta) + \gamma_h^2 + 3\theta\delta_h + \delta_h^2)}{d_h + \gamma_h + \delta_h + \theta} + \\
&\frac{d_h(2\theta^2 + 6\gamma_h(\delta_h + \theta) + 3\gamma_h^2 + 6\theta\delta_h + 3\delta_h^2) + 3d_h^2(\gamma_h + \delta_h + \theta) + d_h^3 + 2\theta^2 d_v}{d_h + \gamma_h + \delta_h + \theta}.
\end{aligned}$$

This implies that $\lambda = -d_h,\ -d_v,\ (-d_h + 2\eta),\ -(d_h + q),\ -(d_h + 2\eta + q)$ are five eigenvalues. The coefficients h_1 is positive and both $h_2 > 0,\ h_3 > 0$ if $R_1 < 1$. Also,

$$\begin{aligned}
h_1 h_2 - h_3 = &(2(d_h + \gamma_h + \delta_h + \theta) + d_v) \\
&\left(\frac{(2 - R_1^2) d_v (d_h + \gamma_h + \delta_h)(d_h + \gamma_h + \delta_h + 2\theta)}{d_h + \gamma_h + \delta_h + \theta} + P_1\right) \\
&- \left(1 - R_1^2\right) d_v (d_h + \gamma_h + \delta_h)(d_h + \gamma_h + \delta_h + 2\theta) \\
= &\left(3 - R_1^2\right) d_v (d_h + \gamma_h + \delta_h)(d_h + \gamma_h + \delta_h + 2\theta) + \\
&2P_1(d_h + \gamma_h + \delta_h + \theta) + P_2 > 0, \text{if } R_1 < 1.
\end{aligned}$$

where $P_2 = d_v \left(\dfrac{(2 - R_1^2) d_v (d_h + \gamma_h + \delta_h)(d_h + \gamma_h + \delta_h + 2\theta)}{d_h + \gamma_h + \delta_h + \theta} + P_1\right)$. Thus all the eigenvalues have negative real parts and hence E_{01} is locally asymptotically stable if $R_1 < 1$. If $R_1 > 1$, then h_0 and h_3 have opposite signs, which implies at least one λ to be positive. Hence, the disease-free equilibrium point E_{01} is unstable if $R_1 > 1$. □

We also have the following lemma.

Lemma 3.3.5 *For the Jacobian matrix $\mathbb{J}_1$, the following statements hold:*

1. $R_1 = 1$ *if and only if* $S(\mathbb{J}_1) = 0$,
2. $R_1 > 1$ *if and only if* $S(\mathbb{J}_1) > 0$,
3. $R_1 < 1$ *if and only if* $S(\mathbb{J}_1) < 0$.

We apply the Krasovkii-LaSalle Theorem Martcheva (2015) to establish the condition for the global stability of the disease-free equilibrium E^{01}.

Theorem 3.3.6 *(**Global stability of** E^{01}) Assume that $\eta \neq 0, \theta \neq 0$ and $k = 0$, then the disease-free equilibrium E^{01} of the system (3.11-3.18) is globally asymptotically stable when $R_1^2 + M < 1$,where*
$M = \dfrac{\beta_v \beta_h \delta_h (d_h + 2\eta)(d_h + \gamma_h + \delta_h + \theta)\phi}{d_v^2 \Lambda (d_h + \eta)(d_h + \gamma_h + \delta_h)(d_h + \gamma_h + \delta_h + 2\theta)} + \dfrac{\theta}{(d_h + \gamma_h + \delta_h + 2\theta)}.$

Proof: Let $s = (S_{hH}(t), I_{hH}(t), R_{hH}(t), S_{vH}(t), I_{vH}(t), S_{hM}(t), I_{hM}(t), R_{hM}(t))$ be any solution of the system (3.11-3.18), then $N_{vH}(t) \leq \dfrac{\phi}{d_v}$. Again, $N_{hH} = S_{hH} + I_{hH} + R_{hH}$, and $N_{hM} = S_{hM} + I_{hM} + R_{hM}$, then $N'_{hH} + N'_{hM} = \Lambda - d_h(N_{hH} + N_{hM}) - \delta_h(I_{hH} + I_{hM}) \geq \Lambda - (d_h + \delta_h)(N_{hH} + N_{hM})$. It follows that $N_{hH} + N_{hM} \geq \dfrac{\Lambda}{d_h + \delta_h}$. Since the solutions $N_{hH}(t)$ and $N_{hM}(t)$ are general and should satisfy the disease-free equilibrium as well, we get $N_{hH}(t) \geq \left(\dfrac{\Lambda(\eta + d_h)}{(d_h + \delta_h)(d_h + 2\eta)}\right)$. Here, we construct a Lyapunov function $V_1(I_{hH}, I_{vH}, I_{hM}) = \dfrac{d_v}{\beta_h} I_{hH} + I_{vH} + \dfrac{d_v}{\beta_h} I_{hM}$. Now, taking the derivative of V_1 with respect to t,

$$
\begin{aligned}
V_1' &= \frac{d_v}{\beta_h} I'_{hH} + I'_{vH} + \frac{d_v}{\beta_h} I'_{hM} \\
&= \frac{d_v I_{vH} S_{hH}}{N_{hH}} + \frac{d_v}{\beta_h}\theta I_{hM} - \frac{d_v}{\beta_h}(\theta + d_h + \delta_h + \gamma_h) I_{hH} + \\
&\frac{\beta_v I_{hH} S_{vH}}{N_{hH}} - d_v I_{vH} + z\theta I_{hM} - \frac{d_v}{\beta_h}(\theta + d_h + \delta_h + \gamma_h) I_{hM} \\
&= \left[\frac{d_v}{\beta_h}\theta + \frac{\beta_v S_{vH}}{N_{hH}} - \frac{d_v}{\beta_h}(\theta + d_h + \delta_h + \gamma_h)\right] I_{hH} - \left[-\frac{d_v S_{hH}}{N_{hH}} + d_v\right] I_{vH} + \\
&\left[\frac{d_v}{\beta_h}\theta - \frac{d_v}{\beta_h}(\theta + d_h + \delta_h + \gamma_h)\right] I_{hM} \\
&\leq \left[\frac{\dfrac{\phi}{d_v}\beta_h \beta_v}{\left(\dfrac{\Lambda(\eta + d_h)}{(d_h + \delta_h)(d_h + 2\eta)}\right) d_v (d_h + \delta_h + \gamma_h)} - 1\right] I_{hH} \\
&= \left[\frac{\beta_v \beta_h (d_h + \delta_h)(d_h + 2\eta)\phi}{d_v^2 \Lambda (d_h + \eta)(d_h + \gamma_h + \delta_h)} - 1\right] I_{hH},
\end{aligned}
$$

After some algebraic manipulations, we get $V_1' < 0$ when $R_1^2 + M < 1$. Therefore, V_1 is a Lyapunov function when $R_1^2 + M < 1$. Let $s = (S_{hH}, I_{hH}, R_{hH}, I_{vH}, S_{hM}, I_{hM}, R_{hM})$ be any solution of the system (3.11-3.18) and $D = \{s : V_1' = 0\}$, then $D \subset \{s : I_{hH} = 0\}$.

If $F \subset D$ is the largest invariant set of the system (3.11-3.18) and s is any solution of the system (3.11-3.18) in F, then for all $t \in R$, s is defined and bounded. Again $F \subseteq \{s : I_{hH} = 0\}$, thus $I_{hH} \equiv 0$. Then from Eq. (3.17), $I_{hM} \equiv 0$. Also, from Eq. (3.15) $I_{vH} \equiv 0$ and from Eq. (3.14) $S_{vH} \equiv \frac{\phi}{d_v}$. Now, the system (3.11-3.18) for the rest four compartments reduce to

$$R'_{hH} = \eta R_{hM} - (\eta + d_h + q)R_{hH}, R'_{hM} = \eta R_{hH} - (\eta + d_h + q)R_{hM}, \tag{3.27}$$

$$S'_{hH} = \Lambda + \eta S_{hM} + qR_{hH} - (\eta + d_h)S_{hH}, S'_{hM} = \eta S_{hH} + qR_{hM} - (\eta + d_h)S_{hM}. \tag{3.28}$$

From Eq.(3.27), we get $(R_{hH} + R_{hM})' = -(d_h + q)(R_{hH} + R_{hM})$. It follows that $R_{hH} \equiv 0$ and $R_{hM} \equiv 0$. Again, from Eq. (3.28), we get $(S_{hH} + S_{hM})' = \Lambda - d_h(S_{hH} + S_{hM})$. It follows that $S_{hH} + S_{hM} \equiv \frac{\Lambda}{d_h}$. Now, substituting $S_{hM} = \frac{\Lambda}{d_h} - S_{hH}$ in Eq.(3.11), we get $S_{hH} \equiv \frac{\Lambda(d_h + \eta)}{d_h(d_h + 2\eta)}$ and then $S_{hM} \equiv \frac{\eta\Lambda}{2\eta d_h + d_h^2}$. Thus, $s = \left(\frac{\Lambda(d_h + \eta)}{d_h(d_h + 2\eta)}, 0, 0, \frac{\phi}{d_v}, \frac{\eta\Lambda}{2\eta d_h + d_h^2}, 0, 0\right)$ and $F \equiv \{E^{01}\}$. Then, applying Krasovkii- LaSalle Theorem Martcheva (2015), the disease-free equilibrium E^{01} is globally asymptotically stable when $R_1^2 + M < 1$. □

We also prove that $R_1 > 1$ provides the condition for uniform persistence of the disease with dynamics given by the system (3.11-3.18) with $\eta \neq 0,\ \theta \neq 0,\ k = 0$.

Theorem 3.3.7 *(**Uniform persistence**) If $R_1 > 1$, then the system (3.11-3.18) is uniformly persistent with respect to $(\Omega_o, \partial\Omega_o)$ in the sense that there is a positive constant $\sigma > 0$ such that every solution*

$$(S_{hH}, I_{hH}, R_{hH}, S_{vH}, I_{vH}, S_{hM}, I_{hM}, R_{hM})$$

with $(S_{hH}(0), I_{hH}(0), R_{hH}(0), S_{vH}(0), I_{vH}(0), S_{hM}(0), I_{hM}(0), R_{hM}(0)) \in \Omega_o$ satisfies $\liminf I_{hH} \geq \sigma,\ \liminf I_{vH} \geq \sigma,\ \liminf I_{hM} \geq \sigma$, *where*

$$\Omega_o = \{(S_{hH}, I_{hH}, R_{hH}, S_{vH}, I_{vH}, S_{hM}, I_{hM}, R_{hM}) \in \Re_+^8 : I_{hH} > 0 \text{ or } I_{vH} > 0 \text{ or } I_{hM} > 0\},$$
$$\partial\Omega_o = \{(S_{hH}, I_{hH}, R_{hH}, S_{vH}, I_{vH}, S_{hM}, I_{hM}, R_{hM}) \in \Re_+^8 : I_{hH} = 0,\ \ I_{vH} = 0,\ I_{hM} = 0\}.$$

To prove uniform persistence of $\{\tau(t)\}_{t\geq 0}$ with respect to $(\Omega_o, \partial\Omega_o)$, we need the following three lemmas.

Lemma 3.3.6 *The sets Ω_o and $\partial\Omega_o$ are positively invariant under the flow induced by the system (3.11-3.18).*

Proof: For any $(S_{hH}(0), I_{hH}(0), R_{hH}(0), S_{vH}(0), I_{vH}(0), S_{hM}(0), I_{hM}(0), R_{hM}(0)) \in \Omega_o$, we have from the first and fourth equations of the system (3.11-3.18)

$$S_{hH}(t) = e^{-\int_0^t B(s_1)ds_1}\left[\int_0^t e^{\int_0^{s_2} B(s_1)ds_1} A(s_2)ds_2 + S_{hH}(0)\right],$$
$$S_{vH}(t) = e^{-\int_0^t F(s_1)ds_1}\left[\int_0^t e^{\int_0^{s_2} F(s_1)ds_1} \phi\, ds_2 + S_{vH}(0)\right],$$

where $A(t) := \Lambda + \eta S_{hM} + qR_{hH} > 0$, $B(t) := \frac{\beta_h I_{vH}}{N_{hH}} + \eta + d_h$, and $F(t) := \frac{\beta_v I_{hH}}{N_{hH}} + d_v$. Again, the Jacobian J_0 corresponding to the second, seventh, and fourth equations of the system is

$$J_0 = \begin{pmatrix} \frac{-\beta_h I_{vH} S_{hH}}{N_{hH}^2} - (\theta + \delta_h + d_h + \gamma_h) & \theta & \frac{\beta_h S_{hH}}{N_{hH}} \\ \theta & -(\theta + \delta_h + d_h + \gamma_h) & 0 \\ \frac{\beta_v S_{vH}}{N_{hH}}\left(1 - \frac{I_{hH}}{N_{hH}}\right) & 0 & -d_v \end{pmatrix}.$$

Since J_0 is an irreducible matrix with non-negative off-diagonal elements then $S(J_0)$ is simple with an associated strongly positive eigenvector Smith and Waltman (1995). Hence the vector $(I_{hH}(t), I_{hM}(t), I_{vH}(t))$ is positive $\forall t > 0$. From the third, sixth, and eighth equations of the system (3.11-3.18), we get

$$R_{hH}(t) = e^{-\int_0^t D(s_1)ds_1}\left[\int_0^t e^{\int_0^{s_2} D(s_1)ds_1} C(s_2)ds_2 + R_{hH}(0)\right],$$
$$S_{hM}(t) = e^{-\int_0^t H(s_1)ds_1}\left[\int_0^t e^{\int_0^{s_2} H(s_1)ds_1} G(s_2)ds_2 + S_{hM}(0)\right],$$
$$R_{hM}(t) = e^{-\int_0^t D(s_1)ds_1}\left[\int_0^t e^{\int_0^{s_2} D(s_1)ds_1} L(s_2)ds_2 + R_{hM}(0)\right],$$

where $C(t) := \gamma_h I_{hH} + \eta R_{hM} > 0$, $D(t) := \eta + d_h + q$, $G(t) := \eta S_{hH} + qR_{hM} > 0$, and $H(t) := \eta + d_h + k$, and $L(t) := \gamma_h I_{hM} + \eta R_{hH} > 0$.
This shows $S_{hH}(t), R_{hH}(t), S_{vH}(t), S_{hM}(t), R_{hM}(t) > 0, \forall t$. Hence the set Ω_o is positively invariant. Since Ω is positively invariant and $\partial\Omega_o$ is relatively closed in Ω_o, it gives $\partial\Omega_o$ is also positively invariant. Thus both Ω_o and $\partial\Omega_o$ are positively invariant under the flow induced by the system (3.11-3.18). □

Lemma 3.3.7 *Every forward orbit of $\tau(t)$ in $M\partial$ converge to E_{01}.*

Proof: Since $P \in M_\partial$ then $\tau(t)P \in M_\partial$ for all $t \geq 0$ then $I_{vH}(t) = 0$ for all $t \geq 0$. Substituting $I_{vH}(t) = 0$ in Eq. (3.15), it follows that $I_{hH}(t) = 0$ for all $t \geq 0$. Again

from the Eq. (3.12), it follows that $I_{hM}(t) = 0$ for all $t \geq 0$. Now from the Eq. (3.13) and Eq. (3.18),

$$\frac{dz}{dt} = \eta Z - (d_h + \eta + q)\, z, \qquad \frac{dZ}{dt} = \eta z - (d_h + \eta + q)\, Z. \tag{3.29}$$

Here, Eq. (3.29) is a system of ordinary linear homogeneous differential equations with constant coefficients, which implies both $z(t), Z(t)$ tend to zero as t approaches to ∞. Also, from Eq. (3.11) and Eq. (3.16), it follows the system of linear non-homogeneous ordinary differential equations with constant coefficients

$$\frac{dx}{dt} = \Lambda + \eta X - (d_h + \eta)\, x, \qquad \frac{dX}{dt} = \eta x - (d_h + \eta)\, X. \tag{3.30}$$

implies that $x(t),\ X(t)$ converge to $\dfrac{\Lambda\,(d_h + \eta)}{d_h\,(d_h + 2\eta)}$ and $\dfrac{\eta\Lambda}{2\eta d_h + d_h^2}$, respectively, as t approaches ∞. Also, $\lim_{t\to\infty} S_{vH}(t) = \dfrac{\phi}{d_v}$. Thus every forward orbit of $\tau(t)$ in M_∂ converges to E_{01}. □

Lemma 3.3.8 *If $R_1 > 1$, then there exists $\rho > 0$ such that*

$$\lim_{t\to\infty} \ Sup\ \ \|\tau(t)P - E_{01}\| \geq \rho, \ \ \forall P \in \Omega_o.$$

i.e E_{01} is uniform weak repeller with $\tau(t)$.

Proof: If possible suppose that there exists $P_o \in \Omega_o$, such that $\lim_{t\to\infty}$ Sup $\|\tau(t)P_o - E_{01}\| < \rho$. Since $\lim_{t\to\infty} N_{hH}(t) \leq \dfrac{\Lambda}{d_h}$, $\lim_{t\to\infty} S_{hH}(t) = \dfrac{\Lambda\,(d_h + \eta)}{d_h\,(d_h + 2\eta)}$, $\lim_{t\to\infty} S_{hM}(t) = \dfrac{\eta\Lambda}{2\eta d_h + d_h^2}$, and $\lim_{t\to\infty} S_{vH}(t) = \dfrac{\phi}{d_v}$, then there exists $t_2 > 0$ and a sufficiently small positive number ρ_o such that $N_{hH}(t) \leq \dfrac{\Lambda}{d_h} + \rho_o$, $S_{hH}(t) \geq \dfrac{\Lambda\,(d_h + \eta)}{d_h\,(d_h + 2\eta)} - \rho_o$, $S_{hM}(t) \geq \dfrac{\eta\Lambda}{2\eta d_h + d_h^2} - \rho_o$, and $S_{vH}(t) \geq \dfrac{\phi}{d_v} - \rho_o$. Here

$$\begin{aligned} kS_{hM} &= \frac{b'\alpha_{vh} I_{vA} S_{hM}}{N_{hA}} = \frac{b'\alpha_{vh} I_{vA} I_{hA} S_{hM}}{I_{hA} N_{hA}} \geq \frac{b'\alpha_{vh} I_{vA} I_{hA} S_{hM}}{M_1 N_{hA}}, (|I_{hA}(t)| \leq M_1 \neq 0, \forall t) \\ &\approx k_1 I_{hA} S_{hM}, \ \text{ where } \frac{b'\alpha_{vh} I_{vA}}{N_{hA} M_1} \approx k_1, \text{Using Mean value theorem} \\ &\approx k_1 k_2 I_{hM} S_{hM} = k_3 I_{hM} S_{hM}, \ I_{hM}(t) \subset I_{hA}(t), \ \forall\, t. \end{aligned}$$

Here, $k = 0$ implies $k_1 \approx 0$ and hence $k_3 \approx 0$. Using these inequalities in Eqs. (3.12), (3.15), (3.17), it follows that

$$I'_{hH} \geq \frac{\beta_h \left(\frac{\Lambda (d_h + \eta)}{d_h (d_h + 2\eta)} - \rho_o \right)}{\frac{\Lambda}{d_h} + \rho_o} I_{vH} + \theta I_{hM} - (\theta + d_h + \delta_h + \gamma_h) I_{hH},$$

$$I'_{vH} \geq \frac{\beta_v \left(\frac{\phi}{d_v} - \rho_o \right)}{\left(\frac{\Lambda}{d_h} + \rho_o \right)} I_{hH} - d_v I_{vH},$$

$$I'_{hM} \geq k_3 \left(\frac{\eta \Lambda}{2\eta d_h + d_h^2} - \rho_o \right) I_{hM} + \theta I_{hH} - (\theta + \delta_h + d_h + \gamma_h) I_{hM},$$

$\forall\ t \geq t_2$.

We now consider the following corresponding auxiliary equations

$$I'_{hH} = \frac{\beta_h \left(\frac{\Lambda (d_h + \eta)}{d_h (d_h + 2\eta)} - \rho_o \right)}{\frac{\Lambda}{d_h} + \rho_o} I_{vH} + \theta I_{hM} - (\theta + d_h + \delta_h + \gamma_h) I_{hH},$$

$$I'_{vH} = \frac{\beta_v \left(\frac{\phi}{d_v} - \rho_o \right)}{\left(\frac{\Lambda}{d_h} + \rho_o \right)} I_{hH} - d_v I_{vH},$$

$$I'_{hM} = k_3 \left(\frac{\eta \Lambda}{2\eta d_h + d_h^2} - \rho_o \right) I_{hM} + \theta I_{hH} - (\theta + \delta_h + d_h + \gamma_h) I_{hM},\ \forall\ t \geq t_2. \quad (3.31)$$

Let $J_{1\rho_o}$ be the Jacobian matrix of the system (3.31) at the disease-free equilibrium point E_{01}

$$J_{1\rho_o} = \begin{pmatrix} -(\theta + \delta_h + d_h + \gamma_h) & \frac{\beta_h \left(\frac{\Lambda (d_h + \eta)}{d_h (d_h + 2\eta)} - \rho_o \right)}{\frac{\Lambda}{d_h} + \rho_o} & \theta \\ \frac{\beta_v \left(\frac{\phi}{d_v} - \rho_o \right)}{\left(\frac{\Lambda}{d_h} + \rho_o \right)} & -d_v & 0 \\ \theta & 0 & -(\theta + \delta_h + d_h + \gamma_h) \end{pmatrix}.$$

Since $R_1 > 1$ then from lemma 4.9 $S(J_1) > 0$, then there exists a sufficiently small $\rho_o > 0$ such that $S(J_{1\rho_o}) > 0$. Here, $J_{1\rho_o}$ is irreducible and has non-negative off-diagonal elements, it follows that $S(J_{1\rho_o})$ is a simple and associates with strongly positive eigenvector $\tilde{v} \in \Re^3_+$ i.e.,

$$(I_{hH}(t), I_{hM}(t), I_{vH}(t)) >> 0\ \ \forall,\ t > t_2.$$

Then there is a positive number a such that $(I_{hH}(t), I_{hM}(t), I_{vH}(t)) \geq a\tilde{v}$. Hence the solution of the system (3.31) is

$$V(t) := ae^{S(J_{1\rho_o})(t-t_2)}\tilde{v}, \forall t \geq t_2 \text{ with } V(t_2) := av.$$

It follows from (Smith and Waltman, 1995, Theorem B.1) that

$$(I_{hH}(t), I_{hM}(t), I_{vH}(t)) \geq ae^{S(J_{1\rho_o})(t-t_2)}\tilde{v}, \ \ \forall\, t \geq t_2.$$

Since $S(J_{1\rho_o}) > 0$, then the solution

$$\lim_{t\to\infty} I_{hH}(t) \to \infty, \ \lim_{t\to\infty} I_{hM}(t) \to \infty, \ \lim_{t\to\infty} I_{vH}(t) \to \infty.$$

This is a contradiction, and hence

$$\lim_{t\to\infty} \ \text{Sup} \ \|\tau(t)P - E_{01}\| \geq \rho, \ \ \forall P \in \Omega_o.$$

□

With the help of the above lemmas, we now establish the persistence Theorem (3.3.7). Proof: Assume that $R_1 > 1$, then it follows from Lemma 3.3.5 that $S(J_1) > 0$. Let $\tau(t)P$ is the solution maps generated by the system (3.11-3.18) with the initial value P. Clearly, the system $\{\tau(t)\}_{t\geq 0}$ admits the global attractor in $\mathbb{R}^8_+$. Here, the stable set of E_{01} is $W^s(E_{01}) = \{P \in \ \ d(\tau(t)P, E_{01}) \to 0 \text{ as } t \to \infty\}$. From the Lemma 3.3.7, E_{01} is a fixed point of $\tau(t)$ and acyclic in $M\partial$, every solution in $M\partial$ approach to E_{01}. Moreover, Lemma 3.3.8 implies that E_{01} is an isolated invariant set in Ω and $W^s(E_{01}) \cap \Omega_o = \phi$. By the acyclicity theorem of uniform persistence for maps Zhao (2001), it follows that $\tau(t)$ is uniformly persistent with respect to $(\Omega_o, \partial\Omega_0)$. Hence there exist $\sigma > 0$ such that $\lim_{t\to\infty} \text{Inf}\ I_{hH} \geq \sigma$, $\lim_{t\to\infty} \text{Inf}\ I_{hM} \geq \sigma$, $\lim_{t\to\infty} \text{Inf}\ I_{vH} \geq \sigma$. This completes the proof. □

3.3.6.3 Case-III: $\eta \neq 0,\ \theta = 0,\ k \neq 0$ (Strict Border Screening and Isolation)

In this case, the local stability of the corresponding disease-free equilibrium point, E_{02}, is given by the theorem below. As mentioned earlier, this disease-free equilibrium asserts the disease-free only within the home country while allowing infected migrants abroad.

Theorem 3.3.8 *The disease free equilibrium point E_{02} of the system (3.11-3.18) is locally asymptotically stable if $R_2 < 1$, and unstable if $R_2 > 1$.*

Proof: The Jacobian matrix of the system (3.11-3.18) at E_{02} is $J_2 = \begin{pmatrix} A^2_{4\times4} & B^2_{4\times4} \\ C^2_{4\times4} & D^2_{4\times4} \end{pmatrix}$, where

$$A^2_{4\times4} = \begin{pmatrix} -a & 0 & q & 0 \\ 0 & -b & 0 & 0 \\ 0 & \gamma_h & -a & 0 \\ 0 & -\dfrac{K_1\phi\beta_v}{(P+Q_3)d_v} & 0 & -d_v \end{pmatrix}, \; B^2_{4\times4} = \begin{pmatrix} -\dfrac{P\beta_h}{P+Q_3} & \eta & 0 & 0 \\ \dfrac{P\beta_h}{P+Q_3} & 0 & 0 & 0 \\ 0 & 0 & 0 & \eta \\ 0 & 0 & 0 & 0 \end{pmatrix},$$

$$C^2_{4\times4} = \begin{pmatrix} 0 & \dfrac{K_1\phi\beta_v}{(P+Q_3)d_v} & 0 & 0 \\ \eta & 0 & 0 & 0 \\ 0 & 0 & 0 & 0 \\ 0 & 0 & \eta & 0 \end{pmatrix}, \; D^2_{4\times4} = \begin{pmatrix} -d_v & 0 & 0 & 0 \\ -d_h-\eta-k & 0 & q & \\ 0 & k & -b & 0 \\ 0 & 0 & \gamma_h & -a \end{pmatrix},$$

$a = d_h + \eta + q$ and $b = d_h + \gamma_h + \delta_h$. Let λ be eigenvalues of the matrix J_2, then the characteristic polynomial is,

$$P(\lambda) = (d_v + \lambda)\, Q(\lambda)\, R(\lambda),$$

where $Q(\lambda) = \lambda^2 + \lambda\,(d_h + d_v + \gamma_h + \delta_h) + (1 - R_2^2)\, d_v\,(d_h + \gamma_h + \delta_h)$, and $R(\lambda) = p_0\lambda^5 + p_1\lambda^4 + p_2\lambda^3 + p_3\lambda^2 + +p_4\lambda + p_5$. $\lambda = -d_v$ is one eigenvalue, and other eigenvalues are given by $Q(\lambda) = 0$ and $R(\lambda) = 0$. From $Q(\lambda) = 0$, the eigenvalues are

$$\lambda_2 = \frac{1}{2}\left(-\sqrt{(d_h + d_v + \gamma_h + \delta_h)^{\,2} - 4\,(1 - R_2^2)\, d_v\,(d_h + \gamma_h + \delta_h)} - (d_h + d_v + \gamma_h + \delta_h)\right),$$

$$\lambda_3 = \frac{1}{2}\left(\sqrt{(d_h + d_v + \gamma_h + \delta_h)^{\,2} - 4\,(1 - R_2^2)\, d_v\,(d_h + \gamma_h + \delta_h)} - (d_h + d_v + \gamma_h + \delta_h)\right).$$

Clearly, $\lambda_2 < 0$ and $\lambda_3 < 0$ if $R_2 < 1$. Furthermore, using Wolfram Mathematica, we showed $p_0, p_1, p_2, p_3, p_4, p_5$ are positive, $p_1p_2p_3 - p_3^2 - p_1^2p_4 > 0$, and $(p_1p_2p_3 - p_3^2 - p_1^2p_4)\,(p_1p_4 - p_5) > (p_1p_2 - p_3)^2\, p_5 + p_1p_5^2$ Gautam et al. (2025, 2022). Then using the Routh Hurwitz theorem, we conclude that all the eigenvalues have negative real parts if $R_2 < 1$. Hence E_{02} is locally asymptotically stable if $R_2 < 1$ and unstable if $R_2 > 1$. □

3.3.7 Analysis of Simplifications Implemented in the Model

3.3.7.1 Approximation with Autonomous System

Note that our model is non-autonomous due to the time-dependent parameter $\psi(t)$, representing the API of India. However, for analytical tractability (Subsection 3.3.4, 3.3.5, and 3.3.6), we approximated the model with the autonomous system. Moreover, since the future API of India can not be obtained, the simulation results for model prediction and control programs (Section 3.3.8) are computed based on the autonomous model with the current API of India. In this section, we examine the potential error that we anticipate from the autonomous model. For this, we compared the predicted cumulative cases for both autonomous and non-autonomous systems for the period 2009-2019 (Figure 8). We observed that the predicted cumulative cases by the autonomous model remain within 5% of the non-autonomous model. For example, from 2009 to 2019, the difference in cumulative cases from the two model systems is only 1000 out of 20,000 base cases. Therefore, the autonomous model provides a reasonable approximation to the non-autonomous model, and the study's main finding remains the same in both models.

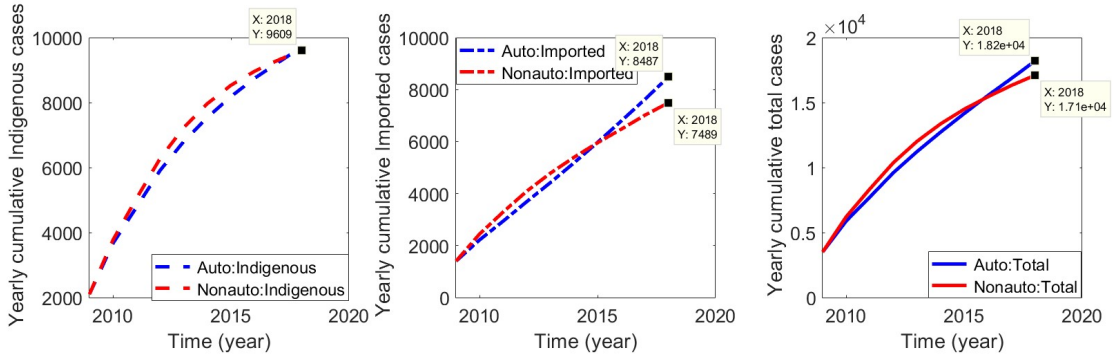

Figure 8: Solutions of autonomous system (blue) and non-autonomous system (red) : Cumulative indigenous(Left), cumulative imported(Middle) and cumulative total (Right).

3.3.7.2 Approximations to the Exposed Class of Mosquitoes and Pathogen Transmission from Recovered Humans

Because of the limited data availability, we have not included two potential phenomena: the incubation period of mosquitoes and pathogen transmission from recovered humans. However, these phenomena have been considered in some previous studies Chitnis et al. (2008); Ngwa and Shu (2000). While these phenomena may not significantly

impact the primary objective of this study, namely the impact of imported cases on the malaria elimination program, we also considered an extended model with these two phenomena incorporated. Fitting this extended model to the data with the same initial values of state variables and parameters (Table 1 and Table 2), we obtained the transmission probability from recovered human to susceptible mosquitoes per bite to be $r = 0.35$ and the incubation period of mosquito as $1/\sigma = 10$ days, consistent with previous studies Chitnis et al. (2008); Xiulei et al. (2020). Notably, per capita mosquito biting rates of $b_1 = 56$ and $b_2 = 48$, estimated with the extended model, are within the 95% confidence interval of the estimates from the simplified model. Moreover, the cumulative case during 2020-2026 predicted by the extended model is 1425, which is close to the estimate of 1348 by the simplified model. Similarly, the predicted new cases in the year 2026 by the extended model is 195, while that by the simplified model is 191. Therefore, the qualitative and quantitative differences between the two models with and without the exposed class of mosquitoes and pathogen transmission from recovered humans are not significant, asserting the robustness of the simplified models shown in Figure 9.

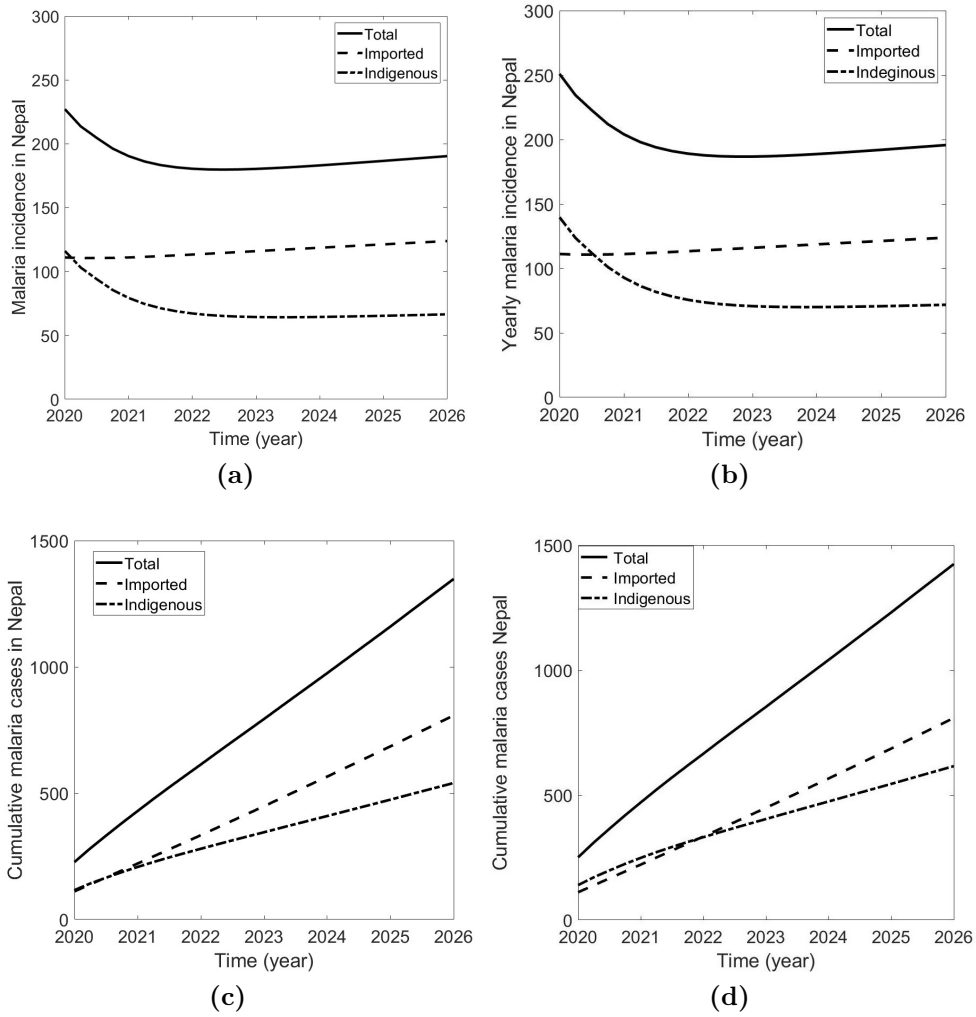

Figure 9: Comparison results . The model-predicted annual incidence rate at the year 2026 for the original model (Figure a) and the model-predicted annual incidence rate at the year 2026 for the simplified model (Figure b). The model-predicted cumulative cases for 2020-2026 for the original model (Figure c) and the model-predicted cumulative cases for 2020-2026 for the simplified model (Figure d).

3.3.8 Malaria Epidemic Prediction and Potential Control in Nepal: Model Simulations

We use our model to predict the malaria epidemic in Nepal and evaluate the potential control strategies. In particular, we focus on whether the goal of malaria elimination from Nepal by 2026 set by the Government of Nepal can be achieved with the current trend and/or potential strategies. We take the year 2020 as the base year and estimate the imported and indigenous malaria cases during the period 2020-2026, and assess the

number of possible control strategies that can be implemented for malaria elimination.

3.3.8.1 Basic Malaria Epidemic Outcome in Nepal

For the basic simulations, we take the API of India, $\psi(t)$, a constant value corresponding to the year 2018. We compute the model predicted values of indigenous and imported new cases for 2020-2026 (Figure 10a). We observe that if the current trend continues, the indigenous malaria cases follow a decreasing trend, but the imported cases increase slightly. We predict the indigenous malaria cases in Nepal will decrease to a yearly incidence of 67 cases in 2026, while the imported cases will remain 124 per year in 2026. As a result, the annual total incidence will remain 191 cases in the year 2026. With this incidence rate, the cumulative indigenous cases and imported cases for the period 2020 to 2026 will reach 540 and 808, respectively, making a total of 1348 cases of malaria in Nepal in this period (Figure 10b). While the magnitude remains relatively low, a slightly elevated level of new cases in 2026, mainly because of the imported cases, shows that the importation of malaria cases from India might remain an obstacle to the Nepal government's goal of malaria elimination by 2026.

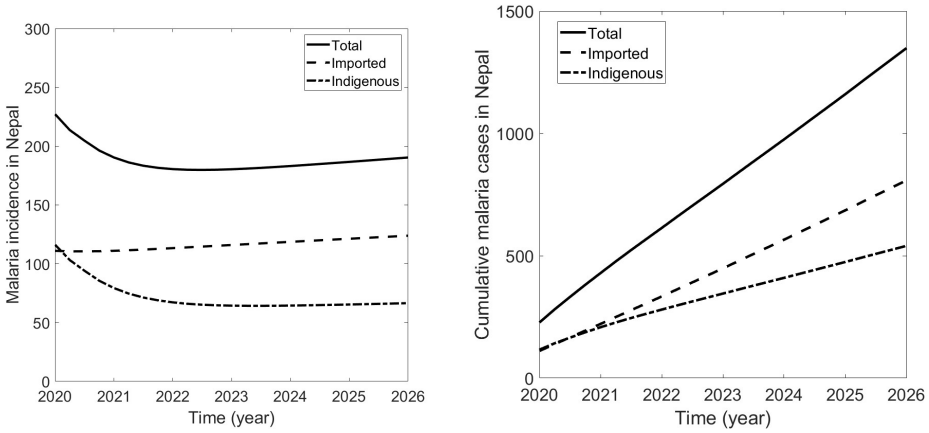

(a) **(b)**

Figure 10: Model prediction of the malaria epidemic in Nepal. (a) The model prediction of the annual incidence of indigenous, imported, and total malaria cases from 2020 to 2026; and (b) the model prediction of the cumulative cases of indigenous, imported and total malaria infection from 2020 to 2026.

3.3.8.2 Impact of the Transmission Abroad on the Epidemic in Home Country

As revealed in the model-predicted epidemic trend, the transmission of malaria abroad that may eventually cause higher imported cases can be a determinant factor for achieving an elimination goal by 2026. The model parameter k, which represents the impact of API of India, can be used to study how the transmission dynamics abroad can impact the epidemic outcome in Nepal. According to the data API of India has had a decreasing trend for the last few years. If the decreasing trend continues, imported cases in Nepal are expected to reduce in the coming years. Our model predicts that the malaria incidence in the year 2026 decreases linearly as the % reduction of API of India increases (Figure 11 Left). For example, reducing the current API (base value $k = 0.1$) by 50% brings down the annual malaria incidence from 191 to 95 in 2026. The linear dependency of cumulative cases on the % reduction of India's API is also seen with a 50% reduction from the base case bringing the cumulative cases from 1,348 to 869 during the period 2020-2026 (Figure 11 Right). These results indicate that the API of India can have an important role in the cases in the home country and eventually on the success of the Nepal government's malaria elimination goal.

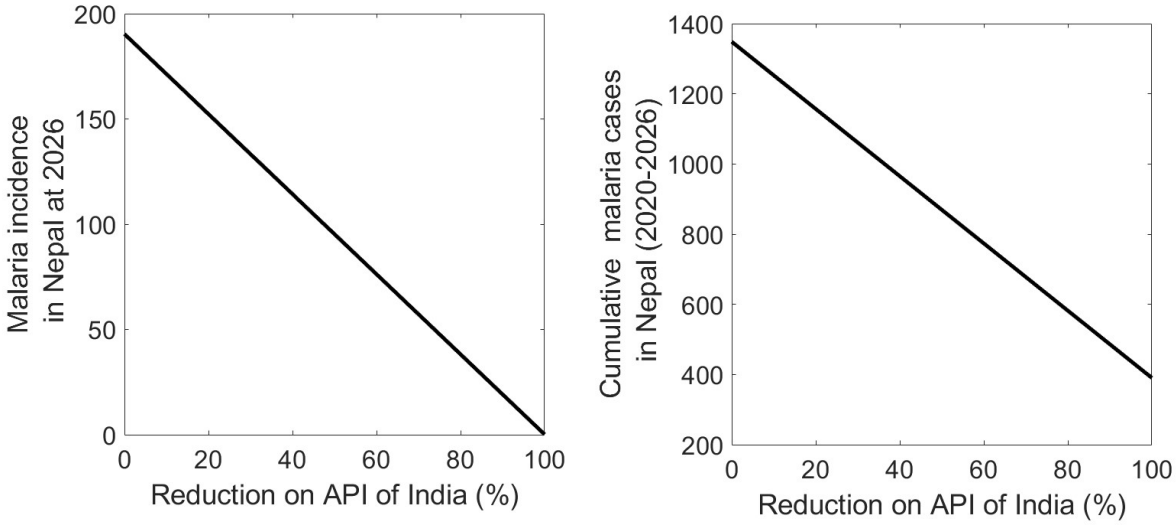

Figure 11: Impact of the API of India. Reduction of total malaria incidence at the year 2026 (Left) and reduction of cumulative malaria cases from 2020-2026 (Right) with Annual Parasitic Incidence (API) of India taking its value 0.1 for the base year 2020.

3.3.8.3 Control of Malaria in Nepal

We consider four potential control strategies: (1) Insecticide-treated nets (ITN), (2) Indoor Residual Spraying (IRS), (3) Border screen and isolation (BSI), and (4) Migration reduction (MR). Implementation of ITN reduces the mosquito biting rate. Assuming ϕ_{ITN} represents the effectiveness of ITN (assuming 100 % coverage), the implementation of this strategy transforms $b \to (1-\phi_{ITN})b$ in our model. Similarly, IRS increases mosquito death, transforming our model as $d_v \to \phi_{IRS} d_v$, where $\phi_{IRS} \geq 1$ is the enhancement of mosquito death rate due to IRS. We denote the effectiveness of BSI by ϕ_{BSI}, $0 \leq \phi_{BSI} \leq 1$ so that the implementation of this strategy results in the transformation $\theta \to (1-\phi_{BSI})\theta$, i.e., reduction of the disease import rate θ by a proportion ϕ_{BSI}. The last strategy, MR, can be attributed to promoting various employment opportunities within the country, thereby reducing the cross-border mobility for seeking employment in India. The strategies can be incorporated into our model by transforming $\eta \to (1-\phi_{MR})\eta$, $\theta \to (1-\phi_{MR})\theta$, where ϕ_{MR}, $0 \leq \phi_{MR} \leq 1$ is the effectiveness of MR.

The mosquito biting rate is one of the most critical parameters of malaria transmission. While we estimated the low biting rate from the data fitting, the estimated value is the average annual rate. In reality, the biting rate can be uncertain as it is affected by various environmental (seasonal), social, and economic factors. To include broader possible scenarios, we present the results for two different biting rates, low biting rate (base case $b = 39.5$ and high biting rate (approximately two times higher than the base case, $b = 100$).

3.3.8.4 Control Strategies for Elimination

The analytical results that we proved in subsection 3.3.5 inform us that malaria can be eliminated from the home country if one of the following conditions can be achieved: absence of cross-border mobility (case I in 3.3.5.1), full protection of transmission abroad (case II in 3.3.5.2), and strict border screening and isolation (case III in 3.3.5.3). According to our theorems, in case I, II, and III, the malaria gets eliminated if $(R_0 < 1, a_{10} > 0)$, $(R_1 < 1, a_{11} > 0)$, and $(R_2 < 1, a_{12} > 0)$, respectively, where a_{10}, a_{11}, and a_{12} are corresponding values of a_1 for case I, II, and III, respectively. We now evaluate whether the control strategies (ϕ_{ITN}, ϕ_{IRS}, ϕ_{BSI}, and ϕ_{MR}) can bring the model to satisfy the condition of eliminating malaria in Nepal.

Our results show that for the low biting rate condition, the elimination of malaria

can be achieved in Nepal regardless of whether any of the control strategies are applied or not because $R_0 < 1, R_1 < 1, R_2 < 1$ and $a_{10} > 0, a_{11} > 0, a_{12} > 0$ remain always true (Figure 12, first row). However, for the high biting rate condition, $R_0 < 1, R_1 < 1, R_2 < 1$ and $a_{10} > 0, a_{11} > 0, a_{12} > 0$ can not be achieved without the control strategies, i.e., for $\phi_{ITN} = \phi_{BSI} = \phi_{MR} = 0$, and $\phi_{IRS} = 1$ (Figure 12, second row). In this case, (ϕ_{BSI}) and (ϕ_{MR}) have no impact on R and a_1. Therefore, the control strategies related to the infected migrant workers and the mobility across the border are not enough for malaria elimination if the biting rate is high. In the high biting rate condition, $(R_0 < 1, a_{10} > 0)$, $(R_1 < 1, a_{11} > 0)$, and $(R_2 < 1, a_{12} > 0)$, i.e., the elimination of malaria, can be obtained if the level of ϕ_{ITN} is greater than 0.35, 0.65, and 0.35, respectively, or the level of ϕ_{IRS} is greater than 1.45, 2.60, 1.50, respectively (Figure 12, second row).

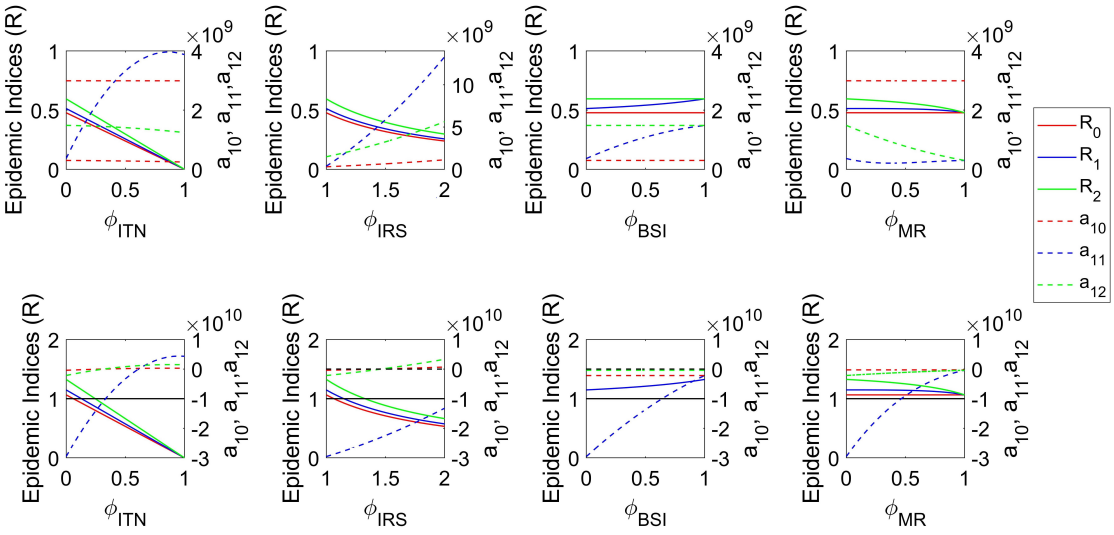

Figure 12: Condition for malaria elimination in Nepal. Threshold indices R_0, R_1, R_2, a_{10}, a_{11}, a_{12} as a function of controls $\phi_{ITN}, \phi_{IRS}, \phi_{BSI}$, and ϕ_{MR} for a low (first row) and high (second row) mosquito biting conditions. Note that the malaria is eliminated if $R_0 < 1, a_{10} > 0$, $R_1 < 1, a_{11} > 0$, and $R_2 < 1, a_{12} > 0$, respectively, where a_{10}, a_{11}, and a_{12} are corresponding values of a_1 for case I (absence of cross-border mobility), case II (full protection of transmission abroad), and case III (strict border screening and isolation), respectively.

3.3.8.5 Control Strategies for Minimal Burden

Here we perform simulations to show how the control strategies ITN, IRS, BSI, and MR impact the annual malaria incidence in 2026 and the cumulative malaria cases for 2020-2026 (Figure 13 and Figure 14). In the low mosquito biting rate condition

(Figure 13, first row), our model predicts that the 50% effectiveness of ITN (i.e., $\phi_{ITN} = 0.5$) reduces the annual malaria incidence in the year 2026 from 191 to 135. As a result, the cumulative cases for 2020-2026 will be reduced from 1,348 to 1001 (Figure 14, first row). An increase in IRS by 1.5 times (i.e., $\phi_{IRS} = 1.5$) will result in an annual incidence rate of 161 in 2026 and a cumulative cases of 1,167 for 2020-2026. Similarly, 50% effectiveness of BSI and MR will reduce the annual incidence rate in the year 2026 to 114 and 100, respectively, and the cumulative cases for 2020-2026 to 903 and 889, respectively.

In a high mosquito biting rate condition (Figure 13, second row, and Figure 14, second row), our model predicts that the 50% effectiveness of ITN (i.e., $\phi_{ITN} = 0.5$) reduces the annual malaria incidence in the year 2026 from 4.25 million to 257 and the cumulative cases for 2020-2026 from 7.8 million to 1,684. Similarly, an increase in IRS by 1.5 times (i.e., $\phi_{IRS} = 1.5$) will result in an annual incidence rate of 106 hundred thousand in 2026 and a cumulative cases of 128 hundred thousand for 2020-2026. 50% effectiveness of BSI and MR will reduce the annual incidence rate in the year 2026 to 4.23 million and 4.13 million, respectively, and the cumulative cases for 2020-2026 to 7.5 million and 6.98 million, respectively.

While each control strategy can maintain a minimum malaria burden, their effect may vary quantitatively. Among these control strategies, MR appears to be the most effective in controlling malaria in Nepal in low mosquito biting rate conditions, while ITN is the most effective control in the high biting rate condition. This indicates that the ideal control strategy may depend on the locations and seasons in which low or high mosquito biting rates are expected. We note that due to the existing open border relationship with a long history between Nepal and India, reducing the cross-border mobility of migrant workers may not be a viable option to implement. Therefore, the optimal border screen and isolation of returning migrant workers along with local approaches, ITN and IRS, can be the most impactful option for controlling and possibly eliminating malaria in Nepal.

In the above calculation, we assumed the 100% coverage of ITN. However, 100% is unlikely to be achieved, especially in resource-limited countries like Nepal. Thus we further observe model prediction for varying coverage and efficacy of ITN. The proportion of coverage ψ_{ITN}, $0 \leq \psi_{ITN} \leq 1$, and efficacy ϕ_{ITN}, $0 \leq \phi_{ITN} \leq 1$, can be incorporated in our model transforming $b \to (1 - \phi_{ITN}\psi_{ITN})\, b$. As presented in Figure 15, our simulations show that 100% efficacy and 100% coverage of ITN significantly reduce the malaria cases in the high mosquito biting case, but the effect

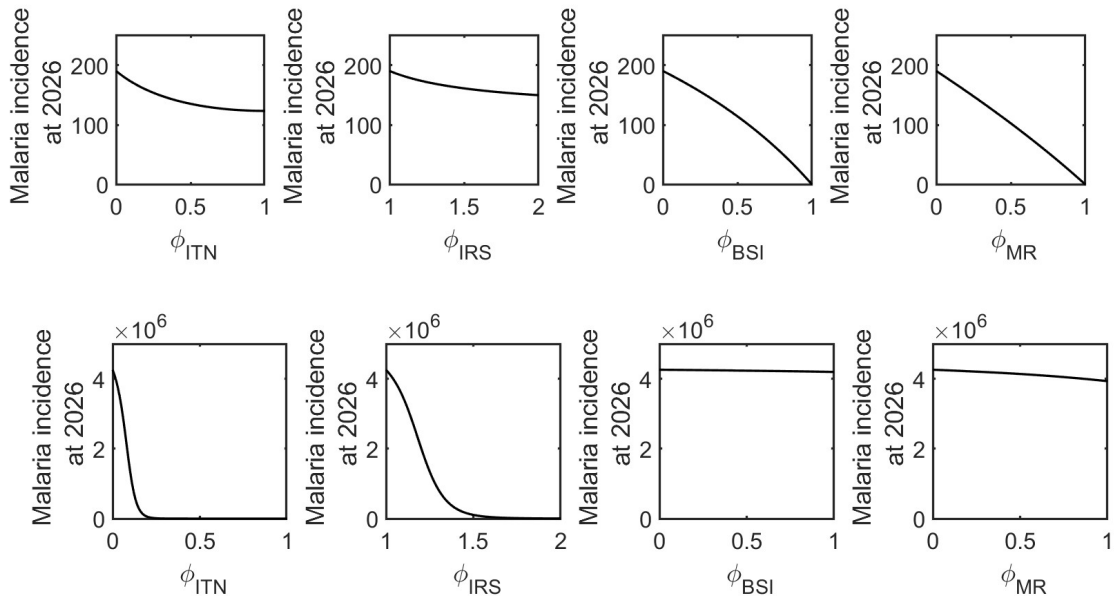

Figure 13: Effects of control strategies on the annual incidence rate. The model-predicted annual incidence rate in the year 2026 for various levels of ITN, IRS, BSI, and MR control in a low biting rate scenario (first row) and a high biting rate scenario (second row).

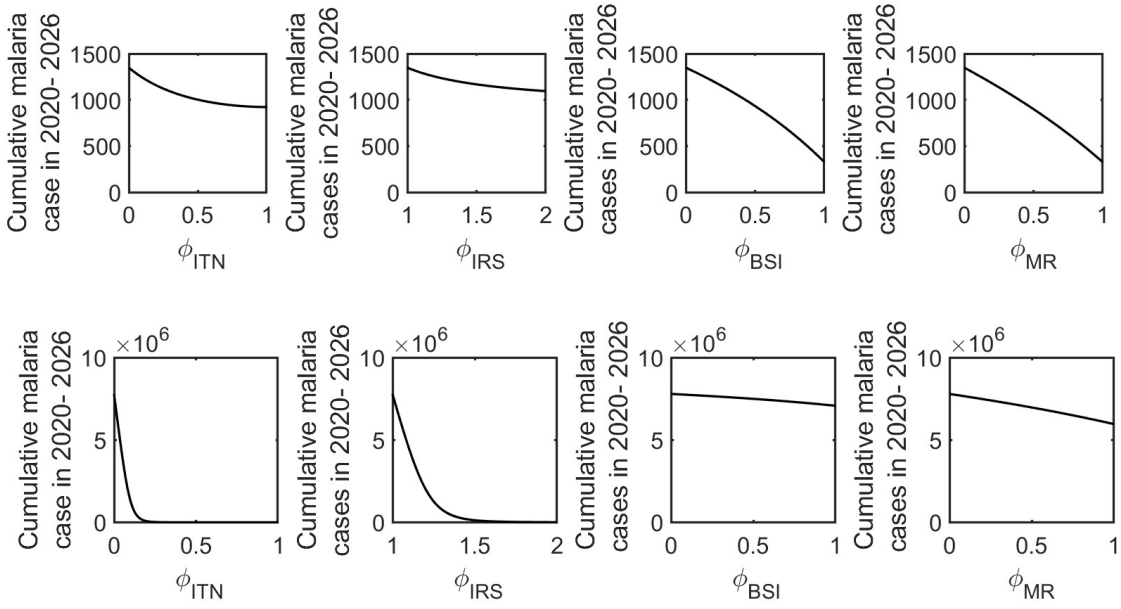

Figure 14: Effects of control strategies on the cumulative cases. The model-predicted cumulative cases for 2020-2026 for various levels of ITN, IRS, BSI, and MR control in a low biting rate scenario (first row) and a high biting rate scenario (second row).

is not significant in the low mosquito biting case. Since Nepal's estimated mosquito biting rate is low, even the 100% coverage and 100% efficacy will reduce malaria cases in 2026 from 191 to 121 only. Thus, in addition to ITN, optimal control strategies should also focus on adequately managing imported cases to eliminate malaria from Nepal by 2026.

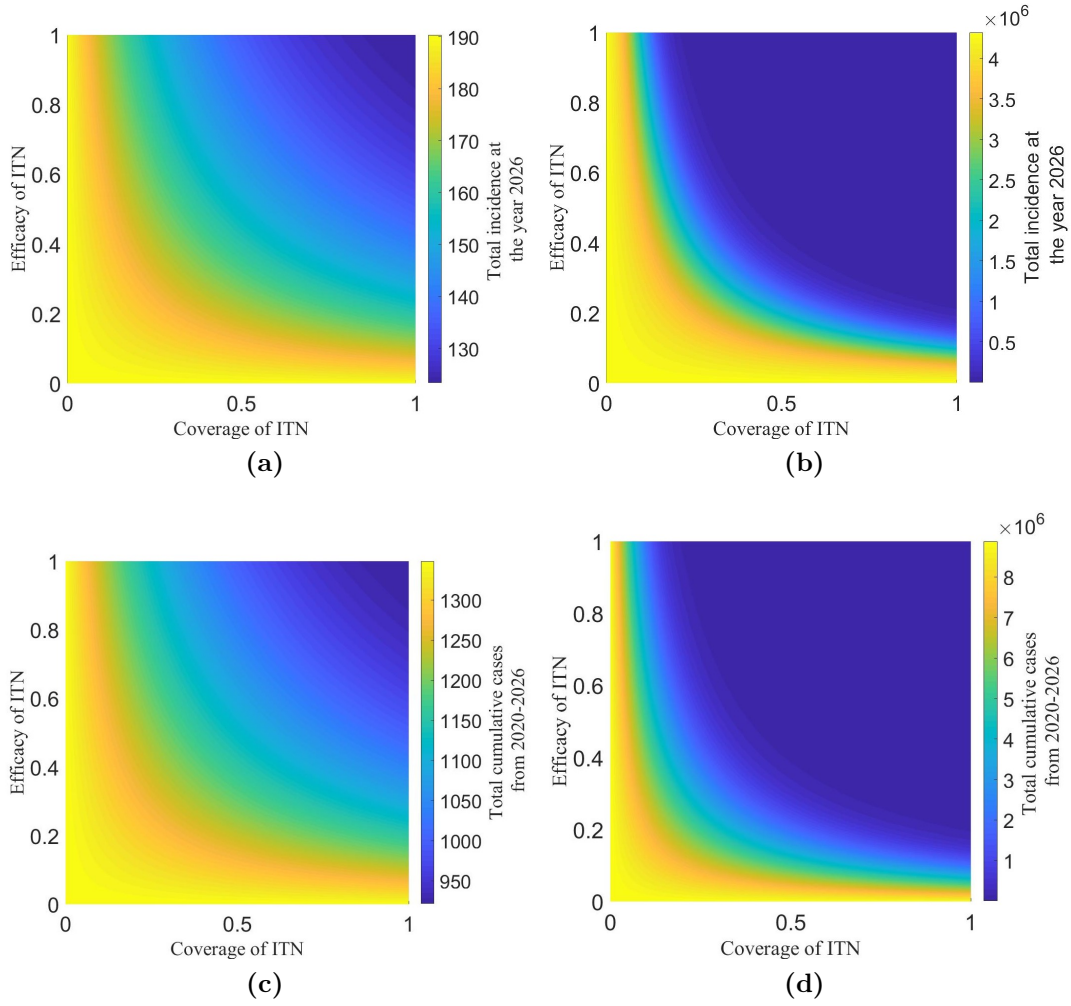

Figure 15: Sensitivity of coverage and efficacy of ITN. The model-predicted annual incidence rate in 2026 for various levels of efficacy and coverage of ITN in a low biting rate scenario (a) and a high biting rate scenario (b). The model-predicted cumulative cases for 2020-2026 for various levels of efficacy and coverage of ITN in a low biting rate scenario (c) and a high biting rate scenario (d).

3.4 Conclusion

Despite a significant decline of malaria cases worldwide, many countries are currently facing difficulty achieving malaria elimination goals from those countries, mainly due to cross-border mobility of migrant workers potentially bringing malaria from abroad. Nepal provides a typical example, which is recently suffering from higher imported cases from India through open-border, posing a severe threat to the Nepal government's goal of eliminating malaria by 2026. In this study, we developed a novel mathematical model validated by the data from Nepal and used our model to analyze the effects of cross-border mobility on the malaria elimination programs for low-endemic countries like Nepal.

Our model analyses and simulations show that malaria can be eliminated from Nepal if strategies promoting the absence of cross-border mobility, complete protection of transmission abroad, or strict border screening and isolation are implemented. In each of these potential strategies, we formulated threshold conditions for the stability of the disease-free equilibriums, providing the level of control strategies, such as ITN, IRS, BSI, and MR, to assert the elimination of malaria from Nepal. In some cases, we mathematically proved the persistence of malaria in Nepal. In one of the cases, namely strict border screening and isolation, our unique model can provide the disease-free condition only within the home country while allowing the disease among migrants abroad. In reality, such disease-free equilibrium is the most viable condition regarding the elimination of malaria from Nepal because achieving elimination from both countries can be challenging with the control strategies by the Nepal government's policy only without making combined strategies by both countries. In addition, we used our model to thoroughly assess all control strategies considered, ITN, IRS, BSI, and MR, to maintain the low level of malaria-endemic in both low and high mosquito biting rate scenarios. Interestingly, our model predicts that MR is the most effective control strategy for the low mosquito biting rate condition, while ITN is the most effective control strategy for the high mosquito biting rate condition. These interesting results suggest that the best control strategy may depend on locations and seasons that determine whether the biting rate is low or high.

There are several limitations of our study. We approximated the incidence rate abroad (India) using the API data of India. The analysis of the full model with accurate dynamics of humans and mosquitoes abroad, along with data from India, can help improve our results. Although the frequent movement of humans and

mosquitoes between bordering cities and the movement of mosquitoes through cross-border transportation may be important, we have not considered these factors in our model because the data of imported cases due to these movements are not available. Therefore, our results are more relevant to the infection importation through cross-border mobility of migrant workers. Our model parameters are estimated with the limited data of malaria cases in Nepal. Uncertainty on the model parameters can be clarified if more frequent data are available. While we estimated the mosquito population based on the previous studies, the implemented values may have some uncertainties. However, our further simulations show that changing the mosquito population size to a realistic limit does not significantly impact on the main qualitative conclusions of our study. Also, some districts of Nepal are directly connected with India making them more vulnerable in comparison to other areas. Therefore, an extension of our model may be necessary to incorporate the spatial heterogeneity of the malaria risk across districts of Nepal.

We also note that we could not prove the persistence theory in Case III (strict border screening and isolation) and Case IV (presence of cross-border mobility, no protection, and no border screening or isolation) because there is no complete disease-free equilibrium in these cases. Extensive mathematical theory may be needed to show the persistence of the disease in such complicated cases. Our analyses show that for some choice of parameters (for example, those making $a_1 < 0$), the disease may persist even if the threshold numbers R_0 (Case I in 3.3.5.1), R_1 (Case II in 3.3.5.2), and R_2 (Case III in 3.3.5.3) are less than 1, indicating a possibility of backward bifurcations. Therefore, a detailed bifurcation analysis for each case (I, II, and III) can be an essential work, which we plan to pursue in future research.

In summary, our model for malaria transmission dynamics, incorporating cross-border mobility between a low endemic country (Nepal) and a high endemic country (India), can provide important insights into an obstacle that cross-border mobility may create to malaria elimination programs. Our analytical and simulation results informing control policies that bring malaria elimination or maintain the epidemic at a low level are helpful for policymakers if implemented in conjunction with more accurate data. The following are the major conclusions and motivation for further research.

1. In the absence of cross-border mobility, reduction of R_0 just below unity may not be enough for malaria elimination at home country and the migrants abroad.

2. In the presence of mobility with complete protection abroad, reduction of R_1

just below unity may not enough for malaria elimination at home and migrants abroad.

3. In the presence of cross-border mobility without protection in abroad and without border screening for infected migrants home country can not be free from malaria until and unless abroad is free from malaria.

4. Mobility Restriction (MR) is most effective strategies for low mosquito biting rates; whereas use of ITN is the best for high biting rates, suggesting season- and location-specific strategies.

5. Thus, it is important to see the disease dynamics when reproduction number below unity through backward bifurcation analysis.

CHAPTER 4

4. BACKWARD BIFURCATION OF MALARIA TRANSMISSION MODEL WITH CROSS-BORDER MOBILITY

In Chapter 3, we developed malaria model with cross-border mobility and performed local and global stability analysis of malaria free equilibrium and uniform persistence theory. In addition, we did model fitting, validation and predicted the level of potential control strategies for control and elimination of malaria in different location and seasons. In this chapter we will perform indepth backward bifurcation analysis of the model.

4.1 Introduction

In disease dynamics, the basic reproduction number, R_0, has been widely considered a critical bifurcation parameter, providing conditions for disease persistence and elimination. If $R_0 < 1$, there is a disease-free equilibrium that is locally asymptotically stable, and the infection dies out. If $R_0 > 1$, there is a locally asymptotically stable endemic equilibrium, and infection persists. More precisely, as R_0 increases through 1, the endemic equilibrium appears, and there is an exchange of stability between the disease-free and endemic equilibrium, referred to as the forward bifurcation Brauer (2004).

However, in some vector-borne disease models like malaria, even if $R_0 < 1$ disease may be endemic in the population; this phenomenon is known as backward bifurcation Brauer (2004). In this case, the classical requirement of the reproduction number being less than unity becomes only necessary but not sufficient for disease elimination Gumel (2012); Fenga et al. (2014). Thus, in the case of vector-borne disease, the new threshold $R_0^* < 1$, often referred to as the transmission threshold, may be required to assert disease elimination. In such dynamics with a backward bifurcation, a bistability situation occurs when R_0 lies in the interval $(R_0^*, 1)$, where the system converges into either disease-free or endemic equilibrium, depending on initial conditions. The initial condition corresponding to the threshold for bistability, the breakpoint density, provides a prevalence level for malaria elimination when $R_0^* < R_0 < 1$. Thus, the backward bifurcation analysis is essential for adequately designing malaria control and elimination programs.

Several existing models of vector-borne diseases have possessed backward bifurcation, primarily due to disease-induced death Xing et al. (2020); Chitnis et al. (2006); Wan and Cui (2009); Feng et al. (2015); Miliyon (2017); Wang et al. (2018); Buonomo and Vargas-De-Leon (2013); kamel Naji and Adnan Thirthar (2020); Sha et al. (2019b); Mohammed-Awel et al. (2017). Some other studies have also shown the possibility of backward bifurcation due to the impact of quarantine Xiulei et al. (2020), income inequality among the susceptible human population Bala and Gimba (2022), and vector biases Chitnis et al. (2006) (biting preference of vector to infectious humans).

Since migration is one of the main obstacles to malaria elimination in many countries Tumwiine et al. (2010); Martens and Hall (2000), a question naturally arises whether cross-border mobility has a role in backward bifurcation. Thus, studying the effects of cross-border mobility on backward bifurcation is crucial. While some studies Tumwiine et al. (2010); Martens and Hall (2000); Acevedo et al. (2015); Gao and Ruan (2012); Kim et al. (2016); Cosner et al. (2009); Cosner (2015); Mukhtar et al. (2020) have considered the effects of host movement on vector-borne disease, we are unaware of any studies that address the backward bifurcation issue of the malaria model with cross-border mobility. Gautam et al. (2022), have developed a malaria model with cross-border mobility and did some basic analysis, persistence theory and estimated some parameters with malaria cases in Nepal; however, the in-depth bifurcation analysis of the nonlinear system of the model and its wide applications to address the real world problems associated with different modes of cross-border mobility left for the future research.

Thus in this study, our main contribution is to examine whether cross-border mobility can bring the backward bifurcation, causing obstacles to malaria elimination even when the basic reproduction number is below unity. The novelty of our results constitutes the establishment of mobility conditions that can solely cause backward bifurcation, underscoring the need to consider cross-border mobility in devising malaria elimination strategies. We further extend our mobility driven backward bifurcation techniques to the case where eradication is impossible due to cross-border mobility; in this case, our analysis allows us to identify mobility-related control strategies to maintain malaria endemic in a low burden level. Now, we summarize some fundamental results from Gautam et al. (2022) and proceed our extensive bifurcation analysis considering different types of mobility in each sections.

4.2 Method

4.2.1 Model Simplification for Bifurcation Analysis

The simplified malaria model with cross-border mobility for the purpose of bifurcation analysis is shown in Figure 16.

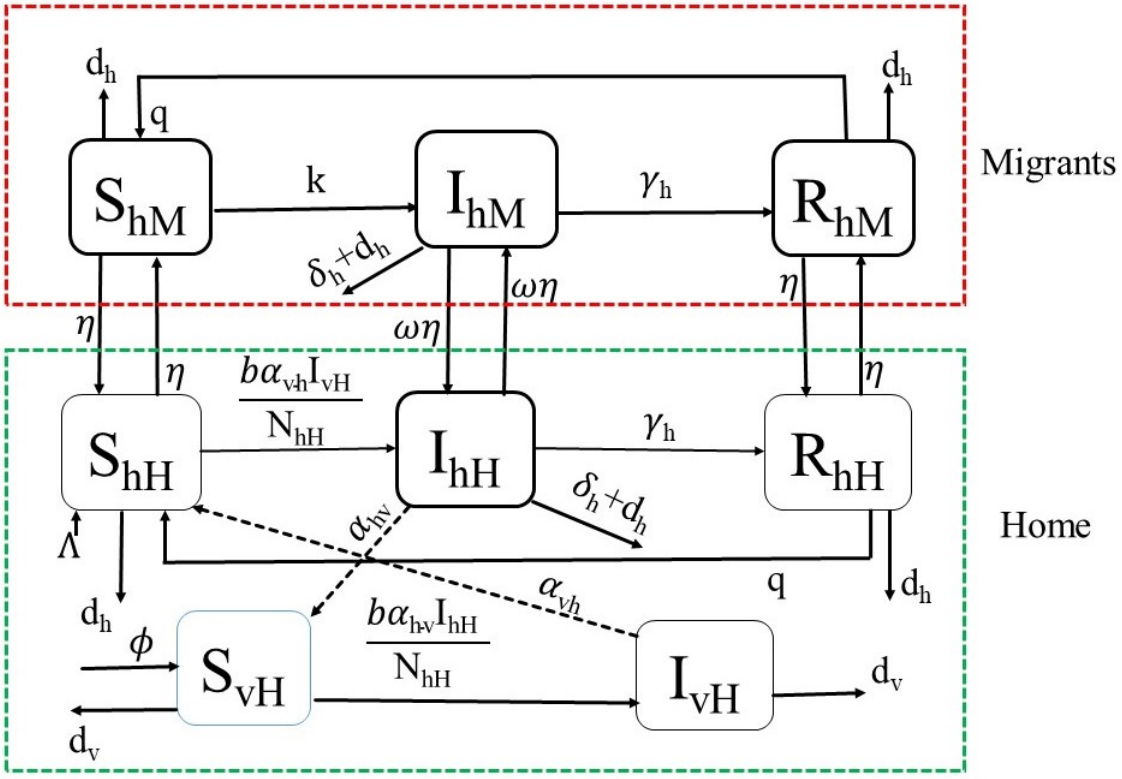

Figure 16: Simplified form of malaria transmission model with cross-border mobility with $\theta = \omega\eta$.

.

A detailed description of the model, considered here for bifurcation analysis, is presented previously Gautam et al. (2022). The model system we consider is as follows:

$$S'_{hH} = \Lambda + \eta S_{hM} + qR_{hH} - \frac{b\alpha_{vh}I_{vH}}{N_{hH}}S_{hH} - (\eta + d_h)S_{hH}, \tag{4.1}$$

$$I'_{hH} = \frac{b\alpha_{vh}I_{vH}}{N_{hH}}S_{hH} + \omega\eta I_{hM} - (\omega\eta + d_h + \delta_h + \gamma_h)I_{hH}, \tag{4.2}$$

$$R'_{hH} = \gamma_h I_{hH} + \eta R_{hM} - (\eta + d_h + q)R_{hH}, \tag{4.3}$$

$$S'_{vH} = \phi - \frac{b\alpha_{hv}I_{hH}}{N_{hH}}S_{vH} - d_v S_{vH}, \tag{4.4}$$

$$I'_{vH} = \frac{b\alpha_{hv}I_{hH}}{N_{hH}}S_{vH} - d_v I_{vH}, \tag{4.5}$$

$$S'_{hM} = \eta S_{hH} + qR_{hM} - kS_{hM} - (d_h + \eta)S_{hM}, \tag{4.6}$$

$$I'_{hM} = kS_{hM} + \omega\eta I_{hH} - (\omega\eta + \delta_h + d_h + \gamma_h)I_{hM}, \tag{4.7}$$

$$R'_{hM} = \gamma_h I_{hM} + \eta R_{hH} - (\eta + d_h + q)R_{hM}. \tag{4.8}$$

For the simulations, we took the values of parameters given in Table 1, which were estimated from the model fitting to the malaria data of Nepal Gautam et al. (2022) with $\eta = 0.04, \omega = 25, b = 43.75$.

Here the equilibria Eq. (3.24) presented slightly different form

$$a_3\lambda_h^{*3} + a_2\lambda_h^{*2} + a_1\lambda_h^* + a_0 = 0, \tag{4.9}$$

where,

$$a_3 = Q_2Q_4d_v\beta_v + 2Q_2Q_4d_v^2 + Q_2^2d_v\beta_v + Q_2^2d_v^2 + Q_4^2d_v^2 > 0,$$
$$a_2 = (p_1 - p_2\beta_h\beta_v), a_1 = (p_3 - p_4\beta_h\beta_v),$$
$$a_0 = -K_1\eta^2\omega k\Lambda\left(d_h + q\right)\left(d_h + 2\eta + q\right)\phi\beta_h\beta_v < 0 \text{ and } p_1,\ p_2,\ p_3,\ p_4$$

are non -negative Gautam et al. (2025).

4.3 Results

4.3.1 Backward Bifurcation Analysis

Using the model (4.1-4.8), we focus on the role of cross-border mobility in the bifurcations corresponding to the elimination or persistence of malaria. To explore this, we analyze two cases in detail: (I) $\eta = 0$ (absence of cross-border mobility); (II) $\eta \neq 0$ (presence of cross-border mobility).

4.3.1.1 Case-I: $\eta = 0$

Equilibria Analysis Since $\eta = 0$, then from the, Eq. (4.9) gives

$$a_3\lambda_h^{*2} + a_2\lambda_h^* + a_1 = 0, \tag{4.10}$$

where, a_3, a_2, and a_1 are simplified to

$$\begin{aligned}
a_3 &= b_0\Lambda d_v\left(d_h+\gamma_h+q\right)\left(\beta_v\left(d_h+q\right)+d_v\left(d_h+\gamma_h+q\right)\right) > 0,\\
a_2 &= \frac{b_0}{dh}\Lambda\left(G_0-R_0^2\right)d_v^2\left(d_h+q\right)\left(d_h+\gamma_h+\delta_h\right)\left(d_h\left(\gamma_h+\delta_h+q\right)+d_h^2+q\delta_h\right),\\
a_1 &= \Lambda\left(1-R_0^2\right)b_0\, d_v^2\left(d_h+q\right)^2\left(d_h+\gamma_h+\delta_h\right)^2,\\
b_0 &= \left(d_h^2\left(\gamma_h+\delta_h+k+q\right)+d_h\left(\gamma_h(k+q)+\delta_h(k+q)+kq\right)+d_h^3+kq\delta_h\right)^2,
\end{aligned}$$

where $G_0 = \dfrac{d_h\left(\beta_v\left(d_h+q\right)+2d_v\left(d_h+\gamma_h+q\right)\right)}{d_v\left(d_h\left(\gamma_h+\delta_h+q\right)+d_h^2+q\delta_h\right)}$. Here $R_0 < 1$ if and only if $a_1 > 0$ and $R_0 < \sqrt{G_0}$ if and only if $a_2 > 0$. Let $\Delta(R_0) = a_2^2 - 4a_1a_3$. Then we have $\Delta(\sqrt{G_0}) = -4a_1a_3 < 0$ when $G_0 < 1$, and $\Delta(1) = a_2^2 > 0$. When $R_0 < 1$, by the intermediate value theorem for continuous function, there exists a unique $R_0^* \in \left(\sqrt{G_0}, 1\right)$ such that $\Delta(R_0^*) = 0$. Therefore, R_0^* is the value of $R_0 < 1$ such that the discriminant of the Eq. (4.10) is zero. Also, for $R_0 < 1$, $\Delta(R_0) > 0$ if and only if $R_0 > R_0^*$, and $\Delta(R_0) < 0$ if and only if $R_0 < R_0^*$ Xing et al. (2020); Feng et al. (2015). Now using $\Delta(R_0^*) = 0$, we obtain $R_0^* = \dfrac{\sqrt{B^2G - 2A + 2\sqrt{M^2 + B^2A(1-G_0)}}}{B}$, where

$$\begin{aligned}
A &= d_h^2\left(d_h+q\right)^2\left(d_h+\gamma_h+\delta_h\right)^2\left(d_h+\gamma_h+q\right)\left(\beta_v\left(d_h+q\right)+d_v\left(d_h+\gamma_h+q\right)\right),\\
B^2 &= d_v\left(d_h+q\right)^2\left(d_h+\gamma_h+\delta_h\right)^2\left(d_h\left(\gamma_h+\delta_h+q\right)+d_h^2+q\delta_h\right)^2,\\
M &= d_h^2\left(d_h+q\right)^2\left(d_h+\gamma_h+\delta_h\right)^2\left(d_h+\gamma_h+q\right)\left(\beta_v\left(d_h+q\right)+d_v\left(d_h+\gamma_h+q\right)\right).
\end{aligned}$$

In Theorem 4.3.1, we present the general results about the existence of endemic equilibria.

Theorem 4.3.1 *Assume that $\eta = 0$ in the system (4.1-4.8), then the following statements hold.*

(i) For $R_0 > 1$, the system has unique endemic equilibrium;

(ii) For $R_0 = 1$, the system has unique endemic equilibrium when $a_2 < 0$ and no endemic equilibrium when $a_2 \geq 0$;

(iii) For $R_0^* < R_0 < 1$, the system has two distinct (upper and lower) endemic equilibria when $a_2 < 0$ and no endemic equilibrium when $a_2 \geq 0$;

(iv) For $R_0 = R_0^*$, the system has unique (coincident) endemic equilibria when $a_2 < 0$ and no endemic equilibrium when $a_2 \geq 0$;

(v) For $R_0 < R_0^*$, the system has no endemic equilibrium.

Proof: Here, the discriminant of Eq. (4.10) is $\Delta = a_2^2 - 4a_1a_3$. (i) For $R_0 > 1$, then $a_1 < 0$. It follows that $\Delta > a_2^2$ and $\lambda_h^* = \dfrac{-a_2 + \sqrt{\Delta}}{2a_3}$ provide unique endemic equilibrium from Eq. (3.22). (ii) Here, $R_0 = 1$, then $a_1 = 0$ and $\lambda_h^* = \dfrac{-a_2}{a_3}$ provide unique endemic equilibrium from Eq. (3.22) when $a_2 < 0$ and no endemic equilibrium when $a_2 \geq 0$. (iii) Since $R_0^* < R_0 < 1$, then $a_1 > 0$ and λ_h^* can not be positive and endemic equilibrium is not possible when $a_2 \geq 0$; however, when $a_2 < 0$, then $0 < \Delta < a_2^2$ and we get two positive values for $\lambda_h^* = \dfrac{-a_2 \pm \sqrt{\Delta}}{2a_3}$ and can obtain two endemic equilibria from Eq. (3.22). (iv) Since $R_0 = R_0^*$, then $\Delta = 0$ and we get two coincident positive values of $\lambda_h^* = \dfrac{-a_2}{2a_3}$ and unique (coincident) endemic equilibria when $a_2 < 0$ but no endemic equilibria when $a_2 \geq 0$. (v) Since $R_0 < R_0^*$, then $\Delta < 0$ and endemic equilibrium does not exist. □

4.3.1.2 Bifurcation Analysis

In this section, we discussed the local behavior of the disease-free and endemic equilibria using the Routh-Hurwitz Theorem and Castillo-Chavez and Song Theorem Martcheva (2015). For the global stability of the disease-free equilibrium, we use the Krasovkii-LaSalle invariance Theorem Martcheva (2015).

Theorem 4.3.2 *(**Forward and backward bifurcations**) Assume that $\eta = 0$, then the model possesses the forward bifurcation at $R_0 = 1$ when $0 \leq \delta_h \leq \delta_h^*$ and the backward bifurcation at $R_0 = 1$ when $\delta_h > \delta_h^*$, where*

$$\delta_h^* = \frac{d_h\left(d_h\beta_v + d_v\gamma_h + d_hd_v + qd_v + q\beta_v\right)}{d_v\left(d_h + q\right)}.$$

Proof: We apply the theorem by Castillo Chavez and Song Martcheva (2015) to derive the condition for forward and backward bifurcations. The system (4.1-4.8) of the model can be written as:

$$\frac{d\vec{x}}{dt} = \vec{f}(\vec{x}, \beta_h),\ \vec{f} : \mathbb{R}^8 \times \mathbb{R} \to \mathbb{R}^8, \vec{f} \in C^2(\mathbb{R}^8 \times \mathbb{R}), \tag{4.11}$$

where $\vec{x} = (S_{hH},\ I_{hH},\ R_{hH},\ S_{vH},\ I_{vH},\ S_{hM},\ I_{hM},\ R_{hM})$,
$\vec{f} = (f_1,\ f_2,\ f_3,\ f_4,\ f_5,\ f_6,\ f_7,\ f_8)$, and $\beta_h^* = \dfrac{\Lambda d_v^2\,(d_h+\gamma_h+\delta_h)}{\phi d_h \beta_v}$ corresponds to $R_0 = 1$ considered as one of the potential bifurcation parameters. Then, the Jacobian of the system at the bifurcation point $(E^0;\ \beta_h^*)$ is

$$J_0 = \begin{pmatrix} P_{5\times 5} & 0_{5\times 3} \\ 0_{3\times 5} & Q_{3\times 3} \end{pmatrix},$$

where

$$P = \begin{pmatrix} -d_h & 0 & q & 0 & -\dfrac{\Lambda d_v^2\,(d_h+\gamma_h+\delta_h)}{\phi d_h \beta_v} \\ 0 & -(d_h+\gamma_h+\delta_h) & 0 & 0 & \dfrac{\Lambda d_v^2\,(d_h+\gamma_h+\delta_h)}{\phi d_h \beta_v} \\ 0 & \gamma_h & -(d_h+q) & 0 & 0 \\ 0 & -\dfrac{\phi d_h \beta_v}{\Lambda d_v} & 0 & -d_v & 0 \\ 0 & \dfrac{\phi d_h \beta_v}{\Lambda d_v} & 0 & 0 & -d_v \end{pmatrix}$$

and

$$Q = \begin{pmatrix} -(d_h+k) & 0 & q \\ k & -(d_h+\gamma_h+\delta_h) & 0 \\ 0 & \gamma_h & -(d_h+q) \end{pmatrix}.$$

Five eigenvalues of the Jacobian J_0 are

$$\lambda = 0, -d_h, -d_v, -(d_h+q), -\left(d_h+d_v+\gamma_h+\delta_h\right),$$

and the rest three eigenvalues are given by the following characteristic polynomial equation of degree three.

$$\lambda^3 + M_2\lambda^2 + M_1\lambda + M_0 = 0, \tag{4.12}$$

where, $M_2 = 3d_h+\gamma_h+\delta_h+k+q$, $M_1 = 2d_h\gamma_h+2d_h\delta_h+2kd_h+2qd_h+3d_h^2+k\gamma_h+k\delta_h+q\gamma_h+q\delta_h+kq$, $M_0 = d_h^2\gamma_h+d_h^2\delta_h+kd_h\gamma_h+kd_h\delta_h+kqd_h+kd_h^2+qd_h\gamma_h+qd_h\delta_h+qd_h^2+d_h^3+kq\delta_h$. Here, $M_0,\ M_1,\ M_2,\ M_3$ all are positive and

$$\begin{aligned} M_1M_2 - M_0 \;=\;& 8d_h^2\,(\gamma_h+\delta_h+k+q) + 8d_h^3 + \gamma_h\left(2\delta_h(k+q)+k^2+3kq+q^2\right) \\ & +\gamma_h^2(k+q) + (k+q)\,(\delta_h+k)\,(\delta_h+q) + \\ & 2d_h\left(\gamma_h^2+\delta_h^2+\gamma_h\,(2\delta_h+3(k+q)) + 3\delta_h(k+q)+k^2+3kq+q^2\right) > 0. \end{aligned}$$

Thus, J_0 has one eigenvalue of zero, four negative, and the remaining three have negative real parts.
Let

$$\vec{v} = (v_1,\ v_2,\ v_3,\ v_4,\ v_5,\ v_6,\ v_7,\ v_8)$$

and

$$\vec{u} = (u_1,\ u_2,\ u_3,\ u_4,\ u_5,\ u_6,\ u_7,\ u_8)^T$$

are the left and right eigenvectors of the zero eigenvalue of J_0, respectively. Solving the matrix equations $\vec{v}J_0 = 0$ and $J_0\vec{u} = 0$, we obtain the components of the eigenvectors $\vec{v}$ and $\vec{u}$ as

$$v_1 = v_3 = v_4 = 0,\ v_5 = \frac{\Lambda v_2 d_v\left(d_h + \gamma_h + \delta_h\right)}{\phi d_h \beta_v},\ v_6 = v_7 = v_8 = 0,$$

,

$$u_1 = -u_2\left(\frac{d_h + \gamma_h + \delta_h}{d_h} - \frac{q\gamma_h}{d_h\left(d_h + q\right)}\right),\ u_3 = \frac{u_2\gamma_h}{d_h + q},$$
$$u_4 = -\frac{u_2\phi d_h\beta_v}{\Lambda d_v^2},\ u_5 = \frac{u_2\phi d_h\beta_v}{\Lambda d_v^2},\ u_6 = u_7 = u_8 = 0,$$

with v_2 and u_2 being free. The parameters a and b defined in Martcheva (2015) are obtained from the equation

$$a = \sum_{m,i,j=1}^{8} v_m u_i u_j \frac{\partial^2 f_m}{\partial x_i \partial x_j}(E_0),\ b = \sum_{m,i=1}^{8} v_m u_i \frac{\partial^2 f_m}{\partial x_i \partial \beta_h}(E_0), \tag{4.13}$$

where f_m be the m^{th} component of $\vec{f}$. To compute the parameter b, we use Eq. (4.13) with $v_m = 0$ for $m = 1,\ 3,\ 4,\ 6,\ 7,\ 8$. Taking partial derivatives of f_2 and f_5 with respect to β_h, we get $\frac{\partial(f_2)}{\partial\beta_h} = \frac{x_1x_5}{x_1+x_2+x_3}$, $\frac{\partial(f_5)}{\partial\beta_h} = 0$, where, $f_2 = \beta_h\frac{x_1x_5}{x_1+x_2+x_3} - \left(d_h+\gamma_h+\delta_h\right)x_2$, $f_5 = \beta_v\frac{x_4x_2}{x_1+x_2+x_3} - x_5d_v$. Using $\vec{v}.\vec{u} = 1$, i.e., $v_2u_2 = \frac{d_v}{d_h+\gamma_h+\delta_h}$. Then, $b = \sum_{m,i=1}^{8} v_m u_i \frac{\partial^2 f_m}{\partial x_i\partial\beta_h}(E_0) = \sum_{i=1}^{8} v_2u_i\frac{\partial^2 f_2}{\partial x_i\partial\beta_h}(E_0) = \sum_{i=1}^{8} v_2u_i\frac{\partial}{\partial x_i}\left(\frac{x_1x_5}{x_1+x_2+x_3}\right)(E_0) = v_2u_5$
$= \frac{\phi d_h\beta_v}{(d_h+\gamma_h+\delta_h)\Lambda d_v} > 0$. Similarly, using Eq. (4.13),

$$\begin{aligned} a = {} & v_2\left(u_1u_1\frac{\partial^2 f_2}{\partial x_1^2} + 2u_1u_2\frac{\partial^2 f_2}{\partial x_1\partial x_2} + 2u_1u_3\frac{\partial^2 f_2}{\partial x_1\partial x_3} + 2u_2u_3\frac{\partial^2 f_2}{\partial x_2\partial x_3} + u_2u_2\frac{\partial^2 f_2}{\partial x_2^2}\right) + \\ & v_2\left(u_3u_3\frac{\partial^2 f_2}{\partial x_3^2} + 2u_1u_5\frac{\partial^2 f_2}{\partial x_1\partial x_5} + 2u_2u_5\frac{\partial^2 f_2}{\partial x_2\partial x_5} + 2u_3u_5\frac{\partial^2 f_2}{\partial x_3\partial x_5}\right) + \\ & v_5\left(u_1u_1\frac{\partial^2 f_5}{\partial x_1^2} + 2u_1u_2\frac{\partial^2 f_5}{\partial x_1\partial x_2} + 2u_1u_3\frac{\partial^2 f_5}{\partial x_1\partial x_3} + 2u_2u_3\frac{\partial^2 f_5}{\partial x_2\partial x_3}\right) + \\ & v_5\left(u_2u_2\frac{\partial^2 f_5}{\partial x_2^2} + u_3u_3\frac{\partial^2 f_5}{\partial x_3^2} + 2u_1u_4\frac{\partial^2 f_5}{\partial x_1\partial x_4} + 2u_2u_4\frac{\partial^2 f_5}{\partial x_2\partial x_4} + 2u_4u_3\frac{\partial^2 f_5}{\partial x_4\partial x_3}\right). \end{aligned} \tag{4.14}$$

After simplification, we get $a = \frac{2d_v\delta_h}{\Lambda} - \frac{2d_h\left(\beta_v\left(d_h+q\right)+d_v\left(d_h+\gamma_h+q\right)\right)}{\Lambda\left(d_h+q\right)}$. Here $a > 0$ if $\delta_h > \frac{d_h\left(d_h\beta_v + d_v\gamma_h + d_hd_v + qd_v + q\beta_v\right)}{d_v\left(d_h+q\right)} = \delta_h^*$. Thus the model possesses the backward bifurcation at $R_0 = 1$ when $\delta_h > \delta_h^*$ and forward bifurcation at $R_0 = 1$ when $0 \leq \delta_h \leq \delta_h^*$.

From the above result, in the absence of cross-border mobility of migrants between the home country and abroad ($\eta = 0$), if $0 \leq \delta_h \leq \delta_h^*$, malaria gets eliminated when $R_0 < 1$. However, if $\delta_h > \delta_h^*$, elimination is possible only when $R_0 < R_0^* < 1$. We also validated the above analytic results with the numerical solutions of the system (4.1-4.8) (Figure 17).

4.3.2 Case-II: $\eta \neq 0$

In the presence of cross-border mobility of the migrant workers ($\eta \neq 0$), the possibility of imported cases depends on malaria transmission abroad. Therefore, we perform our analysis for two subcases: (1) Case IIA (absence of transmission abroad, $\eta \neq 0,\ k = 0$) and (2) Case IIB (presence of transmission abroad, $\eta \neq 0,\ k \neq 0$).

4.3.2.1 Case- IIA ($\eta \neq 0,\ k = 0$)

- *Equilibria Analysis*: Here, Eq.(4.9) reduce to

$$a_3\lambda_h^{*2} + a_2\lambda_h^* + a_1 = 0, \tag{4.15}$$

with $a_3,\ a_2$, and a_1 given by

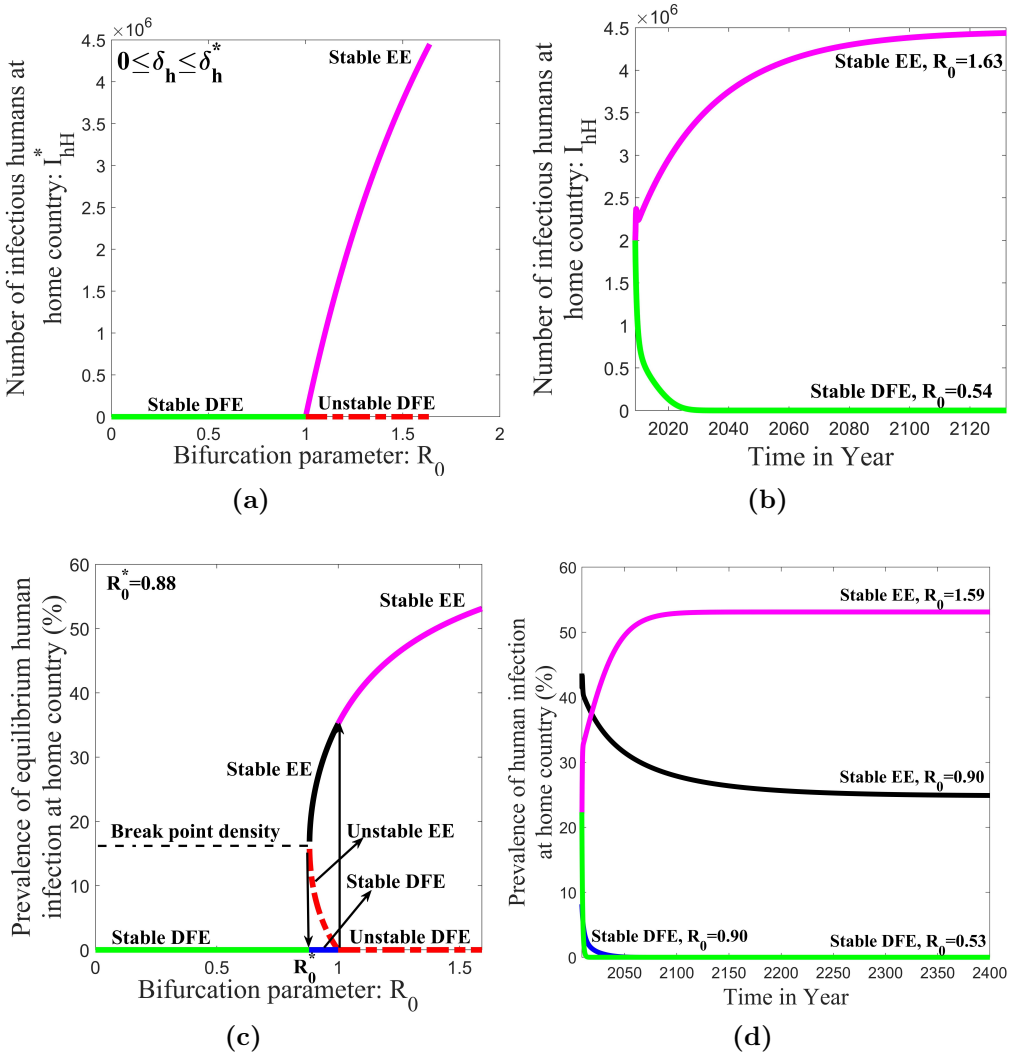

Figure 17: Bifurcation diagrams and model solutions. (a) Forward bifurcation at $R_0 = 1$ when δ_h lies in $0 \leq \delta_h \leq \delta_h^*$ ($\delta_h^* = 0.029$). (b) Model solutions verifying (a), where model solution converges to the unique stable endemic equilibrium when $R_0 = 1.63$ ($R_0 > 1$) (end of the magenta curve) and converges to the stable disease-free equilibrium when $R_0 = 0.54$ ($R_0 < 1$) (end of the green curve), regardless of the initial conditions. (c) Backward bifurcation for $\delta_h = 0.11$ with $R_0^* = 0.88$. (d) Model solutions verifying (c), where model solution converge to the unique stable endemic equilibrium when $R_0 = 1.59$ ($R_0 > 1$) (end of the magenta curve) and for $R_0 = 0.53$ ($R_0 < R_0^* < 1$), model solution converges to the stable disease-free equilibrium (end of the green curve), regardless of the initial conditions. However, for $R_0 = 0.90$ ($R_0^* < R_0 < 1$), the model solution converge to the higher level endemic equilibrium (end of the black curve) when the initial prevalence is above the breakpoint density (horizontal dashed line), and the model solution converges to the disease-free equilibrium (end of the blue curve) when the initial prevalence is below the breakpoint density.

□

$$a_3 = \Lambda\left(Q_2+Q_4\right)d_v d_v\left(d_h+\eta\right)^2\left(\left(Q_2+Q_4\right)d_v+Q_2\beta_v\right) > 0,$$
$$a_2 = A_2\left(G_1 - R_1^2\right),$$
$$A_2 = \frac{\left(\Lambda d_v^2\left(d_h+\eta\right)\left(d_h+\gamma_h+\delta_h\right)\left(d_h+\gamma_h+\delta_h+2\eta\omega\right)\right)}{d_h\left(d_h+2\eta\right)\left(d_h+\gamma_h+\delta_h+\eta\omega\right)},$$
$$a_1 = b_2\left(1-R_1^2\right),$$
$$b_2 = \Lambda\left(d_v\left(d_h+\eta\right)\left(d_h+q\right)\left(d_h+\gamma_h+\delta_h\right)\left(d_h+2\eta+q\right)\left(d_h+\gamma_h+\delta_h+2\omega\eta\right)\right)^2,$$

where $G_1 = \dfrac{Pd_h\left(d_h+2\eta\right)\left(2\left(Q_2+Q_4\right)d_v+Q_2\beta_v\right)\left(d_h+\gamma_h+\delta_h+\eta\omega\right)}{\Lambda K_2 Q_2 d_v\left(d_h+\eta\right)\left(d_h+\gamma_h+\delta_h\right)\left(d_h+\gamma_h+\delta_h+2\eta\omega\right)}$. Here $R_1 < 1$ if and only if $a_1 > 0$ and $R_1 < \sqrt{G_1}$ if and only if $a_2 > 0$. Let $\Delta(R_1) = a_2^2 - 4a_1a_3$. Then we have $\Delta(\sqrt{G_1}) = -4a_1a_3 < 0$ when $R_1 < 1$, and $\Delta(1) = a_2^2 > 0$. It follows that when $R_1 < 1$, the intermediate value theorem for continuous function implies that there exists a unique $R_1^* \in \left(\sqrt{G_1}, 1\right)$ such that $\Delta(R_1^*) = 0$. Therefore, R_1^* is the value of $R_1 < 1$ such that the discriminant of the Eq. (4.15) is zero. Also, for $R_1 < 1$, $\Delta(R_1) > 0$ if and only if $R_1 > R_1^*$, and $\Delta(R_1) < 0$ if and only if $R_1 < R_1^*$ Xing et al. (2020); Feng et al. (2015). Now using $\Delta(R_1^*) = 0$, we obtain $R_1^* = \dfrac{\sqrt{A_2^2G_1 - 2a_3b_2 + 2\sqrt{a_3^2b_2^2 + a_3A_2^2b_2\left(1-G_1\right)}}}{A_2}$. In Theorem 4.3.3, we present the general results about the existence of endemic equilibria.

Theorem 4.3.3 *Assume that $\eta \neq 0$ and $k = 0$ in the system (4.1-4.8), then the following statements hold.*

(i) For $R_1 > 1$, the system has unique endemic equilibrium;

(ii) For $R_1 = 1$, the system has unique endemic equilibrium when $a_2 < 0$ and no endemic equilibrium when $a_2 \geq 0$;

(iii) For $R_1^* < R_1 < 1$, the system has two (higher and lower) endemic equilibria when $a_2 < 0$ and no endemic equilibria when $a_2 \geq 0$;

(iv) For $R_1 = R_1^*$, the system has unique (coincident) equilibria when $a_2 < 0$ and no endemic equilibria when $a_2 \geq 0$;

(v) For $R_1 < R_1^*$, the system has no endemic equilibrium.

Proof is similar to Theorem 4.3.1.

- *Bifurcation Analysis (Case-IIA: $\eta \neq 0,\ k = 0$)*

Again, we use the Castillo Chavez and Song Theorem Martcheva (2015) for the bifurcation analysis. We have already established in Theorem 4.3.2 the role of the disease-induced death rate in possessing the backward bifurcation. Since the primary focus of this study is to examine whether cross-border mobility alone can produce backward bifurcation phenomena, we consider the disease-induced death rate is zero and focus on cross-border mobility in the following sections.

Theorem 4.3.4 *(**Forward and Backward Bifurcation**) Assume that $\eta \neq 0$ and $k = 0$, then the model possesses the forward bifurcation when $0 \leq \omega \leq \omega^*$ at $R_1 = 1$ and possesses the backward bifurcation when $\omega > \omega^* > 1$ at $R_1 = 1$, where $\omega^* = \dfrac{(d_h + \gamma_h)\, A}{\eta\,(d_h + 2\eta + q)\, B}$,*

$$
\begin{aligned}
A = {} & q^2 d_h \beta_v + q^2 d_h d_v + 6\eta q d_h \beta_v + 2q d_h^2 \beta_v + 2\eta q d_v \gamma_h + q d_h d_v \gamma_h + 8\eta q d_h d_v + \\
& 2q d_h^2 d_v + 4\eta^2 d_h \beta_v + 4\eta d_h^2 \beta_v + d_h^3 \beta_v + 2\eta^2 d_v \gamma_h + 3\eta d_h d_v \gamma_h + d_h^2 d_v \gamma_h + \\
& 6\eta^2 d_h d_v + 5\eta d_h^2 d_v + d_h^3 d_v + 3\eta q^2 d_v + 6\eta^2 q d_v + 2\eta q^2 \beta_v + 4\eta^2 q \beta_v, \\
B = {} & q d_v \gamma_h - \left(q d_h \beta_v + 2\eta d_h \beta_v + d_h^2 \beta_v + 2\eta d_v \gamma_h + 2\eta d_h d_v + 2\eta q d_v + 2\eta q \beta_v \right).
\end{aligned}
$$

Proof: We apply the theorem by Castillo Chavez and Song Martcheva (2015) to derive the condition for forward and backward bifurcation. The value of β_h corresponding to $R_1 = 1$ is $\beta_{h1}^* = \dfrac{\Lambda d_v^2 (d_h + \eta)(d_h + \gamma_h)(d_h + 2\eta\omega + \gamma_h)}{\phi d_h \beta_v (d_h + 2\eta)(d_h + \eta\omega + \gamma_h)}$ and E^{01} is the disease-free equilibrium. Then the Jacobian of the system (4.1-4.8) at the bifurcation point $(E^{01};\ \beta_{h1}^*)$ is $J_1 = [M,\ N]$, where

$$
M = \begin{pmatrix}
-(d_h + \eta) & 0 & q & 0 \\
0 & -(d_h + \gamma_h + \omega\eta) & 0 & 0 \\
0 & \gamma_h & -(d_h + \eta + q) & 0 \\
0 & -\dfrac{\phi d_h \beta_v (d_h + 2\eta)}{\Lambda d_v (d_h + \eta)} & 0 & -d_v \\
0 & \dfrac{\phi d_h \beta_v (d_h + 2\eta)}{\Lambda d_v (d_h + \eta)} & 0 & 0 \\
\eta & 0 & 0 & 0 \\
0 & \eta\omega & 0 & 0 \\
0 & 0 & \eta & 0
\end{pmatrix},
$$

and

$$N = \begin{pmatrix} -\beta^*_{h1} & \eta & 0 & 0 \\ \beta^*_{h1} & 0 & \omega\eta & 0 \\ 0 & 0 & 0 & \eta \\ 0 & 0 & 0 & 0 \\ -d_v & 0 & 0 & 0 \\ 0 & -(d_h+\eta) & 0 & q \\ 0 & 0 & -(d_h+\gamma_h+\omega\eta) & 0 \\ 0 & 0 & \gamma_h & -(d_h+\eta+q) \end{pmatrix}.$$

Six eigenvalues of J_1 are $0,\ -d_h,\ -d_v,\ -(d_h+2\eta),\ -(d_h+q),\ -(d_h+2\eta+q)$, and the rest two eigenvalues are obtained from the quadratic equation,

$$(d_h+\gamma_h+\omega\eta)\lambda_1^2 + (d_h+\gamma_h+\omega\eta)\,(2d_h+d_v+2\gamma_h+2\omega\eta)\,\lambda_1 + B_3 = 0, \qquad (4.16)$$

where, $B_3 = d_h\,(2d_v\,(\gamma_h+\omega\eta)+\omega^2\eta^2+3\gamma_h^2+6\gamma_h\omega\eta+\omega^2\eta^2)+d_h^2\,(d_v+3\gamma_h+3\omega\eta)+d_v\,(2\gamma_h\omega\eta+\gamma_h^2+2\omega^2\eta^2)+d_h^3+\gamma_h\,(\gamma_h+\omega\eta)\,(\gamma_h+2\omega\eta)$. Since all the coefficients of the quadratic Eq. (4.16) are positive, then the remaining two eigenvalues of J_1 have also negative real parts. Let $\vec{v} = (v_1,\ v_2,\ v_3,\ v_4,\ v_5,\ v_6,\ v_7,\ v_8)$ and $\vec{u} = (u_1,\ u_2,\ u_3,\ u_4,\ u_5,\ u_6,\ u_7,\ u_8)^T$ are the left and right eigenvectors corresponding to the zero eigenvalue of the matrix J_1. Solving the matrix equations $\vec{v}J_1 = 0$ and $J_1\vec{u} = 0$, we get $v_1 = v_3 = v_4 = v_6 = v_8 = 0, v_5 = \dfrac{\Lambda v_2 d_v\,(d_h+\eta)\,(d_h+\gamma_h)\,(d_h+\gamma_h+2\omega\eta)}{\phi d_h\beta_v\,(d_h+2\eta)\,(d_h+\gamma_h+\omega\eta)}$, and $v_7 = \dfrac{\omega\eta v_2}{d_h+\gamma_h+\omega\eta}$, $u_1 = \dfrac{u_2(Q-R)}{U}$,

$$u_3 = u_2\left(\frac{\omega\eta^2\gamma_h}{(d_h+q)\,(d_h+2\eta+q)\,(d_h+\gamma_h+\omega\eta)} + \frac{\gamma_h\,(d_h+\eta+q)}{(d_h+q)\,(d_h+2\eta+q)}\right),$$

$$u_4 = -\frac{u_2\phi d_h\beta_v\,(d_h+2\eta)}{\Lambda d_v^2\,(d_h+\eta)},\ u_5 = \frac{u_2\phi d_h\beta_v\,(d_h+2\eta)}{\Lambda d_v^2\,(d_h+\eta)},\ u_6 = \frac{u_2(S-T)}{U},$$

$$u_7 = \frac{\omega\eta u_2}{d_h+\gamma_h+\omega\eta},\ u_8 = \frac{u_2\gamma_h\,(\eta d_h+\omega\eta d_h+\omega\eta^2+\eta\gamma_h+\omega\eta^2+\omega\eta q)}{(d_h+q)\,(d_h+2\eta+q)\,(d_h+\gamma_h+\omega\eta)},$$

with $u_2,\ v_2$ free, where,

$$U = d_h\,(d_h+2\eta)\,(d_h+q)\,(d_h+2\eta+q)\,(d_h+\gamma_h+\omega\eta),$$

$$Q = q\gamma_h\left(d_h(2\eta+q)+d_h^2+\eta(2\eta+q)\right)(d_h+\gamma_h+\omega\eta)+q\omega\eta^2\gamma_h\,(2d_h+2\eta+q),$$

$$R = (d_h+\eta)\,(d_h+q)\,(d_h+\gamma_h)\,(d_h+2\eta+q)\,(d_h+\gamma_h+2\omega\eta),$$

$$S = \eta q\gamma_h\,(2d_h+2\eta+q)\,(d_h+\gamma_h+\omega\eta)+q\omega\eta\gamma_h\left(d_h(2\eta+q)+d_h^2+\eta(2\eta+q)\right),$$

$$T = \eta\,(d_h+q)\,(d_h+\gamma_h)\,(d_h+2\eta+q)\,(d_h+\gamma_h+2\omega\eta).$$

Here $\vec{v}.\vec{u} = 1$ implies
$v_2u_2 = \dfrac{d_v\left(d_h+\eta\omega+\gamma_h\right)^2}{\left(d_h+\gamma_h\right)\left(d_h+\eta\omega+\gamma_h\right)\left(d_h+2\eta\omega+\gamma_h\right)+d_v\left(d_h+\eta\omega+\gamma_h\right)^2+\eta^2\omega^2}$.
For the computation of b, $f_2 = \beta_h\dfrac{x_1x_5}{x_1+x_2+x_3} - \left(d_h+\gamma_h\right)x_2$, $f_5 = \beta_v\dfrac{x_4x_2}{x_1+x_2+x_3} - x_5d_v$, $f_7 = \omega\eta x_2 - \left(d_h+\gamma_h+\omega\eta\right)x_7$. Then, taking the partial derivatives of f_2, f_5 and f_7 with respect to β_h, we get $\dfrac{\partial(f_2)}{\partial\beta_h} = \dfrac{x_1x_5}{x_1+x_2+x_3}$, $\dfrac{\partial(f_5)}{\partial\beta_h} = \dfrac{\partial(f_7)}{\partial\beta_h} = 0$. Then, from Eq. (4.13), $b = \sum_{i=1}^{8} v_2u_i\dfrac{\partial^2 f_2}{\partial x_i\partial\beta_h}(E^{01}) = \sum_{i=1}^{8} v_2u_i\dfrac{\partial}{\partial x_i}\left(\dfrac{x_1x_5}{x_1+x_2+x_3}\right)(E^{01}) = v_2u_5 = v_2\dfrac{u_2\phi d_h\beta_v\left(d_h+2\eta\right)}{\Lambda d_v^2\left(d_h+\eta\right)} > 0$. For the computation of a, we use Eq. (4.14) at E^{01} with $\eta \neq 0$ and $k = 0$. After simplification, we get $a = \eta(\omega-1)d_h\gamma_h + \eta(\omega-1)d_h^2 - \dfrac{2\eta d_h\gamma_h\beta_v}{d_v} - \dfrac{d_h^2\gamma_h\beta_v}{d_v} - \dfrac{2\omega\eta^2 d_h\beta_v}{d_v} - \dfrac{2\eta d_h^2\beta_v}{d_v} - \dfrac{\omega\eta d_h^2\beta_v}{d_v} - \dfrac{d_h^3\beta_v}{d_v}$
$- \dfrac{d_h\left(d_h+2\eta\right)\left(\gamma_h\left(d_h+\gamma_h+\omega\eta\right)\left(d_h+\eta+q\right)+\left(d_h+q\right)\left(d_h+\gamma_h+\omega\eta\right)\left(d_h+2\eta+q\right)\right)}{\left(d_h+q\right)\left(d_h+2\eta+q\right)}$
$+ \dfrac{d_h\left(d_h+2\eta\right)\omega\eta^2\gamma_h}{\left(d_h+q\right)\left(d_h+2\eta+q\right)}$. From the expression of a, it is clear that ω should necessarily be greater than 1 for backward bifurcation. Otherwise, a becomes negative, and the model possesses the forward bifurcation. Furthermore, $\omega > \omega^* > 1$ is sufficient for $a > 0$. Therefore, model possesses the forward bifurcation at $R_1 = 1$ for $\omega \leq \omega^*$ and the backward bifurcation if $\omega > \omega^* > 1$, where $\omega^* = \dfrac{\left(d_h+\gamma_h\right)A}{\eta\left(d_h+2\eta+q\right)B}$. □

In the presence of cross-border mobility ($\eta \neq 0$) and the absence of malaria transmission abroad ($k = 0$), malaria elimination in the home country is possible for $\omega \leq \omega^*$ and $R_1 < 1$. However, if $\omega > \omega^* > 1$, elimination of malaria is possible only when $R_1 < R_1^* < 1$. Taking the parameters given in Table 2, we validated the analytic results with the numerical solution of the system (4.1-4.8). The bifurcation diagrams and corresponding model solutions are shown in Figure 18.

- *Sensitivity of Backward Bifurcation Phenomenon (Case-IIA: $\eta \neq 0,\ k = 0$)*

As established in Theorem 4.3.4, the cross-border mobility factor ω can bring the backward bifurcation, resulting in a threshold $R_1^* < 1$ such that malaria eradication requires $R_1 < R_1^* < 1$. In Figure 19, we present the sensitivity of these backward bifurcation phenomena (i.e., the sensitivity of R_1^*) to the cross-border mobility rate (η), the immunity loss rate of human (q), human recovery rate (γ_h), and mosquito death rate (d_v).

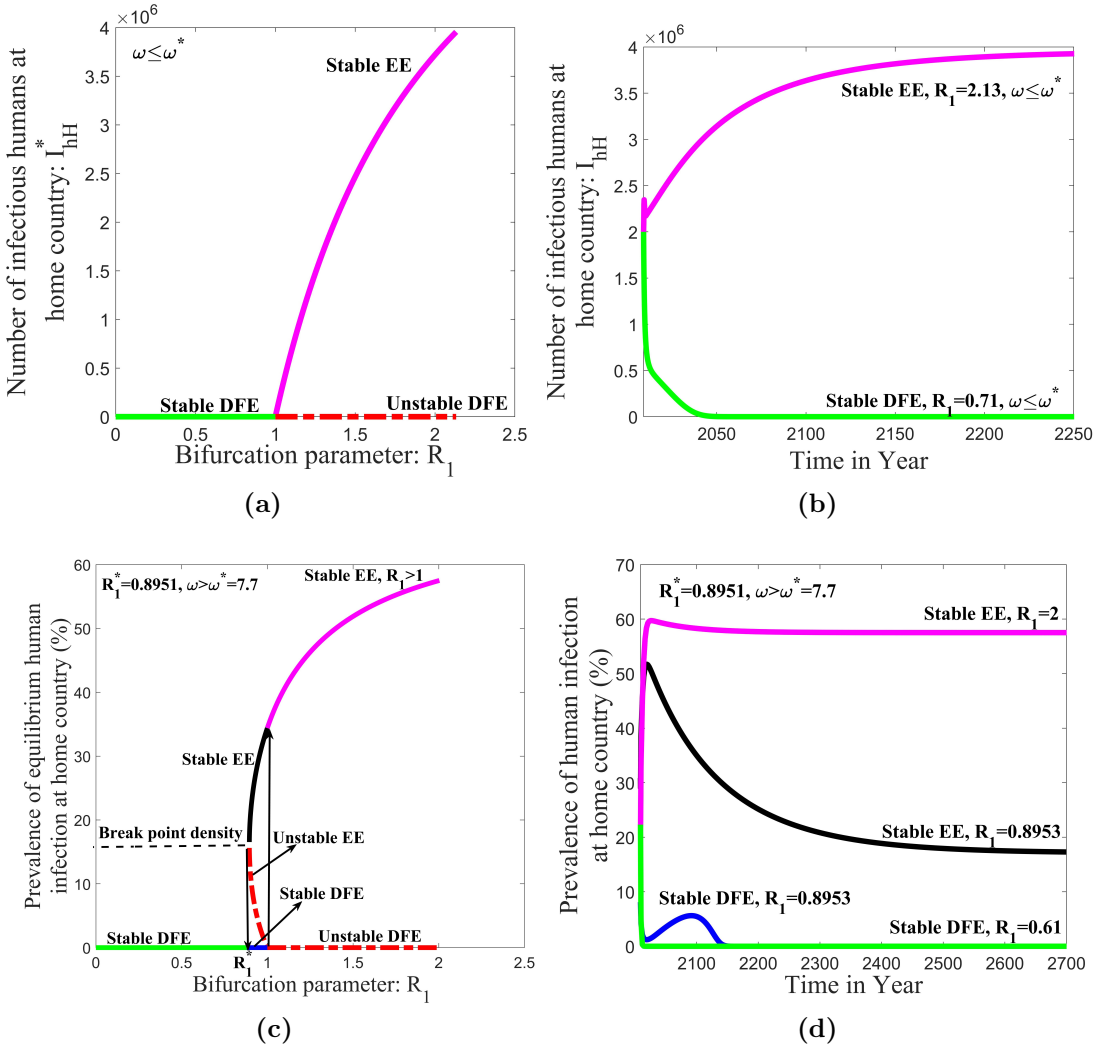

Figure 18: Bifurcation diagrams and time series solutions for $\delta_h = 0$, $\omega^* = 7.7$. (a) Forward bifurcation at $R_1 = 1$ when $\omega \leq \omega^*$ (here $\omega = 1$). (b) Model solutions verifying (a), where the model solution converges to the unique stable endemic equilibrium when $R_1 = 2.13$ ($R_1 > 1$) (end of the magenta curve) and converges to the stable disease-free equilibrium when $R_1 = 0.71$ ($R_1 < 1$) (end of the green curve), independent of initial conditions. (c) Backward bifurcation at $R_1 = 1$ with the transmission threshold $R_1^* = 0.8951, \omega > \omega^*$ (here $\omega = 25$). (d) Model solutions verifying (c); for $R_1 = 2 (R_1 > 1)$, the model solution converges to the unique stable endemic equilibrium (end of the magenta curve), and for $R_1 = 0.61 (R_1 < R_1^* < 1)$, the model solution converges to the unique stable disease-free equilibrium (end of the green curve), independent of initial conditions. However, for $R_1 = 0.8953 (R_1^* < R_1 < 1)$, the model solution converges to the endemic equilibrium (end of the black curve) when the initial prevalence is above the breakpoint density (dashed line), and the model solution converges to the disease-free equilibrium (end of the blue curve) when the initial prevalence is below the breakpoint density.

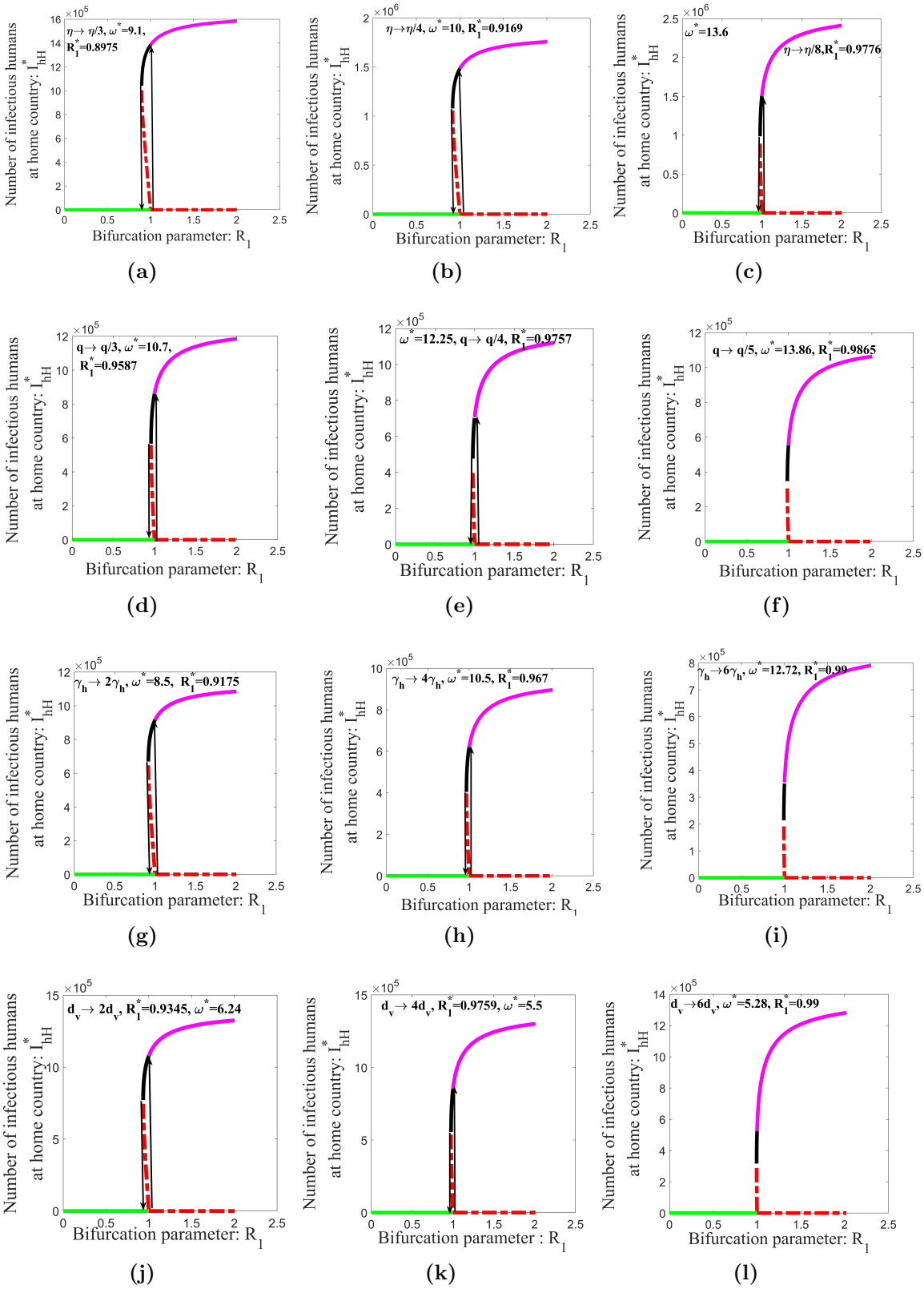

Figure 19: Sensitivity of the backward bifurcation threshold R_1^*.

Figure 19(a), (b), and (c) are for the reduction of the mobility rate (η) from its base value of 0.04 to 0.013, 0.01, and 0.005, respectively. (d), (e), and (f) are for the reduction of immunity loss rate q from its base value of 4 to 1.33, 1, and 0.8, respectively. (g), (h), and (i) are for the increment of human recovery rate γ_h from its base value of 1.85 to 3.7, 7.4 and 11.1, respectively. (j), (k), and (l) are for the increment of mosquito death rate d_v from its base value of 27 to 54, 108 and 162, respectively. If the mobility rate (η) is reduced to 0.013, 0.01, and 0.005 from its base value ($\eta = 0.04$), then the elimination threshold R_1^* increases towards 1 with its values $0.8975, 0.9169$, and 0.9776, respectively (Figure 19, 1st row). With this trend, the threshold R_1^* approaches one when $\eta \to 0$, transforming the backward bifurcation into a forward bifurcation at $\eta = 0$. This result is consistent with Theorem 4.3.2, which shows forward bifurcation for $\eta = 0,\ \delta_h = 0$. The reduction of the immunity loss rate (q) to 1.33 (loss of immunity in nine months), 1 (loss of immunity in one year), and 0.8 (loss of immunity for 15 months) from the base value ($q = 4$), the threshold R_1^* increases to 0.9587, 0.9757, and 0.9865, respectively (Figure 19, 2nd row).

Making the human recovery rate double (three-month recovery time), four-fold (45 days recovery time), and six-fold (27 days recovery time) from its base value $\gamma_h = 1.85$ per year (6.45 months recovery time) increases the thresholds R_1^* to 0.9175, 0.967, and 0.99, respectively (Figure 19, 3rd row). Similarly, making the mosquito mortality rate double, four-fold, and six-fold of its base value ($d_v = 27$) increases the threshold R_1^* to 0.9345, 0.9759, and 0.99, respectively (Figure 19, 4th row). From the 2nd, 3rd, and 4th rows of Figure 19, it is clear that in the presence of cross-border mobility and the absence of malaria transmission abroad ($\eta \neq 0, k = 0$), an increase in the parameters q, γ_h, or d_v increases the threshold R_1^* converging to 1 and transferring the backward bifurcation into the forward bifurcation.

4.3.2.2 Case-IIB: $\eta \neq 0,\ k \neq 0$

- *Equilibria Analysis*

Note that there is no disease-free equilibria in the presence of mobility and infection abroad ($\eta \neq 0,\ k \neq 0$). Here, the product of the roots of Eq. (4.9) is $\dfrac{-a_0}{a_3} > 0$, then Eq. (4.9) has either three positive roots or one positive root with two negative or a complex pair and corresponding endemic equilibria can be obtained from Eq. (3.22). We consider two sub cases: three endemic equilibria (Case-IIB1) and one endemic

equilibrium (Case-IIB2). Eq.(4.9) is transformed into

$$m^3 + cm + d = 0, \tag{4.17}$$

where $\lambda_h^* = m - \frac{a_2}{3a_3}$, $c = \frac{3a_3a_1 - a_2^2}{3a_3^2}$, $d = \frac{2a_2^3 - 9a_3a_2a_1 + 27a_3^2a_0}{27a_3^3}$ and the discriminant D of Eq. (4.17) is $-(4c^3 + 27d^2)$ Wikipedia (2023); Nickalls (2006); Zucker (2008). For the Case-IIB1, $D \geq 0$ (i.e. $c \leq 0$) together with $a_2 < 0$ and $a_1 > 0$ (Descart's rule of sign Eigenwillig (2007)), i.e.,

$$\frac{p_1}{p_2\alpha_{hv}\alpha_{vh}} < b^2 < \frac{p_3}{p_4\alpha_{hv}\alpha_{vh}}. \tag{4.18}$$

If $D = 0$ and $c = 0$, then $d = 0$. In this case, Eq. (4.17) has triple roots and hence Eq. (4.9) has triple positive roots $\lambda_h^* = \frac{-a_2}{3a_3}$. Again, if $D \geq 0$ and $c < 0$ then trigonometric identity

$$4\cos^3\alpha - 3\cos\alpha - \cos3\alpha = 0 \tag{4.19}$$

can be used to obtain three real roots of Eq. (4.17) (double root with one simple root or three distinct roots). Let $t = A\cos\alpha$, then Eq. (4.17) becomes

$$A^3\cos^3\alpha + cA\cos\alpha + d = 0. \tag{4.20}$$

Now, consider the trigonometric identity

$$4\cos^3\alpha - 3\cos\alpha - \cos3\alpha = 0. \tag{4.21}$$

Comparing Eq. (4.20) with Eq. (4.21), we get $\frac{4}{A^3} = \frac{-3}{Ac} = \frac{-\cos3\alpha}{d}$. It follows that $A = 2\sqrt{\frac{-c}{3}}$ and $\cos3\alpha = \frac{3d}{Ac} = \cos\phi$, where $\alpha = \frac{2n\pi \pm \phi}{3}$, and $\phi = \cos^{-1}\left(\frac{9d}{2c\sqrt{-3c}}\right) \in [0, \pi]$. Using the periodicity and even property of the cosine function, $n = 0,\ 1,\ 2$, we get three values of α and then three values of m and hence λ_h^* are $2\sqrt{\frac{-c}{3}}\cos\left(\frac{\phi}{3}\right) - \frac{a_2}{3a_3}$, $2\sqrt{\frac{-c}{3}}\cos\left(\frac{2\pi+\phi}{3}\right) - \frac{a_2}{3a_3}$, $2\sqrt{\frac{-c}{3}}\cos\left(\frac{4\pi+\phi}{3}\right) - \frac{a_2}{3a_3}$, where $\phi = \cos^{-1}\left(\frac{9d}{2c\sqrt{-3c}}\right) \in [0, \pi]$. In particular, if $\phi = 0$, then two of λ_h^* are equal. Now for Case-IIB2, there are two possibilities. (1) One positive λ_h^* exists with two negatives if $D \geq 0,\ c < 0$ together with $a_2 = 0,\ a_1 < 0$, or $a_2 > 0,\ a_1 = 0$, or $a_2 > 0,\ a_1 < 0$ (Descart's rule of sign Eigenwillig (2007)). The value of m and corresponding endemic equilibrium can be obtained using the trigonometric identity Wikipedia (2023); Nickalls (2006); Zucker (2008) as discussed in Case-IIB1. (2)

One positive λ_h^* exists with complex pair when $D < 0$. In this case, if $c = 0$, then $m = (-d)^{\frac{1}{3}}$ and $\lambda_h^* = (-d)^{\frac{1}{3}} - \frac{a_2}{3a_3}$. If $c \neq 0$ then the real root t can be obtained by using the sine or cosine hyperbolic identities according to $c > 0$ or $c < 0$. In each case, corresponding endemic equilibria can be obtained from Eq. (3.22).

- *Bifurcation Analysis (Case-IIB: $\eta \neq 0,\ k \neq 0$)*

As revealed in Eq. (4.18), mosquito biting rate b plays a vital role in the existence of three endemic equilibria when $D \geq 0$. Therefore, we took b as a bifurcation parameter. Note that there is no disease-free equilibrium or reproduction number to establish the threshold criteria. This causes the stability analysis of endemic equilibria to be mathematically untractable. Thus, we numerically demonstrated the possibility of one and three endemic equilibria and their stability. We also estimated the approximate threshold value of the mosquito biting rate (b) for the low endemic level, bi-stability, and high malaria endemic level in the home country of Nepal (Figure 20).

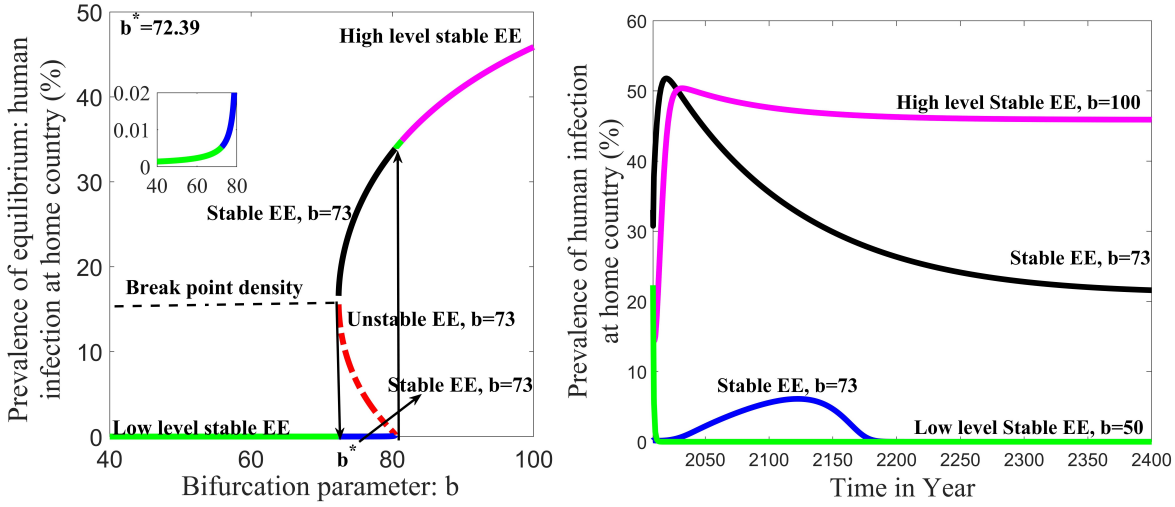

Figure 20: Bifurcation diagram and model solutions with $\delta_h = 0$. (a) Backward bifurcations showing the intervals of b for the existence of lower-level stable endemic equilibrium, bi-stability, and the existence of higher-level stable endemic equilibrium. The lower green section represents one stable endemic equilibrium, with a complex pair representing the lower level of stable endemic equilibrium of malaria in the home country that exists when $b < 72.39$. The upper green section (one endemic equilibrium with a complex pair) and the magenta section (one endemic equilibrium with two negative solutions), respectively, represent the higher level stable endemic equilibrium of malaria in the home country that exists when $b > 80$. The three endemic equilibria in bistability region ($72.39 < b < 80$) are represented by the blue, dotted red, and black lines. (b) Model solutions verifying the backward bifurcation (a), where the model solution converges to a higher level stable endemic equilibrium when $b = 100 (b > 80)$ (end of the magenta curve) and converges to a lower level stable endemic equilibrium when $b = 50 (b < b^*)$ (end of the green curve), regardless of the initial conditions. For $72.39 < b < 80$, bi-stability (ends of the black and blue curves) occurs, i.e., the solution converges to a higher endemic level or lower endemic level depending on the prevalence above or below the breakpoint density, respectively.

- *Sensitivity of Threshold for Malaria Burden (Case-IIB: $\eta \neq 0,\ k \neq 0$)*

In this section, we estimated the impacts of cross-border mobility rate (η), incidence rate abroad (k), mobility factor of infectious migrants (ω), loss of immunity rate (q), increase of mosquito death rate (d_v), and increase of human recovery rate (γ_h) on the threshold (b^*) to maintain lower endemic level, bi-stability, and the higher endemic level of malaria in Nepal (Figures 21 and 22).

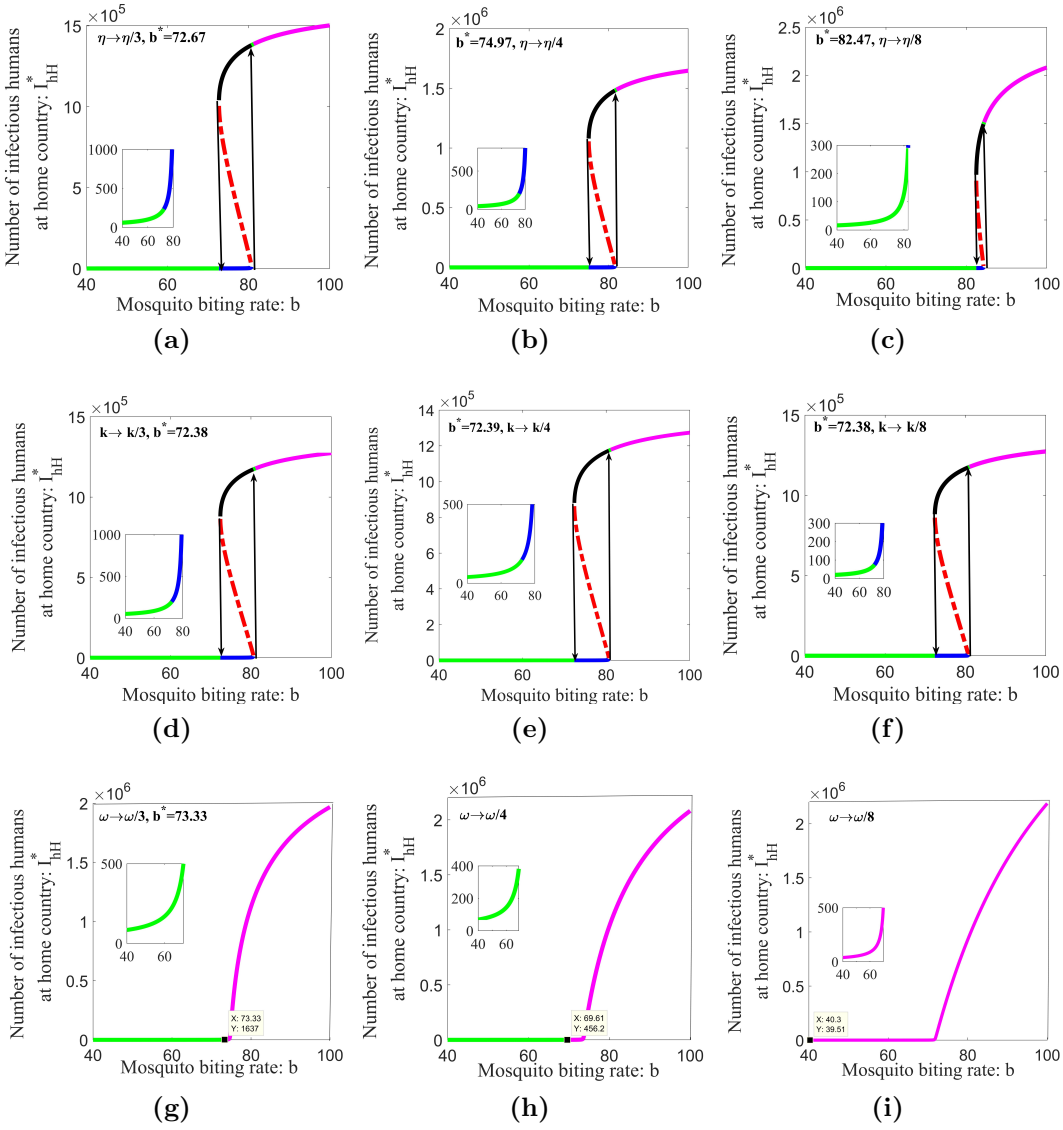

Figure 21: The sensitivity of threshold (b^*) for malaria burden to migration-related parameters with $\delta_h = 0$. (a), (b), and (c) are the successive reduction in mobility rate (η) to 0.013, 0.01 and 0.005, respectively, from its base value ($\eta = 0.02$). (d), (e), and (f) are the successive reduction in incidence rate abroad (k) to 0.000035, 0.000026 and 0.000013, respectively, from its base value ($k = 0.000105$). (g), (h), and (i) are the successive reduction in the mobility factor of infectious migrants (ω) to 8.33, 6.25, and 3.12, respectively, from its base value ($\omega = 25$).

If the mobility rate (η) is reduced to 0.013, 0.01, and 0.005 from its base value ($\eta = 0.04$), malaria can be maintained at a lower endemic level in the home country when the biting rate is less than threshold 72.67 (0.19 bites per day), 75 (0.20 bites per day), and 82 (0.22 bites per day), respectively (Figure 21, 1st row). Here, the range of bistability decreases as η decreases, and eventually, the region vanishes for

$\eta \to 0$, giving the smooth transition from the lower endemic level to the higher endemic level. However, the reduction of incidence rate abroad (k) to 0.000035, 0.000026, and 0.000013 from its base value ($k = 0.000105$) has a negligible impact on the threshold for malaria endemic level (Figure 21, 2nd row). Similarly, reducing the infectious migrants' mobility factor ω to 8.33 from its base value ($\omega = 25$) changes convergence to a higher endemic level to a lower endemic level, and further reduction to 6.25 and 3.15 allow the malaria epidemic to maintain at an even lower level in the home country (Figure 21, 3rd row).

With the reduction of the immunity loss rate (q) to 1.33 (loss of immunity in nine months), 1 (loss of immunity in one-year), and 0.5 (loss of immunity in two years) from its base value $q = 4$ (loss of immunity in three months), the malaria epidemic can be maintained at a lower level in the home country of Nepal when the biting rate is less than 77 (0.21 bites per day), 79 (0.21 bites per day), and 82 (0.22 bites per day), respectively (Figure 22, 1st row). Making the human recovery rate double (three-month recovery time), four-fold (45 days recovery time), and eight-fold (24 days recovery time) of its base value $\gamma_h = 1.85$ per year (about 6 months recovery time), the malaria epidemic can be maintained at a lower level with the controlled biting rate below 100 (0.27 bites per day), 142 (0.38 bites per day), and 1500 (4.1 bites per day), respectively (Figure 22, 2rd row). Similarly, when the biting rate remains below 213 (0.58 bites per day), 632 (1.7 bites per day), and 1500 (4.1 bites per day), making the mosquito mortality rate double (7 days life), four-fold (3.5 days life), and eight-fold (1.5 days life), respectively, of its base value ($d_v = 27$) helps maintain the malaria epidemic at a lower level (Figure 22, 3rd row). Here, decreasing q, increasing γ_h, or increasing d_v eventually provides a curve with smooth transitioning from lower to higher epidemic level.

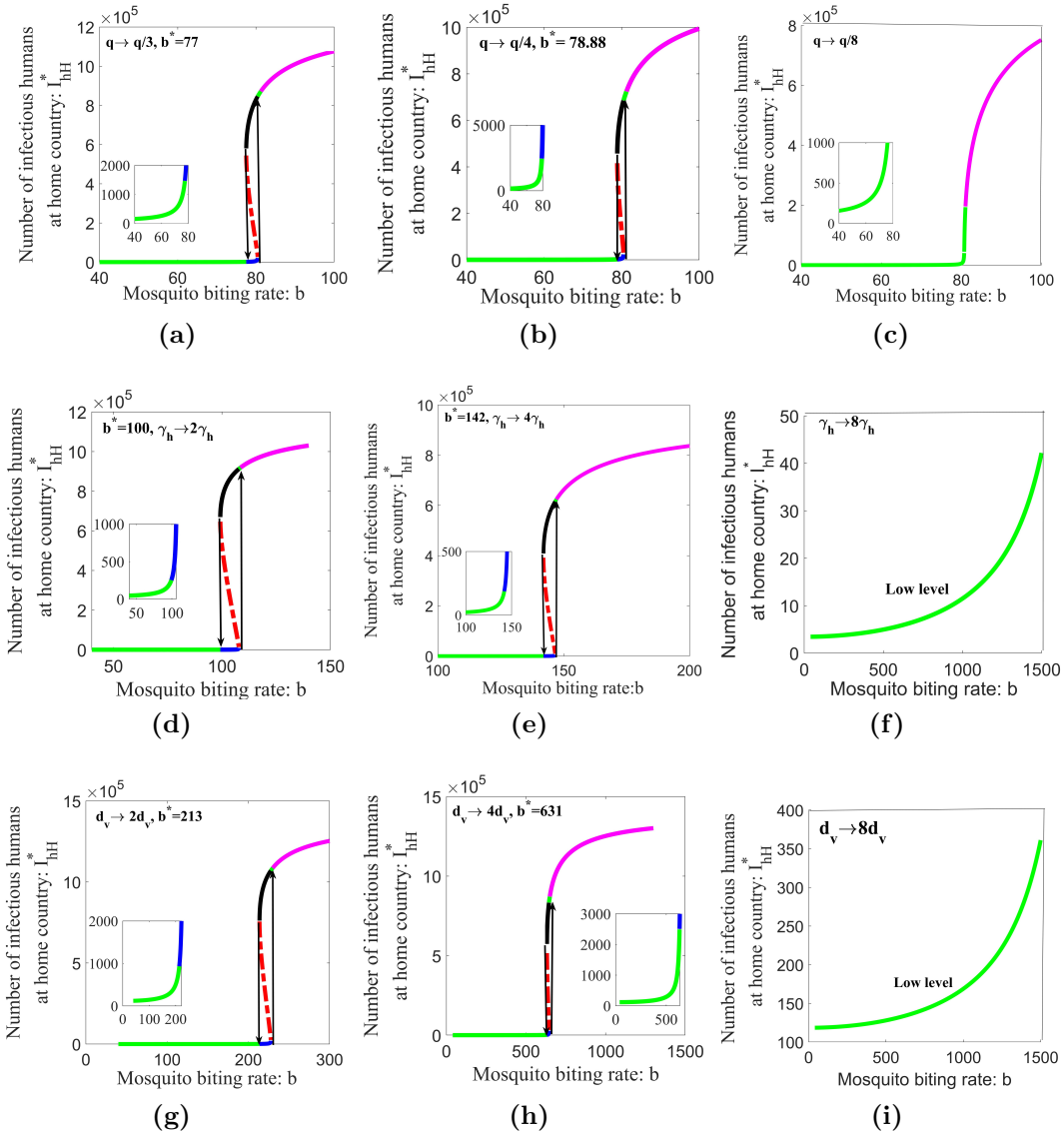

Figure 22: The sensitivity of threshold for malaria burden to humans and mosquito parameters for $\delta_h = 0$. (a), (b), (c) are the impact of the reduction of the immunity loss rate to 1.33, 1 and 0.5, respectively, of its base value q=4. (d), (e), (f) are the impact of two-fold, four-fold, and eight-fold of the recovery rate, respectively, of its base value ($\gamma_h = 1.85$). (g), (h), (i) are the impact of a two-fold, four-fold, and eight-fold increase in the mosquito death rate, respectively, from its base value ($d_v = 27$ i.e.,13.5 days lifetime of a mosquito).

Table 3: Summary of bifurcation analysis of malaria model with cross-border mobility. DFE: disease-free equilibrium, EE: endemic equilibrium, CB: cross-border, FB: forward bifurcation, BB: backward bifurcation, and GS: global stability.

Bifurcation Analysis of malaria model with cross-border mobility		
Case-I($\eta = 0$)	Case-IIA ($\eta \neq 0,\ k = 0$)	Case-IIB ($\eta \neq 0,\ k \neq 0$)
Absence of CB mobility	CB Mobility and protection	CB Mobility without protection
DFE exist	DFE exist	No DFE
FB if $0 \leq \delta_h \leq \delta_h^*$	FB if $\omega \leq \omega^*,\ \delta_h = 0$	One or three EE
BB if $\delta_h > \delta_h^*$	BB if $\omega > \omega^* > 1,\ \delta_h = 0$	Low-high, bi-stability
Elimination: $R_0 < R_0^*$	Elimination: $R_1 < R_1^*$	Endemic
GS, E^0: $R_0 < 1, \delta_h = 0$	GS, E^{01} : $R_1 < 1$, $\delta_h = 0, \omega = 0$	Endemic

4.4 Discussion

Malaria is a major public health challenge worldwide, with millions of cases reported annually, leading to a significant burden of illness and death Xing et al. (2020). Despite the efforts of many countries to eliminate malaria, cases are rising in many places, primarily due to the mobility of migrant workers WHO (2021). This indicates that local malaria control and intervention programs focused locally alone may not be enough to achieve the elimination goal. Therefore, a thorough analysis of why many countries with a long history of low malaria burdens struggle to achieve their elimination plan is necessary. We implemented an in-depth bifurcation analysis to evaluate the role of mobility in hindering the achievement of malaria elimination goals. Our ultimate focus is on the existence of a backward bifurcation, an interesting phenomenon in which the disease cannot be eliminated by simply reducing the basic reproduction number R_0 below unity; instead, another critical threshold R_0^* is required for the elimination of the disease.

Using the malaria model with cross-border mobility developed in our earlier study Gautam et al. (2022), we performed the bifurcation analysis, exploring two critical cases: the absence and presence of cross-border mobility. The condition for forward and backward bifurcation of our model in the lack of cross-border mobility is consistent with the results obtained for some other malaria models Xing et al. (2020); Chitnis et al. (2006); Wan and Cui (2009); Wang et al. (2018); Buonomo and Vargas-De-Leon (2013); kamel Naji and Adnan Thirthar (2020); Sha et al. (2019a). Specifically, the

disease-induced death rate (δ_h) is a primary driver for backward bifurcation. However, our advanced model with cross-border mobility establishes that mobility can be a vital factor responsible for backward bifurcation even without the diseases death. Our results underscoring mobility as a critical factor for backward bifurcation, even in the absence of disease death, significantly contributes to vector-borne diseases, providing a valuable tool to design mobility-focused controls for disease eradication.

Through our bifurcation analysis, we have established a mobility threshold ω^* of infectious migrants, such that the backward bifurcation does not occur in the absence of malaria transmission abroad ($\eta \neq 0, k = 0$) (Theorem 4.3.1.2) when the mobility factor of infectious migrants is below the threshold ($\omega \leq \omega^*$). Note that the mobility of infectious migrants can be reduced through the strict border screening implemented with collaboration between the home country and abroad, and our result on the threshold can help to identify the level of border screening required to avoid backward bifurcation. In this case, we also established a critical threshold R_1^* corresponding to a condition for eradicating disease (Theorem 4.3.3).

In the presence of malaria transmission abroad, our models show that malaria elimination is only possible in the home country unless cross-border mobility is allowed. In the presence of cross-border mobility, two epidemic levels (lower and higher) are possible, as revealed by numerical simulations of our model. We have conducted detailed simulations to identify threshold conditions, depending on various parameters, that help us maintain the epidemic at a lower level. In particular, the mosquito biting rate, which may vary with location, season, and mosquito type, as a bifurcation and control parameter, is one of the determinant factors of whether the epidemic stays at the lower or higher level. It is worth noting that the current status of malaria in Nepal, as predicted by our model with current parameters of Nepal (Table 2), is at the low endemic level but struggles to achieve the elimination goal due to cross-border mobility.

We acknowledge some limitations of our study. We were not able to prove the global stability of the endemic equilibrium for $R_0 > 1$ and $R_1 > 1$ analytically. Instead, we showed persistence for $R_0 > 1$ and $R_1 > 1$ in our previous study Gautam et al. (2022). We could not provide analytical proof of the stability of one or three endemic equilibria when there is a presence of mobility and infection abroad. However, taking the wide range of parameters, we numerically demonstrated the stability of lower and upper endemic equilibria and the instability of the middle endemic equilibrium. Furthermore, our model approximated the incidence rate abroad, keeping the mosquitos role in the

disease spread abroad constant. Analysis of the model with the entire transmission dynamics through mosquitoes abroad as in the home country would provide broad opportunities for model analysis and produce more advanced results.

In summary, we studied in detail how backward bifurcation arises due to the cross-border mobility of migrant workers in the malaria dynamics model. Our central result on the role of mobility in backward bifurcation provides a novel insight into the cross-border mobility rate impacting the persistence and eradication of malaria in the home country. Our results may aid in developing effective malaria elimination strategies for countries like Nepal with low local malaria transmission but vulnerable to obstacles to eradication due to the cross-border mobility across other high epidemic countries. The following are the major conclusions:

1. Cross-border mobility is a primary driver of backward bifurcation.
2. Without cross-border mobility, malaria can be eliminated from Nepal due to negligible disease induced death rate.
3. With mobility, malaria can be eliminated if there is complete protection abroad and controlled mobility rates of infectious migrants below a certain threshold.
4. Cross-border mobility without protection abroad and without border screening, home country can maintains malaria at low levels, but elimination is not possible.

In Chapter 3 and Chapter 4, we discussed about the problem of cross-border mobility and its impact on malaria elimination program of low malaria endemic countries like Nepal. Now in recent years government of Nepal initiated the cross-border collaboration with its neighboring country India for the restriction of imported cases of malaria. If in the best case scenario, there exist the perfect cross-border collaboration then for the complete elimination, the government of Nepal should focus on the relapse case of Vivax malaria which cover almost 90% malaria cases in Nepal. Thus, in the Chapter 5 we will develop and analyze the delay malaria model including the relapses proportion and relapse delay.

CHAPTER 5

5. MODELING MALARIA TRANSMISSION WITH RELAPSE DELAY: IMPACT ON ELIMINATION PLAN OF LOW ENDEMIC COUNTRIES

In this chapter, we discussed about the relapse issue of vivax malaria and its impact on malaria elimination plan of Nepal and other low malaria endemic countries. Although the vivax malaria-infected humans looks like recovered after clearance of blood-stage malaria parasites, there is a high potential for reinfection due to the reactivation of dormant hypnotizes in the liver, even in the absence of mosquito bites. Therefore, achieving the goal of malaria elimination is becoming critical in many countries, including Nepal. In this study, we develop, for the first time, a malaria model that includes relapse delay. Results from thorough mathematical analyses and numerical simulations using malaria parameters from Nepal show that the relapse proportion and relapse delay can play a significant role in malaria dynamics; specifically, increasing relapse delay extends the time to achieve malaria-free equilibrium when $R_0 < 1$. Our model and the related results provide new insights and may help develop strategies to eliminate malaria, including in Nepal.

5.1 Introduction

Malaria remains a significant global health challenge, caused by a protozoan parasite from the genus Plasmodium and transmitted by infected female Anopheles mosquitoes. Malaria in humans is caused by four types of parasites: Plasmodium falciparum (P. falciparum), Plasmodium vivax (P. vivax), Plasmodium malariae (P. malariae), and Plasmodium ovale (P. ovale) Kammanee and Tansuiy (2019). Millions of individuals are affected each year, with vulnerable populations such as children under five, pregnant women, travelers to endemic regions without protection, and those with underlying health conditions like HIV or diabetes being particularly impacted Tasman et al. (2022).

While substantial progress has been made in reducing P. falciparum infections, the reduction of P. vivax and P. ovale infections has proven more challenging. A key factor contributing to this difficulty is the unique ability to relapse from dormant

liver forms, leading to recurrent symptoms weeks or even years after initial treatment Nickalls (2006). Therefore, a patient formerly infected by P. vivax can appear cured but may become infected again without any mosquito bites Kammanee and Tansuiy (2019). This persistence of malaria relapse poses a sustained hurdle for countries in the elimination phase of malaria, including Nepal.

Plasmodium vivax has a complex life cycle compared to other malaria parasites. When an infected mosquito bites a human, it injects sporozoites into the bloodstream. These sporozoites travel to the liver, where they multiply into merozoite and hypnozoite forms. Illness occurs when merozoites invade red blood cells, causing symptoms like fever and chills. Hypnozoites, dormant in the liver, can cause no symptoms initially but may reactivate as merozoites, leading to recurring illness Kammanee and Tansuiy (2019).

These relapses tend to occur more rapidly in tropical regions (i.e., three to six weeks) compared to temperate areas (i.e., six to twelve months) Battle et al. (2014). Additionally, in places where malaria is common, many people may have dormant hypnozoites in their bodies, which can be triggered by illnesses like vivax or falciparum malaria. This explains why vivax malaria often occurs after falciparum malaria, why different genetic types show up during relapses, and why relapse rates are higher in endemic areas compared to controlled areas. The long latency of P. vivax cases may be more widespread than previously believed, substantially hindering efforts to control and combat malaria Tasman et al. (2022); Agyingi et al. (2017); White (2011).

In 2021, the nine countries of the WHO South-East Asia Region contributed 5.4 million cases of malaria. India alone accounted for approximately 79% of all malaria cases in the South-East Asia Region, with P. vivax responsible for 40% of the cases in the region Organization et al. (2022). Malaria, driven by factors like global warming, has spread to hilly and mountainous regions in Nepal, including districts like Mugu, Bajura, and Humla. In 2022, total malaria cases in Nepal were 1917. These cases have now been documented in 51 districts from all seven provinces out of 77 districts of Nepal Post.

In Nepal, P. vivax is the predominant cause of malaria (80% Rijal et al. (2019b)), and it shares co-endemic status with P. falciparum in districts with high malaria prevalence where about 17% of vivax malaria cases are due to relapse during six months Manandhar et al. (2013). The percentage of relapse varies from 4.1% to 28.2%, and in the worst case, up to 90%, depending on the types of malaria treatment

Chloroquine (CQ) only, Chloroquine followed by Primaquine (PQ) , follow-up programs, and many other factors Rijal et al. (2019b); Chu and White (2016).

The literature on malaria modeling begins with Ross (1911) Ross (1911), MacDonald (1957) Macdonald et al. (1957), Anderson and May (1991) Anderson and May (1991b), Tumwiine (2007) Tumwiine et al. (2007), and other researchers who developed mathematical models considering various factors associated with malaria dynamics Traore et al. (2020); Tumwiine et al. (2010); Handari et al. (2019); Wan and Zhu (2012); Aldila (2021); Herdicho et al. (2021); Tasman et al. (2021); Handari et al. (2022); Olaniyi et al. (2022). The first mathematical model to describe the transmission dynamics of P. vivax is Kammanee et al. (2001). This research focuses on the reproduction number, dividing the human population into four compartments. The study Huo et al. (2014) performed stability analysis introducing the model with relapse in vivax infections.

The studies Chamchod and Beier (2013); Ghosh et al. (2020); Wang et al. (2021) developed and analyzed ODE models with reinfection, with recurrent infection, and relapse of vivax malaria. These studies did not incorporate the time delay in disease transmission. The study Wei et al. (2008) formulated an epidemic model of a vector-borne disease with time delay, derived the reproduction number, and discussed the theory of Hopf-bifurcation. Similarly, the studies Chamchod and Britton (2011); Wan et al. (2013) have developed delay malaria models focusing on P. falciparum, including delay corresponding to incubation periods in humans and mosquitoes during malaria transmission.

Existing malaria models using Delay Differential Equation (DDE) have addressed time delays corresponding to incubation periods in mosquito infection Agyingi et al. (2017); Elsheikh et al. (2014); Ngwa et al. (2010), in human infection Chiyaka et al. (2011), and both human and mosquito infection Agyingi et al. (2017). Additionally, the studies Hu et al. (2019); Qiang and Wang (2017); Koutou et al. (2018); Wei et al. (2008); Ruan et al. (2008); Zhang et al. (2020); Pongsumpun and Tang (2007); Wang and Zhao (2017) focused on delay malaria models considering various factors associated with malaria dynamics. However, to the best of our knowledge, there is a gap in modeling the delay due to the reactivation of dormant liver stage vivax parasites. These reactivations cause relapses.

Understanding malaria dynamics due to relapse is urgently needed to assist policy-makers aiming to successfully eliminate malaria. Thus, in this study, we developed and analyzed a mathematical model that incorporates relapse delays, as well as delays

in human-mosquito exposure and immunity loss.

5.2 Method

5.2.1 Mathematical Model

To develop a mathematical model of the transmission dynamics of malaria that incorporates a constant relapse delay, we divide the total human population at risk (N_h) into three distinct groups: those who are susceptible to malaria (S_h), individuals infected with a primary infection (I_p), and those who are infectious due to a relapse of the disease (I_r). Individuals who have completely recovered from a previous malaria infection gradually lose their immunity over time. This immunity loss is characterized by a delay period, τ_1, which ranges from 3 months to fifty years Chitnis et al. (2008). Individuals who have recovered from a previous malaria infection, during which they harbored dormant liver-stage parasites, become re-infectious after a latent period of τ_2. This delay can vary from two weeks to two years White (2011). A person who survives this latent period may experience a relapse or multiple relapses from these dormant parasites.

The female Anopheles mosquito population is divided into two distinct groups: susceptible mosquitoes (S_v) and infectious mosquitoes (I_v). Humans who have been exposed to infectious mosquitoes become infectious themselves after a certain duration, τ_3, which can last from 7 to 90 days Chitnis et al. (2008). A person who survives this duration may develop an active infection and transmit the disease. Mosquitoes that have previously fed on infectious humans become infectious themselves after a span of τ_4, which typically ranges from 10 to 20 days Chitnis et al. (2008). If a mosquito survives this duration, it can transmit malaria parasites to a human host during its next bite.

The rates of human recruitment into the susceptible group and mosquito recruitment into the susceptible group are denoted as Λ and ϕ, respectively. Furthermore, the per capita mosquito biting rate is b, while α_{vh} and α_{hv} are the probabilities of malaria transmission per bite from infectious mosquitoes to susceptible humans and from infectious humans to susceptible mosquitoes, respectively. For the sake of model simplification, we have assumed the same transmission rate from both types of infectious humans (i.e., those with primary infections and those with relapses). Hence, $\beta_h = b\alpha_{vh}$ and $\beta_v = b\alpha_{hv}$ are the transmission rates in humans and mosquitoes, respectively. The

natural and disease-induced death rates of humans are d_h and δ_h, respectively, and the natural death rate of mosquitoes is d_v. Thus, the incidence rates in humans and mosquitoes are
$\frac{\beta_h I_v(t-\tau_3)S_h(t-\tau_3)e^{-d_h\tau_3}}{N_h(t-\tau_3)}$ and $\frac{\beta_v\left(I_p(t-\tau_4)+I_r(t-\tau_4)\right)S_v(t-\tau_4)e^{-d_v\tau_4}}{N_h(t-\tau_4)}$, respectively.

Let ω be the recovery rate of humans, such that after clearance of the malaria parasites from blood, the individual is no longer infectious to a susceptible mosquito but may have hypnozoites in the liver. Among ωI_p, the portion $(1-\epsilon)\omega I_p$, who has cleared malaria parasites from both the blood and liver, moves back to the susceptible class (S_h), losing immunity with delay τ_1. The remaining portion $\epsilon\omega I_p$, who have liver stage parasites, go to the relapse class (I_r), provided that they survive during the time delay τ_2. Thus, parameters ϵ and ϵ_1 are the proportions of the first relapse and multiple relapses, respectively, with delay τ_2. The schematic diagram of the model is given in Figure 23.

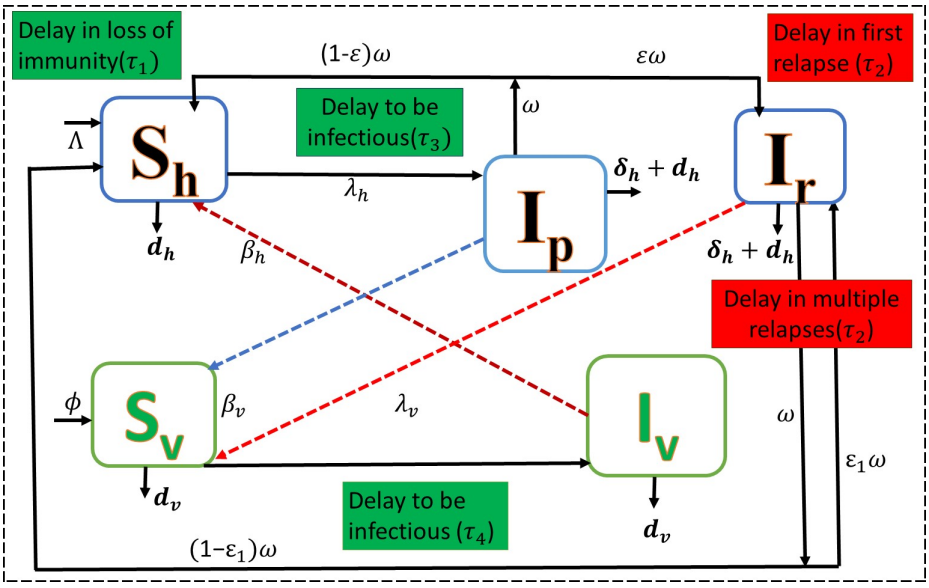

Figure 23: Schematic diagram of the model. The model consists of three human sub-populations: susceptible humans (S_h), infectious humans with primary infection (I_p) (i.e., from the bites of infectious mosquitoes), and infectious humans due to relapses (I_r) (i.e., from the reactivation of dormant stage hypnozoites). Similarly, there are two mosquito subpopulations: susceptible mosquitoes (S_v) and infectious mosquitoes (I_v). The proportions of first-time relapse and multiple relapses are given by ϵ and ϵ_1, respectively. Solid lines represent transitions between susceptible and infectious states in both humans and mosquitoes, which also include the dynamics of relapses and the loss of immunity in humans. Dotted lines represent the interactions between susceptible humans and infectious mosquitoes, as well as the interactions between susceptible mosquitoes and infectious humans. The delay due to waning immunity is τ_1, the delay in single and multiple relapses is τ_2, and the delays in human and mosquito infection are τ_3 and τ_4, respectively.

The model is described by the following set of delay-differential equations:

$$S_h'(t) = \Lambda + (1-\epsilon)\omega I_p(t-\tau_1)e^{-d_h\tau_1} + (1-\epsilon_1)\omega I_r(t-\tau_1)e^{-d_h\tau_1} - \frac{b\alpha_{vh}I_v(t)}{N_h(t)}S_h(t) - d_hS_h(t), \tag{5.1}$$

$$I_p'(t) = \frac{b\alpha_{vh}I_v(t-\tau_3)e^{-d_h\tau_3}}{N_h(t-\tau_3)}S_h(t-\tau_3) - (d_h+\delta_h+\omega)I_p(t), \tag{5.2}$$

$$I_r'(t) = \epsilon\omega I_p(t-\tau_2)e^{-d_h\tau_2} + \epsilon_1\omega I_r(t-\tau_2)e^{-d_h\tau_2} - (d_h+\delta_h+\omega)I_r(t), \tag{5.3}$$

$$S_v'(t) = \phi - \frac{b\alpha_{hv}\left(I_p(t)+I_r(t)\right)}{N_h(t)}S_v(t) - d_vS_v(t), \tag{5.4}$$

$$I_v'(t) = \frac{b\alpha_{hv}\left(I_p(t-\tau_4)+I_r(t-\tau_4)\right)e^{-d_v\tau_4}}{N_h(t-\tau_4)}S_v(t-\tau_4) - d_vI_v(t). \tag{5.5}$$

All the parameters involved in the system (5.1-5.5) are assumed to be non-negative.

The Epidemiology and Disease Control Division, Nepal and our previous study Gautam et al. (2022) highlights imported malaria cases as the main obstacle to Nepal's 2025 elimination target. To address this, the Ministry of Health and Population initiates cross-border collaboration with India, particularly Uttar Pradesh, to curb the influx of cases. Majority of imported cases stem from Nepali migrant workers in Maharashtra and Gujarat. Coordination efforts with Indian states are underway to tackle this challenge effectively Nepal (2022). Thus, we simulate the model to verify the analytical results and to predict local malaria trends in Nepal during the years 2023-2026 assuming no further imported cases after 2023. Our simulation based on the parameters from our previous study Gautam et al. (2022) and available information described below and shown in the Table 4. In the base year 2022, total malaria cases in Nepal were 1917 Post, of which 1764 (92% Rijal et al. (2018); WHO (2023)) were vivax malaria, among which 300 (17% Manandhar et al. (2013)) were infections from relapses within one year.

Among about 30,000,000 population of Nepal in 2022 Gaigbe-Togbe et al., an estimated 8.2 million people are at risk of malaria, as per WHO Nepal (2022). We assumed that the mosquito population is five times higher than the human population Xiulei et al. (2020) and $S_h(0) = 8,198,083$, $I_p(0) = 1617$, $I_r(0) = 300$, $S_v(0) = 40,990,415$, $I_v(0) = 9585$. Here total human population $(N_h) = 8,200,000$, and the crude birth rate of Nepal (in 2022) is 20.2 per year per 1000 population, and so the human recruitment per day (Λ) = Crude Birth Rate per day per individual $\times$ Population at risk = $\frac{20.2 \times 8,200,000}{1000 \times 365} = 454$ per day. Natural death rate of humans $(d_h) = \frac{1}{70 \times 365}$, average lie span of Nepalese people for the year 2022 is 70 years Gaigbe-Togbe et al.. Total mosquito population is (N_v) =Five times Human population at risk Xiulei et al. (2020). Then the mosquito recruitment rate per day was taken as $(\phi) = N_v \times$ birth rate of mosquito per day $\left(\frac{1}{14}\right) = 2,928,571$. The delay time for relapsing varies from two weeks to two years, depending on the type of treatment followed by follow-up programs, location, age, and immunity. The percentage of relapsing in the context of Nepal varies form 4% to 28% in one year Manandhar et al. (2013); Ruan et al. (2008); Rijal et al. (2018).

The descriptions of parameters are given in Table 4.

Table 4: Description of malaria parameters in Nepal

Description	Sym.	Base value
Transmission probability from mosquito to human, per bite	α_{vh}	0.0195 Gautam et al. (2022)
Transmission probability from human to mosquito, per bite	α_{hv}	0.63 Gautam et al. (2022)
Human recruitment rate	Λ	454 day^{-1} (Cal.)
Mosquito recruitment rate	ϕ	2,928,571 day^{-1}(Cal.)
Per capita recovery rate of humans	ω	$\frac{1}{30}$day^{-1} (Assu.)
Per capita natural birth and death rate of mosquitoes	d_v	$\frac{1}{14}$ day $^{-1}$(Assu.)
Per capita disease-induced death rate of humans	δ_h	4.68×10^{-6} day^{-1} Gautam et al. (2022)
Per capita natural death rate of humans	d_h	3.91×10^{-5}day^{-1} (Cal.)
Proportion of first relapse	ϵ	0.28 (Rijal et al. (2019b)) 0.9 Chu and White (2016)
Proportion of multiple relapse	ϵ_1	0.14 (Rijal et al. (2019b))
Immunity waning period	τ_1	365 days (Assu.)
Relapse delay	τ_2	180 days (Assu.)
Latent delay (humans)	τ_3	30 days (Assu.)
Latent delay (mosquitoes)	τ_4	20 days (Assu.)
Biting rate per mosquito	b	0.13 day^{-1} Gautam et al. (2022)

5.3 Results

5.3.1 Existence and Uniqueness of Solutions

Consider $\Omega = \{(x_1,\ x_2,\ x_3,\ x_4,\ x_5) : x_i \geq 0, i = 1,2,3,4,5\} \subset \mathbb{R}^5$ and $\tau_m = \max\{\tau_1, \tau_2, \tau_3, \tau_4\}$. The initial conditions (history function) for the model system (5.1-5.5) are:

$$S_h(t) = \phi_1(t),\ I_p(t) = \phi_2(t),\ I_r(t) = \phi_3(t),\ S_v(t) = \phi_4(t),\ I_v(t) = \phi_5(t) \qquad (5.6)$$

with $\phi_i(t) \geq 0$ and $\phi_i(0) > 0$ for $i = 1,2,3,4,5$, and $t \in [-\tau_m, 0)$ and $(\phi_1, \phi_2, \phi_3, \phi_4, \phi_5) \in C([-\tau_m, 0], \Omega)$, where $C([-\tau_m, 0], \Omega)$ be the Banach Space of continuous functions defined from $[-\tau_m, 0]$ to Ω with supremum norm. According to the fundamental theory

of functional differential equations Hale and Lunel (2013), the system with initial conditions admits a unique solution.

5.3.2 Positivity and Boundedness of Solutions

Now, we establish the following theorems regarding the system's positivity and boundedness of solutions.

Theorem 5.3.1 *All the solutions of the system (5.1-5.5) with initial conditions* $S_h(0) > 0, S_v(0) > 0$*, together with* $I_p(0), I_r(0), I_v(0) \geq 0$ *are positive for* $t > 0$.

Proof: We apply the method of contradiction to show the positivity of the solutions to the system (5.1-5.5) as in Vaidya and Peter (2021); Chen et al. (2016); Diabate et al. (2022). First we show that, $S_v(t) > 0$ for all $t > 0$. Suppose $S_v(t) > 0$ is not possible for all $t > 0$, then there exist first time point $t = t_v > 0$ such that $S_v(t_v) = 0$. Then from the Eq. (5.4), we get $S_v'(t)|(t = t_v) = \phi > 0$. It follows that there is a constant η small enough such that $S_v(t) < 0$ for $t_v - \eta < t < t_v$, which contradicts the fact that $S_v(t) > 0$ for $t_v - \eta < t < t_v$ and $S_v(t_v) = 0$ for the first time. Thus $S_v(t) > 0$ for all $t > 0$.
Next, we show that, $S_h(t) > 0$ for all $t > 0$. Suppose that $S_h(t) > 0$ for all $t > 0$ is not possible, then there exist $t = t_s > 0$ (first time point) such that $S_h(t_s) = 0$, then from Eq. (5.1), we get $S_h'(t)|(t = t_s) = \Lambda + (1-\epsilon)\omega I_p(t_s - \tau_m)e^{-d_h\tau_m} + (1-\epsilon_1)\omega I_r(t_s - \tau_m)e^{-d_h\tau_m}$. Let $t_I = t_s - \tau_m$. Now we claim $(1-\epsilon)\omega I_p(t_I)e^{-d_h\tau_m} + (1-\epsilon_1)\omega I_r(t_I)e^{-d_h\tau_m}$ can not be negative. Suppose if possible $(1-\epsilon)\omega I_p(t_I)e^{-d_h\tau_m} + (1-\epsilon_1)\omega I_r(t_I)e^{-d_h\tau_m} < 0$. Then there exist first time point t_p $(0 < t_p < t_I < t_s)$ such that at least one of $I_p(t_p), I_r(t_p)$ should be zero. i.e., $\min\{I_p(t_p), I_r(t_p)\} = 0$. If $I_r(t_p) = 0$ and $I_p(t_p) \geq 0$, then from the Eq. (5.3), $I_r'(t)|(t = t_p) = \epsilon\omega I_p(t_p - \tau_m)e^{-d_h\tau_m} + \epsilon_1\omega I_r(t_p - \tau_m)e^{-d_h\tau_m} > 0$. Which contradicts t_p is the first time point such that $I_r(t_p) = 0$. Therefore, $I_r(t_p) > 0$. Similarly, we can show that $I_p(t_p) > 0$ and contradicts our assumption $(1-\epsilon)\omega I_p(t_I)e^{-d_h\tau_m} + (1-\epsilon_1)\omega I_r(t_I)e^{-d_h\tau_m} < 0$. Therefore, $S_h'(t)|(t = t_s) = \Lambda + (1-\epsilon)\omega I_p(t_s - \tau_m)e^{-d_h\tau_m} + (1-\epsilon_1)\omega I_r(t_s - \tau_m)e^{-d_h\tau_m} > 0$. It follows that there is a constant ζ small enough such that $S_h(t) < 0$ for $t_s - \zeta < t < t_s$, which contradicts the fact that $S_h(t) > 0$ for $t_s - \zeta < t < t_s$ and $S_h(t_s) = 0$ for the first time. Thus $S_h(t) > 0$ for all $t > 0$. Similarly, using the same approach, we can show that $I_p(t) > 0,\ I_r(t) > 0, I_v(t) > 0$ for all $t > 0$. Hence, the solution set $\{S_h, I_p, I_r, S_v, I_v\}$ of the system (5.1-5.5) is always non-negative. □
We now prove that these non-negative solutions are bounded in Theorem 5.3.2.

Theorem 5.3.2 *All the solutions of the system (5.1-5.5) with initial conditions* $S_h(0) > 0, S_v(0) > 0$*, together with* $I_p(0), I_r(0), I_v(0) \geq 0$*, are bounded for* $t > 0$*.*

Proof: Now, we show that the mosquito population is bounded for all time t.
We denote $V(t) = S_v(t) + I_v(t + \tau_4)$, then using the system (5.4-5.5), we get

$$V'(t) \quad = \phi - \frac{b\alpha_{hv}\left(I_p(t) + I_r(t)\right)}{N_h(t)} S_v(t)\left(1 - e^{-d_v\tau_4}\right) - d_v V(t).$$

Since $\frac{b\alpha_{hv}\left(I_p(t) + I_r(t)\right)}{N_h(t)} S_v(t)\left(1 - e^{-d_v\tau_4}\right) \geq 0$, then, we have a linear differential equation, $V'(t) \leq \phi - d_v V(t)$. Solving, we get $V(t) \leq \frac{\phi}{d_v}\left(1 - e^{-d_v t}\right) + V(0)e^{-d_v t}$. Taking $t \to \infty$, $N_v(t) = V(t) \leq \frac{\phi}{d_v}$. Hence, the mosquito population, $N_v(t)$, is ultimately bounded all the time.
For the human population, taking $H(t) = S_h(t + \tau_m) + I_p(t + 2\tau_m) + I_r(t + \tau_m)$, then from the system (5.1-5.3), we have

$$\begin{aligned} H'(t) \qquad &= \Lambda + (1-\epsilon)\omega I_p(t)e^{-d_h\tau_m} + (1-\epsilon_1)\omega I_r(t)e^{-d_h\tau_m} - d_h S_h(t+\tau_m) \\ &- \frac{b\alpha_{vh} I_v(t+\tau_m)\left(1 - e^{-d_h\tau_m}\right)}{N_h(t+\tau_m)} S_h(t+\tau_m) - (d_h + \delta_h + \omega) I_p(t + 2\tau_m) + \\ &\epsilon\omega I_p(t)e^{-d_h\tau_m} + \epsilon_1\omega I_r(t)e^{-d_h\tau_m} - (d_h + \delta_h + \omega) I_r(t + \tau_m). \end{aligned}$$

Since $\frac{b\alpha_{vh} I_v(t+\tau_m)\left(1 - e^{-d_h\tau_m}\right)}{N_h(t+\tau_m)} S_h(t + \tau_m) \geq 0$, then

$$\begin{aligned} H'(t) \quad &\leq \Lambda - d_h H(t) + \epsilon\omega I_p(t)e^{-d_h\tau_m} + \epsilon_1\omega I_r(t)e^{-d_h\tau_m} \\ &-(\omega + \delta_h) I_p(t + 2\tau_m) - (\delta_h + \omega) I_r(t + \tau_m). \end{aligned}$$

Now there are two cases:
Case(i): If $\epsilon\omega I_p(t)e^{-d_h\tau_m} + \epsilon_1\omega I_r(t)e^{-d_h\tau_m} \leq (\omega + \delta_h) I_p(t + 2\tau_m) + (\delta_h + \omega) I_r(t + \tau_m)$. It follows that

$H'(t) < \Lambda - d_h H(t)$ and $H(t) \leq \frac{\Lambda}{d_h}\left(1 - e^{-d_h t}\right) + H(0)e^{-d_h t}$, hence for $t \to \infty$, $N_h(t) = H(t) \leq \frac{\Lambda}{d_h}$.

Case (ii): If $(\omega+\delta_h) I_p(t+2\tau_m)+(\delta_h+\omega) I_r(t+\tau_m) < \epsilon\omega I_p(t)e^{-d_h\tau_m}+\epsilon_1\omega I_r(t)e^{-d_h\tau_m}, \forall t$. Then, it follows that

$$I_p(t + 2\tau_m) + I_r(t + \tau_m) \quad < \frac{\epsilon\omega I_p(t)e^{-d_h\tau_m} + \epsilon_1\omega I_r(t)e^{-d_h\tau_m}}{(\omega + \delta_h)} < \epsilon I_p(t)e^{-d_h\tau_m} + \epsilon_1 I_r(t)e^{-d_h\tau_m} < I_p(t) + I_r(t).$$

Therefore, $I_p(t+2\tau_m) < I_p(t), I_r(t+\tau_m) < I_r(t)$ and ensure both $I_p(t)$ and $I_r(t)$ are strictly decreasing functions. In addition, both $I_p(t)$ and $I_r(t)$ are non-negative, so both are bounded. Now, using boundedness of $I_p(t)$ and $I_r(t)$ in the Eq. (5.1), $S_h(t)$ is also bounded. Thus, the human population $N_h(t)$ is also bounded. □

5.3.3 Existence of Equilibria

At equilibrium, the system is not of delay equations but of non-linear algebraic equations. Let $\left(S_h^*, I_p^*, I_r^*, S_v^*, I_v^*\right)$ be an equilibrium solution of the system (5.1-5.5). Then, solving the system, we get

$$
\begin{aligned}
S_h^* &= \frac{\Lambda\left(d_h+\delta_h+\omega\right)e^{d_h\tau_1+d_h\tau_3}\left(\delta_h e^{d_h\tau_2}+d_h e^{d_h\tau_2}+\omega\left(e^{d_h\tau_2}-\epsilon_1\right)\right)}{Q_2\lambda_h^*+Q_1}, \qquad (5.7)\\
I_p^* &= \frac{\Lambda\lambda_h^* e^{d_h(\tau_1+\tau_2)}\left(\omega(1-\epsilon_1 e^{-d_h\tau_2})+d_h+\delta_h\right)}{Q_2\lambda_h^*+Q_1},\\
I_r^* &= \frac{\Lambda\omega\epsilon\lambda_h^*+Q_1}{Q_2\lambda_h^*+Q_1},\\
I_v^* &= \frac{\phi\lambda_h^*\beta_v\left(\delta_h e^{d_h\tau_2}+d_h e^{d_h\tau_2}+\omega\left(e^{d_h\tau_2}+\epsilon-\epsilon_1\right)\right)}{V\lambda_h^*+U},\\
S_v^* &= \frac{\phi-I_v^* d_v}{d_v},\\
&\text{where } \lambda_h^* = \frac{\beta_h I_v^*}{N_h^*},\ \beta_h = b\alpha_{vh}, \beta_v = b\alpha_{hv}, \qquad (5.8)
\end{aligned}
$$

where

$$
\begin{aligned}
Q_2 &= \omega^2\left(e^{d_h\tau_1+d_h\tau_3}-1\right)\left(e^{d_h\tau_2}-\epsilon_1\right)+\epsilon\omega^2\left(e^{d_h\tau_2}-1\right)+\delta_h^2 e^{d_h(\tau_1+\tau_2+\tau_3)}+ \qquad (5.9)\\
&\quad \omega\left(d_h+\delta_h\right)e^{d_h\tau_2}\left(e^{d_h\tau_1+d_h\tau_3}-1\right)+\omega\left(d_h+\delta_h\right)e^{d_h\tau_1+d_h\tau_3}\left(e^{d_h\tau_2}-\epsilon_1\right)+\\
&\quad 2d_h\delta_h e^{d_h(\tau_1+\tau_2+\tau_3)}+\omega\epsilon\delta_h e^{d_h\tau_2}+d_h^2 e^{d_h(\tau_1+\tau_2+\tau_3)}+\omega\epsilon d_h e^{d_h\tau_2},\\
Q_1 &= d_h\left(d_h+\delta_h+\omega\right)e^{d_h\tau_1+d_h\tau_3}\left(\delta_h e^{d_h\tau_2}+d_h e^{d_h\tau_2}+\omega\left(e^{d_h\tau_2}-\epsilon_1\right)\right),\\
U &= d_v^2\left(d_h+\delta_h+\omega\right)\left(\delta_h e^{d_h\tau_2}+d_h e^{d_h\tau_2}+\omega\left(e^{d_h\tau_2}-\epsilon_1\right)\right)e^{d_v\tau_4+d_h\tau_3},\\
V &= d_v\left(d_v e^{d_v\tau_4}+\beta_v\right)\left(\delta_h e^{d_h\tau_2}+d_h e^{d_h\tau_2}+\omega\left(e^{d_h\tau_2}+\epsilon-\epsilon_1\right)\right),
\end{aligned}
$$

where Q_1, Q_2, U, V are non-negative. Therefore, if λ_h^* is positive, then $S_h^*,\ I_p^*,\ I_r^*, I_v^*$ are positive and the malaria endemic equilibrium is obtained. However, for $\lambda_h^* = 0$, we get the malaria-free equilibrium. After some algebraic manipulation with the system (5.1-5.5), we get the cubic Eq. (5.10)

$$
\left(L_3\left(\lambda_h^*\right)^2+L_2\left(\lambda_h^*\right)+L_1\right)\lambda_h^* = 0, \qquad (5.10)
$$

where L_i for $i = 1, 2, 3$ with their signs as described in Eq. (5.19). By solving the Eq. (5.10) we can obtain the disease-free and endemic equilibria.

5.3.3.1 Malaria-free Equilibrium and Basic Reproduction Number

Now the $\lambda_h^* = 0$, obtained from Eq. (5.10), provides the malaria free equilibrium

$$\mathbb{E}^0 = \left(S_h^0,\ I_p^0,\ I_r^0,\ S_v^0,\ I_v^0\right) = \left(\frac{\Lambda}{d_h},\ 0,\ 0,\ \frac{\phi}{d_v},\ 0\right).$$

To derive the basic reproduction number, we used next generation matrix method described in Van den Driessche (2017); Diekmann et al. (1990). In the system (5.1-5.5), there are three infected compartments I_p, I_r and I_v. Let $I_p = y_1, I_r = y_2$ and $I_v = y_3$. Here, the incidence rates for the three infectious compartments I_p, I_r and I_v are $\mathscr{F}_1(t) = \dfrac{b\alpha_{vh} I_v(t-\tau_3) e^{-d_h\tau_3}}{N_h(t-\tau_3)} S_h(t-\tau_3), \mathscr{F}_2(t) = 0,$
$\mathscr{F}_3(t) = \dfrac{b\alpha_{hv}\left(I_p(t-\tau_4) + I_r(t-\tau_4)\right) e^{-d_v\tau_4}}{N_h(t-\tau_4)} S_v(t-\tau_4)$, respectively. Similarly, the transfer rates from these compartments are $\mathscr{V}_1(t) = (d_h + \delta_h + \omega) I_p(t), \mathscr{V}_2(t) = -\epsilon\omega I_p(t-\tau_2) e^{-d_h\tau_2} - \epsilon_1\omega I_r(t-\tau_2) e^{-d_h\tau_2} + (d_h + \delta_h + \omega) I_r(t), \mathscr{V}_3(t) = d_v I_v(t)$ respectively.

We now introduce two matrices:

$$\mathbb{F} = \left[\frac{\partial \mathscr{F}_i}{\partial y_j}\left(\mathbb{E}^0\right)\right] = \begin{pmatrix} 0 & 0 & \beta_h e^{-d_h\tau_3} \\ 0 & 0 & 0 \\ \dfrac{\phi d_h \beta_v e^{-d_v\tau_4}}{\Lambda d_v} & \dfrac{\phi d_h \beta_v e^{-d_v\tau_4}}{\Lambda d_v} & 0 \end{pmatrix},$$

$$\mathbb{V} = \left[\frac{\partial \mathscr{V}_i}{\partial y_j}\left(\mathbb{E}^0\right)\right] = \begin{pmatrix} d_h + \delta_h + \omega & 0 & 0 \\ -\omega\epsilon e^{-d_h\tau_2} & -\omega\epsilon_1 e^{-d_h\tau_2} + d_h + \delta_h + \omega & 0 \\ 0 & 0 & d_v \end{pmatrix}.$$

These matrices provide the $\mathbb{F}\mathbb{V}^{-1}$ and the basic reproduction number R_0 corresponds to the spectral radius of $\mathbb{F}\mathbb{V}^{-1}$:

$$R_0 = \rho(\mathbb{F}\mathbb{V}^{-1}) = \sqrt{\frac{e^{-(d_h\tau_3 + d_v\tau_4)} \phi d_h \beta_h \beta_v \left(\left(\omega\epsilon - \omega\epsilon_1\right) e^{-d_h\tau_2} + d_h + \delta_h + \omega\right)}{\Lambda d_v^2 \left(d_h + \delta_h + \omega\right)\left(d_h + \delta_h + \omega - \omega\epsilon_1 e^{-d_h\tau_2}\right)}}.$$

Next, we investigated the sensitivity of R_0 to the relapse delay (τ_2), proportion of first time relapse (ϵ), and proportion of multiple relapse (ϵ_1) (Figure 24).

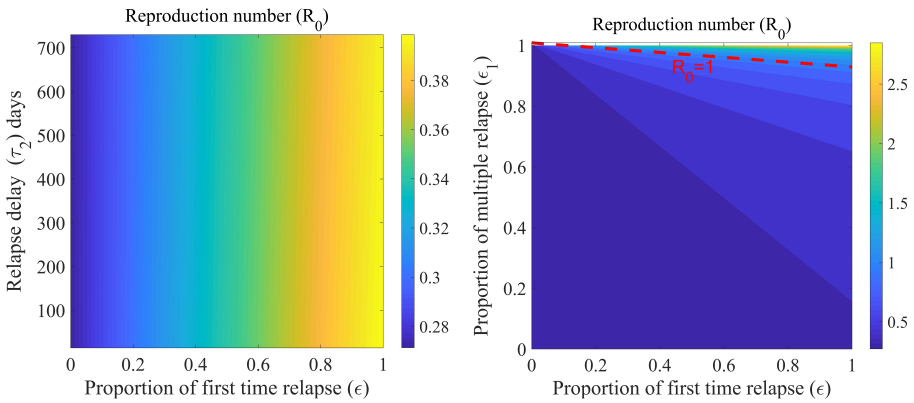

(a) **(b)**

Figure 24: Sensitivity of basic reproduction number (R_0) to the relapse delay (τ_2), the proportion of first time relapse (ϵ) and the proportion of multiple relapses (ϵ_1).

Increasing relapse delay (τ_2) reduces R_0 slowly, while increasing relapse proportion (ϵ) and multiple relapse proportion (ϵ_1) increases R_0 rapidly (Figure 24(a, b)). For the malaria parameters of Nepal presented in Table 4, despite the 100% of recovered individual from primary malaria cases experiencing relapse over a period of two weeks to two years, then also malaria remains under control in Nepal (Figure 24(a)). Also, only exceptionally high percentage of recovered human from primary infection get relapse together with recovered human from relapse class get multiple relapses in exceptionally higher percentage will create a problem to control malaria in Nepal. Otherwise, malaria level is in fully control but the problem of elimination is remains critical.

5.3.4 Model Analysis Considering one Delay (τ_2)

Since our main interest is to evaluate the role of the relapse delay (τ_2) and the proportion of relapses for the persistence and elimination of malaria, we considered the model without other delays for the stability analysis of the malaria-free equilibrium when $R_0 < 1$, and existence of endemic equilibria and Hopf bifurcation analysis when $R_0 > 1$.

5.3.4.1 Stability Analysis of the Malaria-free Equilibrium

For the simplification of model analysis, we take the proportion of first time relapse and multiple relapses to be equal, i.e., $\epsilon_1 = \epsilon$. Then

$$R_0|(\epsilon = \epsilon_1) = \sqrt{\frac{\phi d_h \beta_h \beta_v}{\Lambda d_v^2 \left(d_h + \delta_h + \omega - \epsilon\omega\ e^{-d_h\tau_2}\right)}}.$$

Let $\vec{x(t)}$ be the transpose of the vector $(S_h(t), I_p(t), I_r(t), S_v(t), I_v(t))$. Then linearizing the system (5.1-5.5) at the malaria-free equilibrium $\mathbb{E}^0$, we obtain

$$\frac{d}{dt}\vec{x}(t) = \mathbb{M}^0\vec{x}(t) + \mathbb{N}^0\vec{x}(t-\tau_2) \tag{5.11}$$

where $\mathbb{M}^0 = \begin{pmatrix} -d_h & \omega(1-\epsilon) & \omega(1-\epsilon) & 0 & -\beta_h \\ 0 & -k & 0 & 0 & \beta_h \\ 0 & 0 & \omega - k & 0 & 0 \\ 0 & -\dfrac{\phi d_h \beta_v}{\Lambda d_v} & -\dfrac{\phi d_h \beta_v}{\Lambda d_v} & -d_v & 0 \\ 0 & \dfrac{\phi d_h \beta_v}{\Lambda d_v} & \dfrac{\phi d_h \beta_v}{\Lambda d_v} & 0 & -d_v \end{pmatrix}$,

$\mathbb{N}^0 = \begin{pmatrix} 0 & 0 & 0 & 0 & 0 \\ 0 & 0 & 0 & 0 & 0 \\ 0 & \omega\epsilon e^{-d_h\tau_2} & \omega\epsilon e^{-d_h\tau_2} & 0 & 0 \\ 0 & 0 & 0 & 0 & 0 \\ 0 & 0 & 0 & 0 & 0 \end{pmatrix}$. Let λ be an eigenvalue, and det(A) be the determinant of the matrix A.

The characteristic equation of Eq. (5.11) is $\det(\mathbb{M}^0 + \mathbb{N}^0 e^{-\lambda\tau_2} - \lambda\mathbb{I}_{5\times 5}) = 0$, i.e.,

$$\begin{vmatrix} -(d_h+\lambda) & \omega(1-\epsilon) & \omega(1-\epsilon) & 0 & -\beta_h \\ 0 & -(k+\lambda) & 0 & 0 & \beta_h \\ 0 & \omega\epsilon e^{-(d_h+\lambda)\tau_2} & \omega\epsilon e^{-(d_h+\lambda)\tau_2} - (k+\lambda) & 0 & 0 \\ 0 & -\dfrac{\phi d_h \beta_v}{\Lambda d_v} & -\dfrac{\phi d_h \beta_v}{\Lambda d_v} & -(d_v+\lambda) & 0 \\ 0 & \dfrac{\phi d_h \beta_v}{\Lambda d_v} & \dfrac{\phi d_h \beta_v}{\Lambda d_v} & 0 & -(d_v+\lambda) \end{vmatrix} = 0,$$

where $k = d_h + \delta_h + \omega$. It has two negative eigenvalues $\lambda = -d_h, -d_v$ and the remaining

eigenvalues can be obtained form the equation $P(\lambda) = 0$, where

$$
\begin{aligned}
P(\lambda) &= A_3\lambda^3 + A_2\lambda^2 + A_1\lambda + A_0, \text{where} \qquad (5.12)\\
A_3 &= 1,\ A_2 = 2d_h + d_v + 2\delta_h + 2\omega - \omega\epsilon e^{-(d_h+\lambda)\tau_2},\\
A_1 &= \omega\left(d_h + \delta_h\right)\left(2 - \epsilon e^{-(d_h+\lambda)\tau_2}\right) + \left(\omega d_v + \omega^2\right)\left(1 - \epsilon e^{-(d_h+\lambda)\tau_2}\right) + \left(1 - R_0^2\right)\omega d_v\\
&\quad + 2d_h\delta_h + \left(2 - R_0^2\right) d_v\left(d_h + \delta_h\right) + R_0^2\omega\epsilon d_v e^{-d_h\tau_2} + d_h^2 + \delta_h^2,\\
A_0 &= d_v\left(d_h + \delta_h + \omega\right)\left(\left(1 - R_0^2\right)\left(d_h + \delta_h + \omega\right) - \omega\epsilon e^{-d_h\tau_2}\left(e^{-\lambda\tau_2} - R_0^2\right)\right).
\end{aligned}
$$

In this case $p(\lambda) = 0$ is equivalent with $L(\lambda) = M(\lambda)$, where $L(\lambda) = A_3\lambda^3 + A_2\lambda^2 + A_1\lambda$, $M(\lambda) = -A_0$.

Theorem 5.3.3 *For $\tau_2 = 0$, the malaria-free equilibrium is locally asymptotically stable for $R_0 < 1$ and unstable for $R_0 > 1$.*

Proof: In this case, the characteristic equation Eq. (5.12) is reduced to a polynomial equation. It follows that $A_3 = 1,\ A_2 = 2d_h + d_v + 2\delta_h + (2 - \epsilon)\omega,\ A_1 = d_h\left(\left(2 - R_0^2\right) d_v + 2\delta_h + 2\omega - \omega\epsilon\right) + d_v\left(\left(2 - R_0^2\right)\delta_h + \left(1 - R_0^2\right)\omega + R_0^2\omega\epsilon + \omega(1 - \epsilon)\right) + d_h^2 + \left(\delta_h + \omega\right)\left(\delta_h + \omega(1 - \epsilon)\right)$, and
$A_0 = \left(1 - R_0^2\right) d_v\left(d_h + \delta_h + \omega\right)\left(d_h + \delta_h + \omega(1 - \epsilon)\right)$. Therefore, $A_i > 0$ for all i, and
$A_1A_2 - A_0 = d_h^2\left(\left(4 - R_0^2\right) d_v + 6\delta_h + 3\omega(2 - \epsilon)\right) + d_v^2\left(\left(2 - R_0^2\right)\delta_h + \omega\left(\left(2 - \epsilon\right) - R_0^2(1 - \epsilon)\right)\right)$
$+ 2d_h^3 + \left(\delta_h + \omega\right)\left(\omega(4 - 3\epsilon)\delta_h + 2\delta_h^2 + \omega^2(\epsilon - 2)(\epsilon - 1)\right) + d_v\left(2\delta_h + \omega(2 - \epsilon)\right)^2$
$- d_vR_0^2\left(\delta_h + \omega(1 - \epsilon)\right)^2 + d_h 2d_v\left(\left(4 - R_0^2\right)\delta_h + \left(1 - R_0^2\right)\omega + R_0^2\omega\epsilon + \omega(3 - 2\epsilon)\right)$
$+ d_h\left(2 - R_0^2\right) d_v^2 + 6\omega(2 - \epsilon)\delta_h + 6\delta_h^2 + \omega^2\left(\epsilon^2 - 6\epsilon + 6\right) > 0$. Hence, from the Routh-Hurwitz criteria, the malaria-free equilibrium is locally asymptotically stable when $R_0 < 1$. However, for $R_0 > 1$, $A_0 < 0$, and the malaria-free equilibrium becomes unstable. □

Theorem 5.3.4 *For all $\tau_2 > 0$, the malaria-free equilibrium is locally asymptotically stable for $R_0 < 1$ and unstable for $R_0 > 1$.*

Proof: To prove Theorem 5.3.4, we need to establish the following three results, for all τ_2:

(i) Eq. (5.12) has no non-negative real roots when $R_0 < 1$;

(ii) Eq. (5.12) cannot have purely imaginary roots of the form $\lambda = i\alpha,\ \alpha > 0$ for $R_0 < 1$; and

(iii) Eq. (5.12) has non-negative real eigenvalues or has eigenvalues with positive real parts when $R_0 > 1$.

Proof (i): Setting $L(\lambda) = A_3\lambda^3 + A_2\lambda^2 + A_1\lambda$ and $M(\lambda) = -A_0$, then Eq. (5.12) can be written as $L(\lambda) = M(\lambda)$. Then $L(\lambda) \geq 0$ for $\lambda \geq 0$ but $M(\lambda)$ is a decreasing function of λ with $M(0) = (R_0^2 - 1)\, d_v\, (d_h + \delta_h + \omega)\left(d_h + \delta_h + \omega - \epsilon\omega e^{-d_h\tau_2}\right) < 0$ for $R_0 < 1$. Thus the Eq. (5.12) has no non-negative real roots.

Proof (ii): In this case, Eq. (5.12) can be written as

$$\lambda^3 + b_2\lambda^2 + b_1\lambda + b_0 + \left(c_2\lambda^2 + c_1\lambda + c_0\right) e^{-(d_h+\lambda)\tau_2} = 0, \tag{5.13}$$

where

$b_2 = 2d_h + d_v + 2\delta_h + 2\omega, c_2 = -\omega\epsilon,$
$b_1 = (d_h + \delta_h + \omega)\left(d_h + \left(2 - R_0^2\right) d_v + \delta_h + \omega\right) + R_0^2\omega\epsilon d_v e^{-d_h\tau_2},$
$c_1 = -\omega\epsilon\,(d_h + d_v + \delta_h + \omega)\,,$
$b_0 = d_v\,(d_h + \delta_h + \omega)\left(\left(1 - R_0^2\right)(d_h + \delta_h + \omega) + R_0^2\omega\epsilon e^{-d_h\tau_2}\right), c_0 = -\omega\epsilon d_v\,(d_h + \delta_h + \omega)\,.$

Suppose, if possible there exists some τ_2 for which Eq. (5.13) has roots with non-negative real parts for $R_0 < 1$, then they must be a pair of purely imaginary roots for some $\tau_2 > 0$. Suppose, if possible $\lambda = i\alpha$ is a root of Eq. (5.13) for $R_0 < 1$. Then substituting $\lambda = i\alpha$ into the equation and collecting the real and imaginary parts, we obtain

$$\begin{aligned} \alpha^2 b_2 - b_0 &= e^{-d_h\tau_2}\left(cos(\alpha\tau_2)\left(c_0 - \alpha^2 c_2\right) + \alpha c_1 sin(\alpha\tau_2)\right), \\ \alpha^3 - \alpha b_1 &= e^{-d_h\tau_2}\left(\alpha c_1 cos(\alpha\tau_2) - sin(\alpha\tau_2)\left(c_0 - \alpha^2 c_2\right)\right). \end{aligned} \tag{5.14}$$

Now squaring and adding,

$$\alpha^6 + \alpha^4\left(b_2^2 - 2b_1 - c_2^2 e^{-2d_h\tau_2}\right) + \alpha^2\left(b_1^2 - 2b_0 b_2 - c_1^2 e^{-2d_h\tau_2} + 2c_0 c_2 e^{-2d_h\tau_2}\right) + b_0^2 - c_0^2 e^{-2d_h\tau_2} = 0. \tag{5.15}$$

Now taking $z = \alpha^2$,

$$z^3 + z^2\left(b_2^2 - 2b_1 - c_2^2 e^{-2d_h\tau_2}\right) + z\left(b_1^2 - 2b_0 b_2 - c_1^2 e^{-2d_h\tau_2} + 2c_0 c_2 e^{-2d_h\tau_2}\right) + b_0^2 - c_0^2 e^{-2d_h\tau_2} = 0. \tag{5.16}$$

Let

$$f(z) := z^3 + B_2 z^2 + B_1 z + B_0 = 0, \tag{5.17}$$

where

$$B_0 = d_v^2 \left(d_h + \delta_h + \omega\right)^2 \left(\left(R_0^2 \omega \epsilon e^{-d_h \tau_2} + \omega \epsilon e^{-d_h \tau_2} + \left(1 - R_0^2\right)\left(\delta_h + \omega\right)\right) + \left(1 - R_0^2\right) d_h\right)$$
$$\left(\left(1 - R_0^2\right)\left(-\omega \epsilon e^{-d_h \tau_2} + \delta_h + \omega\right) + \left(1 - R_0^2\right) d_h\right),$$
$$B_1 = \omega^2 \left(\delta_h + \omega\right)^2 e^{-2d_h \tau_2}\left(e^{2d_h \tau_2} - \epsilon^2\right) + 2R_0^2 \omega d_v e^{-d_h \tau_2}\left(\delta_h + \omega\right)^2\left(e^{d_h \tau_2} - \epsilon\right) + d_h^4$$
$$+ 2\omega \delta_h \left(\delta_h + \omega\right)^2 + 2R_0^2 d_v \delta_h \left(\delta_h + \omega\right)^2 + \left(1 - R_0^2\right)^2 \omega^2 d_v^2 \delta_h^2 \left(\delta_h + \omega\right)^2$$
$$+ \omega^2 d_v^2\left(1 - \epsilon^2 e^{-2d_h \tau_2}\right) + 2R_0^2\left(1 - R_0^2\right)\omega^2 \epsilon d_v^2 e^{-d_h \tau_2} + R_0^4 \omega^2 \epsilon^2 d_v^2 e^{-2d_h \tau_2} + 4\left(1 - R_0^2\right)\omega d_v^2 \delta_h$$
$$+ 2R_0^2 \omega \epsilon d_v^2 \delta_h e^{-d_h \tau_2} + 2R_0^4 \omega d_v^2 \delta_h\left(1 - \epsilon e^{-d_h \tau_2}\right) + 2\left(1 - R_0^2\right) d_v^2 \delta_h^2 + R_0^4 d_v^2 \delta_h^2$$
$$+ 2d_h^3\left(R_0^2 d_v + 2\left(\delta_h + \omega\right)\right) + d_h^2\left(\omega^2\left(6 - \epsilon^2 e^{-2d_h \tau_2}\right) + 2R_0^2 d_v\left(\omega\left(3 - \epsilon e^{-d_h \tau_2}\right) + 3\delta_h\right)\right)$$
$$+ d_h^2\left(\left(R_0^4 - 2R_0^2 + 2\right) d_v^2 + 12\omega \delta_h + 6\delta_h^2\right) + 2d_h\left(\omega^2 \delta_h\left(6 - \epsilon^2 e^{-2d_h \tau_2}\right) + \omega^3\left(2 - \epsilon^2 e^{-2d_h \tau_2}\right)\right)$$
$$+ 2d_h\left(R_0^2 d_v e^{-d_h \tau_2}\left(\delta_h + \omega\right)\left(3\delta_h e^{d_h \tau_2} + 3\omega e^{d_h \tau_2} - 2\omega \epsilon\right) + 6\omega \delta_h^2 + 2\delta_h^3\right) +$$
$$2d_h d_v^2\left(R_0^4\left(\omega - \omega \epsilon e^{-d_h \tau_2} + \delta_h\right) + R_0^2 \omega \epsilon e^{-d_h \tau_2} + 2\left(1 - R_0^2\right)\left(\delta_h + \omega\right)\right),$$
$$B_2 = 2\omega^2 - \omega^2 \epsilon^2 e^{-2d_h \tau_2} + 2d_h\left(R_0^2 d_v + 2\left(\delta_h + \omega\right)\right) + 2R_0^2 d_v\left(\omega - \omega \epsilon e^{-d_h \tau_2} + \delta_h\right) + 2d_h^2 + d_v^2 +$$
$$4\omega \delta_h + 2\delta_h^2.$$

Thus all $B_i > 0$ for $R_0 < 1$, then using Descart's rule of sign Eq. (5.16) does not have positive roots. Hence $\lambda = i\alpha$ does not exist as a root of Eq. (5.13) for $R_0 < 1$.
Proof (iii): Now we rewrite the characteristic equation $P(\lambda) = 0$ as $L(\lambda) = M(\lambda)$, where $L(\lambda) = A_3\lambda^3 + A_2\lambda^2 + A_1\lambda$ and $M(\lambda) = -A_0$. Considering the real eigenvalues, $L(0) = 0$, $\lim_{\lambda \to \infty} L(\lambda) = \infty$ and $M(0) = \left(R_0^2 - 1\right) d_v \left(d_h + \delta_h + \omega\right)\left(d_h + \delta_h + \omega - \epsilon\omega e^{-d_h \tau_2}\right) > 0$ for $R_0 > 1$. Then there must exist at least one positive $\lambda = \lambda^*$ such that $L(\lambda^*) = M(\lambda^*)$, i.e., λ^* is a positive eigenvalue of the characteristic equation $P(\lambda) = 0$ and hence, the malaria-free equilibrium becomes unstable for $R_0 > 1$. □

5.3.4.2 Impact of Relapse Delay and Proportion of Relapse on Malaria Burden in Nepal

Here, we perform simulations using the parameters in Table 4 to show how the proportion of first time relapse (ϵ), the proportion of multiple relapses (ϵ_1), and the relapse delay (τ_2) impact the malaria dynamics in Nepal from the beginning of the year 2023 to the end of 2025 (Figure 25 (a,b,c) respectively). Increasing the proportion of first time relapse (Figure 25(a)), our model predicts that if 80% of the recovered humans from primary infection get first time relapse, there will be 8 malaria cases at the end of 2025. However, if the relapse percentage is below 35%, then Nepal will be malaria free at the end of 2025.
Similarly, from (Figure 25(b)), our model predicts that if 28% of recovered humans

from relapse class get multiple relapse, there will be 4 malaria cases at the end of 2025. However, if the multiple relapse proportion is below 16%, then Nepal will be malaria free at end of 2025.

Also, from (Figure 25(c)), our model predicts that if the relapse delay is one year, there will be 16 malaria cases at the end of 2025. However if the relapse delay is below six months, Nepal will be malaria free at the end of 2025. In this case malaria cases remains almost constant when number of days in duration is less than the corresponding τ_2. However, number of malaria cases strictly increasing with increasing relapse delay when duration exceed τ_2. Next, we perform simulations to show how the

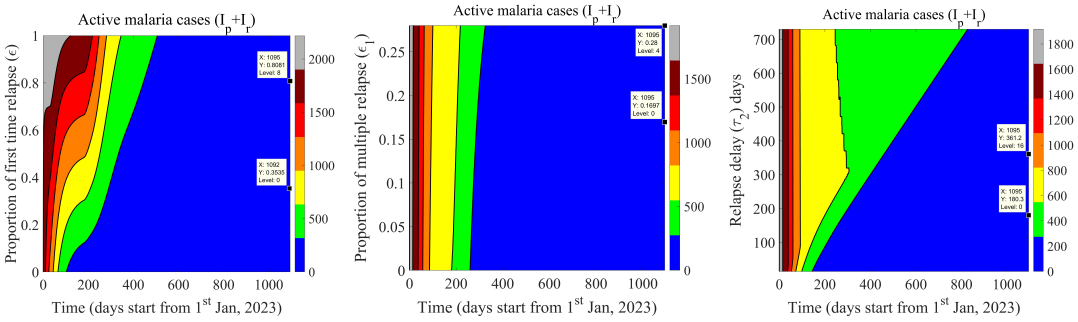

Figure 25: Time series solutions of total infections due to the impact of the proportion of first time relapse (ϵ), the proportion of multiple relapses (ϵ_1), and the relapse delay (τ_2). Number of days start from January 1, 2023. In each (a,b,c) , $R_0 < 1$.

variation in two of three relapse parameters (i.e., the proportion of first time relapse (ϵ), the proportion of multiple relapses (ϵ_1), and the relapse delay (τ_2)) impact malaria dynamics in Nepal at the end of the year 2025 (Figure 26 (a)(b)(c) respectively). Increasing the proportion of first time relapse, together with relapse delay, our model predicts that in the worst case if 100% of those recovered from primary infection experiences relapse after six months then there will be still 14 malaria cases in Nepal at the end of 2025. However, if the percentage of relapse of those recovered from primary infection after six months is below 45% then Nepal will be malaria free at the end of 2025 (Figure 26(a)). Similarly, increasing the multiple relapse proportion together with relapse delay, our model predicts that if the relapse delay is less than four months, Nepal will be malaria free at the end of 2025 only when the multiple relapse proportion remains below 28% (Figure 26(b)).

However, if the relapse delay is six months, then Nepal will be malaria free at the end of 2025 only when the multiple relapse proportion is below 20%. Again, increasing the proportion of first time relapse, together with the multiple relapse proportion, our

model predicts that if in the worst case that the relapse proportion and the multiple relapse proportion are 100%, there will be 3486 malaria cases at the end of 2025 (Figure 26(c)). However, if the relapse proportion and the multiple relapse proportion remain below 20%, Nepal will be malaria free at the end of 2025. In Figure 26(a,b), R_0 remains below 1 however in Figure 26(c), R_0 switch below 1 to above 1 while varying ϵ and ϵ_1.

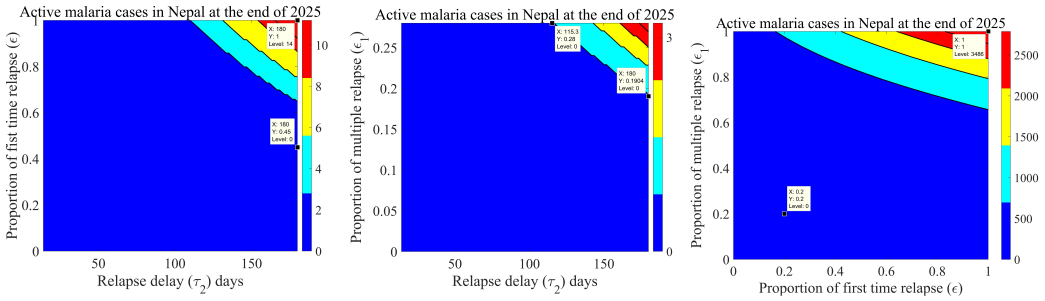

(a) **(b)** **(c)**

Figure 26: Malaria levels after three years from Jan 1^{st}, 2023 with respect to the proportion of first relapse (ϵ), the proportion of multiple relapses (ϵ_1), and the relapse delay (τ_2). In (a,b), R_0 remains 1 however in (c), R_0 switches below 1 to above 1 while varying ϵ and ϵ_1.

5.3.4.3 Sensitivity of Relapse Delay and Relapse Proportions on Time to Malaria Eradication

Here we perform simulations to show how the variation of two of three relapse parameters impacts the first time point to achieve malaria elimination in Nepal (Figure 27 (a)(b)(c) respectively). In particular, starting from Jan 1^{st}, 2023, when 25% of recovered humans from the I_p class relapses after two weeks, then the system achieves the malaria-free point after 467 days . Similarly, when 25% of recovered humans relapses after six months, then the system achieves the malaria-free point after 1004 days (almost end of the year 2025) (Figure 27(a)). Moreover, when 25% of recovered humans from the I_r class relapses after two weeks, then the system achieves the malaria-free point after 523 days (before the end of 2025). However, when 25% of recovered humans relapses after six months, then the system achieves the malaria-free point after 1315 days (After the end of 2026) (Figure 27(b)). Likewise, when 20% of recovered humans from the I_p and I_r classes relapse after about six months, then the system achieves the malaria-free point at the end of 2025 (1095 days). However, when 25% of recovered humans from the I_p and I_r classes relapses after six months, then

the system achieves the malaria-free point after 1295 days (middle of 2026) (Figure 27(c)).

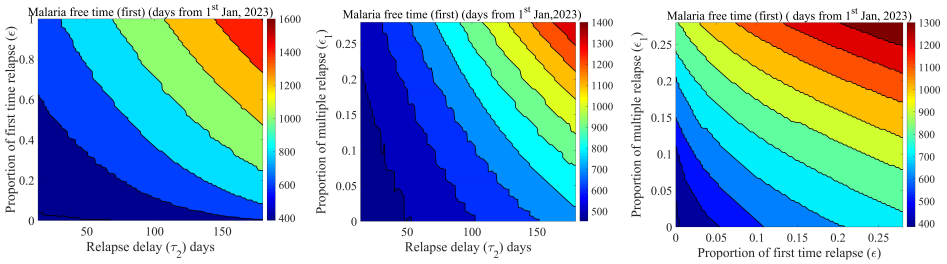

(a) **(b)** **(c)**

Figure 27: Sensitivity of the time (in days) for the system to achieve the disease-free point, varying the proportion of first relapse (ϵ), the proportion of multiple relapses (ϵ_1), and the relapse delay(τ_2). Days starting from 1^{st} Jan, 2023. For all (a,b,c), $R_0 < 1$.

5.3.5 Malaria Endemic Equilibria and Stability

In this section we will discuss about the existence of malaria endemic equilibrium, stability and Hopf bifurcation when $R_0 > 1$.

5.3.5.1 Malaria Endemic Equilibrium

The equilibria Eq. (5.10) reduces to

$$L_3 \left(\lambda_h^*\right)^2 + L_2 \lambda_h^* + L_1 = 0, \tag{5.18}$$

where

$$\begin{aligned} L_3 &= \Lambda d_v \left(d_v + \beta_v\right) \left(\delta_h e^{d_h \tau_2} + d_h e^{d_h \tau_2} + \omega \left(e^{d_h \tau_2} + \epsilon - \epsilon_1\right)\right)^2, \\ L_1 &= \Lambda \left(1 - R_0^2\right) d_v^2 \left(d_h + \delta_h + \omega\right)^2 \left(e^{d_h \tau_2} \left(d_h + \delta_h + \omega\right) - \omega \epsilon_1\right)^2, \end{aligned} \tag{5.19}$$

where $L_3 > 0$ and $L_1 < 0$ for $R_0 > 1$ and L_2 varies with the choice of parameters. Thus, there exists a unique malaria endemic equilibrium when $R_0 > 1$. Plugging the unique positive value of λ_h^* obtained from Eq. (5.18) in the Subsection (5.3.3) we

obtain unique endemic equilibrium:

$$S_h^* = \frac{\Lambda\left(\delta_h e^{d_h\tau_2} + d_h e^{d_h\tau_2} + \omega\left(e^{d_h\tau_2} - \epsilon\right)\right)}{\lambda_h^*\left(\delta_h e^{d_h\tau_2} + \omega\epsilon\left(e^{d_h\tau_2} - 1\right)\right) + d_h\left(\delta_h e^{d_h\tau_2} + \lambda_h^* e^{d_h\tau_2} + \omega\left(e^{d_h\tau_2} - \epsilon\right)\right) + d_h^2 e^{d_h\tau_2}},$$

$$I_p^* = \frac{\Lambda\lambda_h^*\left(\left(d_h + \delta_h\right)e^{d_h\tau_2} + \omega\left(e^{d_h\tau_2} - \epsilon\right)\right)}{k\left(\lambda_h^*\left(\delta_h e^{d_h\tau_2} + \omega\epsilon\left(e^{d_h\tau_2} - 1\right)\right) + d_h\left(\delta_h e^{d_h\tau_2} + \lambda_h^* e^{d_h\tau_2} + \omega\left(e^{d_h\tau_2} - \epsilon\right)\right) + d_h^2 e^{d_h\tau_2}\right)},$$

$$I_r^* = \frac{\Lambda\omega\epsilon\lambda_h^*}{k\left(\lambda_h^*\left(\delta_h e^{d_h\tau_2} + \omega\epsilon\left(e^{d_h\tau_2} - 1\right)\right) + d_h\left(\delta_h e^{d_h\tau_2} + \lambda_h^* e^{d_h\tau_2} + \omega\left(e^{d_h\tau_2} - \epsilon\right)\right) + d_h^2 e^{d_h\tau_2}\right)},$$

$$I_v^* = \frac{\phi\lambda_h^*\beta_v e^{d_h\tau_2}}{d_v\left(\lambda_h^*\beta_v e^{d_h\tau_2} + d_v\left(\delta_h e^{d_h\tau_2} + \lambda_h^* e^{d_h\tau_2} + \omega\left(e^{d_h\tau_2} - \epsilon\right) + d_h e^{d_h\tau_2}\right)\right)},$$

$$N_h^* = \frac{\Lambda\left(\delta_h e^{d_h\tau_2} + \lambda_h^* e^{d_h\tau_2} + \omega e^{d_h\tau_2} + d_h e^{d_h\tau_2} - \omega\epsilon\right)}{\lambda_h^*\left(\delta_h e^{d_h\tau_2} + \omega\epsilon\left(e^{d_h\tau_2} - 1\right)\right) + d_h\left(\delta_h e^{d_h\tau_2} + \lambda_h^* e^{d_h\tau_2} + \omega\left(e^{d_h\tau_2} - \epsilon\right)\right) + d_h^2 e^{d_h\tau_2}},$$

$$\lambda_v^* = \frac{\lambda_h^*\beta_v e^{d_h\tau_2}}{\delta_h e^{d_h\tau_2} + \lambda_h^* e^{d_h\tau_2} + \omega(e^{d_h\tau_2} - \epsilon) + d_h e^{d_h\tau_2}}.$$

5.3.5.2 Stability Analysis of Malaria Endemic Equilibrium

The Jacobian of the system at the malaria endemic equilibrium is

$$\mathbb{J}_1 := \begin{pmatrix} -\left(d_h + \lambda_h^*\left(1 - \frac{S_h^*}{N_h^*}\right)\right) & \frac{\lambda_h^* S_h^*}{N_h^*} + \omega(1-\epsilon) & \frac{\lambda_h^* S_h^*}{N_h^*} + \omega\left(1-\epsilon\right) & -\frac{\beta_h S_h^*}{N_h^*} \\ \lambda_h^*\left(1 - \frac{S_h^*}{N_h^*}\right) & -\left(k + \frac{\lambda_h^* S_h^*}{N_h^*}\right) & -\frac{\lambda_h^* S_h^*}{N_h^*} & \frac{\beta_h S_h^*}{N_h^*} \\ 0 & \omega\epsilon e^{-d_h\tau_2} & -\left(-\omega\epsilon e^{-d_h\tau_2} + k\right) & 0 \\ -\frac{\lambda_v^*\left(\frac{\phi}{d_v} - i_v^*\right)}{N_h^*} & \frac{\left(\frac{\phi}{d_v} - i_v^*\right)(\beta_v - \lambda_v^*)}{N_h^*} & \frac{\left(\frac{\phi}{d_v} - i_v^*\right)(\beta_v - \lambda_v^*)}{N_h^*} & -(d_v + \lambda_v^*) \end{pmatrix}.$$

Let λ be an eigenvalue of the Jacobian $(\mathbb{J}_1)$. Then the characteristic equation is

$$\begin{vmatrix} a_1 - \lambda & a_2 & a_2 & a_3 \\ a_4 & a_5 - \lambda & a_6 & a_7 \\ 0 & a_8 e^{-(\lambda+\tau_2)d_h} & a_8 e^{-(\lambda+\tau_2)d_h} + a_9 - \lambda & 0 \\ a_{10} & a_{11} & a_{11} & a_{12} - \lambda \end{vmatrix} = 0,$$

where $a_1 = -\left(d_h + \lambda_h^*\left(1 - \frac{S_h^*}{N_h^*}\right)\right),\ a_2 = \frac{\lambda_h^* S_h^*}{N_h^*} + \omega(1-\epsilon),\ a_3 = -\frac{\beta_h S_h^*}{N_h^*},$
$a_4 = \lambda_h^*\left(1 - \frac{S_h^*}{N_h^*}\right),\ a_5 = -(d_h + \delta_h + \frac{\lambda_h^* S_h^*}{N_h^*} + \omega), a_6 = -\frac{\lambda_h^* S_h^*}{N_h^*},$
$a_7 = \frac{\beta_h S_h^*}{N_h^*},\ a_8 = \omega\epsilon,\ a_9 = -(d_h + \delta_h + \omega),$
$a_{10} = -\frac{\lambda_v^*\left(\frac{\phi}{d_v} - i_v^*\right)}{N_h^*}, a_{11} = \frac{\left(\frac{\phi}{d_v} - (i_v)^*\right)(\beta_v - (\lambda_v)^*)}{N_h^*},\ a_{12} = -(d_v + \lambda_v^*).$ The

characteristic equation reduces to

$$\lambda^4 + B_3\lambda^3 + B_2\lambda^2 + B_1\lambda + B_0 + \left(C_3\lambda^3 + C_2\lambda^2 + C_1\lambda + C_0\right) e^{-(d_h+\lambda)\tau_2} = 0, \quad (5.20)$$

where,

$$\begin{aligned}
B_3 &= -\left(a_1 + a_5 + a_9 + a_{12}\right), B_2 = a_9a_{12} + a_5\left(a_9 + a_{12}\right) + a_1\left(a_5 + a_9 + a_{12}\right) \\
&\quad - a_2a_4 - a_3a_{10} - a_7a_{11}, \\
B_1 &= a_3\left(a_5 + a_9\right)a_{10} + a_7\left(a_1 + a_9\right)a_{11} + a_2a_4\left(a_9 + a_{12}\right) - a_2a_7a_{10} - a_3a_4a_{11} - a_5a_9a_{12} \\
&\quad - a_1\left(a_9a_{12} + a_5\left(a_9 + a_{12}\right)\right), \\
B_0 &= a_9\left(a_2a_7a_{10} + a_3a_4a_{11} + a_1a_5a_{12}\right) - a_9\left(a_3a_5a_{10} + a_1a_7a_{11} + a_2a_4a_{12}\right), \\
C_3 &= -a_8, C_2 = a_8\left(a_1 + a_5 - a_6 + a_{12}\right), C_1 = a_8\left(a_1a_6 + a_{12}a_6 + a_3a_{10}\right) \\
&\quad - a_8\left(a_5a_{12} + a_1\left(a_5 + a_{12}\right)\right), \\
C_0 &= a_8\left(a_3a_6a_{10} + a_1a_5a_{12}\right) - a_8\left(a_3a_5a_{10} + a_1a_6a_{12}\right).
\end{aligned}$$

Theorem 5.3.5 *For $\tau_2 = 0$, the endemic equilibrium is locally asymptotically stable when $R_0 > 1$ and $D_3D_2D_1 - D_1^2 - D_3^2D_0 > 0$, where $D_i = B_i + C_i > 0$ for all i.*

Proof: For $\tau_2 = 0$, the characteristic equation Eq. (5.20) becomes

$$\lambda^4 + D_3\lambda^3 + D_2\lambda^2 + D_1\lambda + D_0 = 0, \quad (5.21)$$

where $D_i = B_i + C_i$ for all i. Using the Routh-Hurwitz criteria, the malaria endemic equilibrium is locally asymptotically stable when $D_i > 0$ for all i together with $D_3D_2D_1 - D_1^2 - D_3^2D_0 > 0$ Martcheva (2015). □

When $\tau_2 = 0$ all roots of Eq (5.20) lie on the left side of the imaginary axis, indicating stability at the endemic equilibrium. As τ_2 increases from 0, a root of Eq (5.20) can cross the imaginary axis to the right side. The critical case occurs when $\lambda = i\alpha$, as a root can shift to either the right or left side with a small perturbation when situated on the imaginary axis Busenberg and Cooke (2012). Upon substituting in the Eq. (5.20) and collecting real and imaginary parts we get

$$\begin{aligned}
\alpha^4 - \alpha^2B_2 + B_0 &= \cos\alpha\tau_2\left(\alpha^2C_2 - C_0\right)e^{-d_h\tau_2} + \sin\alpha\tau_2\left(\alpha^3C_3 - C_1\alpha\right)e^{-d_h\tau_2}, \quad (5.22) \\
\alpha B_1 - \alpha^3B_3 &= \cos\alpha\tau_2\left(\alpha^3C_3 - C_1\alpha\right)e^{-d_h\tau_2} - \sin\alpha\tau_2\left(\alpha^2C_2 - C_0\right)e^{-d_h\tau_2}.
\end{aligned}$$

Now squaring and adding, we get

$$\alpha^8 + H_3\alpha^6 + H_2\alpha^4 + H_1\alpha^2 + H_0 = 0, \tag{5.23}$$

Taking $b = \alpha^2$, we have

$$b^4 + H_3b^3 + H_2b^2 + H_1b + H_0 = 0, \tag{5.24}$$

where we obtain the following:

$$\begin{aligned}
H_3 &= B_3^2 - 2B_2 - C_3^2e^{-2d_h\tau_2},\\
H_2 &= B_2^2 - 2B_1B_3 + 2B_0 + (2C_1C_3 - C_2^2)e^{-2d_h\tau_2},\\
H_1 &= B_1^2 - 2B_0B_2 + (2C_0C_2 - C_1^2)e^{-2d_h\tau_2},\ H_0 = B_0^2 - C_0^2e^{-2d_h\tau_2}.
\end{aligned}$$

Now transforming the equation by $b = u - \dfrac{H_3}{4}$ into depressed quartic form:

$$u^4 + Au^2 + Bu + C = 0, \tag{5.25}$$

where $A = 8H_2 - 3H_3, B = H_3^3 - 4H_3H_2 + 8H_1, C = -3H_3^4 + 16H_2H_3^2 - 64H_3H_1 + 256H_0$. Let $u^4 + Au^2 + Bu + C = (u^2 - Lu + M)(u^2 + Lu + N)$. Then, we have $M + N = A + L^2$, $M - N = B/L$, $MN = C$. Using the identity $(M + N)^2 = (M - N)^2 + 4MN$, it follows that $L^2(L^2 + A)^2 - B^2 - 4L^2C = 0$ and we get $t^3 + 2At^2 + (A^2 - 4C)t - B^2 = 0$, where $t = L^2$. By inspection (for fixed coefficients) or using Cardon's method Lestari et al. (2020), we can obtain the value of t, and L, M, N can be obtained. Then we can obtain u and hence possible values of b. If $b > 0$, then $\lambda = \pm i\alpha$ exist and the model undergoes a Hopf bifurcation.

Now, we proceed with two cases. Case I: If a positive value of b is not possible, and Eq. (5.20) has no purely imaginary roots for all $\tau_2 > 0$, placing all of Eq. (5.20)'s roots in the left half of the complex plane. Then the following Theorem (5.3.6), holds.

Theorem 5.3.6 *If Case I is satisfied together with $R_0 > 1$, then the malaria endemic equilibrium is asymptotically stable for all $\tau_2 > 0$ provided that it is stable for $\tau_2 = 0$ Misra et al. (2018).*

Case II: If the Eq. (5.24) has at least one positive root b^* for $R_0 > 1$, then Eq. (5.20) has pair of purely imaginary roots $\pm i\alpha^*$ and model undergoes Hopf bifurcations.

Remark: If Eq. (5.24) has more than one positive real root, then Eq. (5.20) has more than one pair of purely imaginary roots, and the system possesses a finite number of stability switches as delay parameter τ_2 increases.

5.3.5.3 Malaria Dynamics with Decay Oscillations for $R_0 > 1$

Taking parameters fixed from Table 4 and initial conditions from data on malaria in Nepal (2022), we obtain solutions with damped oscillations, as shown in Figure 28 (a,b) and as discussed in Case (I). It is worth noting that simulating the model with a wide range of parameters with $\tau_2 > 0$, we get decaying oscillations, verifying Case I. However, simulating the model with a wide range of the parameter values given in Table 4, we did not obtain Case (II).

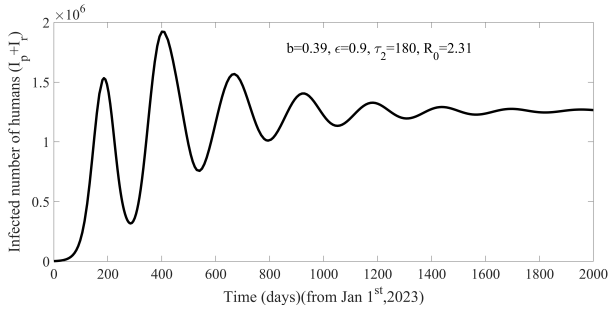

(a)

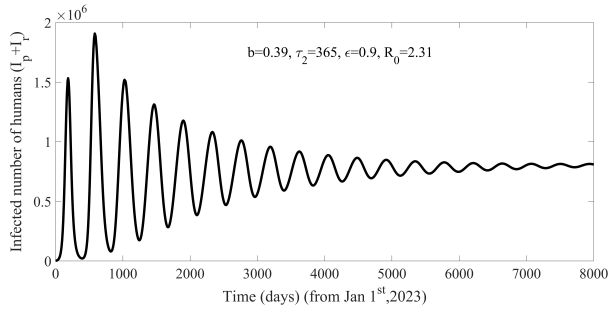

(b)

Figure 28: Model solutions with damped oscillations when varying τ_2 without other delays, when $R_0 > 1$. In (a), when the relapse delay is six months and 90% of those recovered from the I_p class have a first time relapse, malaria becomes endemic in the population, with decaying oscillations. In (b), the impact of increasing the relapse period to one year is shown. In this case, the disease dynamics are quite slow, taking a longer time to achieve a stable endemic level, with persistence of oscillations over a long time.

5.3.6 Simulations Results Considering all Four Delays

Here, we examine the Hopf bifurcation phenomenon and the sensitivity of oscillations to each four delays and and the relapse proportion. We assumed $b = 0.6, \alpha_{vh} = 0.33, \alpha_{hv} = 0.59, \Lambda = 8, \omega = 0.56, d_h = 0.0029, \delta_h = 0.00171, d_v = 0.03, \phi = 80, \tau_1 = 9, \tau_2 =$

$0.02, \tau_3 = 20, \tau_4 = 20, \epsilon = 0.6, \epsilon_1 = 0.1, R_0 = 1.82$, $S_h(0) = 500, I_p(0) = 300, I_r(0) = 0, S_v(0) = 1000, I_v(0) = 300$, and obtained the Hopf Bifurcation (Figure 29). In addition with same initial conditions and parameters, tspan =1500, we see the impact of increasing each delays at a time fixing others on the oscillations of the $I_p + I_r$ at the time of last fifty days (1450-1500). we observed that all delay parameters are highly sensitive to protect the regular outbreak of infection (Figure 30).

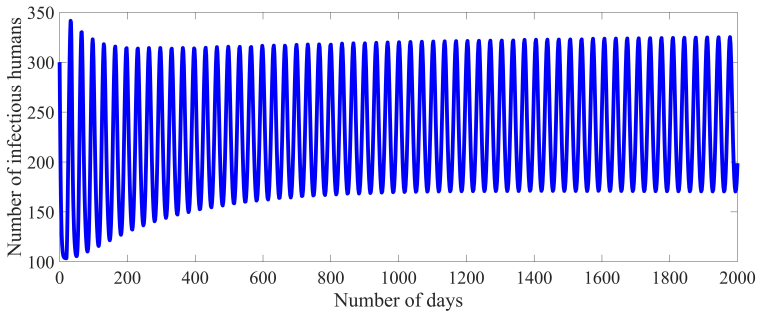

(a)

Figure 29: Hopf bifurcations when taking all delays.

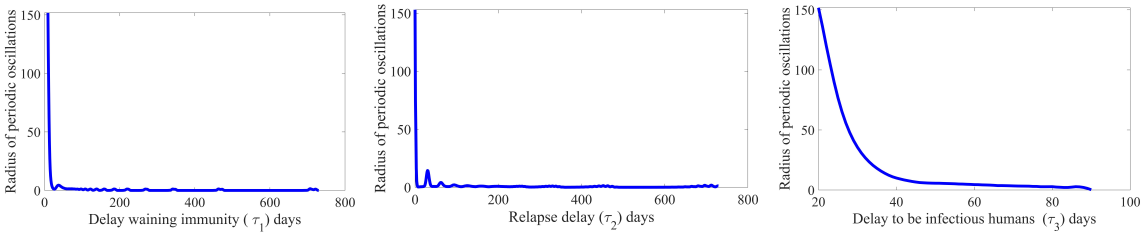

(a) **(b)** **(c)**

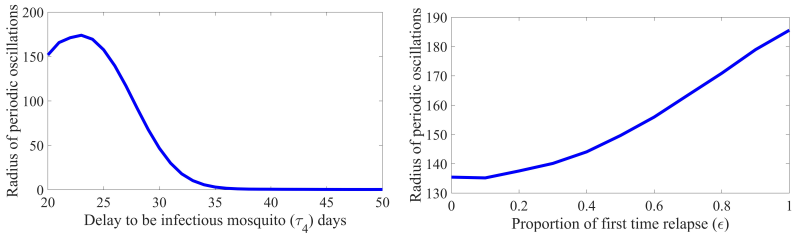

(d) **(e)**

Figure 30: Sensitivity of Hopf bifurcations to the delays and relapse proportions . The sensitivity of the Hopf bifurcation to $\tau_1, \tau_2, \tau_3, \tau_4$ are shown in parts (a, b, c, d) , respectively. The sensitivity of the Hopf bifurcation to the proportion of relapse ϵ is shown in part (e).

5.4 Conclusion

Addressing the persistence of *Plasmodium vivax* and *Plasmodium ovale* in global malaria eradication is challenging due to reactivation of the dormant stage parasites in the liver and previously-infected individuals becoming infectious again due to relapse Yan et al. (2023). Existing models Chamchod and Beier (2013); Ghosh et al. (2020); Wang et al. (2021) considered relapse from recovered humans using a system of ordinary differential equations, but these studies did not fully address the impacts of the relapse proportion and relapse delay on malaria dynamics. In this study, we developed, for the first time, a malaria model that accounts for the delay in the reactivation of dormant liver-stage parasites, leading to malaria reinfection.

Using our model, we performed a basic analysis and derived the basic reproduction number, R_0 for all four delays. However, in the absence of other delays, we showed that the malaria-free equilibrium is asymptotically stable when $R_0 < 1$, and unstable when $R_0 > 1$ for all values of the relapse delay, τ_2. In addition, a unique endemic equilibrium point exists and we obtained the condition for Hopf bifurcation when $R_0 > 1$. To verify the theoretical results, we performed simulation results of the model with the malaria data of Nepal and predicted the local malaria burden of Nepal from the beginning of the year 2023 to the end of the year 2025 in the absence of imported cases.

As predicted by the analysis of our model, the relapse delay and proportions of relapses substantially affects different aspects of malaria dynamics. Particularly, a long relapse delay reduces the basic reproduction number and takes a longer time to achieve the disease-free equilibrium when $R_0 < 1$, and a short delay in relapse increases the basic reproduction number and achieves the disease-free equilibrium rapidly when $R_0 < 1$. Similarly, increasing the proportion relapsing result increase in reproduction number and decreases the rate of convergence of the solution to the malaria-free equilibrium when $R_0 < 1$. In the absence of imported cases, our model predicts that If 50% of recovered individuals from the primary infection experience a first relapse, followed by 14% of those from the relapse group having multiple relapses within five months, Nepal is expected to be malaria-free by the end of 2025. If only 28% of recovered individuals from the primary infection experience a first relapse, followed by 25% of those from the relapse group having multiple relapses within five months, Nepal cannot achieve malaria-free status by the end of 2025.

If 50% of recovered individuals from the primary infection experience a first relapse,

followed by 14% of those from the relapse group having multiple relapses within two months, Nepal is projected to be malaria-free by the end of 2024. If 50% of recovered individuals from the primary infection experience a first relapse, followed by 14% of those from the relapse group having multiple relapses within six months, Nepal will not achieve malaria-free status by the end of 2025 (Figure 27(a,b)). Thus, our study underscores the need for consideration of relapse delays and the proportion of relapse in modeling to accurately predict malaria dynamics. Furthermore, we obtained periodic oscillations with Hopf bifurcations when $R_0 > 1$. We also evaluated the sensitivity of periodic oscillations to all delays as well as to relapse proportion. In this case, the radius of periodic oscillations is highly sensitive to all delays; hence increasing the delays helps to protect from regular outbreak and the solution converges to the malaria endemic equilibrium when $R_0 > 1$. However, the radius of periodic oscillations increases with higher proportions of first time relapse. Thus, control strategies to reduce the proportion of first time relapse will be highly impactful in protecting from regular outbreak Via Hopf- Bifurcation.

We acknowledge certain limitations in our study. Firstly, due to the unavailability of primary infection and relapse-induced infection datasets, we had to rely on parameters obtained from existing literature and malaria cases of the base year for our simulations. Our simulation results are based on after successful implementation of planning of cross border collaboration of Nepal government and other countries and complete restriction on imported cases after 2023 Nepal (2022), which is the major limitation of this study. Given a more robust dataset, simulations utilizing estimated parameters would further improve our predictions. Additionally, the majority of our analysis primarily focused on varying the delay in relapse and proportion of relapses to concentrate our examination on relpase specific impact. Given the inherent complexity of the model, mainly due to the presence of four distinct types of delays, we were limited to testing the stability of the infected equilibrium and the phenomenon of Hopf bifurcation through numerical techniques across a wide range of parameter values. Although we observed the possibility of multiple endemic equilibria when $R_0 < 1$ and the potential of backward bifurcation, we limit our study only to the endemic equilibria and assessment of Hopf bifurcation when $R_0 > 1$. In summary, our novel delay-dynamics malaria model, which incorporates the consideration of the relapse delay, revealed that the timing of relapse and the proportion of both single and multiple relapses play a crucial role in shaping malaria dynamics. Our research underscores the importance of factoring in the relapse delay when modeling malaria dynamics to enhance the accuracy of prediction.

CHAPTER 6

6.SUMMARY AND CONCLUSION

6.1 Summary

Malaria remains a significant health challenge in Nepal, primarily due to imported cases from cross-border mobility, especially from India, and the high prevalence of Plasmodium vivax, which tends to relapse over time. These factors pose substantial barriers to Nepal's goal of malaria elimination by 2026. This dissertation addresses these issues by developing mathematical models that incorporate cross-border mobility and relapse malaria cases, along with comprehensive model analysis and simulations to understand their impact on malaria dynamics and the elimination target.

Chapter 1 includes an overview of the global malaria elimination programs, imported malaria cases in a global context, literature reviews of malaria modeling, research objectives and outlines. Chapter 2 details the life cycle of malaria parasites, the biology of malaria transmission, symptoms, testing tools and techniques, and treatments. It also covers the fundamental terminologies and theorems for malaria modeling, detailing the analysis and simulation techniques used throughout the dissertation.

In Chapter 3, we developed mathematical model that incorporates cross-border mobility and imported malaria cases. This chapter estimates malaria cases for 2026 and evaluates control strategies for minimizing the burden and achieving elimination, considering different levels of mosquito biting rates. It also covers stability analysis and persistence theory. In Chapter 4, we perform an in-depth backward bifurcation analysis of the model, examining various cases of mobility and deriving the threshold value for the mobility-associated parameter, ω, necessary for achieving malaria elimination. In Chapter 5, we develop a malaria model that includes relapse delays and the proportion of relapses, including multiple relapses. Based on relapse parameters, this chapter estimates the time required for the system to achieve malaria pre-elimination equilibrium. Chapter 6 summarizes the summary and conclusions of the dissertation. Overall, this study involves the development of mathematical models addressing real-world issues related to the mobility of people and the associated challenges for malaria elimination, along with the relapse problem of P. vivax and P. ovale malaria parasites. It also addresses potential control strategies for successful elimination and maintaining malaria at a minimal level in worst-case scenarios. Numerical simulations and analyses

are conducted using MATLAB R2018a (The MathWorks, Inc.) and Mathematica.

6.2 Conclusion

In this study, we developed two malaria models to address the issues of imported malaria cases due to cross-border mobility of migrant workers and relapse malaria cases of Vivax and Ovale, based on malaria incidence in Nepal. Since 2014, imported cases have consistently exceeded local cases, with nearly 80% of cases being Vivax. Through our models, we gained significant insights into malaria transmission dynamics and identified effective control strategies. We developed a mathematical model that incorporates cross-border mobility. In the absence of cross-border mobility, reducing the epidemic threshold R_0 just below unity may not be sufficient for malaria elimination in the home country and among migrants abroad. In the presence of mobility with complete protection abroad, reducing R_1 just below unity may still be inadequate for eliminating malaria both at home and among the migrant population. Furthermore, without protection abroad and border screening, the home country cannot be free from malaria until the abroad is malaria-free. Thus, it is important to analyze the disease dynamics when the threshold numbers are below unity through backward bifurcation analysis.

We simplified the model with cross-border mobility for an extensive backward bifurcation analysis and proved analytically that the mobility of infectious migrant workers contributes to the phenomenon of backward bifurcation. This is a major finding in our study and in the field of backward bifurcation literature. The analysis showed that without cross-border mobility, backward bifurcation occurs only if the disease-induced mortality rate is above a certain threshold. However, with ongoing cross-border mobility and complete protection from malaria transmission abroad, elimination is achievable only if the mobility rate of infectious migrants is kept below a critical threshold. Without protection abroad and border screening, malaria elimination is not possible unless the abroad is malaria-free. In this case, we determined the mosquito biting rate threshold needed to maintain malaria at a low level in the home country.

Simulation of the model with Nepal's malaria parameters showed that if cross-border mobility is completely restricted, malaria can be eliminated from Nepal by 2026 due to the negligible disease-induced death rate. Currently, there is no protection policy for Nepalese migrants abroad, and mobility continues. Thus, Nepal can maintain a low malaria level with local control strategies, but elimination is not possible until malaria

is eliminated in India. However, if policies are implemented to protect migrants abroad and adopt strict border screening to keep the mobility of infectious migrants below a threshold, malaria elimination in Nepal is possible. Additionally, Mobility Restriction (MR) is the most effective strategy for low mosquito biting rates, while ITN is best for high biting rates, suggesting season- and location-specific strategies.

In our previous malaria model with cross-border mobility, we acknowledged the limitation of not including relapse malaria cases. Our ordinary differential equation model assumed an instantaneous rate, whereas most real-world results are impacted by some historical functions. To address these limitations, we developed a delay malaria model incorporating relapse. It is important to note that in recent years, the Nepal government has initiated collaboration with Indian authorities to restrict the cross-border mobility of infectious migrants.

We introduced a comprehensive malaria transmission model that accounts for relapse delays in the absence of imported cases. Our findings indicate that relapse dynamics significantly affect malaria transmission. Specifically, increasing relapse delays prolong the time to achieve malaria-free equilibrium when $R_0 < 1$ but accelerate the convergence to endemic equilibrium when $R_0 > 1$. These insights highlight the importance of addressing relapse cases to achieve effective malaria control.

Overall, this dissertation underscores the critical impact of cross-border mobility and relapse dynamics on malaria transmission in Nepal. It highlights the necessity of stringent control measures, particularly Mobility Restriction, to meet the 2026 malaria elimination target. The developed models and simulations offer valuable insights that can inform policy decisions and practical strategies, not only for Nepal but also for other countries facing similar challenges. Ensuring complete protection from malaria transmission abroad and controlling the mobility of infectious migrants are essential steps toward successful malaria elimination.

Our study made two recommendations to the policy level for successful malaria elimination in Nepal by 2026: (a) Implement a counseling program about protection tools for migrants before moving abroad, together with rigorous border screening and isolation, to achieve malaria elimination in Nepal by 2026 if there are no relapse cases. (b) Establish and enforce a comprehensive radical cure treatment protocol alongside a structured follow-up program to maintain relapse proportions below a certain level, as indicated by our simulations, if there are no imported cases.

6.3 Future research directions

The following areas will be the potential research areas to asses the global malaria eradication.

1. Malaria transmission model incorporating the mosquito mobility from endemic to non-endemic region.
2. The malaria model incorporating cross-border mobility and relapse in low endemic countries.
3. Risk based malaria model with high, moderate and low risk regions of Nepal.
4. Malaria model incorporating the temperature variation.
5. Risk of infection and risk of hospitalization in vector-borne diseases.

References

L. J Abu-Raddad, P Patnaik, and J. G Kublin. Dual infection with hiv and malaria fuels the spread of both diseases in sub-saharan africa. *Science*, **314**(5805):1603–1606, 2006.

M. A Acevedo, O Prosper, K Lopiano, N Ruktanonchai, T. T Caughlin, M Martcheva, C. W Osenberg, and D. L Smith. Spatial heterogeneity, host movement and mosquito-borne disease transmission. *PloS one*, **10**(6):e0127552, 2015.

E Agyingi, T Wiandt, and M Ngwa. Stability and hopf bifurcation of a two species malaria model with time delays. *Letters in Biomathematics*, **4**(1):59–76, 2017.

S Akbari, N. K Vaidya, and L. M Wahl. The time distribution of sulfadoxine-pyrimethamine protection from malaria. *Bulletin of mathematical biology*, **74**: 2733–2751, 2012.

D Aldila. A superinfection model on malaria transmission: Analysis on the invasion basic reproduction number. *Commun. Math. Biol. Neurosci.*, **2021**:Article–ID, 2021.

R. M Anderson. *The population dynamics of infectious diseases: theory and applications*. Springer, 2013a.

R M Anderson. *The population dynamics of infectious diseases: theory and applications*. Springer, 2013b.

R. M Anderson and R. M May. *Infectious diseases of humans: dynamics and control*. Oxford university press, 1991a.

R M Anderson and R M May. *Infectious diseases of humans: dynamics and control*. Oxford university press, 1991b.

R. M. Anderson and R. M. May. *Infectious Diseases of Humans: Dynamics and Control*. Oxford University Press, 1992.

S Antinori, L Galimberti, L Milazzo, and M Corbellino. Biology of human malaria plasmodia including plasmodium knowlesi. *Mediterranean journal of hematology and infectious diseases*, **4**(1), 2012.

L. E Aragon and C Espinal. Expansion de la frontera, expansion de la enfermeded: movilidad geografica y salud en la amazonia. *Enfoque Integral de la Salud Humana en la Amazonia*, pages 429–456, 1992.

S Arik, B Traore, B Sangare, and S Traore. A mathematical model of malaria transmission with structured vector population and seasonality. *Journal of Applied Mathematics*, **2017**:6754097, January 2017. ISSN 1110-757X. doi: 10.1155/2017/6754097. URL `https://doi.org/10.1155/2017/6754097`.

H. H. Askling, F Bruneel, G Burchard, F Castelli, P. L. Chiodini, M. P. Grobusch, R Lopez-Velez, M Paul, and E Petersen. Management of imported malaria in europe. *Malaria Journal*, **11**:328, 2012.

NTJ Bailey. *The Biomathematics of Malaria*. Charles Griffin and Company Ltd, London, 1982.

S. I Bala and B Gimba. Modeling the impacts of income inequality on malaria transmission dynamics. *International Journal of Engineering Research and Applications*, **12**(2):31–46, 2022.

H. T. Banks, S. Hu, and W. C. Thompson. *Modeling and Inverse Problems in the Presence of Uncertainty*. CRC Press, Boca Raton, FL, 2014.

K. E Battle, M. S Karhunen, S Bhatt, P. W Gething, R. E Howes, N Golding, T. P Van Boeckel, J. P Messina, G.D Shanks, D. L Smith, et al. Geographical variation in plasmodium vivax relapse. *Malaria journal*, **13**(1):1–16, 2014.

J. C Beier. Malaria parasite development in mosquitoes. *Annual review of entomology*, **43**(1):519–543, 1998.

A Berman and R. J Plemmons. *Nonnegative matrices in the mathematical sciences*. SIAM, 1994.

D Bernoulli. An attempt at a new analysis of the mortality caused by smallpox and of the advantages of inoculation to prevent it. *Inoculation against Smallpox*, 1760. Translated and reprinted in Bull. Hist. Med. 1946;20:21-30.

J Bradley, F Monti, A. M Rehman, C Schwabe, D Vargas, G Garcia, D Hergott, M Riloha, and I Kleinschmidt. Infection importation: a key challenge to malaria elimination on bioko island, equatorial guinea. *Malaria journal*, **14**(1):1–7, 2015.

F Brauer. Backward bifurcations in simple vaccination models. *Journal of Mathematical Analysis and Applications*, **298**(2):418–431, 2004.

F Brauer. Backward bifurcations in simple vaccination/treatment models. *Journal of Biological Dynamics*, **5**(5):410–418, 2011. doi: 10.1080/17513758.2010.510584. URL `https://doi.org/10.1080/17513758.2010.510584`.

F Brauer, P van den Driessche, and J Wu. *Mathematical Epidemiology*. Springer, 2008.

B Buonomo and C Vargas-De-Leon. Stability and bifurcation analysis of a vector-bias model of malaria transmission. *Mathematical Biosciences*, **242**(1):59–67, 2013.

S Busenberg and K Cooke. *Vertically Transmitted Diseases: Models and Dynamics*, volume **23**. Springer Science & Business Media, 2012. ISBN 978-1-4612-1458-7. doi: 10.1007/978-1-4612-1458-7.

C Castillo-Chavez and B Song. Dynamical models of tuberculosis and their applications. *Mathematical Biosciences and Engineering*, **1**(2):361–404, April 2004. ISSN 1547-1063. doi: 10.3934/mbe.2004.1.361.

F Chamchod and JC Beier. Modeling plasmodium vivax: relapses, treatment, seasonality, and g6pd deficiency. *Journal of theoretical biology*, **316**:25–34, 2013.

F Chamchod and N F Britton. Analysis of a vector-bias model on malaria transmission. *Bulletin of Mathematical Biology*, **73**(3):639–657, March 2011. ISSN 1522-9602. doi: 10.1007/s11538-010-9535-8.

S-S Chen, C-Y Cheng, and Y Takeuchi. Stability analysis in delayed within-host viral dynamics with both viral and cellular infections. *Journal of Mathematical Analysis and Applications*, **442**(2):642–672, 2016.

N Chitnis, J M Cushing, and JM Hyman. Bifurcation analysis of a mathematical model for malaria transmission. *SIAM Journal on Applied Mathematics*, **67**(1): 24–45, 2006.

N Chitnis, J M Hyman, and JM Cushing. Determining important parameters in the spread of malaria through the sensitivity analysis of a mathematical model. *Bulletin of Mathematical Biology*, **70**:1272–1296, 2008.

C Chiyaka, W Garira, and S Dube. Effects of treatment and drug resistance on the transmission dynamics of malaria in endemic areas. *Theoretical Population Biology*, **75**(1):14–29, February 2009. ISSN 0040-5809. doi: 10.1016/j.tpb.2008.10.003.

C Chiyaka, Z Mukandavire, and P Das. Global dynamics of a malaria model with partial immunity and two discrete time delays. *International Journal of Biomathematics*, **4** (02):135–147, 2011.

CS Chu and N J White. Management of relapsing plasmodium vivax malaria. *Expert Review of Anti-infective Therapy*, **14**(10):885–900, October 2016. ISSN 1478-7210. doi: 10.1080/14787210.2016.1220306.

C O Cornelio and O F Seriano. Malaria in south sudan 1: introduction and pathophysiology. *South Sudan Medical Journal*, **4**(1):7–9, 2011.

C Cosner. Models for the effects of host movement in vector-borne disease systems. *Mathematical Biosciences*, **270**:192–197, 2015.

C Cosner, J C Beier, R S Cantrell, D Impoinvil, L Kapitanski, M D Potts, A Troyo, and S Ruan. The effects of human movement on the persistence of vector-borne diseases. *Journal of theoretical biology*, **258**(4):550–560, 2009.

EG Cox F. History of the discovery of the malaria parasites and their vectors. *Parasites and vectors*, **3**(1):1–9, 2010.

L. S David, J. D Chris, and N Amadou. Age and immunity: important factors in the transmission of malaria. *Journal of Infectious Diseases*, **201**(3):337–345, 2010. doi: 10.1086/649830.

M Dhimal, B Ahrens, and U Kuch. Species composition, seasonal occurrence, habitat preference and altitudinal distribution of malaria and other disease vectors in eastern nepal. *Parasites & Vectors*, **7**(1):1–11, January 2014a. ISSN 1756-3305. doi: 10.1186/1756-3305-7-540.

M Dhimal, B Ahrens, and U Kuch. Malaria control in nepal 1963–2012: Challenges on the path towards elimination. *Malaria Journal*, **13**(1):1–14, January 2014b. ISSN 1475-2875. doi: 10.1186/1475-2875-13-241.

AB Diabate, B Sangare, and O Koutou. Mathematical modeling of the dynamics of vector-borne diseases transmitted by mosquitoes: Taking into account aquatic stages and gonotrophic cycle. *Nonautonomous Dynamical Systems*, **9**(1):205–236, January 2022. ISSN 2364-1843. doi: 10.1515/ndyn-2022-0123.

O Diekmann, JAP Heesterbeek, and J A.J. Metz. On the definition and the computation of the basic reproduction ratio r_0 in models for infectious diseases in

heterogeneous populations. *Journal of Mathematical Biology*, **28**:365–382, June 1990. ISSN 0303-6812. doi: 10.1007/BF00178324.

K Dietz, L Molineaux, and A Thomas. A malaria model tested in the african savannah. *Bulletin of the World Health Organization*, **50**(3-4):347, 1974.

EDCD. Malaria elimination program, 2020. URL `https://edcd.gov.np/section/malaria-elimination-program`. Accessed: 2020-07-30.

A Eigenwillig. On multiple roots in descartes rule and their distance to roots of higher derivatives. *Journal of Computational and Applied Mathematics*, **200**(1):226–230, 2007.

S M-AS Elsheikh, K C Patidar, and R Ouifki. Analysis of a malaria model with a distributed delay. *The IMA Journal of Applied Mathematics*, **79**(6):1139–1160, 2014.

Epidemiology and disease control division Nepal. Malaria elimination program. `https://edcd.gov.np/section/malaria-elimination-program`, 2019. Online; accessed 31-July-2023.

X Feng, S Ruan, Z Teng, and K Wang. Stability and backward bifurcation in a malaria transmission model with applications to the control of malaria in china. *Mathematical biosciences*, **266**:52–64, 2015.

X. Feng, L. Zhang, F. Huang, J. Yin, H. Tu, H. Xiao, and S. Zhou. Imported malaria cases in china: Epidemiological characteristics and risk factors. *Malaria Journal*, **19**:392, 2020.

X Fenga, Z Tenga, K Wangb, and F Zhangc. Backward bifurcation and global stability in an epidemic model with treatment and vaccination. *Discrete and Continuous Dynamical Systems-Series B*, **19**(4), 2014.

J A N Filipe, E M Riley, C J Drakeley, C J Sutherland, and A C Ghani. Determination of the processes driving the acquisition of immunity to malaria using a mathematical transmission model. *PLoS computational biology*, **3**(12):e255, 2007.

Centers for Disease Control, Prevention, et al. Global health, division of parasitic diseases and malaria. *ParasitesScabies. Available online: https://www. cdc. gov/parasites/scabies/index. html (accessed on 30 March 2023)*, 2018.

F Forouzannia and A B Gumel. Mathematical analysis of an age-structured model for malaria transmission dynamics. *Mathematical biosciences*, **247**:80–94, 2014.

V Gaigbe-Togbe, L Bassarsky, D Gu, T Spoorenberg, and L Zeifman. World population prospects 2022; united nations: New york, ny, usa, 2022. *Google Scholar*.

D Gao and S Ruan. A multipatch malaria model with logistic growth populations. *SIAM journal on applied mathematics*, **72**(3):819–841, 2012.

R Gautam, A Pokharel, K Adhikari, KN Uprety, and N K Vaidya. Modeling malaria transmission in nepal: impact of imported cases through cross-border mobility. *Journal of Biological Dynamics*, **16**(1):528–564, 2022.

R Gautam, K Adhikari, A Pokharel, K. N Uprety, and N. K Vaidya. Role of cross-border mobility on the backward bifurcation of malaria transmission model: Implications for malaria control in nepal. *Nonlinear Analysis: Real World Applications*, **81**: 104173, 2025.

M Ghosh, S Olaniyi, and O S Obabiyi. Mathematical analysis of reinfection and relapse in malaria dynamics. *Applied Mathematics and Computation*, **373**:125044, 2020.

C Golgi. Sulle febbri malariche estivo-autunnali. *Rendiconti dell'Accademia dei Lincei*, **2**:155–158, 1886.

Ministry of Health GoN and EDCD Population. Nepal malaria strategic plan 2014-2025, 2016. URL `https://edcd.gov.np/resource-detail/nepal-strategic-plan-2014-2015`.

L Green and D Thompson. Comprehensive strategies for malaria control: An overview. *Global Health Journal*, **10**(2):101–115, 2020.

J T Griffin, T D Hollingsworth, L C Okell, T S Churcher, M White, W Hinsley, T Bousema, C J Drakeley, NM Ferguson, M-G Basanez, et al. Reducing plasmodium falciparum malaria transmission in africa: a model-based evaluation of intervention strategies. *PLoS medicine*, **7**(8):e1000324, 2010.

DM Grobman. Homeomorphism system of differential equations. *DAN USSR*, **128**(5): 880–881, 1959.

A B Gumel. Causes of backward bifurcations in some epidemiological models. *Journal of Mathematical Analysis and Applications*, **395**(1):355–365, 2012.

T. U H. Juliette, R Isobel, F Seth, R Marian-Andrei, L Shengjie, C Justin, J. W Daniel, M Swapnil, and B Samir. Using hawkes processes to model imported and local malaria cases in near-elimination settings. pages 1–24, 2020.

J K Hale and SM V Lunel. *Introduction to functional differential equations*, volume **99**. Springer Science & Business Media, 2013.

B D Handari, F Vitra, R Ahya, S T Nadya, and D Aldila. Optimal control in a malaria model: intervention of fumigation and bed nets. *Advances in Difference Equations*, **2019**(1):497, 2019.

B D Handari, R A Ramadhani, C W Chukwu, SHA Khoshnaw, and D Aldila. An optimal control model to understand the potential impact of the new vaccine and transmission-blocking drugs for malaria: A case study in papua and west papua, indonesia. *Vaccines*, **10**(8):1174, 2022.

E Harris and J White. Advancements in malaria diagnosis: Loop-mediated isothermal amplification (lamp). *Clinical Microbiology Reviews*, **28**(3):456–471, 2015.

P Hartman. A lemma in the theory of structural stability of differential equations. *Proceedings of the American Mathematical Society*, **11**(4):610–620, 1960.

IM Hastings. A model for the origins and spread of drug-resistant malaria. *Parasitology*, **115**(2):133–141, August 1997. ISSN 0031-1820. doi: 10.1017/S0031182097001356.

F F Herdicho, W Chukwu, H Tasman, et al. An optimal control of malaria transmission model with mosquito seasonal factor. *Results in Physics*, **25**:104238, 2021.

M W Hirsch, S Smale, and R L Devaney. *Differential Equations, Dynamical Systems, and an Introduction to Chaos*. Academic Press, 2012.

M Hongyu, X Xiaohua, P Alans, and W Hulin. On identifiability of nonlinear ode models and applications in viral dynamics. *SIAM Review*, **53**(1):3–39, 2011.

M B Hoshen and A P Morse. A weather-driven model of malaria transmission. *Malaria journal*, **3**:1–14, 2004.

Z Hu, S Yin, and H Wang. Stability and hopf bifurcation of a vector-borne disease model with saturated infection rate and reinfection. *Computational and Mathematical Methods in Medicine*, **2019**, 2019.

H-Fg Huo, G-M Qiu, et al. Stability of a mathematical model of malaria transmission with relapse. In *Abstract and Applied Analysis*, volume **2014**. Hindawi, 2014. doi: 10.1155/2014/364751.

R Isobel, R C Jos Eduardo, M. C Zulma, R Manuel Gomez, B. G Caterina G Kyle, S Kammerle, G.T. W Patrick, C. G Azra, B Samir, and et al. Estimating spatiotemporally varying malaria reproduction numbers in a near elimination setting. *Nat Commun*, **9**(1):2476–2484, 2018.

S Jeffrey and M Pia. The economic and social burden of malaria. *Nature*, **415**:680–685, 2002.

M Jones and E Brown. The origin of the term "malaria": An historical perspective. *Journal of Tropical Medicine*, **12**(3):201–210, 2005. Explores the derivation and historical context of the term "malaria".

M Jones and E White. Microscopic diagnosis of malaria: Methods and accuracy. *Tropical Medicine and International Health*, **19**(6):622–627, 2014.

K. C. Kain, M. A. Harrington, and S Tennyson. Imported malaria cases: Geographic distribution and epidemiology. *Clinical Infectious Diseases*, **27**(1):1–8, 1998.

R. kamel Naji and A. and Adnan Thirthar. Stability and bifurcation of an sis epidemic model with saturated incidence rate and treatment function. *Iranian Journal of Mathematical Sciences and Informatics*, **15**(2):129–146, 2020.

A Kammanee and O Tansuiy. A mathematical model of transmission of plasmodium vivax malaria with a constant time delay from infection to infectious. *Communications of the Korean Mathematical Society*, **34**(2):685–699, March 2019. ISSN 1225-1763. doi: 10.4134/CKMS.c180665.

A Kammanee, N Kanyamee, and IM Tang. Basic reproduction number for the transmission of plasmodium vivax malaria. *The Southeast Asian Journal of Tropical Medicine and Public Health*, **32**(4):702–706, December 2001. ISSN 0125-1562.

M J. Keeling and P Rohani. *Modeling Infectious Diseases in Humans and Animals*. Princeton University Press, 2008.

S Kim, A Tridane, and D E Chang. Human migrations and mosquito-borne diseases in africa. *Mathematical Population Studies*, **23**(2):123–146, 2016.

JC Koella. On the use of mathematical models of malaria transmission. *Acta tropica*, **49**(1):1–25, 1991.

J C Kohler and A Bowra. Exploring anti-corruption, transparency, and accountability in the world health organization, the united nations development programme, the world bank group, and the global fund to fight aids, tuberculosis and malaria. *Globalization and health*, **16**:1–10, 2020.

O Koutou, B Traore, and B Sangare. Mathematical modeling of malaria transmission global dynamics: taking into account the immature stages of the vectors. *Advances in Difference Equations*, **2018**:1.

O Koutou, B Traore, and B Sangare. Mathematical model of malaria transmission dynamics with distributed delay and a wide class of nonlinear incidence rates. *Cogent Mathematics & Statistics*, **5**(1):1564531, 2018.

CLA Laveran. A new protozoon found in the blood of malarial patients. *Lancet*, **1**: 327–328, 1881. Original discovery of the Plasmodium parasite as the causative agent of malaria.

A Le Menach, A J Tatem, J M Cohen, S I Hay, H Randell, AP Patil, and D L Smith. Travel risk, malaria importation and malaria transmission in zanzibar. *Scientific Reports*, **1**(1):93, September 2011. ISSN 2045-2322. doi: 10.1038/srep00093.

K E Lestari, US Pasaribu, SW Indratno, and H Garminia. Generating roots of cubic polynomials by cardano's approach on correspondence analysis. *Heliyon*, **6**(6), 2020.

Y. Liu, J. Sun, H. Lu, H. Yang, and Q. Liu. Malaria in southeast asia: Epidemiology and risk factors. *BMC Public Health*, **14**:129, 2014.

Y Lou and X-Q Zhao. A climate-based malaria transmission model with structured vector population. *SIAM Journal on Applied Mathematics*, **70**(6):2023–2044, 2010.

W MacCallum. On the sexual reproductive forms of a malaria-like parasite found in birds; with a note on the exflagellation of malaria parasites. *Journal of Experimental Medicine*, **2**(4):371–386, 1897. doi: 10.1084/jem.2.4.371.

G Macdonald et al. The analysis of infection rates in diseases in which super infection occurs. *Tropical diseases bulletin*, **47**:907–915, 1950.

G Macdonald et al. The epidemiology and control of malaria. *The Epidemiology and Control of Malaria.*, 1957.

S Manandhar, C L Bhusal, U Ghimire, S P Singh, D B Karmacharya, and S M Dixit. A study on relapse/re-infection rate of plasmodium vivax malaria and identification of the predominant genotypes of p. vivax in two endemic districts of nepal. *Malaria Journal*, **12**(1):1–8, 2013.

E Marchiafava and A Celli. Ulteriore ricerche sulle febbri malariche estivo-autunnali. *Riforma Med*, **1**:1–14, 1885.

M Martcheva. *An introduction to mathematical epidemiology*, volume **61**. Springer, 2015.

P Martens and L Hall. Malaria on the move: human population movement and malaria transmission. *Emerging infectious diseases*, **6**(2):103, 2000.

WJ Martens, L W Niessen, J Rotmans, T H Jetten, and A J McMichael. Potential impact of global climate change on malaria risk. *Environmental health perspectives*, **103**(5):458–464, 1995.

T Miliyon. Backward bifurcation in sirs malaria model. *arXiv: Populations and Evolution*, 2017.

J Miller and D Clark. *Diagnosis and Treatment Process of Malaria Disease*. Academic Press, London, UK, 2018.

D A Milner. Malaria pathogenesis. *Cold Spring Harbor perspectives in medicine*, **8**(1): a025569, 2018.

AK Misra, R K Rai, and Y Takeuchi. Modeling the effect of time delay in budget allocation to control an epidemic through awareness. *International Journal of Biomathematics*, **11**(02):1850027, 2018.

J Mohammed-Awel, R Zhao, E Numfor, and S Lenhart. Management strategies in a malaria model combining human and transmission-blocking vaccines. *Discrete and Continuous Dynamical Systems-B*, **22**(3):977, 2017.

C Moler. *Numerical Computing with MATLAB*. Society for Industrial and Applied Mathematics (SIAM), 2004.

P Muentener, P Schlagenhauf, and R Steffen. Imported malaria in industrialized countries 1993–1998: Epidemiology and analysis of risk factors. *Tropical Medicine and International Health*, **4**(1):72–76, 1999.

A YA Mukhtar, J B Munyakazi, and R Ouifki. Assessing the role of human mobility on malaria transmission. *Mathematical Biosciences*, **320**:108304, 2020.

J A Najera, M Gonzalez-Silva, and PL Alonso. Some lessons for the future from the global malaria eradication programme (1955–1969). *PLoS medicine*, **8**(1):e1000412, 2011.

National Vector Borne Disease Control Programme. Malaria site india: Comprehensive data on malaria in india. `http://www.malariasite.com/india-malaria-data`, 2020. Accessed: 2020-12-15.

The Rising Nepal. Imported cases threaten target to malaria elimination by 2025: Experts, 2022. URL `https://risingnepaldaily.com/news/11937`.

G A Ngwa. Modelling the dynamics of endemic malaria in growing populations. *Discrete and Continuous Dynamical Systems Series B*, **4**:1173–1202, December 2004. ISSN 1553-5231. doi: 10.3934/dcdsb.2004.4.1173.

G A Ngwa and W S Shu. A mathematical model for endemic malaria with variable human and mosquito populations. *Mathematical and Computer Modelling*, **32**(7-8): 747–763, October 2000. ISSN 0895-7177. doi: 10.1016/S0895-7177(00)00207-0.

G A Ngwa, A M Niger, and A B Gumel. Mathematical assessment of the role of non-linear birth and maturation delay in the population dynamics of the malaria vector. *Applied Mathematics and Computation*, **217**(7):3286–3313, 2010.

RWD Nickalls. Viete, descartes and the cubic equation. *The Mathematical Gazette*, **90**(518):203–208, 2006.

GoN Ministry of Health and Population. National malaria surveillance guidelines 2019, 2019. URL `https://www.edcd.gov.np/resources/download/national-malaria-surveillance-guidelines-2019`.

Ministry of Health and Government of India Family Welfare. National framework for malaria elimination in india (2016-2030). 2020. URL `http://origin.searo.who.int/india/publications/national_framework_malaria_elimination_india_2016_2030.pdf`.

GON Ministry of Labour and Government of Nepal Employment. Labour migration for employment: A status report for nepal: 2015/2016–2016/2017, 2018.

Ministry of Labour and GoN Employment. Migration and remittances: The case of nepal, 2020. About 5.5 million Nepalese, including 1.9 million male workers, were living abroad, mostly in India.

KO Okosun and O D Makinde. Modelling the impact of drug resistance in malaria transmission and its optimal control analysis. 2011.

S Olaniyi, M Mukamuri, KO Okosun, and OA Adepoju. Mathematical analysis of a social hierarchy-structured model for malaria transmission dynamics. *Results in Physics*, **34**:104991, 2022.

World Health Organization. Dohs, annual report (2017/2018), 2018. URL `https://publichealthupdate.com/department-of-health-services-dohs-annual-report-2074-75-2017-18/`.

World Health Organization et al. Global technical strategy for malaria 2016–2030, 2021 update. *Geneva: World Health Organization*, pages 1–40, 2021.

World Health Organization et al. *World malaria report 2022*. World Health Organization, 2022.

R M Oxborough. Trends in us presidents malaria initiative-funded indoor residual spray coverage and insecticide choice in sub-saharan africa (2008–2015): urgent need for affordable, long-lasting insecticides. *Malaria journal*, **15**(1):146, 2016.

P E Parham and E Michael. Modeling the effects of weather and climate change on malaria transmission. *Environmental health perspectives*, **118**(5):620–626, 2010.

P Pongsumpun and I-M Tang. Transmission model for plasmodium vivax malaria: Conditions for bifurcation. *International Journal of Bioengineering and Life Sciences*, **1**(5):58–65, May 2007. ISSN 2251-1789.

The Kathmandu Post. *Budget cuts by government and donors hinder Nepals fight against malaria*. URL `https://kathmandupost.com/health/2023/04/27/budget-cuts-by-government-and-donors-hinder-nepal-s-fight-against-malaria`.

L Qiang and B-G Wang. An almost periodic malaria transmission model with time-delayed input of vector. *Discrete & Continuous Dynamical Systems-Series B*, **22**(4), 2017.

M Rafikov, L Bevilacqua, and APP Wyse. Optimal control strategy of malaria vector using genetically modified mosquitoes. *Journal of Theoretical Biology*, **258**(3): 418–425, 2009.

M Rahman, K Bekele-Maxwell, L L Cates, HT Banks, and N K Vaidya. Modeling zika virus transmission dynamics: parameter estimates, disease characteristics, and prevention. *Scientific Reports*, **9**(1):10575, 2019.

K R Rijal, B Adhikari, P Ghimire, M R Banjara, B Hanboonkunupakarn, M Imwong, K Chotivanich, K P Ceintury, B K Lal, GD Thakur, et al. Epidemiology of plasmodium vivax malaria infection in nepal. *The American journal of tropical medicine and hygiene*, **99**(3):680, 2018.

K R Rijal, B Adhikari, N Adhikari, S P Dumre, M S Banjara, U T Shrestha, MR Banjara, N Singh, L Ortegea, BK Lal, et al. Micro-stratification of malaria risk in nepal: implications for malaria control and elimination. *Tropical Medicine and Health*, **47**: 1–12, 2019a.

K R Rijal, B Adhikari, P Ghimire, MR Banjara, T G Das, B Hanboonkunupakarn, M Imwong, K Chotivanich, N PJ Day, NJ White, et al. Efficacy of primaquine in preventing short-and long-latency plasmodium vivax relapses in nepal. *The Journal of Infectious Diseases*, **220**(3):448–456, August 2019b. ISSN 1537-6613. doi: 10.1093/infdis/jiz168.

S Roberts and M Johnson. Current antimalarial therapies and their uses: An overview. *International Journal of Antimicrobial Agents*, **45**(3):251–259, 2016.

R Ross. On some peculiar pigmented cells found in two mosquitoes fed on malarial blood. *BMJ*, **2**(1928):1786–1788, 1897. doi: 10.1136/bmj.2.1994.1786.

R Ross. *The prevention of malaria*. John Murray, 1911.

S Ruan, D Xiao, and J C Beier. On the delayed ross–macdonald model for malaria transmission. *Bulletin of mathematical biology*, **70**(4):1098–1114, 2008.

A Sandia Mago. Venezuela: Malaria y movilidad humana estacional de las comunidades indigenas del rio riecito del estado apure: Salud y sociedad. *Fermentum*, (8-9): 103–123, 1993.

CD Schunn, D Wallach, et al. Evaluating goodness-of-fit in comparison of models to data. *Psychologie der Kognition: Reden and vortrage anlasslich der emeritierung von Werner Tack*, pages 115–154, 2005.

A Sha, S Samanta, M Martcheva, and J Chattopadhyay. Backward bifurcation, oscillations and chaos in an eco-epidemiological model with fear effect. *Journal of biological dynamics*, **13**(1):301–327, 2019a.

A Sha, S Samanta, M Martcheva, and J Chattopadhyay. Backward bifurcation, oscillations and chaos in an eco-epidemiological model with fear effect. *Journal of biological dynamics*, **13**(1):301–327, 2019b.

BS Shanker, RP Uttam, K Mukti, U Murari, N-B Kesara, and M Phunuch. Epidemiological situations and control strategies of vector-borne diseases in nepal during 1998-2016. *Journal of Health Research*, **33**(6):478–493, 2019.

D L Smith, S I Hay, A M Noor, and R W Snow. Predicting changing malaria risk after expanded insecticide-treated net coverage in africa. *Trends in parasitology*, **25** (11):511–516, 2009.

H L Smith and P Waltman. *The theory of the chemostat: dynamics of microbial competition*, volume 13. Cambridge university press, 1995.

J Smith. *A History of Malaria and its Control*. Oxford University Press, Oxford, UK, 1999. Discusses the introduction of the term "malaria" by Francisco Torti in 1718.

J Smith and P Brown. Malaria diagnosis: The importance of accurate detection and diagnosis. *Journal of Infectious Diseases*, **210**(4):120–130, 2015.

G Strang. *Linear Algebra and Its Applications*. Cengage Learning, 2016.

E M Stuckey, J Stevenson, K Galactionova, A Y Baidjoe, T Bousema, W Odongo, S Kariuki, C Drakeley, T A Smith, J Cox, et al. Modeling the cost effectiveness of malaria control interventions in the highlands of western kenya. *PloS one*, **9**(10): e107700, 2014.

J. W. Sturrock Hugh, JM. Novotny, S Kunene, S Dlamini, Z Zulu, J M. Cohen, M S. Hsiang, B Greenhouse, and R D. Gosling. Reactive case detection for malaria elimination: Real-life experience from an ongoing program in swaziland. *PLOS ONE*, **8**(5):1–8, 05 2013.

H Tasman, UD Purwati, FF Herdicho, CW Chukwu, et al. An optimal control problem of malaria model with seasonality effect using real data. *Commun. Math. Biol. Neurosci.*, **2021**:Article–ID, 2021.

H Tasman, D Aldila, P A Dumbela, M Z Ndii, F F Herdicho, and CW Chukwu. Assessing the impact of relapse, reinfection and recrudescence on malaria eradication policy: a bifurcation and optimal control analysis. *Tropical Medicine and Infectious Disease*, **7**(10):263, 2022.

A Tattem, J Smith, and P Brown. The geography of climate change. *Global Environmental Change*, **45**:123–136, 2017.

S. C Thomas, M. C Justin, N Joseph, N Nyasatu, K Simon, and C Simon. Measuring the path toward malaria elimination. *Science*, **13**(6189):1230–1232, 2014.

TNH. Government launches new malaria campaign. Technical report, The New Humanitarian, 2012. URL `https://reliefweb.int/report/nepal/government-launches-new-malaria-campaign?fbclid=IwAR3qKbafo8FBxejGsA_f49cIpIXQONMSYHd4Y64tgWJCoe-9cj2jXGv08i0`.

L Torres-Sorando and DJ. Rodriguez. Models of spatio-temporal dynamics in malaria. *Ecological Modelling*, **104**(2-3):231–240, 1997.

B Traore, O Koutou, and B Sangare. A global mathematical model of malaria transmission dynamics with structured mosquito population and temperature variations. *Nonlinear Analysis: Real World Applications*, **53**:103081, 2020.

J Tumwiine, JYT Mugisha, and LS Luboobi. A mathematical model for the dynamics of malaria in a human host and mosquito vector with temporary immunity. *Applied mathematics and computation*, **189**(2):1953–1965, 2007.

J Tumwiine, JYT Mugisha, and LS Luboobi. A host-vector model for malaria with infective immigrants. *Journal of Mathematical Analysis and Applications*, **361**(1): 139–149, 2010.

NK Vaidya and M Peter. Modeling intracellular delay in within-host hiv dynamics under conditioning of drugs of abuse. *Bulletin of Mathematical Biology*, **83**(7):81, 2021.

NK Vaidya and J Wu. Hiv epidemic in far-western nepal: effect of seasonal labor migration to india. *BMC Public Health*, **11**(310):1–11, 2011a.

NK Vaidya and J Wu. Hiv epidemic in far-western nepal: effect of seasonal labor migration to india. *BMC public health*, **11**:1–11, 2011b.

P Van den Driessche. Reproduction numbers of infectious disease models. *Infectious Disease Modelling*, **2**(3):288–303, 2017.

P Van den Driessche and J Watmough. Reproduction numbers and sub-threshold endemic equilibria for compartmental models of disease transmission. *Mathematical biosciences*, **180**(1-2):29–48, 2002.

P Van den Driessche and J Watmough. Further notes on the basic reproduction number. *Mathematical epidemiology*, pages 159–178, 2008.

J Wairimu, F Chirove, M Ronoh, and D M Malonza. Modeling the effects of insecticides resistance on malaria vector control in endemic regions of kenya. *Biosystems*, **174**: 49–59, 2018.

H Wan and J-A Cui. A model for the transmission of malaria. *Discrete and Continuous Dynamical Systems. Series B*, **11**(2):479–496, 2009.

H Wan and H Zhu. The impact of resource and temperature on malaria transmission. *Journal of Biological Systems*, **20**(03):285–302, 2012.

H Wan, J Cui, et al. A malaria model with two delays. *Discrete Dynamics in Nature and Society*, **2013**, July 2013. ISSN 1026-0226. doi: 10.1155/2013/546195.

J Wang, X-Z Li, and S Bhattacharya. The backward bifurcation of a model for malaria infection. *International Journal of Biomathematics*, **11**(02):1850018, 2018.

S-F Wang, L Hu, and L-F Nie. Global dynamics and optimal control of an age-structure malaria transmission model with vaccination and relapse. *Chaos, Solitons & Fractals*, **150**:111216, 2021.

X Wang and X-Q Zhao. A periodic vector-bias malaria model with incubation period. *SIAM Journal on Applied Mathematics*, **77**(1):181–201, January 2017. ISSN 0036-1399. doi: 10.1137/16M1057904.

H-M Wei, X-Z Li, and M Martcheva. An epidemic model of a vector-borne disease with direct transmission and time delay. *Journal of Mathematical Analysis and Applications*, **342**(2):895–908, June 2008. ISSN 0022-247X. doi: 10.1016/j.jmaa.2008.01.042.

M T White, L Conteh, R Cibulskis, and A C Ghani. Costs and cost-effectiveness of malaria control interventions-a systematic review. *Malaria journal*, **10**:1–14, 2011.

NJ White. Determinants of relapse periodicity in plasmodium vivax malaria. *Malaria journal*, **10**(1):1–36, 2011.

WHO. *Malaria Control: A Field Guide*. WHO Press, 2019.

WHO. World malaria report,2021. Report, WHO, 2021.

WHO. *WHO Malaria Policy Advisory Group (MPAG) Meeting Report, 18-20 April 2023*. MPAG Reports. World Health Organization, Geneva, Switzerland, 1st edition, 2023. ISBN 978-92-4-006998-3. Available at: https://www.who.int/publications/i/item/9789240069983.

Wiki. 2001 nepal census, 2001. URL `https://en.wikipedia.org/wiki/2001_Nepal_census`.

Wiki. 2011 nepal census, 2011. URL `https://en.wikipedia.org/wiki/20011_Nepal_census`.

Wikipedia. Cubic equation. `https://en.wikipedia.org/wiki/Cubic_equation`, 2023. [Online; accessed 14-April-2023].

S Williams and M Johnson. Evaluating the performance of rapid diagnostic tests for malaria. *Malaria Journal*, **13**:150, 2014.

E Worrall, J Hill, J Webster, and J Mortimer. Experience of targeting subsidies on insecticide-treated nets: what do we know and what are the knowledge gaps? *Tropical medicine and international health*, **10**(1):19–31, 2005.

Y Xing, Z Guo, and J Liu. Backward bifurcation in a malaria transmission model. *Journal of Biological Dynamics*, **14**(1):368–388, 2020.

J Xiulei, J Shuwan, and G Daozhou. Mathematical analysis of the rossmacdonald model with quarantine. *Bulletin of Mathematical Biology*, **82**(4):47, 2020.

H Yan, S Wei, Y Sui, S Lu, W Zhang, X Feng, Y Liu, T Zhang, W Ruan, J Xia, et al. Analysis of the relapse of imported plasmodium vivax and plasmodium ovale in five provinces of china. *Malaria Journal*, **22**(1):209, 2023.

HM Yang. Malaria transmission model for different levels of acquired immunity and temperature-dependent parameters (vector). *Revista de saude publica*, **34**:223–231, 2000.

Y Zhang, S Liu, and Z Bai. A periodic malaria model with two delays. *Physica A: Statistical Mechanics and its Applications*, **541**:123327, 2020.

X-Q Zhao. Uniform persistence in processes with application to nonautonomous competitive models. *Journal of mathematical analysis and applications*, **258**(1): 87–101, 2001.

F Zhilan and W Dominik. A model for malaria with relapse: Analytical and numerical analysis. *Mathematical Biosciences*, 184(1):23–38, 2003.

G. Zhou, Y. A. Afrane, S. Munga, D. Zhong, L. Cui, and G. Yan. Trends in malaria in africa: Progress and challenges. *International Journal of Environmental Research and Public Health*, **13**(2):123, 2016.

IJ Zucker. 92.34 the cubic equation-a new look at the irreducible case. *The Mathematical Gazette*, **92**(524):264–268, 2008.

Appendix

Publications

1. **Gautam, R.,** Pokharel, A., Adhikari, K., Uprety, K.N. and Vaidya, N.K., 2022. Modeling malaria transmission in Nepal: impact of imported cases through cross-border mobility. Journal of Biological Dynamics, 16(1),528-564.

2. **Gautam, R**., Adhikari, K., Pokharel, A., Uprety, K. N.,& Vaidya, N. K. (2025). Role of cross-border mobility on the backward bifurcation of malaria transmission model: Implications for malaria control in Nepal. Nonlinear Analysis: Real World Applications, 81, 104173.

3. Adhikari, K. **Gautam, R.,** Pokharel, A., Uprety KN. Vaidya, NK. Transmission dynamics of COVID-19 in Nepal: Mathematical model uncovering effective controls, Journal of Theoretical Biology, Volume 521, 2021, 110680, ISSN 0022-5193,
https://doi.org/10.1016/j.jtbi.2021.110680.

4. Pokharel A., Adhikari K., **Gautam R.,** Uprety KN., Vaidya NK., Modeling transmission dynamics of measles in Nepal and its control with monitored vaccination program. Math Biosci Eng. 2022 Jan 1;19(8):8554-79.

5. Pokharel A., Adhikari K., **Gautam R.,** Uprety KN., Vaidya NK., Modeling Measles Transmission in Adults and Children: Implications to Vaccination for Eradication. Infectious Disease Modelling.

6. Adhikari, K., **Gautam, R.,** Pokharel, A., Uprety KN., Vaidya, NK., Data-Driven Models for the Risk of Infection and Hospitalization during a Pandemic: Case Study on COVID-19 in Nepal. *Journal of Theoretical Biology.*

7. Adhikari, K., **Gautam, R.,** Pokharel, A., Uprety KN., Dhimal M.N, Vaidya, NK., Insight into delta variant dominated second wave of COVID-19 in Nepal, Epidemics (2022) 100642.

8. Adhikari K., Dhan Bahadur Shrestha DB., **Gautam R.,** Pokharel A. Transmission Dynamics of COVID-19 in Nepal. Humanities and Social Sciences Journal, Volume 13, Number 1, 2021, 155-169.

9. Chanda NB., Adhikari K., **Gautam R.,** Pokharel A., Uprety KN., Estimating effects of nonpharmaceutical interventions of COVID-19 in Sudurpaschim province, Nepal. *Journal of Institute of Science and Technology*, Vol. 28 No. 1 (2023), DOI: https://doi.org/10.3126/jist.v28i1.49044.

10. Gautam Dwarika., **Gautam R.,**.,Adhikari K., Pokharel A., Uprety KN., Transmission Dynamics of Dengue Disease in the Rupandehi District of Nepal. *Journal of Nepal Mathematical Society (JNMS)*, (2024), June.

11. Pokharel A., Adhikari K., **Gautam R**. 2024. Modelling the Impact of Vaccination on the Control of Measles in Nepal, T*he Nepali Mathematical Sciences Report* (2024),41(1), 1534, doi; https://doi.org10.3126/nmsr.v41i1.67453.

12. **Gautam, R.,** Adhikari, K., Pokharel,A., Ghosh,B., Schwartz,E. J., Uprety, K.N. and Vaidya, N.K., 2022. Modeling malaria transmission with relapse delay: Impact on elimination plan of low endemic countries. (Submitted)

Presentation to the department

- Sixth Progress presentation: Modeling malaria transmission with delay in relapse: impact of relapse in elimination plan of low endemic countries, on the dated 2080-06-14, Central Department of Mathematics, Research Committee, IOST.
- Contributed Talk in PhD festival 2080: Modeling malaria transmission with delay in relapse: impact of relapse in elimination plan of low endemic countries, on the dated 2080-06-21, Central Department of Mathematics
- Fifth Progress presentation: Modeling malaria transmission with delay in relapse: impact of relapse in elimination plan of low endemic countries, on the dated 2080-06-14, Central Department of Mathematics, Research Committee, IOST.
- Fourth Progress presentation: Role of the Cross-border Mobility on the Backward bifurcation of malaria transmission model: Implications for con- trol and elimination of malaria in Nepal, on the dated 2079-10-16, Central Department of Mathematics, Research Committee, IOST.
- Third Progress presentation (Refinement of Data Fitting and Model Analysis and ready manuscript to submit in one of the reputed international journal) on the dated 2077-10-12, Central Department of Mathematics, Research Committee, IOST.
- Second Progress presentation (Rigorous Analysis of the Model including cross-border mobility and its impact for malaria elimination programs), on the dated 2077-05-26, Central Department of Mathematics, Research Committee, IOST.
- First Progress presentation (Literature Review, Model Formulation, Model Validation, Data Fitting and Parameters Estimation),on the dated 2077-02-25, Central Department of Mathematics, Research Committee, IOST.

Conferences/Workshops/Seminors

- **Poster presentation in PhD festival 2080:** Modeling malaria transmission with delay in relapse: impact of relapse in elimination plan of low endemic countries, on the dated 2080-06-21, Central Department of Mathematics.

- **Presentation:** Bifurcation Analysis of malaria transmission model:Applications in elimination of malaria from Nepal. Third International Conference on Applications of Mathematics to Nonlinear Sciences.(25 May, 2023, Pokhara organize by ANMA and NMS)).

- **Presentation:** Bifurcation Analysis of malaria transmission model:Applications in elimination of malaria from Nepal. National Conference on Mathemat- ics & Its Applications (NCMA-2022) (11-13 June, 2022, Ilam).

- **Presentation:** Modeling malaria transmission in Nepal: impact of im- ported cases through cross-border mobility. (12 October, 2022, IIT, In- dore(Through CIMPA research help project)).

- **Facilitator:** Data visualization in epidemic models. Infectious diseases workshop on "Mathematical Modeling for epidemic control and preven tion" (21-24, June 2022). Nepal health research council.

- **Participation and presentation:** CIMPA Summer Research School in Mathematical Epidemiology (09/05/2022 to 20/05/2022). Dhaka University, Bangaladesh.

- **Participation** in the 13th Conference on Dynamical Systems Applied to Biology and Natural Sciences (DSABNS 2022) Mathematical and Theo- retical Biology Group (MTB),Feb. 8- 11, 2022.

- **Presentation :** Bifurcation Analysis of Malaria Transmission Including Cross-Border Mobility. Recent Trends in Mathematical Modeling and its Applications (NCRTMMA 2021) August 23-27.

- **Presentation:** Bifurcation Analysis of Malaria Transmission Model: in the 3rd International Conference on Frontiers of Science and Technology-2021 (ICFST-2021) India, scheduled on August 13-14, 2021 in virtual mode.

- **Presentation** in ICCA NEPAL 2021, organized by Nepal Mathematical Society: Bifurcation Analysis of Malaria Including the Cross-Border Mo- bility between Nepal and India.

- **Poster presentation**: Bifurcation Analysis: Malaria Model with Cross- Border Mobility in the 3rd Annual Meeting of the SIAM Texas-Louisiana Section, October 16 - 18, 2020.

- **Participation** in the 3rd Annual Meeting of the SIAM Texas-Louisiana Section Hosted by Texas A& M University.

- **Participation** in the talk on the topic of "The Basic Reproduction Number R_0 in Infectious Disease: Implication to COVID-19 Epidemic in Nepal" by Naveen K Vaidya organized by Nepal Statistical Society Virtual Zoom meeting, 9:30-10:30 am, August 29, 2020.

Scholarly Awards/honors

- **PhD Research Fellowship:** GRAID (Graduate Research Assistantships in Developing Countries) Program, International Mathematical Union (IMU). Fellowship period: 06/01/2021 05/31/2025.

- **PhD Fellowship and Research Supports Grant:** University Grants Commission (UGC), PhD Fellowship period: 2021-2024.

- **NMS-Fellowship-2020:** Nepal Mathematical Society.

- **Awarded paper: Gautam, R.,** Pokharel, A., Adhikari, K., Uprety, K. N., & Vaidya, N. K. (2022). Modeling malaria transmission in Nepal: impact of imported cases through cross-border mobility. Journal of Biological Dynamics, 16(1), 528-564. (Awarded as the best international paper of the year 2022-2023).

- **Awarded paper:** Adhikari, K., **Gautam, R.,** Pokharel, A., Uprety, K. N., & Vaidya, N. K. (2021). Transmission dynamics of COVID-19 in Nepal: Mathematical model uncovering effective controls. Journal of theoretical biology, 521, 110680.- (Awarded as the best international paper of the year 2021).

- CIMPA Research Visit Travel Support 9/16/2022-10/15/2022 for Indian Institute of Technology, Indore (IITI), India.

JOURNAL OF BIOLOGICAL DYNAMICS
2022, VOL. 16, NO. 1, 528–564
https://doi.org/10.1080/17513758.2022.2096935

Modeling malaria transmission in Nepal: impact of imported cases through cross-border mobility

Ramesh Gautam[a], Anjana Pokharel[b], Khagendra Adhikari[c], Kedar Nath Uprety[d] and Naveen K. Vaidya[e,f,g]

[a]Ratna Rajya Laxmi Campus, Tribhuvan University, KTM, Nepal; [b]Padma Kanya Multiple Campus, Tribhuvan University, KTM, Nepal; [c]Amrit Campus, Tribhuvan University, KTM, Nepal; [d]Central Department of Mathematics, Tribhuvan University, KTM, Nepal; [e]Department of Mathematics and Statistics, San Diego State University, San Diego, CA, USA; [f]Computational Science Research Center, San Diego State University, San Diego, CA, USA; [g]Viral Information Institute, San Diego State University, San Diego, CA, USA

ABSTRACT

The cross-border mobility of malaria cases poses an obstacle to malaria elimination programmes in many countries, including Nepal. Here, we develop a novel mathematical model to study how the imported malaria cases through the Nepal-India open-border affect the Nepal government's goal of eliminating malaria by 2026. Mathematical analyses and numerical simulations of our model, validated by malaria case data from Nepal, indicate that eliminating malaria from Nepal is possible if strategies promoting the absence of cross-border mobility, complete protection of transmission abroad, or strict border screening and isolation are implemented. For each strategy, we establish the conditions for the elimination of malaria. We further use our model to identify the control strategies that can help maintain a low endemic level. Our results show that the ideal control strategies should be designed according to the average mosquito biting rates that may depend on the location and season.

ARTICLE HISTORY
Received 30 June 2021
Accepted 24 June 2022

KEYWORDS
Cross-border mobility; malaria elimination programme; imported malaria cases; mathematical model; Nepal

MATHEMATICS SUBJECT CLASSIFICATIONS 2010
34D20; 37N25; 92B05; 92C50

1. Introduction

Malaria continues to pose a global health burden and is one of the leading causes of death in many developing countries [11]. In 2019, about 229 million cases of malaria and 409 thousand malaria-related deaths were estimated worldwide, mainly in African countries [30,67]. Despite the continuous control efforts with programmes targeting elimination, malaria cases have slightly increased globally for the past few years. According to the WHO reports, the total number of worldwide malaria cases in 2016, 2017, 2018, 2019, and 2020 are 214, 217, 219, 228, and 229 million, respectively. In pursuit of malaria elimination, broad access to human mobility has been a primary obstacle to successful malaria control in many countries, including Nepal [23]. In particular, the human mobility between low and high endemic countries results in the importation of malaria cases from high to low endemic countries, causing potentiality for the resurgence of malaria

CONTACT Naveen K. Vaidya nvaidya@sdsu.edu

Supplemental data for this article can be accessed here. https://doi.org/10.1080/17513758.2022.2096935

in low endemic countries. Notably, the cross-border migrants contribute to the transfer of malaria cases from high to low endemic countries [33]. For example, even though the elimination of malaria from Spain was declared in 1964, about 10,000 cases were reported, mostly in travellers and migrants, in a later year. Similarly, about 12,000 to 15,000 cases of malaria are imported to European Union (EU) every year, with the majority to France, the UK, and Germany from West Africa [32,59,68]. Given the significant obstacle to malaria elimination due to human mobility across borders, studying the impact of the imported cases through cross-border mobility on the malaria elimination programmes is critical.

Nepal is one of the countries facing the direct consequence of a cross-border transfer of malaria cases due to its open border provision with India. Although the malaria elimination programmes in Nepal started in 1958 [25], the trend of malaria cases remained fluctuated between 1963 and 2018, with a peak in 1985 (more than 42,321 cases) [22,28]. After 1985, the number of cases steadily declined, and the transmission rate eventually reached a low level of 0.08 per 1000 annual parasite incidence (API) among the risk population in 2018 [66]. With this rapidly decreasing- trend, the Nepal government has set the goal of zero indigenous malaria by 2022 and malaria elimination by 2026 [29]. However, the porous border between Nepal and India has been a severe concern for achieving these goals because even though the number of total cases declined from 2009 (3500 cases) to 2018 (1065 cases) by 69%, the net imported cases increased during this period by approximately 40 to 58% [28]. Most of these imported cases reported a history of travel to malaria-endemic areas of India [29]. An increase in imported cases has posed an uncertainty about the elimination programmes to meet Nepal's goal set. Mathematical modelling can provide a valuable tool to predict the potential impact of such imported cases on malaria elimination from Nepal.

Since the first differential equation-based model introduced by Ronald Ross in 1911 [12], various mathematical models have been developed to study the impact of control and prevention policies on the incidence of malaria in many endemic regions [6,18,19,36,42,48,54]. These models have been further extended by incorporating age structure, loss of immunity, the effect of social, economic, and environmental factors, human migration, drug resistance of vector, the impact of bed-nets, multi-groups, and multi patches [2–4,7,10,16,20,31,37,45–47,52,61–63]. Even though some mathematical models [8,17,39,51,58] include cross-border mobility, there remains uncertainty on the various aspects of the role of imported cases in vector-borne disease, particularly malaria transmission. Except for some descriptive, analytical, and retrospective studies [21,25,55,57,66], none of the previous models focused on the dynamics of indigenous and imported malaria cases in the context of Nepal, which is in critical condition of achieving the 2026 malaria elimination goal due to cross-border mobility of migrant workers.

Motivated from a previous study [64], which addressed the impact of cross-border mobility on HIV-AIDS epidemics in Nepal, we develop a novel transmission dynamics model of malaria by incorporating the imported cases through the cross-border mobility into a basic malaria model. Using the data of malaria cases in Nepal, we estimate the critical parameters of malaria dynamics in Nepal. We thoroughly analyze our model to study the impact of cross-border mobility on disease eradication and threshold dynamics.

We further use our model to predict the future trend of imported and indigenous malaria cases and evaluate the different control strategies to achieve the malaria elimination goal by 2026.

2. Mathematical model

2.1. Model formulation

To develop a transmission dynamics model of malaria, we divide the total population of the home country into two groups: the population living in the home country (N_{hH}) and the population living abroad as migrant workers (N_{hM}). Each of these groups is further divided into three subgroups: susceptible (S_{hH}), infectious (I_{hH}), and recovered (R_{hH}) in the home country and susceptible (S_{hM}), infectious (I_{hM}), and recovered (R_{hM}) living abroad as migrant workers. Moreover, we consider susceptible and infectious mosquito populations in the home country (S_{vH}, I_{vH}) and abroad (S_{vA}, I_{vA}). We note that the migrant workers, N_{hM}, are included in the total human population abroad (N_{hA}) and thus the corresponding abroad groups, susceptible (S_{hA}), infectious (I_{hA}), and recovered (R_{hA}) include S_{hM}, I_{hM}, and R_{hM}, respectively.

In our model, malaria transmission occurs from infected mosquitoes to susceptible humans and from infected humans to susceptible mosquitoes through mosquito bites. We assume that b and b' are the per capita biting rates of mosquitoes in the home country and abroad, respectively. α_{vh} and α'_{vh} are the probability in the home country and abroad, respectively, that an infectious mosquito transmit malaria to a susceptible human in a single bite. Similarly, α_{hv} and α'_{hv} are the probability in the home country and abroad, respectively, that the malaria is transmitted from infectious human to a susceptible mosquito in a single infectious bite. For the home country, the total number of bites (per time) from all the infectious mosquitoes is bI_{vH} (infectious bites). Among these bites, the susceptible humans get $\frac{bI_{vH}S_{hH}}{N_{hH}}$ infectious bites. Therefore, the incidence rate of humans (i.e. the new human infections per unit time) is $\frac{b\alpha_{vh}I_{vH}S_{hH}}{N_{hH}}$ [2,14,15,34,40,71,72]. Similarly, the incidence rate for humans in abroad is $\frac{b'\alpha'_{vh}I_{vA}S_{hA}}{N_{hA}}$. Also, the total number of bites (per time) made by the susceptible mosquitoes in the home country is bS_{vH}. Among these bites, the total number of bites from the infectious humans (infectious bites) is $\frac{bS_{vH}I_{hH}}{N_{hH}}$. Therefore, the Incidence rate of mosquitoes (i.e. the new mosquito infections per unit time) is $\frac{b\alpha_{hv}I_{hH}S_{vH}}{N_{hH}}$. Similarly, the incidence rates for mosquitoes in abroad is $\frac{b'\alpha'_{hv}I_{hA}S_{vA}}{N_{hA}}$.

The infectious humans recover with the rate γ_h, and the recovered individuals lose their immunity and move back to the susceptible class at the rate q. Because of the short lifespan of mosquitoes, we do not consider the recovered class for the mosquitoes population. The parameters Λ and d_h represent the recruitment rate and the natural death rate of humans, respectively, while the parameters ϕ and d_v represent the recruitment rate and the death rate of mosquitoes, respectively. We assume that η represents the per capita cross-border mobility rate for susceptible populations (S_{hH}, S_{hM}) and recovered populations (R_{hH}, R_{hM}). Since infected individuals may behave differently in their travels from and to the home country, we take p and θ as the cross-border mobility rate for infectious individuals from

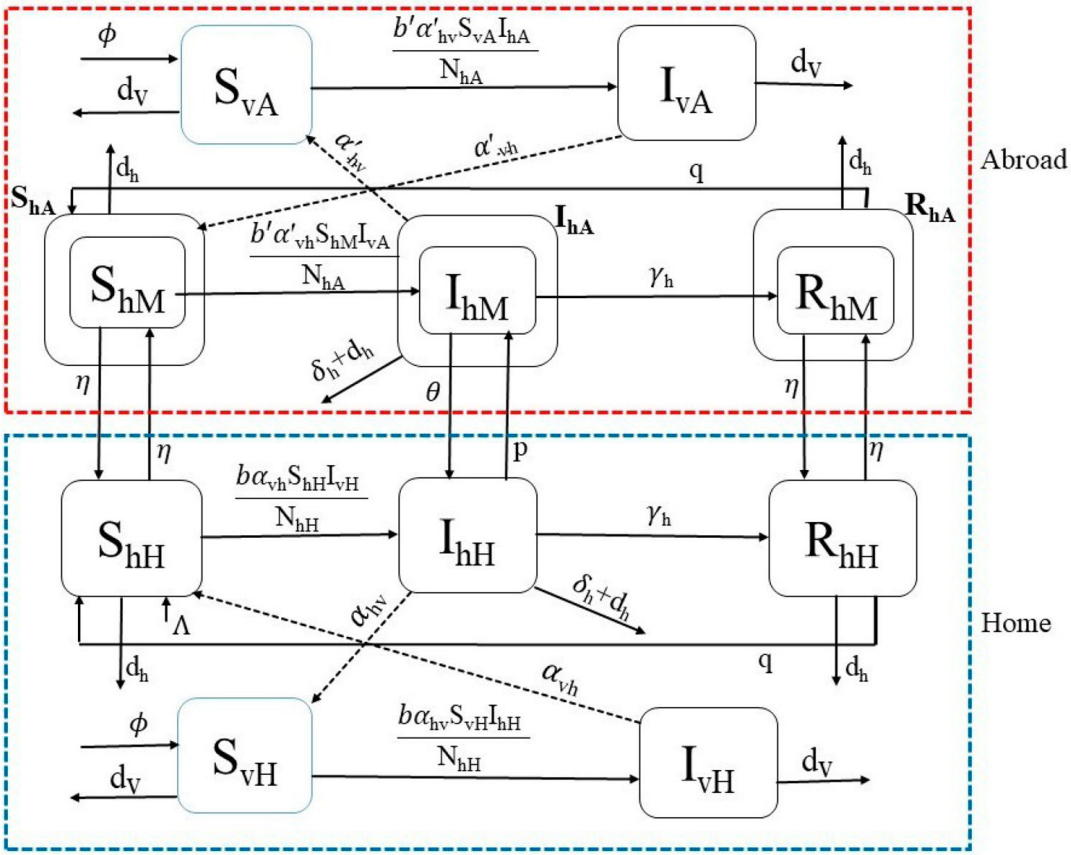

Figure 1. Malaria transmission dynamics with cross-border mobility. The upper SI-SIRS (inside red dashed line) and lower SI-SIRS (inside blue dashed line) represent the dynamics of malaria abroad and in the home country. The solid arrows represent the transfer of populations, and the dotted arrows represent the interaction between the susceptible human and infectious female Anopheles mosquitoes and infectious humans with susceptible female Anopheles mosquitoes. Here, subscripts H, A, and M refer to home, abroad, and migrant, respectively, and the subscript h and v refer to human and vector (mosquito), respectively.

and to the home country, respectively. In the model, θI_{hM} and $\frac{b\alpha_{vh}I_{vH}S_{hH}}{N_{hH}}$ represent the imported and indigenous malaria incidence at home country, respectively.

The schematic diagram of our model is presented in Figure 1. The system of equations describing the transmission dynamics of malaria discussed above is as follows:

$$S'_{hH} = \Lambda + \eta S_{hM} + qR_{hH} - \frac{b\alpha_{vh}I_{vH}}{N_{hH}}S_{hH} - (\eta + d_h)S_{hH}, \tag{1}$$

$$I'_{hH} = \frac{b\alpha_{vh}I_{vH}}{N_{hH}}S_{hH} + \theta I_{hM} - (p + d_h + \delta_h + \gamma_h)I_{hH}, \tag{2}$$

$$R'_{hH} = \gamma_h I_{hH} + \eta R_{hM} - (\eta + d_h + q)R_{hH}, \tag{3}$$

$$S'_{vH} = \phi - \frac{b\alpha_{hv}I_{hH}}{N_{hH}}S_{vH} - d_v S_{vH}, \tag{4}$$

$$I'_{vH} = \frac{b\alpha_{hv}I_{hH}}{N_{hH}}S_{vH} - d_v I_{vH}, \tag{5}$$

$$S'_{hM} = \eta S_{hH} + qR_{hM} - \frac{b'\alpha'_{vh}I_{vA}}{N_{hA}}S_{hM} - (d_h + \eta)S_{hM}, \tag{6}$$

$$I'_{hM} = \frac{b'\alpha'_{vh}I_{vA}}{N_{hA}}S_{hM} + pI_{hH} - (\theta + \delta_h + d_h + \gamma_h)I_{hM}, \tag{7}$$

$$R'_{hM} = \gamma_h I_{hM} + \eta R_{hH} - (\eta + d_h + q)R_{hM}, \tag{8}$$

$$S'_{vA} = \phi - \frac{b'\alpha'_{hv}I_{hA}}{N_{hA}}S_{vA} - d_v S_{vA}, \tag{9}$$

$$I'_{vA} = \frac{b'\alpha'_{hv}I_{hA}}{N_{hA}}S_{vA} - d_v I_{vA}. \tag{10}$$

2.2. Approximation to incidence rate abroad

Since the detailed dynamics of malaria abroad makes the model extremely complex and uncertain, we introduce an index $\psi(t)$ called Annual Parasite Incidence (API), for which the data are publicly available. We introduce this index into the model to approximate the incidence rate abroad. Here $\psi(t)$ is defined as the number of positive cases of malaria per population under surveillance, i.e. $\psi(t) = \frac{I_{hA}(t)}{N_{hA}(t)}$. The incidence rate of humans in abroad is given by

$$\lambda'_h = \frac{b'\alpha'_{vh}I_{vA}(t)}{N_{hA}(t)} = \frac{b'\alpha'_{vh}I_{vA}(t)}{I_{hA}(t)}\psi(t).$$

Both $b'\alpha'_{vh}I_{vA}(t)$ and $I_{hA}(t)$ are differentiable functions in the interval $[0, T]$, where T is the final time of the disease dynamics considered. Assuming that $I_{hA}(t) \neq 0, \forall\, t \in [0, T]$, the mean value theorem of integral calculus allows us to approximate the integral of the continuous function $\frac{b'\alpha'_{vh}I_{vA}(t)}{I_{hA}(t)}$ with a constant $\zeta = \frac{b'\alpha'_{vh}}{T}\int_0^T \frac{I_{vA}(t)}{I_{hA}(t)}\,\mathrm{d}t \approx b'\alpha'_{vh}\frac{I_{vA}(t_0)}{I_{hA}(t_0)}$ for some $t_0 \in (0, T)$. Thus, we approximate the incidence rate abroad by $\lambda'_h = \zeta\psi(t)$ and estimate the value of ζ from the data fitting. With this approximation, the system (1)–(10) reduces to the system of the following eight differential equations.

$$S'_{hH} = \Lambda + \eta S_{hM} + qR_{hH} - \frac{b\alpha_{vh}I_{vH}}{N_{hH}}S_{hH} - (\eta + d_h)S_{hH}, \tag{11}$$

$$I'_{hH} = \frac{b\alpha_{vh}I_{vH}}{N_{hH}}S_{hH} + \theta I_{hM} - (p + d_h + \delta_h + \gamma_h)I_{hH}, \tag{12}$$

$$R'_{hH} = \gamma_h I_{hH} + \eta R_{hM} - (\eta + d_h + q)R_{hH}, \tag{13}$$

$$S'_{vH} = \phi - \frac{b\alpha_{hv}I_{hH}}{N_{hH}}S_{vH} - d_v S_{vH}, \tag{14}$$

$$I'_{vH} = \frac{b\alpha_{hv}I_{hH}}{N_{hH}}S_{vH} - d_v I_{vH}, \tag{15}$$

$$S'_{hM} = \eta S_{hH} + qR_{hM} - \zeta\psi(t)S_{hM} - (d_h + \eta)S_{hM}, \tag{16}$$

$$I'_{hM} = \zeta\psi(t)S_{hM} + pI_{hH} - (\theta + \delta_h + d_h + \gamma_h)I_{hM}, \tag{17}$$

$$R'_{hM} = \gamma_h I_{hM} + \eta R_{hH} - (\eta + d_h + q)R_{hM}. \tag{18}$$

3. Parameters and model validation

3.1. Data

In this study, we used the data containing both indigenous and imported malaria cases in Nepal. Since the total cases were not classified as imported and indigenous before 2009, we considered the data only from 2009 to 2019 for our model fitting. The primary data sources related to malaria cases in Nepal are the National Malaria Surveillance Guidelines 2019 published by the Government of Nepal, Ministry of Health and Population Department of Health Services Epidemiology and Disease Control Division (EDCD) [21,28]. In addition, we also obtained the data of Annual Parasitic Incidence (API) of India from the Malaria Site India [41,44].

3.2. Parameter estimation

The population of Nepal was estimated to be 23,151,423 in 2001 [69] and 26,494,504 in 2011 [70]. Taking the average population growth per year from 2001 to 2011, we estimated the population of Nepal in 2009 (the base year of our dynamics, i.e. $t = 0$) to be 25,825,888. About 5.5 million Nepalese, including 1.9 million male workers, were living abroad [38], mostly in India. These migrant workers bring malaria upon their return home, contributing the significant number of imported malaria cases in Nepal [29]. Note that the majority of Nepalese migrants working in India are male [64]. Therefore, we took $N_{hM}(0) = 1.9$ million. With 5.5 million living abroad, the population inside Nepal is approximately 20,325,888. Since most of the hilly and mountainous regions of Nepal are considered risk free zone of malaria, leaving only about 48% of Nepalese residing in other regions in high, moderate or low risk area [50], we estimated $N_{hH}(0) = 9{,}756{,}426$. Moreover, we used the information from the data and divided the total population into different compartments and obtained $S_{hH}(0) = 9{,}754{,}000$, $I_{hH}(0) = 2000$, $R_{hH}(0) = 426$, $S_{hM}(0) = 1{,}898{,}300$, $I_{hM}(0) = 1400$, $R_{hM}(0) = 300$, $S_{vH}(0) = 9{,}754{,}176$, and $I_{vH}(0) = 2250$. About 37.5% of the total migrant workers (∼179,464) travelled from Nepal to India in 2009 [27]. This allows us to estimate per capita annual mobility rate of migrants from Nepal to India as $\eta = \frac{\text{Number of migrants from Nepal to India}}{\text{Total risk population of malaria in Nepal}} = \frac{179,464}{9,756,426} = 0.0183$ (per human per year).

The Crude Birth Rate (CBR), i.e. the number of live birth per year per 1000 people, of Nepal for the year 2009 was 23.189 [70], which implies the human recruitment rate per year for the population in the risk area is $\Lambda = 48\%$ of $\frac{23.189 \times 25{,}825{,}888}{1000} = 287{,}460$. Since the average life expectancy of Nepalese individuals in 2009 was 67.178 years [60], the natural death rate of humans per year is taken as $d_h = 0.0149$ per year. The number of deaths due to malaria in the base year [26] was 6, so we calculated $\delta_h = 0.0017$ per year. The duration of immunity for recovered people varies widely from region to region, and we took the immunity period to be 3 months, i.e. $q = 4$ per year [15]. For model fitting, we assumed that all the cases are recorded and that malaria-infected Nepalese do not move to India as workers while sick. Therefore, we took $p = 0$.

The population of female Anopheles mosquitoes has been estimated to be 1–10 times the human population [13,15,34]. Thus we took the mosquito population equal to base year human population 9,756,426. Based on the previous studies [1,9,13,15,34], we took the probability of disease transmission, per bite, from an infectious mosquito to a susceptible

human as $\alpha_{vh} = 0.0195$, and from an infectious human to a susceptible mosquito as $\alpha_{hv} = 0.63$. Similarly, the human recovery rate and the mosquito death rate were obtained from previous studies as $\gamma_h = 1.85$ per year and $d_v = 27.9113$ per year [1,9,13,15,34]. The remaining parameters, θ, ζ, and b, were estimated from the data fitting.

3.3. Model fitting to the data

As per the national planning of malaria elimination by 2026, the Government of Nepal introduced the strategic plan in 2014, which includes the distribution of Long Lasting Insecticide Treated Nets (LLINs) and Indoor Residual Spraying (IRS) intended to reduce mosquito bites [29]. Thus in our model fitting, we allow the different biting rates for the period before ($b = b_1$) and after ($b = b_2$) 2014.

The available data are the yearly indigenous malaria incidence, the yearly imported malaria incidence, and the total malaria incidence in Nepal. From the solution of our model, the indigenous, the imported, and the total malaria incidences at time t, denoted by $L(t)$, $I(t)$, and $T(t)$, respectively, can be computed using the following expressions:

$$L(t) = \frac{b\alpha_{vh}S_{hH}I_{vH}}{N_{hH}}, \quad I(t) = \theta I_{hM}, \quad T(t) = \frac{b\alpha_{vh}S_{hH}I_{vH}}{N_{hH}} + \theta I_{hM}. \tag{19}$$

The model system of differential equations was solved numerically using the fourth-order Runge-Kutta method. Using the solutions, we obtained the best-fit parameters using the nonlinear least-squares regression method that minimizes the following sum of the squared residuals:

$$J(\phi) = \sum_{k=1}^{n} \left[(L(t_k) - \bar{L}(t_k))^2 + (I(t_k) - \bar{I}(t_k))^2 + (T(t_k) - \bar{T}(t_k))^2 \right], \tag{20}$$

where $L(t_k), I(t_k), T(t_k)$ and $\bar{L}(t_k), \bar{I}(t_k), \bar{T}(t_k)$ are the model predicted incidences and those given in the available data. In our data fitting, we used the total 30 data points to estimate four parameters $\Phi = (\theta, \zeta, b_1, b_2)$. The ratio of data to the free parameters used in our model, i.e. 7:1, is well within the recommended range of 5:1–10:1 [53]. Also, three types of data (indigenous, imported, and total) included in fitting provide additional feature of malaria infection. To obtain the confidence limits for the estimated parameters, we computed standard errors from the sensitivity matrix S using the techniques described previously [49]. Furthermore, we computed the rank of the matrix $S^T S$ and found the matrix to be of the full rank (rank = 4), which ascertain the identifiability of these parameters of the model [43]. All computations were carried out in MATLAB (The MathWorks, Inc.).

In Figure 2, we present the model prediction, along with the data, of the indigenous, the imported, and the total malaria incidence. The model fits have captured the dynamics pattern of the multiple data well, and the model prediction is also consistent with the cumulative data (Figure 2), thereby validating the model. All estimated parameters, as well as the fixed parameters, are provided in Table 2. As indicated by the data [29], the model solutions also show the decreasing trend of the malaria cases from 2009, with the indigenous case being more than the imported case until 2014. However, after 2014, the imported case overtook the indigenous case, indicating the alarming situation originating from the imported cases.

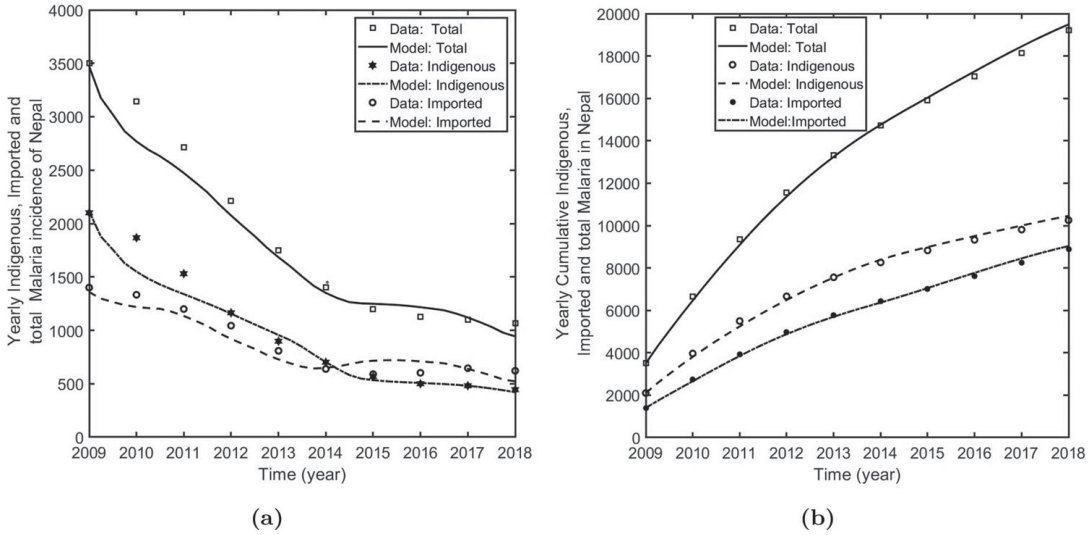

Figure 2. Model fitting to the data. (a) Solution of the fitted model along with the data of indigenous, imported, and total malaria incidences in Nepal, and (b) Model prediction of cumulative indigenous, cumulative imported, and cumulative total cases in Nepal.

Our estimates show that the biting rate of mosquitoes is $b_1 = 48.0$ (95% CI: [38.13, 57.87]) before 2014, and $b_2 = 39.5$ (95% CI: [29.63, 49.37]) after 2014. These estimated values are consistent with the values provided in many previous studies [15,34]. Similarly, we estimated the disease import rate $\theta = 0.98$ (95% CI: [0.42, 1.54]) and the parameter corresponding to the incidence rate in India $\zeta = 0.00105$ (95% CI: [0.0005, 0.0016]).

4. Model analysis

Note that our model is non-autonomous due to the presence of time-dependent parameter $\psi(t)$. Since $\psi(t)$ depends on the policy implemented abroad, the time-dependent nature of this parameter remains unknown, and the analysis of this non-autonomous model is complicated and uncertain. Therefore, for the purpose of analysis, we consider the autonomous form of the model by taking a constant $k = (\zeta/T)\int_0^T \psi(t)\,\mathrm{d}t$ as an approximation to the incidence rate abroad.

4.1. Basic properties of model: positivity and boundedness

In this section, we show that the solutions of all the state variables are non-negative and bounded in order to demonstrate that the model is well-posed and biologically valid for describing malaria transmission dynamics. The results are presented in the following theorem.

Theorem 4.1: *If* $S_{hH}(0) > 0, I_{hH}(0) \geq 0, R_{hH}(0) \geq 0, S_{hM}(0) \geq 0, I_{hM}(0) \geq 0, R_{hM}(0) \geq 0, S_{vH}(0) > 0, I_{vH}(0) \geq 0$, *then the solution set* $\{S_{hH}(t), I_{hH}(t), R_{hH}(t), S_{hM}(t), I_{hM}(t), R_{hM}(t), S_{vH}(t), I_{vH}(t)\}$ *of the system* (11)–(18) *is always non-negative and bounded.*

Proof: See Appendix A.1. ■

Using the above conditions, we derive that for any $\epsilon > 0$, there exists $t_\epsilon > 0$ such that the solution of the system with $t \geq t_\epsilon$ lies in the compact set $\Omega = \Omega_h \times \Omega_v$, where

$$\Omega_h = \left\{ (S_{hH}, I_{hH}, R_{hH}, S_{hM}, I_{hM}, R_{hM}) \in \Re^6_+ : N_h \leq \frac{\Lambda}{d_h} + \epsilon \right\}$$

and

$$\Omega_v = \left\{ (S_{vH}, I_{vH}) \in \Re^2_+ : N_v \leq \frac{\phi}{d_v} + \epsilon \right\}.$$

4.2. Existence of equilibria

For convenience, we let $S_{hH} = x, I_{hH} = y, R_{hH} = z, S_{hM} = X, I_{hM} = Y, R_{hM} = Z, S_{vH} = l$, and $I_{vH} = m$, and we take $(x^*, y^*, z^*, l^*, m^*, X^*, Y^*, Z^*)$ to represent the equilibrium point of the system (11)–(18). For simplicity, we assume that also for the infectious compartments, the mobility rate is equal in both ways, from home to abroad and vice versa, i.e. $\theta = p$. Taking,

$$\lambda_h^* = \beta_h \frac{m^*}{N_{hH}^*}, \quad \lambda_v^* = \beta_v \frac{y^*}{N_{hH}^*}, \quad \beta_v = b\alpha_{hv}, \quad \beta_h = b\alpha_{vh}, \tag{21}$$

the system (11)–(18) provides

$$\begin{aligned} x^* &= \frac{P}{K_1 + K_2\,\lambda_h^*}, \quad y^* = \frac{Q_1 + Q_2\lambda_h^*}{K_1 + K_2\,\lambda_h^*}, \quad z^* = \frac{Q_3 + Q_4\lambda_h^*}{K_1 + K_2\,\lambda_h^*}, \\ X^* &= \frac{S_1 + S_2\lambda_h^*}{K_1 + K_2\,\lambda_h^*}, \quad Y^* = \frac{T_1 + T_2\lambda_h^*}{K_1 + K_2\,\lambda_h^*}, \quad Z^* = \frac{U_1 + U_2\lambda_h^*}{K_1 + K_2\,\lambda_h^*}, \end{aligned} \tag{22}$$

where $P, Q_1, Q_2, Q_3, Q_4, S_1, S_2, T_1, T_2, U_1, U_2, K_1, K_2$ are non-negative constants with the combination of model parameters computed using Wolfram Mathematica. The closed-forms of these expressions are provided in Supplementary Material A (page 1–3). With some algebraic manipulation, we obtain

$$\begin{aligned} N_{hH}^* &= \frac{P + Q_1 + Q_3 + \lambda_h^*(Q_2 + Q_4)}{K_1 + K_2\,\lambda_h^*}, \quad \lambda_v^* = \frac{\beta_v(Q_1 + Q_2\lambda_h^*)}{P + Q_1 + Q_3 + \lambda_h^*(Q_2 + Q_4)}, \\ m^* &= \frac{\phi\beta_v(Q_1 + Q_2\lambda_h^*)}{d_v\left(\beta_v Q_1 + d_v P + Q_1 d_v + Q_3 d_v + (Q_2 d_v + Q_4 d_v + \beta_v Q_2)\lambda_h^*\right)}, \quad l^* = \frac{\phi - m^* d_v}{d_v}. \end{aligned} \tag{23}$$

Then, from (21) and (23), we obtain

$$a_0\lambda_h^{*3} + a_1\lambda_h^{*2} + a_2\lambda_h^* + a_3 = 0, \tag{24}$$

where,

$$\begin{aligned} a_0 &= Q_2Q_4d_v\beta_v + 2Q_2Q_4d_v^2 + Q_2^2d_v\beta_v + Q_2^2d_v^2 + Q_4^2d_v^2 > 0, \\ a_1 &= PQ_2d_v\beta_v + 2PQ_2d_v^2 + 2PQ_4d_v^2 + Q_2Q_3d_v\beta_v + Q_1Q_4d_v\beta_v + 2Q_2Q_3d_v^2 + 2Q_1Q_4d_v^2 \end{aligned}$$

$$+ 2Q_1Q_2d_v\beta_v + 2Q_1Q_2d_v^2 + 2Q_3Q_4d_v^2 - K_2Q_2\phi\beta_h\beta_v,$$

$$a_2 = P^2d_v^2 + PQ_1d_v\beta_v + 2PQ_1d_v^2 + 2PQ_3d_v^2 + Q_1Q_3d_v\beta_v + 2Q_1Q_3d_v^2 + Q_1^2d_v\beta_v + Q_1^2d_v^2 + Q_3^2d_v^2 - K_2Q_1\phi\beta_h\beta_v - K_1Q_2\phi\beta_h\beta_v,$$

$$a_3 = -K_1Q_1\phi\beta_h\beta_v \leq 0.$$

Since the primary focus of our study is to evaluate the impact of imported cases via cross-border mobility on the local malaria transmission and control, we now analyze the existence of equilibria for four important cases stated based on the mobility and outside transmission parameters η, θ, and k. The cases we consider are: (I) $\eta = 0, \theta = 0, k \neq 0$ (absence of cross-border mobility); (II) $\eta \neq 0, \theta \neq 0, k = 0$ (complete protection of transmission abroad); (III) $\eta \neq 0, \theta = 0, k \neq 0$ (strict border screening and isolation); and (IV) $\eta \neq 0, \theta \neq 0, k \neq 0$ (presence of cross-border mobility, no protection, and no border screening or isolation). We now perform equilibria analysis for each of these four cases in the following subsections.

4.2.1. Case-I: $\eta = 0, \theta = 0, k \neq 0$ (absence of cross-border mobility)

In this case, Q_1, Q_3, S_1, T_1, U_1 are zero and $P \neq 0, K_1 \neq 0$, implying that one root of (24) is zero, i.e. $\lambda_h^* = 0$. Then, from (22) and (23), we obtain a disease-free equilibrium point, E_0, given by

$$E_0 = \left(\frac{\Lambda}{d_h}, 0, 0, \frac{\phi}{d_v}, 0, 0, 0, 0\right).$$

We now derive the epidemic threshold index, R_0, corresponding to this disease-free equilibrium point (E_0) by using the second-generation matrix method [24,65] (the details are provided in Appendix A.2) and obtain

$$R_0 = \sqrt{\frac{\phi d_h \beta_h \beta_v}{\Lambda(d_h + \delta_h + \gamma_h)d_v^2}}.$$

We also confirm that our expression of R_0 is consistent with the one derived from the first principle [35,65] (see Appendix A.3). The other two roots of (24) are given by $\lambda_h^* = \frac{-a_1 \pm \sqrt{a_1^2 - 4a_0a_2}}{2a_0}$. Note that $a_0 > 0$. Also, it is easy to verify that if $R_0 > 1$, then $a_2 < 0$, which implies one value of λ_h^*, i.e. $\frac{-a_1 + \sqrt{a_1^2 - 4a_0a_2}}{2a_0}$, is positive. This provides us with one endemic equilibrium point of the system. Similarly, if $R_0 < 1$, then $a_2 < 0$. In this case, the system provides either two positive values of λ_h^*, i.e. two endemic equilibrium points, if $a_1 < 0$ or no positive λ_h^*, i.e. no endemic equilibrium point, if $a_1 > 0$.

4.2.2. Case-II: $\eta \neq 0, \theta \neq 0, k = 0$ (complete protection of transmission abroad)

In this case, Q_1, Q_3, T_1, U_1 are zero, and P, S_1, K_1 are positive, which shows one of λ_h^* to be zero from (24). Then from (22) and (23), we obtain another disease-free equilibrium point, E_{01}, given by

$$E_{01} = \left(\frac{\Lambda\,(d_h + \eta)}{d_h\,(d_h + 2\eta)}, 0, 0, \frac{\phi}{d_v}, 0, \frac{\eta\Lambda}{2\eta d_h + d_h^2}, 0, 0\right).$$

We also obtain the epidemic threshold index, R_1, corresponding to this disease-free equilibrium point, E_{01}, as follows (see Appendix A.4)

$$R_1 = R_0\sqrt{1 + \frac{\eta\,(d_h + \gamma_h + \delta_h) + (\eta - \theta)\,d_h}{(d_h + \eta)\,(d_h + \gamma_h + \delta_h + 2\theta)}}.$$

Note that the migrant workers presumably travel less while they are infected. This implies $\eta - \theta \geq 0$ and hence $R_1 \geq R_0$ in general. Similar to Case I above, we can easily verify that if $R_1 > 1$, we obtain only one endemic equilibrium point, and if $R_1 < 1$, we obtain two equilibrium points (or no equilibrium point) depending on whether $a_1 < 0$ (or $a_1 > 0$).

4.2.3. Case-III: $\eta \neq 0, \theta = 0, k \neq 0$ (strict border screening and isolation)

In this case, Q_1 is 0, and $K_1, P, Q_3, S_1, T_1, U_1$ are positive. One root of the Equation (24) is zero, giving a disease-free equilibrium point, E_{02}. However, this disease-free equilibrium condition asserts the absence of the disease only within the home country while allowing the disease among migrants abroad. The expression for E_{02} is given by

$$E_{02} = \left(\frac{P}{K_1}, 0, \frac{Q_3}{K_1}, \frac{\phi}{d_v}, 0, \frac{S_1}{K_1}, \frac{T_1}{K_1}, \frac{U_1}{K_1}\right),$$

and the corresponding epidemic threshold index is (see Appendix A.5)

$$R_2 = \sqrt{\frac{PK_1\phi\beta_h\beta_v}{(P + Q_3)^2 d_v^2\,(d_h + \gamma_h + \delta_h)}}.$$

Note that $\eta = 0$ implies $R_2 = R_0$ as expected. Again, as in Case I and II above, here also we obtain only one endemic equilibrium point for $R_2 > 1$ and two equilibrium points (or no equilibrium point) depending on whether $a_1 < 0$ (or $a_1 > 0$) for $R_2 < 1$.

4.2.4. Case-IV: $\eta \neq 0, \theta \neq 0, k \neq 0$ (presence of cross-border mobility, no protection, and no border screening or isolation)

In this case, $a_3 \neq 0$ implying $\lambda_h^* \neq 0$ (from (24)) and $m^* \neq 0$ (from (21)). This implies that the disease-free equilibrium point does not exist, indicating that malaria eradication is not possible as long as there is a presence of cross-border mobility, absence of protection abroad, and absence of border screening and isolation.

To analyze possible endemic equilibrium points, we represent α, β, and γ to be the three possible roots of the cubic equation (24). The product of roots, $\alpha\beta\gamma = -\frac{a_3}{a_0}$. Since $a_0 > 0$ and $a_3 < 0$, $\alpha\beta\gamma > 0$. This shows that all three roots can not be negative real numbers. Also, (24) can not have one negative real root and two complex roots because otherwise, two complex roots $\alpha = a + ib, \beta = a - ib$ and one negative real root γ provides $\alpha\beta\gamma = (a^2 + b^2)\gamma < 0$, which is not possible here. Thus, the Equation (24) provides at least one positive value of λ_h^*, and hence the system admits at least one endemic equilibrium point.

To identify whether the system has 1, 2, or 3 endemic equilibrium points, we first transform the Equation (24) in terms of the equilibrium infected humans, y^*, to obtain $F_L(y^*) = F_R(y^*)$, where $F_L(y^*) = -M_2 y^* - M_3$ and $F_R(y^*) = M_0(y^*)^3 + M_1(y^*)^2$. The

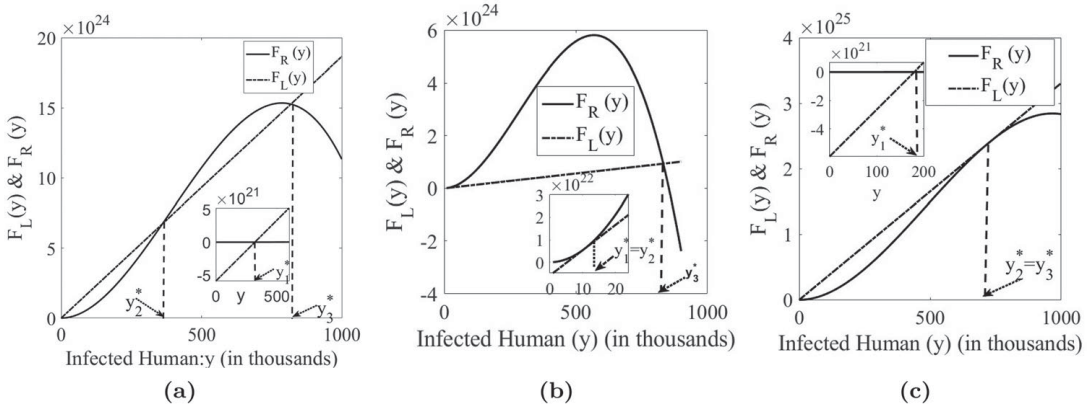

Figure 3. Endemic equilibriums. (a) Graphs of $F_L(y)$ and $F_R(y)$ with possible three intersections corresponding to three endemic equilibrium points. (b) Graphs of $F_L(y)$ and $F_R(y)$ with exactly two endemic equilibrium points $y_1^* = y_2^*$ and y_3^*. Decreasing the slope of $F_L(y)$ further gives only one equilibrium point y_3^* (a high epidemic level). (c) Graphs of $F_L(y)$ and $F_R(y)$ with exactly two endemic equilibrium points y_1^* and $y_2^* = y_3^*$. Increasing the slope of $F_L(y)$ further gives only one equilibrium point y_1^* (a low epidemic level).

equilibrium values of y^*, i.e. y_1^*, y_2^*, y_3^*, are then given by the intersection of the curves $F_L(y)$ and $F_R(y)$ (Figure 3). As shown in Figure 3, the slope $-M_2$ of the linear function $F_L(y)$, which can be explained in terms of the infection rate β_h, can help determine the existence of 1, 2, or 3 equilibria. An increase in β_h (i.e. a decrease in the slope of $F_L(y)$) makes the equilibrium point y_1^* and y_3^* move to the right and y_2^* move to the left, eventually giving $y_1^* = y_2^*$ corresponding to two equilibria $y_1^* = y_2^*$ and y_3^* (Figure 3(b)). Increasing β_h further, y_1^* and y_2^* disappear, and only one equilibrium point y_3^* exists. Since the equilibrium point y_3^* attains the highest value, we can correspond this situation to the worst-case scenario, i.e. a high endemic level. Similarly, decreasing β_h (i.e. increasing the slope of the linear function $F_L(y)$) causes y_1^* and y_3^* to move to the left and y_2^* to move to the right. At some point, y_2^* and y_3^* coincide with each other, giving only two equilibrium points y_1^* and $y_2^* = y_3^*$. If β_h is decreased further, then y_2^* and y_3^* disappear, leaving only y_1^* as an endemic equilibrium point. Since y_1^* corresponds to the smallest equilibrium point, the case in which the only y_1^* exists can be considered as the endemic condition with the minimum burden. Therefore, increasing the slope $-M_2$ (for example, decreasing β_h), making it less than its threshold value (corresponding to $y_2^* = y_3^*$), can be a vital control strategy to maintain the endemic at a low level.

In summary, the parameter a_3, which is always non-positive, provides an important threshold for disease-free equilibrium to occur ($a_3 = 0$). As long as $a_3 \neq 0$ (i.e. $a_3 < 0$), there is no DFE, and the system always provides at least one endemic equilibrium. The absence of DFE with at least one endemic equilibrium can be attributable to ongoing infection abroad and the importation of malaria cases through cross-border mobility, making $a_3 \neq 0$. When $a_3 = 0$ (presence of DFE), 1 or 2 endemic equilibrium points exist according to the sign of other parameters (a_1, a_2), which depend upon the thresholds R_0, R_1, or R_2. Similarly, when $a_3 < 0$ (absence of DFE), 1 to 3 endemic equilibrium points exist according to the sign of other coefficients.

4.3. Stability analysis and uniform persistence

In this section, we provide some analytical results related to the stability and uniform persistence of the system, specifically, the local stability of the disease-free equilibrium points and the uniform persistence for Case-I and Case-II. In addition, for Case-III, we provide the local stability of the disease-free equilibrium point that corresponds to the absence of disease within the home country only. We were unable to prove the uniform persistence for Case-III and Case-IV because of the complexity of the model, presumably due to the absence of the overall disease-free equilibrium point in these cases.

4.3.1. Case-I: $\eta = 0, \theta = 0, k \neq 0$ (absence of cross-border mobility)

We prove the local stability of the disease-free equilibrium E_0 as stated in the following theorem.

Theorem 4.2: *The disease free equilibrium point E_0 of the system* (11)–(18) *is locally asymptotically stable if $R_0 < 1$, and unstable if $R_0 > 1$.*

Proof: See Appendix A.6. ■

From the eigenvalues of the Jacobian matrix J at E_0 (Appendix A.6), we have the following lemma.

Lemma 4.3: *For the Jacobian matrix J, the following statements hold:*

(1) $R_0 = 1$ *if and only if* $S(J) = 0$,
(2) $R_0 > 1$ *if and only if* $S(J) > 0$,
(3) $R_0 < 1$ *if and only if* $S(J) < 0$,

where $S(J) := \max\{\mathrm{Re}(\lambda) : \lambda$ *is eigenvalue of the jacobian of system at DFE* $E_0\}$.

We now establish that $R_0 > 1$ can also provide a condition for the uniform persistence of the disease in the home country in the absence of cross-border mobility. Here, we use the following notations and definitions.

$$\Omega_o = \{(S_{hH}(t), I_{hH}(t), \ldots, I_{vH}(t)) \in \Re^5_+ : S_{hH}(t) > 0, I_{hH}(t) > 0, \ldots, I_{vH}(t) > 0\},$$

$$\partial\Omega_o = \{(S_{hH}(t), I_{hH}(t), \ldots, I_{vH}(t)) \in \Re^5_+ : I_{hH}(t) = 0 \text{ or } I_{vH}(t) = 0\},$$

$$\Omega = \Omega_o \cup \partial\Omega_o = \Re^5_+.$$

In the absence of cross-border mobility, it is enough to consider only the decoupled system (11)–(15). We assume that $\tau(t)P$ is the solution maps generated by the decoupled system (11)–(15) with initial value P. We denote $M_\partial = \{P \in \partial\Omega_o : \tau(t)P \in \partial\Omega_o\}$, and $\omega(P) = \{y : \tau(t)P \to y \text{ as } t \to \infty\}$. We first state and prove the following three lemmas.

Lemma 4.4: *The sets Ω_o and $\partial\Omega_o$ are positively invariant under the flow induced by the decoupled system* (11)–(15) *of the home country.*

Proof: See Appendix A.7. ■

Lemma 4.5: *Every forward orbit of $\tau(t)$ in $M\partial$ converge to E_0, i.e. E_0 is the fixed point of $\tau(t)$ and acyclic in $M\partial$.*

Proof: See Appendix A.8. ■

Lemma 4.6: *If $R_0 > 1$, then there exists $\rho > 0$ such that*

$$\lim_{t\to\infty} Sup \ \|\tau(t)P - E_0\| \geq \rho, \quad \forall\, P \in \Omega_o.$$

i.e. E_0 is uniform weak repeller with $\tau(t)$.

Proof: See Appendix A.9. ■

We are now ready to state the following theorem, which establishes the condition for malaria persistence in Nepal when cross-border mobility is absent.

Theorem 4.7: *Let $R_0 > 1$, then the decoupled system (11)–(15) of home country is uniformly persistent with respect to $(\Omega_o, \partial\Omega_o)$ in the sense that there is a positive constant $\sigma > 0$ such that every solution $(S_{hH}(t), I_{hH}(t), R_{hH}(t), S_{vH}(t), I_{vH}(t))$ of (11)–(15) with $(S_{hH}(0), I_{hH}(0), R_{hH}(0), S_{vH}(0), I_{vH}(0)) \in \Omega_o$ satisfies*

$$\lim_{t\to\infty} Inf\, I_{hH} \geq \sigma, \lim_{t\to\infty} Inf\, I_{vH} \geq \sigma \tag{25}$$

Proof: Assume that $R_0 > 1$, then it follows from Lemma 4.3 that $S(J) > 0$. Let $\tau(t)P$ is the solution maps generated by the decoupled system (11)–(15) with initial value $P \in \Omega_o$. Clearly, the system $\{\tau(t)\}_{t\geq 0}$ admits the global attractor in $\Re^5_+$. From the Lemma 4.5, E_0 is a fixed point of $\tau(t)$ and acyclic in $M\partial$, every solution in $M\partial$ approaches E_0. Moreover, Lemma 4.6 implies that E_0 is an isolated invariant set in Ω and $W^s(E_0) \cap \Omega_o = \phi$. By the acyclicity theorem of uniform persistence for maps [73], it follows that $\tau(t)$ is uniformly persistent with respect to $(\Omega_o, \partial\Omega_0)$. Hence there exists $\sigma > 0$ such that $\lim_{t\to\infty} \text{Inf}\, I_{hH} \geq \sigma, \lim_{t\to\infty} \text{Inf}\, I_{vH} \geq \sigma$. This completes the proof. ■

4.3.2. Case-II: $\eta \neq 0, \theta \neq 0, k = 0$ (complete protection of transmission abroad)

The local stability of the disease-free equilibrium E_{01}, corresponding to the case when complete protection of transmission is in force outside Nepal, is given by the following theorem.

Theorem 4.8: *The disease free equilibrium point E_{01} of the system (11)–(18) is locally asymptotically stable if $R_1 < 1$, and unstable if $R_1 > 1$.*

Proof: See Appendix A.10. ■

We also have the following lemma.

Lemma 4.9: *For the Jacobian matrix J_1 (Appendix A.10), the following statements hold:*

(1) $R_1 = 1$ *if and only if* $S(J_1) = 0$,

(2) $R_1 > 1$ *if and only if* $S(J_1) > 0$,
(3) $R_1 < 1$ *if and only if* $S(J_1) < 0$.

We also prove that $R_1 > 1$ provides the condition for uniform persistence of the disease with dynamics given by the system (11)–(18) with $\eta \neq 0, \theta \neq 0, k = 0$. Here, we use the following notations and definitions.

$$\Omega_o = \{(S_{hH}(t), I_{hH}(t), \ldots, R_{hM}(t)) \in \Re^8_+ : S_{hH}(t) > 0, I_{hH}(t) > 0, \ldots, R_{hM}(t) > 0\},$$

$$\partial\Omega_o = \{(S_{hH}(t), I_{hH}(t), \ldots, R_{hM}(t)) \in \Re^8_+ : I_{hH}(t) = 0 \text{ or } I_{vH}(t) = 0 \text{ or } I_{hM}(t) = 0\}.$$

To prove uniform persistence of $\{\tau(t)\}_{t\geq 0}$ with respect to $(\Omega_o, \partial\Omega_o)$, we need the following three lemmas.

Lemma 4.10: *The sets* Ω_o *and* $\partial\Omega_o$ *are positively invariant under the flow induced by the system* (11)–(18).

Proof: See Appendix A.11. ■

Lemma 4.11: *Every forward orbit of* $\tau(t)$ *in* $M\partial$ *converge to* E_{01}.

Proof: See Appendix A.12 ■

Lemma 4.12: *If* $R_1 > 1$, *then there exists* $\rho > 0$ *such that*

$$\lim_{t\to\infty} Sup \ \|\tau(t)P - E_{01}\| \geq \rho, \quad \forall\, P \in \Omega_o.$$

i.e. E_{01} *is uniform weak repeller with* $\tau(t)$.

Proof: See Appendix A.13. ■

With the help of the above lemmas, we now establish the following persistence theorem.

Theorem 4.13: *If* $R_1 > 1$, *then the system* (11)–(18) *is uniformly persistent with respect to* $(\Omega_o, \partial\Omega_o)$ *in the sense that there is a positive constant* $\sigma > 0$ *such that every solution* $(S_{hH}(t), I_{hH}(t), R_{hH}(t), S_{vH}(t), I_{vH}(t), S_{hM}(t), I_{hM}(t), R_{hM}(t))$ *with* $(S_{hH}(0), I_{hH}(0), R_{hH}(0), S_{vH}(0), I_{vH}(0), S_{hM}(0), I_{hM}(0), R_{hM}(0)) \in \Omega_o$ *satisfies* $\lim_{t\to\infty} Inf\, I_{hH} \geq \sigma, \lim_{t\to\infty} Inf\, I_{vH} \geq \sigma, \lim_{t\to\infty} Inf\, I_{hA} \geq \sigma$.

Proof: Assume that $R_1 > 1$, then it follows from Lemma 4.9 that $S(J_1) > 0$. Let $\tau(t)P$ is the solution maps generated by the system (11)–(18) with the initial value P. Clearly, the system $\{\tau(t)\}_{t\geq 0}$ admits the global attractor in $\Re^8_+$. Here, the stable set of E_{01} is $W^s(E_{01}) = \{P \in d(\tau(t)P, E_{01}) \to 0 \text{ as } t \to \infty\}$. From the Lemma 4.11, E_{01} is a fixed point of $\tau(t)$ and acyclic in $M\partial$, every solution in $M\partial$ approach to E_{01}. Moreover, Lemma 4.12 implies that E_{01} is an isolated invariant set in Ω and $W^s(E_{01}) \cap \Omega_o = \phi$. By the acyclicity theorem of uniform persistence for maps [73], it follows that $\tau(t)$ is uniformly persistent with respect to $(\Omega_o, \partial\Omega_0)$. Hence there exist $\sigma > 0$ such that $\lim_{t\to\infty} \text{Inf}\, I_{hH} \geq \sigma, \lim_{t\to\infty} \text{Inf}\, I_{hM} \geq \sigma, \lim_{t\to\infty} \text{Inf}\, I_{vH} \geq \sigma$. This completes the proof. ■

4.3.3. Case-III: $\eta \neq 0, \theta = 0, k \neq 0$ (strict border screening and isolation)

In this case, the local stability of the corresponding disease-free equilibrium point, E_{02}, is given by the theorem below. As mentioned earlier, this disease-free equilibrium asserts the disease-free only within the home country while allowing infected migrants abroad.

Theorem 4.14: *The disease free equilibrium point E_{02} of the system* (11)–(18) *is locally asymptotically stable if $R_2 < 1$, and unstable if $R_2 > 1$.*

Proof: See Appendix A.14. ■

4.4. Analysis of simplifications implemented in the model

4.4.1. Approximation with autonomous sytem

Note that our model is non-autonomous due to the time-dependent parameter $\psi(t)$, representing the API of India. However, for analytical tractability (Subsections 4.1, 4.2, and 4.3), we approximated the model with the autonomous system. Moreover, since the future API of India can not be obtained, the simulation results for model prediction and control programmes (Section 5) are computed based on the autonomous model with the current API of India. In this section, we examine the potential error that we anticipate from the autonomous model. For this, we compared the predicted cumulative cases for both autonomous and non-autonomous systems for the period 2009–2019 (see in page-1 of Supplementary Material B). We observed that the predicted cumulative cases by the autonomous model remain within 5% of the non-autonomous model. For example, from 2009 to 2019, the difference in cumulative cases from the two model systems is only 1000 out of 20,000 base cases. Therefore, the autonomous model provides a reasonable approximation to the non-autonomous model, and the study's main finding remains the same in both models.

4.4.2. Approximations to the exposed class of mosquitoes and pathogen transmission from recovered humans

Because of the limited data availability, we have not included two potential phenomena: the incubation period of mosquitoes and pathogen transmission from recovered humans. However, these phenomena have been considered in some previous studies [15,47]. While these phenomena may not significantly impact the primary objective of this study, namely the impact of imported cases on the malaria elimination programme, we also considered an extended model with these two phenomena incorporated. Fitting this extended model to the data with the same initial values of state variables and parameters (Tables 1 and 2), we obtained the transmission probability from recovered human to susceptible mosquitoes per bite to be $r = 0.35$ and the incubation period of mosquito as $1/\sigma = 10$ days, consistent with previous studies [15,34]. Notably, per capita mosquito biting rates of $b_1 = 56$ and $b_2 = 48$, estimated with the extended model, are within the 95% confidence interval of the estimates from the simplified model.

Moreover, the cumulative case during 2020–2026 predicted by the extended model is 1425, which is close to the estimate of 1348 by the simplified model. Similarly, the predicted new cases in the year 2026 by the extended model is 195, while that by the simplified model is 191. Therefore, the qualitative and quantitative differences between the two models with

Table 1. Base value of demographic variables of malaria in Nepal.

Description	State variables	Base Value	Reference
Risk humans population in Nepal	$N_{hH}(0)$	9,756,426	Calculated
Susceptible humans in Nepal	$S_{hH}(0)$	9,754,000	Calculated
Infectious humans in Nepal	$I_{hH}(0)$	2000	Assumed
Recovered humans in Nepal	$R_{hH}(0)$	426	Assumed
Susceptible Migrants in India	$S_{hM}(0)$	1,898,300	[29]
Infectious Migrants in India	$I_{hM}(0)$	1400	Assumed
Recovered Migrants in India	$R_{hM}(0)$	300	Assumed
Susceptible mosquitoes in Nepal	$S_{vH}(0)$	9,754,176	Assumed
Infectious mosquitoes in Nepal	$I_{vH}(0)$	2250	Assumed

Table 2. Model parameters of incidence of malaria in Nepal.

Description	Parameters	Base value and unit	Reference
Probability of malaria transmission from an infectious mosquito (per bite) to a susceptible human	α_{vh}	0.0195	[1,13]
Probability of malaria transmission from an infectious human to a susceptible mosquito (per bite)	α_{hv}	0.63	[5,9,13]
Humans recruitment rate	Λ	287,460 Number $\times$ yr^{-1}	Calculated
Per capita recovery rate of humans	γ_h	1.85 yr^{-1}	[1,13]
Per capita natural birth and death rate of mosquitoes	d_v	27.9113 yr^{-1}	[1,13]
Per capita disease induced death rate of humans	δ_h	0.00171 yr^{-1}	Calculated
Per capita natural death rate of humans	d_h	0.0149 yr^{-1}	Calculated
Per capita mobility rate of healthy humans	η	0.0183 yr^{-1}	Calculated
Per capita disease import rate of humans	θ	0.98 yr^{-1} [0.4172, 1.5428]	Estimated
Per capita disease export rate of humans	p	0 yr^{-1}	Assumed
Per capita rate of Immunity loss of humans	q	4 yr^{-1}	[15]
Parameter related with incidence rate in India	ζ	0.00105 yr^{-1} [0.0005, 0.0016]	Estimated
Per capita biting rate of mosquitoes at home country up to 2014	b_1	48 yr^{-1} [39.6537, 66.3463]	Estimated
Per capita biting rate of mosquitoes at home country after 2014	b_2	39.5 yr^{-1} [29.6318, 49.3682]	Estimated

and without the exposed class of mosquitoes and pathogen transmission from recovered humans are not significant, asserting the robustness of the simplified models(see in page 2-4 of Supplementary Material B).

5. Malaria epidemic prediction and potential control in Nepal: model simulations

We use our model to predict the malaria epidemic in Nepal and evaluate the potential control strategies. In particular, we focus on whether the goal of malaria elimination from Nepal by 2026 set by the Government of Nepal can be achieved with the current trend and/or potential strategies. We take the year 2020 as the base year and estimate the imported and indigenous malaria cases during the period 2020–2026, and assess the number of possible control strategies that can be implemented for malaria elimination.

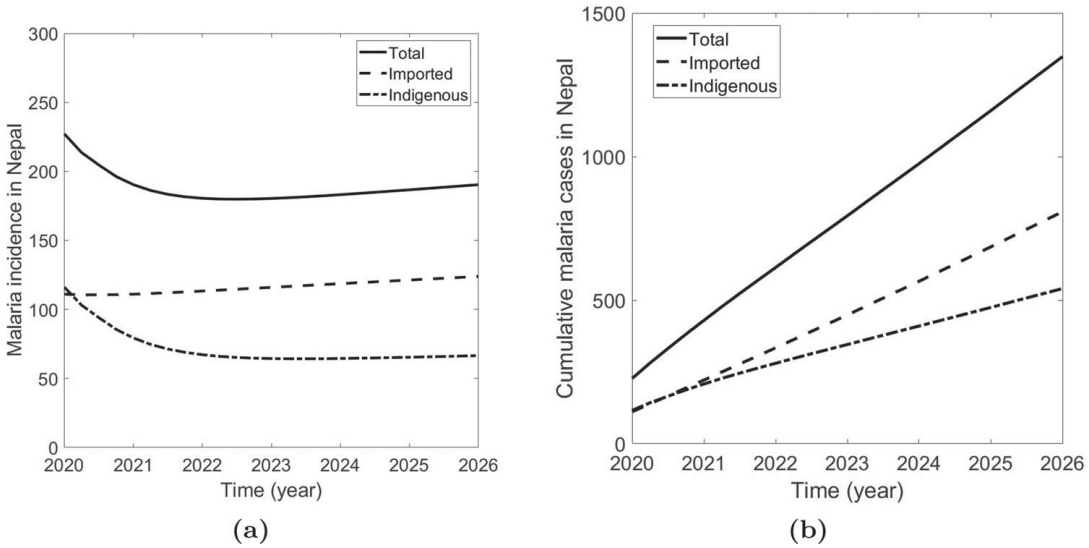

Figure 4. Model prediction of the malaria epidemic in Nepal. (a) The model prediction of the annual incidence of indigenous, imported, and total malaria cases from 2020 to 2026; and (b) the model prediction of the cumulative cases of indigenous, imported and total malaria infection from 2020 to 2026.

5.1. Basic malaria epidemic outcome in Nepal

For the basic simulations, we take the API of India, $\psi(t)$, a constant value corresponding to the year 2018. We compute the model predicted values of indigenous and imported new cases for 2020–2026 (Figure 4(a)). We observe that if the current trend continues, the indigenous malaria cases follow a decreasing trend, but the imported cases increase slightly. We predict the indigenous malaria cases in Nepal will decrease to a yearly incidence of 67 cases in 2026, while the imported cases will remain 124 per year in 2026. As a result, the annual total incidence will remain 191 cases in the year 2026. With this incidence rate, the cumulative indigenous cases and imported cases for the period 2020 to 2026 will reach 540 and 808, respectively, making a total of 1348 cases of malaria in Nepal in this period (Figure 4(b)). While the magnitude remains relatively low, a slightly elevated level of new cases in 2026, mainly because of the imported cases, shows that the importation of malaria cases from India might remain an obstacle to the Nepal government's goal of malaria elimination by 2026.

5.2. Impact of the transmission abroad on the epidemic in home country

As revealed in the model-predicted epidemic trend, the transmission of malaria abroad that may eventually cause higher imported cases can be a determinant factor for achieving an elimination goal by 2026. The model parameter k, which represents the impact of API of India, can be used to study how the transmission dynamics abroad can impact the epidemic outcome in Nepal. According to the data API of India has had a decreasing trend for the last few years. If the decreasing trend continues, imported cases in Nepal are expected to reduce in the coming years. Our model predicts that the malaria incidence in the year 2026 decreases linearly as the % reduction of API of India increases (Figure 5). For example, reducing the current API (base value $k = 0.1$) by 50% brings down the annual

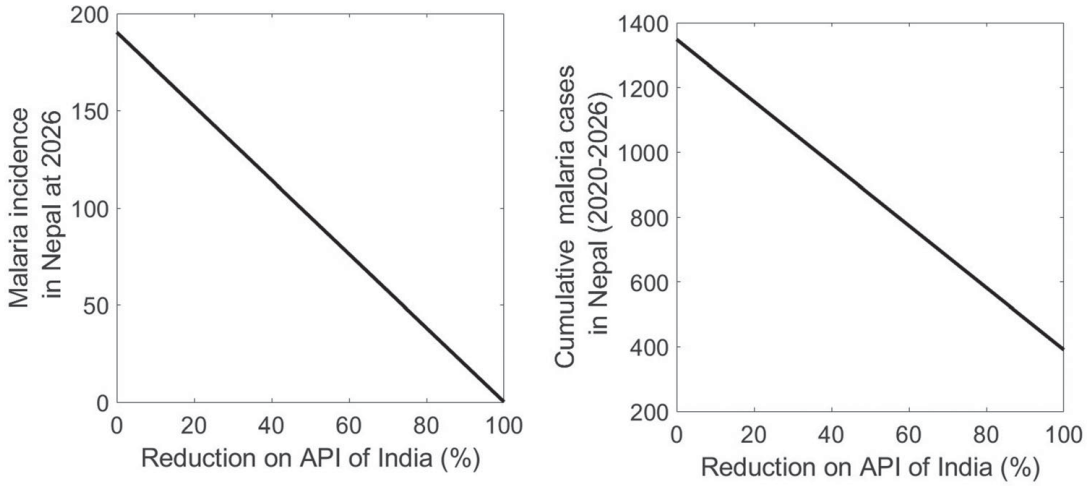

Figure 5. Impact of the API of India. Reduction of total malaria incidence at the year 2026 (Left) and reduction of cumulative malaria cases from 2020–2026 (Right) with Annual Parasitic Incidence (API) of India taking its value 0.1 for the base year 2020.

malaria incidence from 191 to 95 in 2026. The linear dependency of cumulative cases on the % reduction of India's API is also seen with a 50% reduction from the base case bringing the cumulative cases from 1,348 to 869 during the period 2020–2026 (Figure 5). These results indicate that the API of India can have an important role in the cases in the home country and eventually on the success of the Nepal government's malaria elimination goal.

5.3. Control of malaria in Nepal

We consider four potential control strategies: (1) Insecticide-treated nets (ITN), (2) Indoor Residual Spraying (IRS), (3) Border screen and isolation (BSI), and (4) Migration reduction (MR). Implementation of ITN reduces the mosquito biting rate. Assuming ϕ_{ITN} represents the effectiveness of ITN (assuming 100% coverage), the implementation of this strategy transforms $b \to (1-\phi_{ITN})b$ in our model. Similarly, IRS increases mosquito death, transforming our model as $d_v \to \phi_{IRS} d_v$, where $\phi_{IRS} \geq 1$ is the enhancement of mosquito death rate due to IRS. We denote the effectiveness of BSI by ϕ_{BSI}, $0 \leq \phi_{BSI} \leq 1$ so that the implementation of this strategy results in the transformation $\theta \to (1-\phi_{BSI})\theta$, i.e. reduction of the disease import rate θ by a proportion ϕ_{BSI}. The last strategy, MR, can be attributed to promoting various employment opportunities within the country, thereby reducing the cross-border mobility for seeking employment in India. The strategies can be incorporated into our model by transforming $\eta \to (1-\phi_{MR})\eta, \theta \to (1-\phi_{MR})\theta$, where ϕ_{MR}, $0 \leq \phi_{MR} \leq 1$ is the effectiveness of MR.

The mosquito biting rate is one of the most critical parameters of malaria transmission. While we estimated the low biting rate from the data fitting, the estimated value is the average annual rate. In reality, the biting rate can be uncertain as it is affected by various environmental (seasonal), social, and economic factors. To include broader possible scenarios, we present the results for two different biting rates, low biting rate (base

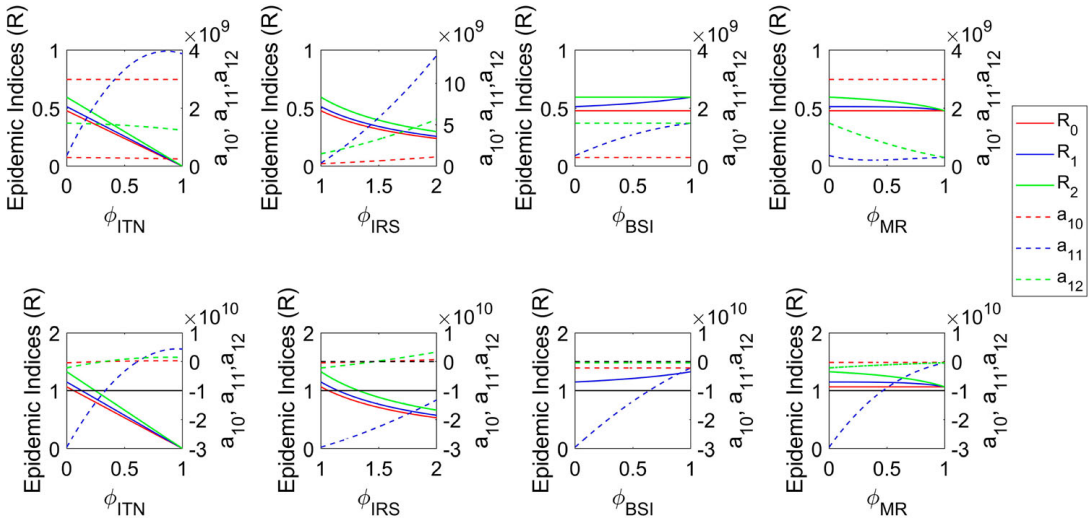

Figure 6. Condition for malaria elimination in Nepal. Threshold indices $R_0, R_1, R_2, a_{10}, a_{11}, a_{12}$ as a function of controls $\phi_{ITN}, \phi_{IRS}, \phi_{BSI}$, and ϕ_{MR} for a low (first row) and high (second row) mosquito biting conditions. Note that the malaria is eliminated if $R_0 < 1, a_{10} > 0$, $R_1 < 1, a_{11} > 0$, and $R_2 < 1, a_{12} > 0$, respectively, where a_{10}, a_{11}, and a_{12} are corresponding values of a_1 for case I (absence of cross-border mobility), case II (full protection of transmission abroad), and case III (strict border screening and isolation), respectively.

case $b = 39.5$ and high biting rate (approximately two times higher than the base case, $b = 100$).

5.3.1. Control strategies for elimination

The analytical results that we proved in Subsection 4.2 inform us that malaria can be eliminated from the home country if one of the following conditions can be achieved: absence of cross-border mobility (case I in Subsection 4.2.1), full protection of transmission abroad (case II in Subsection 4.2.2), and strict border screening and isolation (case III in Subsection 4.2.3). According to our theorems, in case I, II, and III, the malaria gets eliminated if $(R_0 < 1, a_{10} > 0)$, $(R_1 < 1, a_{11} > 0)$, and $(R_2 < 1, a_{12} > 0)$, respectively, where a_{10}, a_{11}, and a_{12} are corresponding values of a_1 for case I, II, and III, respectively. We now evaluate whether the control strategies ($\phi_{ITN}, \phi_{IRS}, \phi_{BSI}$, and ϕ_{MR}) can bring the model to satisfy the condition of eliminating malaria in Nepal.

Our results show that for the low biting rate condition, the elimination of malaria can be achieved in Nepal regardless of whether any of the control strategies are applied or not because $R_0 < 1, R_1 < 1, R_2 < 1$ and $a_{10} > 0, a_{11} > 0, a_{12} > 0$ remain always true (Figure 6, first row). However, for the high biting rate condition, $R_0 < 1, R_1 < 1, R_2 < 1$ and $a_{10} > 0, a_{11} > 0, a_{12} > 0$ can not be achieved without the control strategies, i.e. for $\phi_{ITN} = \phi_{BSI} = \phi_{MR} = 0$, and $\phi_{IRS} = 1$ (Figure 6, second row). In this case, (ϕ_{BSI}) and (ϕ_{MR}) have no impact on R and a_1. Therefore, the control strategies related to the infected migrant workers and the mobility across the border are not enough for malaria elimination if the biting rate is high. In the high biting rate condition, $(R_0 < 1, a_{10} > 0)$, $(R_1 < 1, a_{11} > 0)$, and $(R_2 < 1, a_{12} > 0)$, i.e. the elimination of malaria, can be obtained if the level of ϕ_{ITN} is greater than 0.35, 0.65, and 0.35, respectively, or the level of ϕ_{IRS} is greater than 1.45, 2.60, 1.50, respectively (Figure 6, second row).

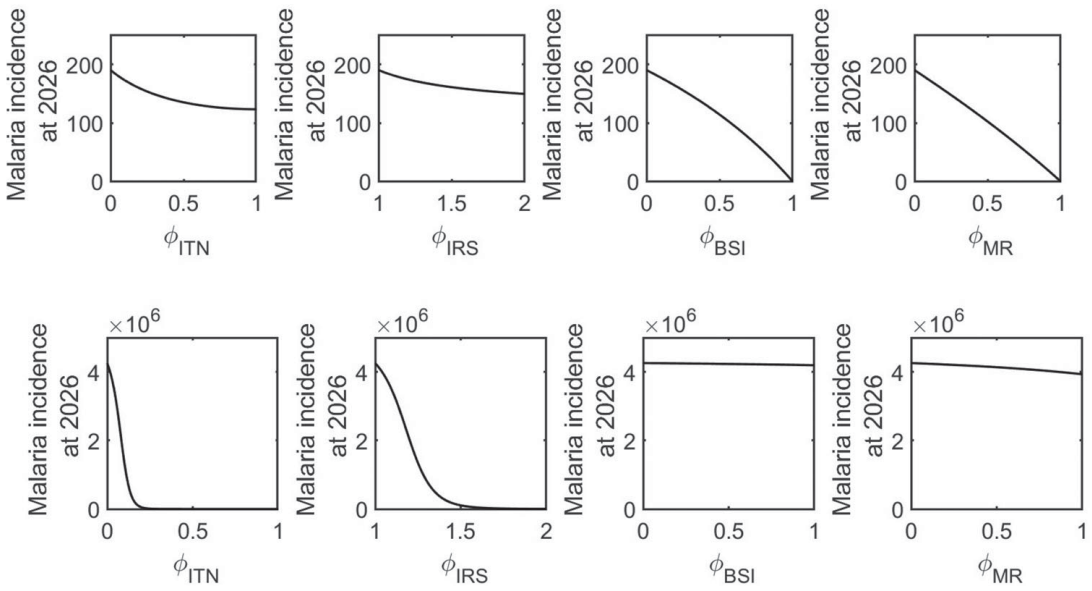

Figure 7. Effects of control strategies on the annual incidence rate. The model-predicted annual incidence rate in the year 2026 for various levels of ITN, IRS, BSI, and MR control in a low biting rate scenario (first row) and a high biting rate scenario (second row).

5.3.2. Control strategies for minimal burden

Here we perform simulations to show how the control strategies ITN, IRS, BSI, and MR impact the annual malaria incidence in 2026 and the cumulative malaria cases for 2020–2026 (Figures 7 and 8). In the low mosquito biting rate condition (Figure 7, first row), our model predicts that the 50% effectiveness of ITN (i.e. $\phi_{ITN} = 0.5$) reduces the annual malaria incidence in the year 2026 from 191 to 135. As a result, the cumulative cases for 2020–2026 will be reduced from 1348 to 1001 (Figure 8, first row). An increase in IRS by 1.5 times (i.e. $\phi_{IRS} = 1.5$) will result in an annual incidence rate of 161 in 2026 and a cumulative cases of 1167 for 2020–2026. Similarly, 50% effectiveness of BSI and MR will reduce the annual incidence rate in the year 2026 to 114 and 100, respectively, and the cumulative cases for 2020–2026 to 903 and 889, respectively.

In a high mosquito biting rate condition (Figure 7, second row, and Figure 8, second row), our model predicts that the 50% effectiveness of ITN (i.e. $\phi_{ITN} = 0.5$) reduces the annual malaria incidence in the year 2026 from 4.25 million to 257 and the cumulative cases for 2020–2026 from 7.8 million to 1684. Similarly, an increase in IRS by 1.5 times (i.e. $\phi_{IRS} = 1.5$) will result in an annual incidence rate of 106 hundred thousand in 2026 and a cumulative cases of 128 hundred thousand for 2020–2026. 50% effectiveness of BSI and MR will reduce the annual incidence rate in the year 2026 to 4.23 million and 4.13 million, respectively, and the cumulative cases for 2020–2026 to 7.5 million and 6.98 million, respectively.

While each control strategy can maintain a minimum malaria burden, their effect may vary quantitatively. Among these control strategies, MR appears to be the most effective in controlling malaria in Nepal in low mosquito biting rate conditions, while ITN is the most effective control in the high biting rate condition. This indicates that the ideal control strategy may depend on the locations and seasons in which low or high mosquito biting rates are expected. We note that due to the existing open border relationship with a long

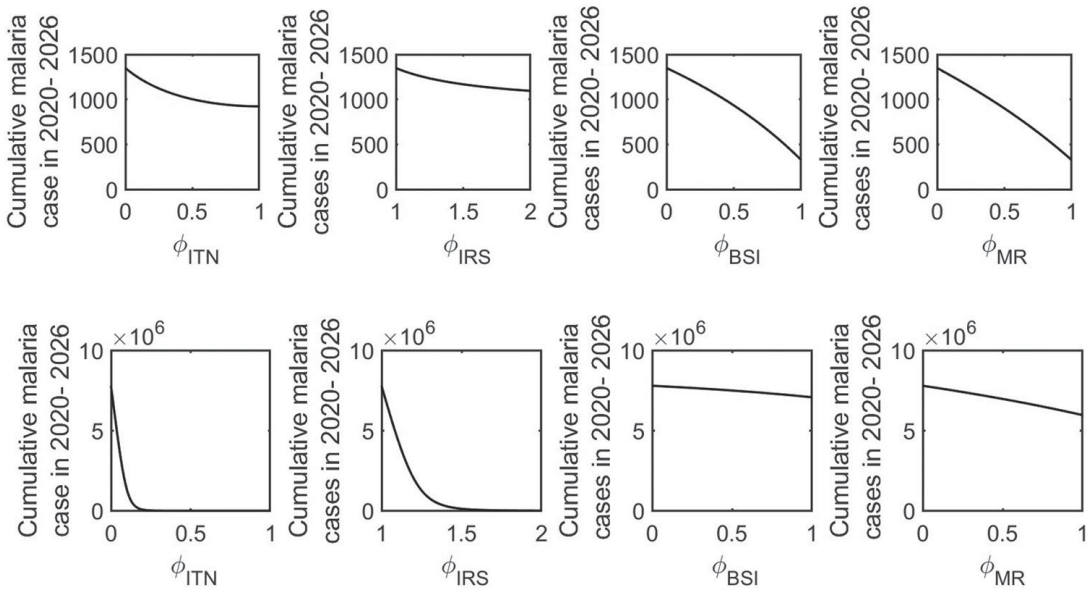

Figure 8. Effects of control strategies on the cumulative cases. The model-predicted cumulative cases for 2020–2026 for various levels of ITN, IRS, BSI, and MR control in a low biting rate scenario (first row) and a high biting rate scenario (second row).

history between Nepal and India, reducing the cross-border mobility of migrant workers may not be a viable option to implement. Therefore, the optimal border screen and isolation of returning migrant workers along with local approaches, ITN and IRS, can be the most impactful option for controlling and possibly eliminating malaria in Nepal.

In the above calculation, we assumed the 100% coverage of ITN. However, 100% is unlikely to be achieved, especially in resource-limited countries like Nepal. Thus we further observe model prediction for varying coverage and efficacy of ITN. The proportion of coverage ψ_{ITN}, $0 \leq \psi_{ITN} \leq 1$, and efficacy ϕ_{ITN}, $0 \leq \phi_{ITN} \leq 1$, can be incorporated in our model transforming $b \to (1 - \phi_{ITN}\psi_{ITN})b$. As presented in Figure 9, our simulations show that 100% efficacy and 100% coverage of ITN significantly reduce the malaria cases in the high mosquito biting case, but the effect is not significant in the low mosquito biting case. Since Nepal's estimated mosquito biting rate is low, even the 100% coverage and 100% efficacy will reduce malaria cases in 2026 from 191 to 121 only. Thus, in addition to ITN, optimal control strategies should also focus on adequately managing imported cases to eliminate malaria from Nepal by 2026.

6. Conclusion

Despite a significant decline of malaria cases worldwide, many countries are currently facing difficulty achieving malaria elimination goals from those countries, mainly due to cross-border mobility of migrant workers potentially bringing malaria from abroad. Nepal provides a typical example, which is recently suffering from higher imported cases from India through open-border, posing a severe threat to the Nepal government's goal of eliminating malaria by 2026. In this study, we developed a novel mathematical model validated by the data from Nepal and used our model to analyze the effects of cross-border mobility on the malaria elimination programmes for low-endemic countries like Nepal.

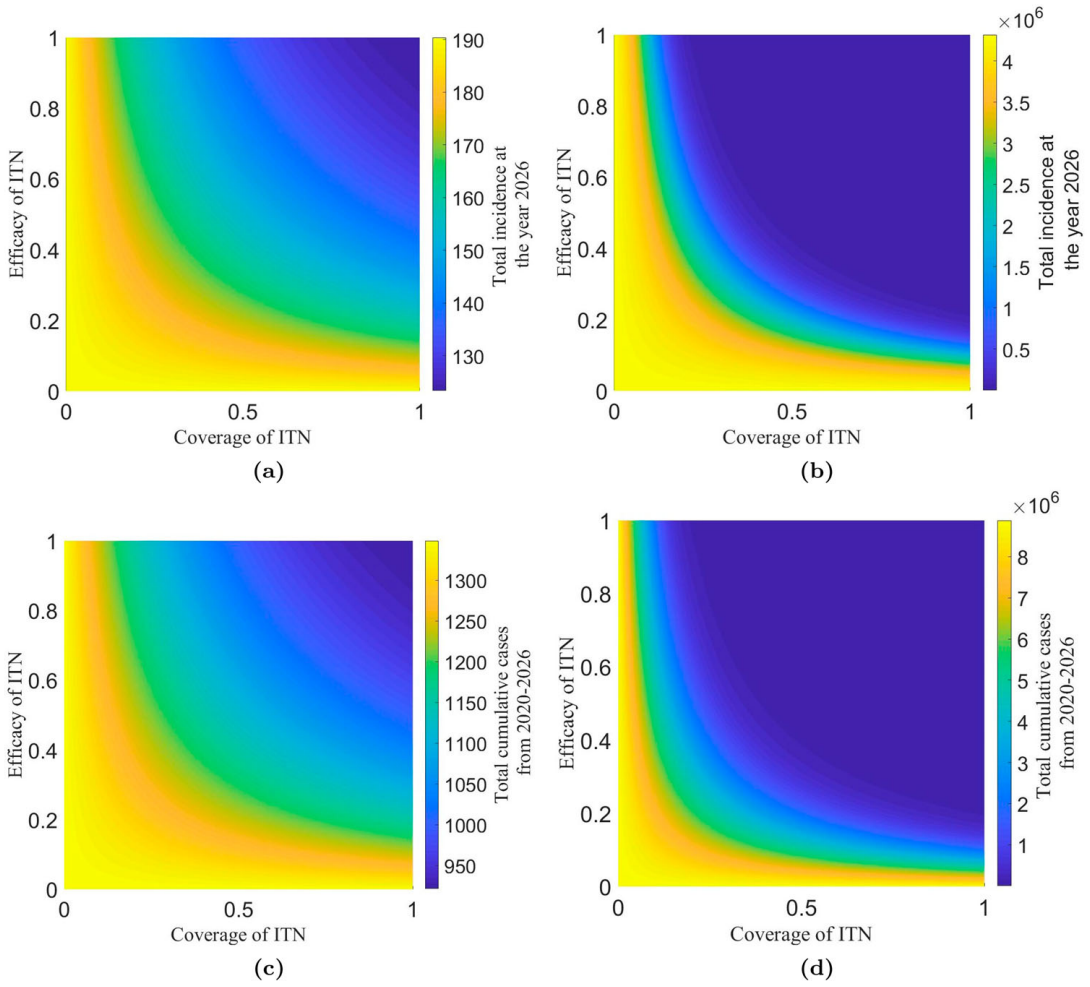

Figure 9. Sensitivity of coverage and efficacy of ITN. The model-predicted annual incidence rate in 2026 for various levels of efficacy and coverage of ITN in a low biting rate scenario (a) and a high biting rate scenario (b). The model-predicted cumulative cases for 2020–2026 for various levels of efficacy and coverage of ITN in a low biting rate scenario (c) and a high biting rate scenario (d).

Our model analyzes and simulations show that malaria can be eliminated from Nepal if strategies promoting the absence of cross-border mobility, complete protection of transmission abroad, or strict border screening and isolation are implemented. In each of these potential strategies, we formulated threshold conditions for the stability of the disease-free equilibriums, providing the level of control strategies, such as ITN, IRS, BSI, and MR, to assert the elimination of malaria from Nepal. In some cases, we mathematically proved the persistence of malaria in Nepal. In one of the cases, namely strict border screening and isolation, our unique model can provide the disease-free condition only within the home country while allowing the disease among migrants abroad. In reality, such disease-free equilibrium is the most viable condition regarding the elimination of malaria from Nepal because achieving elimination from both countries can be challenging with the control strategies by the Nepal government's policy only without making combined strategies by both countries. In addition, we used our model to thoroughly assess all control strategies considered, ITN, IRS, BSI, and MR, to maintain the low level of malaria-endemic in both low and high mosquito biting rate scenarios. Interestingly, our model predicts that MR is

the most effective control strategy for the low mosquito biting rate condition, while ITN is the most effective control strategy for the high mosquito biting rate condition. These interesting results suggest that the best control strategy may depend on locations and seasons that determine whether the biting rate is low or high.

There are several limitations of our study. We approximated the incidence rate abroad (India) using the API data of India. The analysis of the full model with accurate dynamics of humans and mosquitoes abroad, along with data from India, can help improve our results. Although the frequent movement of humans and mosquitoes between bordering cities and the movement of mosquitoes through cross-border transportation may be important, we have not considered these factors in our model because the data of imported cases due to these movements are not available. Therefore, our results are more relevant to the infection importation through cross-border mobility of migrant workers. Our model parameters are estimated with the limited data of malaria cases in Nepal. Uncertainty on the model parameters can be clarified if more frequent data are available. While we estimated the mosquito population based on the previous studies, the implemented values may have some uncertainties. However, our further simulations show that changing the mosquito population size to a realistic limit does not significantly impact on the main qualitative conclusions of our study. Also, some districts of Nepal are directly connected with India making them more vulnerable in comparison to other areas. Therefore, an extension of our model may be necessary to incorporate the spatial heterogeneity of the malaria risk across districts of Nepal.

We also note that we could not prove the persistence theory in Case III (strict border screening and isolation) and Case IV (presence of cross-border mobility, no protection, and no border screening or isolation) because there is no complete disease-free equilibrium in these cases. Extensive mathematical theory may be needed to show the persistence of the disease in such complicated cases. Our analyses show that for some choice of parameters (for example, those making $a_1 < 0$), the disease may persist even if the threshold numbers R_0 (Case I in Subsection 4.2.1), R_1 (Case II in Subsection 4.2.2), and R_2 (Case III in Subsection 4.2.3) are less than 1, indicating a possibility of backward bifurcations. Therefore, a detailed bifurcation analysis for each case (I, II, and III) can be an essential work, which we plan to pursue in future research.

In summary, our model for malaria transmission dynamics, incorporating cross-border mobility between a low endemic country (Nepal) and a high endemic country (India), can provide important insights into an obstacle that cross-border mobility may create to malaria elimination programmes. Our analytical and simulation results informing control policies that bring malaria elimination or maintain the epidemic at a low level are helpful for policymakers if implemented in conjunction with more accurate data.

Acknowledgements

This research was supported by the GRAID (Graduate Research Assistantships in Developing Countries) awards from the International Mathematical Union (IMU). RG acknowledges the University Grants Commission (UGC) for Ph.D. Faculty Fellowship and the Nepal Mathematical Society (NMS) for the NMS Ph.D. Fellowship Award 2020. KA acknowledges the Nepal Academy of Science and Technology (NAST) for Ph.D. Fellowship and the Nepal Mathematical Society (NMS) for the NMS Ph.D. Fellowship Award 2020. AP acknowledges the Nepal Mathematical Society (NMS)

for the NMS Ph.D. Fellowship Award 2020. The work of NV was supported by NSF grants DMS-1951793, DMS-1616299, DMS-1836647, and DEB-2030479 from the National Science Foundation of USA, and the UGP Award from San Diego State University.

Disclosure statement

No potential conflict of interest was reported by the author(s).

Funding

This research was supported by the GRAID (Graduate Research Assistantships in Developing Countries) awards from the International Mathematical Union (IMU). RG acknowledges the University Grants Commission (UGC) for Ph.D.Faculty Fellowship and the Nepal Mathematical Society (NMS) for the NMS Ph.D. Fellowship Award 2020. KA acknowledges the Nepal Academy of Science and Technology (NAST) for Ph.D. Fellowship and the Nepal Mathematical Society (NMS) for the NMS Ph.D. Fellowship Award 2020. AP acknowledges the Nepal Mathematical Society (NMS) for the NMS Ph.D. Fellowship Award 2020. The work of NV was supported by NSF grants DMS-1951793, DMS-1616299, DMS-1836647, and DEB-2030479 from the National Science Foundation of USA, and the UGP Award from San Diego State University.

References

[1] L.J. Abu-Raddad, P. Patnaik, and J.G. Kublin, *Dual infection with HIV and malaria fuels the spread of both diseases in sub-saharan africa*, Science 314(5805) (2006), pp. 1603–1606. ISSN 00368075, 10959203. Available at http://www.jstor.org/stable/20032992.

[2] F.B. Agusto, S.Y. Del Valle, K.W. Blayneh, C.N. Ngonghala, M.J. Goncalves, N. Li, R. Zhao, and H.Gong, *The impact of bed-net use on malaria prevalence*, J. Theor. Biol. 320 (2013), pp. 58–65. ISSN 0022-5193. Available at https://www.sciencedirect.com/science/article/pii/S0022519312006315.

[3] R.M. Anderson and M. Robert, *Infectious Diseases of Humans: Dynamics and Control*, Oxford University Press, Oxford, 1991. ISBN 9780198540403.

[4] R.M. Anderson, R.M. May, and B. Anderson, *The Population Dynamics of Infectious Diseases: Theory and Applications. Population and Community Biology*, Springer, New York, 1982. ISBN 13: 978–0198540403.

[5] J.L. Aron, *Mathematical modelling of immunity to malaria*, Math. Biosci. 90(1) (1988), pp. 385–396. ISSN 0025–5564.

[6] D. Bassidy, F. Avner, and Y. Abdul-Aziz, *Mathematical model for optimal use of sulfadoxine-pyrimethamine as a temporary malaria vaccine*, Bull. Math. Biol. 72(4) (2010), pp. 914–930.

[7] D. Bichara and C. Castillo-Chavez, *Vector-borne diseases models with residence times – a lagrangian perspective*, Math. Biosci. 281 (2016), pp. 128–138.

[8] J. Bradley, F. Monti, A.M. Rehman, C. Schwabe, D. Vargas, G. Garcia, D. Hergott, M. Riloha, and I.Kleinschmidt, *Infection importation: A key challenge to malaria elimination on bioko island, equatorial guinea*, Malar. J. 14(1) (2015), pp. 46–53.

[9] C. Castillo-Chavez and B. Song, *Dynamical model of tuberculiosis and their application*, Math. Biosci. Eng. 1(2) (2004), pp. 361–404.

[10] C. Castillo-Chavez, D. Bichara, and B.R. Morina, *Perspectives on the role of mobility, behavior, and time scales in the spread of diseases*, PNAS 113 (2016), pp. 14582–14588.

[11] CDC, *Malaria's impact worldwide*, 2020. Available at https://www.cdc.gov/malaria/malaria_worldwide/impact.html.

[12] Centre for Diseases Control and Prevention, CDC, *Ross and the discovery that mosquitoes transmit malaria parasites*, 2020. Available at https://www.cdc.gov/malaria/about/history/ross.html.

[13] F. Chamchod and N.F. Britton, *Analysis of a vector-bias model on malaria transmission*, Bull. Math. Biol. 73(3) (2011), pp. 639–657. Available at https://doi:10.1007/s11538-010-9545-0.

[14] N. Chitnis, J.M. Cushing, and J. Hyman, *Bifurcation analysis of a mathematical model for malaria transmission*, SIAM J. Appl. Math. 67(1) (2006), pp. 24–45.
[15] N. Chitnis, J.M. Hyman, and J.M. Cushing, *Determining important parameters in the spread of malaria through the sensitivity analysis of a mathematical model*, Bull. Math. Biol. 70 (2008), pp. 1272–1296.
[16] C. Chiyaka, W. Garira, and S. Dube, *Effects of treatment and drug resistance on the transmission dynamics of malaria in endemic areas*, Theor. Popul. Biol. 75(1) (2009), pp. 14–29. ISSN 0040–5809.
[17] T.S. Churcher, J.M. Cohen, J. Novotny, N. Ntshalintshali, S. Kunene, and S. Cauchemez, *Measuring the path toward malaria elimination*, Science 13(6189) (2014), pp. 1230–1232.
[18] G. Covell, *Epidemiology and control of malaria*, BMJ 2(5059) (1957), pp. 1477–1477. ISSN 0007-1447. Available at https://www.bmj.com/content/2/5059/1477.1.
[19] B. Dembele and A.-A. Yakubu, *Optimal treated mosquito bed nets and insecticides for eradication of malaria in missira*, Discrete Contin. Dyn. Syst. B 17(6) (2012), pp. 1831–1840.
[20] B. Derdei and I. Abderrahman, *Multi-patch and multi-group epidemic models: A new framework*, J. Math. Biol. 77 (2018), pp. 107–134.
[21] M. Dhimal, B. Ahrens, and U. Kuch, *Malaria control in Nepal 1963–2012: Challenges on the path towards elimination*, Malar. J. 13(1) (2014), pp. 241–255.
[22] M. Dhimal, B. Ahrens, and U. Kuch, *Species composition, seasonal occurrence, habitat preference and altitudinal distribution of malaria and other disease vectors in Eastern Nepal*, Parasit. Vectors 7(1) (2014), pp. 540–551.
[23] S. Dhiman, *Are malaria elimination efforts on right track? an analysis of gains achieved and challenges ahead*, Infect. Dis. Poverty 8(1) (2019), pp. 14–33.
[24] O. Diekmann, J.A.P. Heesterbeek, and J.A.J. Metz, *On the definition and the computation of the basic reproduction ratio r0 in models for infectious diseases in heterogeneous populations*, J. Math. Biol. 28(4) (1990), pp. 365–382.
[25] Epidemiology and Diseases Control Division (EDCD), Nepal, *Malaria elimination program*, 2020. Available at https://edcd.gov.np/section/malaria-elimination-program.
[26] GON, *Government launches new malaria campaign*, Tech. Rep., The New Humanitarian, 2012. Available at https://reliefweb.int/report/nepal/government-launches-new-malaria-campaign?fbclid=IwAR3qKbafo8FBxejGsA_f49cIpIXQONMSYHd4Y64tgWJCoe-9cj2jXGv08i0.
[27] Government of Nepal, Ministry of Health and Population, *Labour migration for employment: A status report of Nepal 2015/16*, 2018. Available at https://nepal.iom.int/sites/default/files/publication/LabourMigration_for_Employment-A_StatusReport_for_Nepal_201516201617_Eng.PDF.
[28] Government of Nepal Ministry of Health and Population, *National malaria surveillance guidelines 2019*, 2019. Available at https://www.edcd.gov.np/resources/download/national-malaria-surveillance-guidelines-2019.
[29] Government of Nepal, Ministry of Health and Population, EDCD, *Nepal malaria strategic plan 2014–2025*, 2016. Available at https://edcd.gov.np/resource-detail/nepal-strategic-plan-2014-2015.
[30] Government of Nepal, Ministry of Health and Population, EDCD, *World malaria report-2019*, 2020. Available at https://www.who.int/publications/i/item/9789241565721.
[31] I.M. Hastings, *A model for the origins and spread of drug-resistant malaria*, Parasitology 115(2) (1997), pp. 133–141.
[32] Z. Herrador, B. Fernandez-Martinez, V. Quesada-Cubo, O. Diaz-Garcia, R. Cano, A. Benito, and D.Gómez-Barroso, *Imported cases of malaria in spain:observational study using nationally reported statistics and surveillance data, 2002-2015*, Malar. J. 18(1) (2019), pp. 230–241.
[33] IOM UN Migration, *Malaria and mobility: Adressing malaria control and elimination in migration and human movement*, 2020. Available at https://www.iom.int/sites/default/files/our_work/DMM/Migration-Health/mhd_infosheet_malaria_and_mobility_25.04.2020.pdf.
[34] X. Jin, S. Jin, and D. Gao, *Mathematical analysis of the ross–macdonald model with quarantine*, Bull. Math. Biol. 82(4) (2020), p. 47.

[35] M.J. Keeling and P. Rohani, *Modeling Infectious Diseases in Humans and Animals*, Princeton University Press, Princeton, 2008. ISBN 9780691116174. Available at http://www.jstor.org/stable/j.ctvcm4gk0.
[36] W.O. Kermack and A.G. McKendrick, *A contribution to the mathematical theory of epidemics*, Proc. R. Soc. Lond. Ser. A 115(772) (1927), pp. 700–721. ISSN 09501207. Available at http://www.jstor.org/stable/94815.
[37] O. Koutou, B. Traore, and B. Sangare, *Mathematical modeling of malaria transmission global dynamics: Taking into account the immature stages of the vectors*, Adv. Differ. Equ. 2018 (2018), p. 220.
[38] L. Kumar, *Emigration of nepalese people and its impact*, Econ. J. Dev. Issues 19 (July 2017), p. 77.
[39] A. Le Menach, A.J. Tatem, J.M. Cohen, S.I. Hay, H. Randell, A.P. Patil, and D.L. Smith, *Travel risk, malaria importation and malaria transmission in zanzibar*, Sci. Rep. 1 (2011), p. 91. ISSN 2045–2322.
[40] Y. Lou and X.-Q. Zhao, *A climate-based malaria transmission model with structured vector population*, SIAM J. Appl. Math. 70(6) (2010), pp. 2023–2044.
[41] Malaria Site, *Malaria in India*, 2019. Available at https://www.malariasite.com/malaria-india/.
[42] S. Mandal, R.R. Sarkar, and S. Singh, *Mathematical models of malaria – a review*, Malar. J. 10(1) (2011), pp. 202–221.
[43] H. Miao, X. Xia, A. Perelson, and H. Wu, *On identifiability of nonlinear ode models and applications in viral dynamics*, SIAM Rev. 53(1) (2011), pp. 3–39.
[44] Ministry of Health and Family Welfare, Government of India, *Family Welfare: National framework for malaria elimination in India (2016–2030)*, 2020. Available at http://origin.searo.who.int/india/publications/national_framework_malaria_elimination_india_2016_2030.pdf.
[45] C. Ngonghala, S. Del Valle, R. Zhao, and J. Mohammed-Awel, *Quantifying the impact of decay in bed-net efficacy on malaria transmission*, J. Theor. Biol. 363, pp. 247-261. (2014).
[46] G.A. Ngwa, *Modelling the dynamics of endemic malaria in growing populations*, Discrete Contin. Dyn. Syst. Ser. B 4(4) (2004), pp. 1173–1202.
[47] G. Ngwa and W. Shu, *A mathematical model for endemic malaria with variable human and mosquito populations*, Math. Comput. Model. 32(7) (2000), pp. 747–763. ISSN 0895–7177.
[48] K.O. Okosun, R. Ouifki, and N. Marcus, *Optimal control analysis of a malaria disease transmission model that includes treatment and vaccination with waning immunity*, Biosystems 106(2-3) (2011), pp. 136–145.
[49] M. Rahman, K.B. Maxwell, L.L. Cates, H.T. Banks, and N.K. Vaidya, *Modeling zika virus transmission dynamics: Parameter estimates, disease characteristics, and prevention*, Sci. Rep. 9(1) (July 2019), pp. 1–13.
[50] K.R. Rijal, B. Adhikari, N. Adhikari, S.P. Dumre, M.S. Banjara, U.T. Shrestha, M.R. Banjara, N.Singh, L. Ortegea, B.K. Lal, G.D. Thakur, and P. Ghimire, *Micro-stratification of malaria risk in Nepal: Implications for malaria control and elimination*, Trop. Med. Health. 47(1) (June 2019), pp. 21–33.
[51] I. Routledge, J.E.R. Chevez, Z.M. Cucunuba, M.G. Rodriguez, C. Guinovart, K.B. Gustafson, K.Schneider, P.G.T. Walker, A.C. Ghani, and S. Bhatt, *Estimating spatiotemporally varying malaria reproduction numbers in a near elimination setting*, Nat. Commun. 9(1) (2018), pp. 2476–2484.
[52] J. Sachs and P. Malaney, *The economic and social burden of malaria*, Nature 415 (2002), pp. 680–685.
[53] C.D. Schunn and D.P. Wallach, *Evaluating goodness-of-fit in comparison of models to data*. in *Psychologie der Kognition: Reden and Vorträge anlässlich der Emeritierung von Werner Tack*, W. Tack, ed., Saarbrueken, Germany: University of Saarland Press, 2005, pp. 115–135.
[54] F.R. Sharpe and A.J. Lotka, *Contribution to the analysis of malaria epidemiology. IV. Incubation lag*, Am. J. Epidemiol. 3(supp1) (January 1923), pp. 96–112. ISSN 0002–9262.
[55] S.B. Shrestha, U.R. Pyakurel, M. Khanal, M. Upadhyay, K. Na-Bangchang, and P. Muhamad, *Epidemiological situations and control strategies of vector-borne diseases in Nepal during 1998–2016*, J. Health Res. 33(6) (2019), pp. 478–493.

[56] H. Smith and P. Waltman, *The Theory of the Chemostat*, Cambridge University Press, Atlanta, 1995. ISBN 0-521-47027-7.
[57] J.L. Smith, P. Ghimire, K.R. Rijal, A. Maglior, S. Hollis, R. Andrade-Pacheco, G. Das Thakur, N.Adhikari, U. Thapa Shrestha, M.R. Banjara, B.K. Lal, J.O. Jacobson, and A. Bennett, *Designing malaria surveillance strategies for mobile and migrant populations in Nepal: A mixed-methods study*, Malar. J. 18(1) (2019), pp. 158–177.
[58] H.J.W. Sturrock, J.M. Novotny, S. Kunene, S. Dlamini, Z. Zulu, J.M. Cohen, M.S. Hsiang, B.Greenhouse, and R.D. Gosling, *Reactive case detection for malaria elimination: Real-life experience from an ongoing program in swaziland*, PLoS ONE 8(5) (May 2013), pp. 1–8.
[59] A.J. Tatem, P. Jia, D. Ordanovich, M. Falkner, Z. Huang, R. Howes, I.H. Simon, P.W. Gethin, and D.LSmith, *The geography of imported malaria to non-endemic countries: A meta-analysis of nationally reported statistics*, Lancet Infect. Dis. 17(1) (2017), pp. 98–107.
[60] The World Bank, *Birth rate, crude (per 1000-Nepal)*, 2020. Available at https://data.worldbank.org/indicator/SP.DYN.CBRT.IN?locations=NP.
[61] L.J. Torres-Sorando and D. Rodríguez, *Models of spatio-temporal dynamics in malaria*, Ecol. Modell. 104(2) (1997), pp. 231–240. ISSN 0304–3800.
[62] B. Traore, B. Sangare, and S. Traore, *A mathematical model of malaria transmission with structured vector population and seasonality*, J. Appl. Math. 2017 (2017), Article ID 6754097.
[63] H.J.T. Unwin, I. Routledge, S. Flaxman, M.-A. Rizoiu, S. Lai, J. Cohen, D.J. Weiss, S. Mishra, and S.Bhatt, *Using hawkes processes to model imported and local malaria cases in near-elimination settings*, PLoS Comput. Biol. 17(4) (2021), e1008830. https://doi.org/10.1371/journal.pcbi.1008830
[64] N.K. Vaidya and W. Jianhong, *HIV epidemic in far-Western Nepal: Effect of seasonal labor migration to India*, BMC Public Health 11(310) (2011), pp. 1–11.
[65] P. van den Driessche and J. Watmough, *Reproduction numbers and sub-threshold endemic equilibria for compartmental models of disease transmission*, Math. Biosci. 180(1) (2002), pp. 29–48. ISSN 0025–5564.
[66] WHO, *Department of health services, annual report*, 2018. Available at https://publichealthupdate.com/department-of-health-services-dohs-annual-report-2074-75-2017-18/.
[67] WHO, *Latest data on malaria trends in 87 countries*, Tech. Rep., World Health Organization, 2020. Available at https://www.who.int/teams/global-malaria-programme/reports/world-malaria-report-2020?fbclid=IwAR0D-ryfYEWJ-yvyC7HJib271Rz3iAanP57sArjjOWDOXd2cR1FcHSvd0Zg.
[68] WHO, *World malaria report 2019*, 2020. Available at https://www.who.int/malaria/publications/world-malaria-report-2019/World-Malaria-Report-2019-briefing-kit-eng.pdf.
[69] Wiki, *2001 Nepal census*, 2001. Available at https://en.wikipedia.org/wiki/2001_Nepal_census.
[70] Wiki, *Nepal census*, 2011. Available at https://en.wikipedia.org/wiki/20011_Nepal_census.
[71] Y. Xing, Z. Guo, and J. Liu, *Backward bifurcation in a malaria transmission model*, J. Biol. Dyn.14(1) (2020), pp. 368–388. PMID: 32462991.
[72] H. Yin, C. Yang, X. Zhang, and J. Li, *Dynamics of malaria transmission model with sterile mosquitoes*, J. Biol. Dyn. 12(1) (2018), pp. 577–595.
[73] X.-Q. Zhao, *Uniform persistence in processes with application to nonautonomous competitive models*, J. Math. Anal. Appl. 258(1) (2001), pp. 87–101. ISSN 0022-247X.

Appendices

Appendix 1

A.1 Proof of Theorem 4.1

First, we prove that all the solutions are bounded. From Equations (11), (12), and (13), we get

$$\frac{\mathrm{d}S_{hH}}{\mathrm{d}t} = \Lambda + qR_{hH} + \eta S_{hM} - \frac{b\alpha_{vh}S_{hH}I_{vH}}{N_{hH}} - (\eta + d_h)S_{hH}$$

$$> -\frac{b\alpha_{vh}S_{hH}I_{vH}}{N_{hH}} - (\eta + d_h)S_{hH}$$

$$\Rightarrow \quad S_{hH} > S_{hH}(0)\exp\left(-\int_0^t \left(\frac{b\alpha_{vh}I_{vH}}{N_{hH}} + \eta + d_h\right)\mathrm{d}t\right) \geq 0;$$

$$\frac{\mathrm{d}I_{hH}}{\mathrm{d}t} = \frac{b\alpha_{vh}S_{hH}I_{vH}}{N_{hH}} + \theta I_{hM} - (\theta + d_h + \delta_h + \gamma_h)I_{hH} \geq -(\theta + d_h + \delta_h + \gamma_h)I_{hH}$$

$$\Rightarrow \quad I_{hH} \geq I_{hH}(0)\exp\left(-\int_0^t (\theta + d_h + \delta_h + \gamma_h)\,\mathrm{d}t\right) \geq 0;$$

$$\text{and} \quad \frac{\mathrm{d}R_{hH}}{\mathrm{d}t} = \gamma_h I_{hH} + \eta R_{hA} - (\eta + d_h + q)R_{hH} \geq -(\eta + d_h + q)R_{hH}$$

$$\Rightarrow \quad R_{hH} \geq R_{hH}(0)\exp\left(-\int_0^t (\eta + d_h + q)\,\mathrm{d}t\right) \geq 0.$$

Similarly, from Equations (16), (17), and (18), we get

$$\frac{\mathrm{d}S_{hM}}{\mathrm{d}t} = \eta S_{hH} + qR_{hM} - (k + d_h + \eta)S_{hM} \geq -(k + d_h + \eta)S_{hM}$$

$$\Rightarrow \quad S_{hM} \geq S_{hM}(0)\exp\left(-\int_0^t (\eta + k + d_h)\,\mathrm{d}t\right) \geq 0;$$

$$\frac{\mathrm{d}I_{hM}}{\mathrm{d}t} = kS_{hM} + \theta I_{hH} - (\theta + \delta_h + d_h + \gamma_h)I_{hM} \geq -(\theta + \delta_h + d_h + \gamma_h)I_{hM}$$

$$\Rightarrow \quad I_{hM} \geq I_{hM}(0)\exp\left(-\int_0^t (\theta + d_h + \delta_h + \gamma_h)\,\mathrm{d}t\right) \geq 0;$$

$$\text{and} \quad \frac{\mathrm{d}R_{hM}}{\mathrm{d}t} = \gamma_h I_{hM} + \eta R_{hH} - (\eta + d_h)R_{hM} \geq -(\eta + d_h + q)R_{hM}$$

$$\Rightarrow \quad R_{hM} \geq R_{hM}(0)\exp\left(-\int_0^t (\eta + d_h + q)\,\mathrm{d}t\right) \geq 0.$$

Also, from (14) and (15),

$$\frac{\mathrm{d}S_{vH}}{\mathrm{d}t} = \phi - \frac{b\alpha_{hv}S_{vH}I_{hH}}{N_{hH}} - d_v S_{vH} > -\frac{b\alpha_{hv}S_{vH}I_{hH}}{N_{hH}} - d_v S_{vH}$$

$$\Rightarrow \quad S_{vH} > S_{vH}(0)\exp\left(-\int_0^t \left(\frac{b\alpha_{hv}I_{hH}}{N_{hH}} + dv\right)\mathrm{d}t\right) \geq 0;$$

$$\text{and} \quad \frac{\mathrm{d}I_{vH}}{\mathrm{d}t} = \frac{b\alpha_{hv}S_{vH}I_{hH}}{N_{hH}} - d_v I_{vH} \geq -d_v I_{vH}$$

$$\Rightarrow \quad I_{vH} \geq I_{vH}(0)\exp\left(-\int_0^t (d_v)\,\mathrm{d}t\right) \geq 0.$$

Hence the solution set $\{(S_{hH}(t), I_{hH}(t), R_{hH}(t), S_{hM}(t), I_{hM}(t), R_{hM}(t), S_{vH}(t), I_{vH}(t))\}$ of the system (11)–(18) is always non-negative. We now prove that these non-negative solutions are bounded. Adding (11)–(13) and (16)–(18), we obtain

$$\frac{\mathrm{d}N_h}{\mathrm{d}t} = \Lambda - d_h N_h - \delta_h I_{hH} - \delta_h I_{hM} \leq \Lambda - d_h N_h,$$

which implies $\lim_{t\to\infty} N_h \leq \frac{\Lambda}{d_h}$. Hence, the human population, $N_h(t)$, is ultimately bounded.

Again, adding (14) and (15), we obtain

$$\frac{\mathrm{d}N_v}{\mathrm{d}t} = \phi - d_v N_v,$$

which implies $\lim_{t\to\infty} N_v = \frac{\phi}{d_v}$. Hence, the mosquito population $N_v(t)$ is ultimately bounded. Thus all state variables representing the populations are non-negative and bounded.

A.2 Derivation of the epidemic index R_0 from the next generation matrix method

From the system (11)–(18), the newly infectious matrix F_i and its Jacobian matrix F at the disease-free equilibrium point E_0 are

$$F_i = \begin{pmatrix} \frac{\beta_h S_{hH} I_{vH}}{N_{hH}} \\ \frac{\beta_v S_{vH} I_{hH}}{N_{hH}} \\ kS_{hM} \end{pmatrix}, \quad F = \begin{pmatrix} 0 & \beta_h & 0 \\ \frac{\beta_v \phi\, d_h}{\Lambda d_v} & 0 & 0 \\ 0 & 0 & 0 \end{pmatrix}.$$

Again, the transfer matrix V_i and its Jacobian matrix V at the disease-free equilibrium point,

$$V_i = \begin{pmatrix} (\theta + \delta_h + \gamma_h + d_h) I_{hH} - \theta\, I_{hM} \\ d_v i_{vH} \\ (\theta + \gamma_h + \delta_h + d_h) I_{hA} - \theta\, I_{hH} \end{pmatrix}, \quad V = \begin{pmatrix} d_h + \delta_h + \gamma_h & 0 & 0 \\ 0 & d_v & 0 \\ 0 & 0 & \gamma_h + \delta_h + d_h \end{pmatrix}.$$

Here the dominant eigenvalue of FV^{-1} gives the following epidemic index.

$$R_0 = \sqrt{\frac{\phi d_h \beta_h \beta_v}{(d_h + \gamma_h + \delta_h)\, \Lambda d_v^2}}.$$

A.3 Derivation of R_0 from the first principle method

The overall basic reproduction number (R_0) of malaria is equal to the geometric mean of the basic reproduction numbers of malaria transmission from an infected human to susceptible mosquitoes (R_H) and the transmission of malaria from an infected mosquito to susceptible humans (R_V). Here $\frac{b}{N_{hH}}$ is the average number of bites made by a mosquito to a human in unit time. Each mosquito bites at a constant rate, whereas the rate at which humans are bitten will vary with respect to the density of mosquitoes within the area. The expected number of infected mosquitoes from an infected human in his infectious period (assuming that all mosquitoes are susceptible) is given by $R_H = \frac{b\,\alpha_{hv} N_v^0}{(d_h+\delta_h+\gamma_h)N_h^0} = \frac{b\alpha_{hv}\phi d_h}{(d_h+\delta_h+\gamma_h)\Lambda d_v}$. Similarly, the expected number of susceptible humans that become infected due to contact with one infected mosquito in its infectious period (assuming that all humans are susceptible) are given by $R_V = \frac{b\,\alpha_{vh} N_h^0}{N_h^0 d_v} = \frac{b\alpha_{vh}}{d_v}$. Then, we get

$$R_0 = \sqrt{R_H \times R_V} = \sqrt{\frac{\phi d_h \beta_h \beta_v}{\Lambda (d_h + \delta_h + \gamma_h) d_v^2}}.$$

A.4 Derivation of the epidemic index R_1

From the system (11)–(18), the newly infectious matrix F_i and its Jacobian matrix F at the disease-free equilibrium point E_{01} are

$$F_i = \begin{pmatrix} \frac{b\alpha_{vh} S_{hH} I_{vH}}{N_{hH}} \\ \frac{b\alpha_{hv} S_{vH} I_{hH}}{N_{hH}} \\ kS_{hM} \end{pmatrix}, \quad F = \begin{pmatrix} 0 & \beta_h & 0 \\ \frac{\phi d_h \beta_v\, (d_h + 2\eta)}{\Lambda d_v\, (d_h + \eta)} & 0 & 0 \\ 0 & 0 & 0 \end{pmatrix}.$$

Again, the transfer matrix V_i and its Jacobian matrix V at the disease-free equilibrium point E_{01} are,

$$V_i = \begin{pmatrix} (\theta + \delta_h + \gamma_h + d_h)I_{hH} - \theta\, I_{hM} \\ d_v i_{vH} \\ (\theta + \gamma_h + \delta_h + d_h)I_{hM} - \theta\, I_{hH} \end{pmatrix}, \quad V = \begin{pmatrix} d_h + \gamma_h + \delta_h + \theta & 0 & -\theta \\ 0 & d_v & 0 \\ -\theta & 0 & d_h + \gamma_h + \delta_h + \theta \end{pmatrix}.$$

Then the dominant eigenvalue of FV^{-1} gives the epidemic index R_1:

$$R_1 = R_0\sqrt{1 + \frac{(\eta\,(d_h + \gamma_h + \delta_h) - \theta d_h)}{(d_h + \eta)\,(d_h + \gamma_h + \delta_h + 2\theta)}}.$$

A.5 Derivation of the epidemic index R_2

From the system (11)–(18), the newly infectious matrix F_i and its Jacobian matrix F at the disease-free equilibrium point E_{02} are

$$F_i = \begin{pmatrix} \dfrac{b\alpha_{vh}S_{hH}I_{vH}}{N_{hH}} \\ \dfrac{b\alpha_{hv}S_{vH}I_{hH}}{N_{hH}} \\ kS_{hM} \end{pmatrix}, \quad F = \begin{pmatrix} 0 & \dfrac{P\beta_h}{P + Q_3} & 0 \\ \dfrac{K_1\phi\beta_v}{(P + Q_3)d_v} & 0 & 0 \\ 0 & 0 & 0 \end{pmatrix}$$

Again, the transfer matrix V_i and its Jacobian matrix V at the disease-free equilibrium point E_{02} are

$$V_i = \begin{pmatrix} (\theta + \delta_h + \gamma_h + d_h)I_{hH} - \theta\, I_{hM} \\ d_v i_{vH} \\ (\theta + \gamma_h + \delta_h + d_h)I_{hM} - \theta\, I_{hH} \end{pmatrix}, \quad V = \begin{pmatrix} d_h + \gamma_h + \delta_h & 0 & 0 \\ 0 & d_v & 0 \\ 0 & 0 & d_h + \gamma_h + \delta_h \end{pmatrix}.$$

Then the dominant eigenvalue of FV^{-1} provides the epidemic index R_2.

$$R_2 = \sqrt{\frac{PK_1\phi\beta_h\beta_v}{(P + Q_3)^2 d_v^2\,(d_h + \gamma_h + \delta_h)}}$$

Appendix 2

A.6 Proof of Theorem 4.2

The local stability of E_0 is determined by the following Jacobian matrix of (11)–(18) evaluated at E_0: $J = \begin{pmatrix} J_{H,5\times5} & 0_{5\times3} \\ 0_{3\times5} & J_{A,3\times3} \end{pmatrix}$, where

$$J_{H,5\times5} = \begin{pmatrix} -d_h & 0 & q & 0 & -\beta_h \\ 0 & -F & 0 & 0 & \beta_h \\ 0 & \gamma_h & -G & 0 & 0 \\ 0 & -\dfrac{\phi d_h\beta_v}{\Lambda} & 0 & -d_v & 0 \\ 0 & \dfrac{\phi d_h\beta_v}{\Lambda} & 0 & 0 & -d_v \end{pmatrix}, \quad J_{A,3\times3} = \begin{pmatrix} -H & 0 & q \\ k & -F & 0 \\ 0 & \gamma_h & -G \end{pmatrix},$$

$F = (d_h + \gamma_h + \delta_h), G = (d_h + q)$, and $H = (d_h + k)$. The roots of the characteristic polynomial equation of J_H are

$$\lambda_1 = -d_h, \lambda_2 = -d_h + q, \lambda_3 = -d_v,$$

$$\lambda_4 = \frac{-(d_h + d_v + \gamma_h + \delta_h) - \sqrt{(d_h + d_v + \gamma_h + \delta_h)^2 - 4d_v\,(d_h + \delta_h + \gamma_h)\left(1 - R_0^2\right)}}{2},$$

$$\lambda_5 = \frac{-(d_h + d_v + \gamma_h + \delta_h) + \sqrt{(d_h + d_v + \gamma_h + \delta_h)^2 - 4d_v\,(d_h + \delta_h + \gamma_h)\left(1 - R_0^2\right)}}{2}.$$

The roots, λ, of the characteristic polynomial equation of the matrix J_A are given by

$$\lambda^3 + e_1\lambda^2 + e_2\lambda + e_3 = 0,$$

where
$$e_1 = 3d_h + \gamma_h + \delta_h + k + q,$$
$$e_2 = 2d_h\gamma_h + 2d_h\delta_h + 2kd_h + 2qd_h + 3d_h^2 + k\gamma_h + k\delta_h + q\gamma_h + q\delta_h + kq,$$
$$e_3 = d_h^2\gamma_h + d_h^2\delta_h + kd_h\gamma_h + kd_h\delta_h + kqd_h + kd_h^2 + qd_h\gamma_h + qd_h\delta_h + qd_h^2 + d_h^3 + kq\delta_h.$$
$$\begin{aligned} e_1e_2 - e_3 = {} & 4d_h\gamma_h\delta_h + 8d_h^2\gamma_h + 2d_h\gamma_h^2 + 8d_h^2\delta_h + 2d_h\delta_h^2 + 2k^2d_h \\ & + 6kd_h\gamma_h + 6kd_h\delta_h + 6kqd_h + 8kd_h^2 + 2q^2d_h + 6qd_h\gamma_h + 6qd_h\delta_h + 8qd_h^2 \\ & + 8d_h^3 + k^2\gamma_h + k^2\delta_h + 2k\gamma_h\delta_h + k\gamma_h^2 + k\delta_h^2 + 3kq\gamma_h + 2kq\delta_h \\ & + q^2\gamma_h + q^2\delta_h + 2q\gamma_h\delta_h + q\gamma_h^2 + q\delta_h^2 + k^2q + kq^2 > 0. \end{aligned}$$

Here, $e_1, e_2, e_3, e_1e_2 - e_3$ are positive. Using Routh Hurwitz criteria, all the eigenvalues of J_A have negative real part. Therefore, all the eigenvalues of J_H are negative when $R_0 < 1$. Thus the disease-free equilibrium point E_0 is locally asymptotically stable if $R_0 < 1$, and unstable if $R_0 > 1$.

A.7 Proof of the Lemma 4.4

For any $(S_{hH}(0), I_{hH}(0), R_{hH}(0), S_{vH}(0), I_{vH}(0)) \in \Omega_o$, we have from the first and fourth equations of the system,

$$S_{hH}(t) = e^{-\int_0^t B(s_1)\,ds_1}\left[\int_0^t e^{\int_0^{s_2} B(s_1)\,ds_1} A(s_2)\,ds_2 + S_{hH}(0)\right],$$
$$S_{vH}(t) = e^{-\int_0^t F(s_1)\,ds_1}\left[\int_0^t e^{\int_0^{s_2} F(s_1)\,ds_1} \phi\,ds_2 + S_{vH}(0)\right],$$

where, $A(t) := \Lambda + qR_{hH} > 0$, $B(t) := \frac{\beta_h I_{vH}}{N_{hH}} + d_h$, and $F(t) := \frac{\beta_v I_{hH}}{N_{hH}} + d_v$. The Jacobian matrix J_0 corresponding to the second and fifth equations of the system is

$$J_0 = \begin{pmatrix} \dfrac{-\beta_h I_{vH} S_{hH}}{N_{hH}^2} - (\delta_h + d_h + \gamma_h) & \dfrac{\beta_h S_{hH}}{N_{hH}} \\ \dfrac{\beta_v S_{vH}}{N_{hH}}\left(1 - \dfrac{I_{hH}}{N_{hH}}\right) & -d_v \end{pmatrix}.$$

Since J_0 is an irreducible matrix with non negative off diagonal elements then $S(J_0)$ is simple with an associated strongly positive eigenvector [56]. Hence the vector $(I_{hH}(t), I_{vH}(t))$ is positive for all $t > 0$. Again from the third equation of the system,

$$R_{hH}(t) = e^{-\int_0^t D(s_1)\,ds_1}\left[\int_0^t e^{\int_0^{s_2} D(s_1)\,ds_1} C(s_2)\,ds_2 + R_{hH}(0)\right]$$

where $C(t) = \gamma_h I_{hH} > 0$ and $D(t) = d_h + q$. $S_{hH}(t), R_{hH}(t), S_{vH}(t) > 0, \forall\, t > 0$. Hence the sets Ω_o is positively invariant. Since Ω is positively invariant and $\partial\Omega_o$ is relatively closed in Ω_o, it gives $\partial\Omega_o$ is also positively invariant. Thus both Ω_o and $\partial\Omega_o$ are positively invariant under the flow induced by the decoupled system (11)–(15).

A.8 Proof of the Lemma 4.5

Since $P \in M_\partial$, $\tau(t)P \in M_\partial$ for all $t \geq 0$. From the definition of M_∂, $I_{vH}(t) = 0$, $\forall\ t \geq 0$. Using $I_{vH}(t) = 0$ in (15), it follows that $I_{hH}(t) = 0$ for all $t \geq 0$. Then from the first, third, and fourth equation of (11)–(15),

$$\frac{dS_{hH}}{dt} + d_hS_{hH} = \Lambda, \quad \frac{dR_{hH}}{dt} + (d_h + q)R_{hH} = 0, \quad \frac{dS_{vH}}{dt} + d_vS_{vH} = \phi.$$

Solving the first order linear ordinary differential equations, we have $\lim_{t\to\infty} S_{hH}(t) = \frac{\Lambda}{d_h}, \lim_{t\to\infty} R_{hH}(t) = 0, \lim_{t\to\infty} S_{vH}(t) = \frac{\phi}{d_v}$. It follows that any forward orbit of $\tau(t)$ in M_∂ converges to E_0.

A.9 Proof of the Lemma 4.6

Suppose, if possible, there exists $P_o \in \Omega_o$, such that $\lim_{t\to\infty} \text{Sup}\, \|\tau(t)P_o - E_0\| < \rho$. Since $\lim_{t\to\infty} N_{hH}(t) \leq \frac{\Lambda}{d_h}$ and $\lim_{t\to\infty} S_{vH}(t) = \frac{\phi}{d_v}$ then there exists $t_2 > 0$, $\forall t \geq t_2$ and a sufficiently small positive number ρ_o such that $N_{hH}(t) \leq \frac{\Lambda}{d_h} + \rho_o$ and $S_{hH}(t) \geq \frac{\Lambda}{d_h} - \rho_o$ and $S_{vH}(t) \geq \frac{\phi}{d_v} - \rho_o$. Using these inequalities in Equations (12) and (15), we obtain

$$
\begin{aligned}
I'_{hH} &\geq \beta_h \left(1 - \frac{2\rho_0}{\frac{\Lambda}{d_h} + \rho_0}\right) I_{vH} - (d_h + \delta_h + \gamma_h) I_{hH}, \\
I'_{vH} &\geq \frac{\beta_v \left(\frac{\phi}{d_v} - \rho_o\right)}{\left(\frac{\Lambda}{d_h} + \rho_o\right)} I_{hH} - d_v I_{vH}.
\end{aligned}
$$

We consider the corresponding auxiliary equations

$$
\begin{aligned}
I'_{hH} &= \beta_h \left(1 - \frac{2\rho_0}{\frac{\Lambda}{d_h} + \rho_0}\right) I_{vH} - (d_h + \delta_h + \gamma_h) I_{hH}, \\
I'_{vH} &= \frac{\beta_v \left(\frac{\phi}{d_v} - \rho_o\right)}{\left(\frac{\Lambda}{d_h} + \rho_o\right)} I_{hH} - d_v I_{vH}, \quad \forall\, t \geq t_2.
\end{aligned}
\tag{A1}
$$

Let J_{ρ_o} be the Jacobian of the system (A1), then

$$
J_{\rho_o} = \begin{pmatrix}
-(\delta_h + d_h + \gamma_h) & \beta_h \left(1 - \frac{2\rho_0}{\frac{\Lambda}{d_h} + \rho_0}\right) \\
\frac{\beta_v \left(\frac{\phi}{d_v} - \rho_o\right)}{\left(\frac{\Lambda}{d_h} + \rho_o\right)} & -d_v
\end{pmatrix}
$$

Since $S(J) > 0$, there exists a sufficiently small $\rho_o > 0$ such that $S(J_{\rho_o}) > 0$. Since J_{ρ_o} is irreducible and has non-negative off-diagonal elements, it follows that $S(J_{\rho_o})$ is a simple and associates with strongly positive eigenvector $\tilde{\nu} \in \Re^2_+$, i.e. $(I_{hH}(t), I_{vH}(t)) >> 0\ \forall\ t \geq t_2$. Then there is a positive number a such that $(I_{hH}(t), I_{vH}(t)) \geq a\tilde{\nu}$ and hence the solution of the system (A1) is

$$
V(t) := a e^{S(J_{\rho_o})(t-t_2)} \tilde{\nu}, \quad \forall\, t \geq t_2
$$

with $V(t_2) := a\tilde{\nu}$. Hence it follows from [56, Theorem B.1] that

$$
(I_{hH}(t), I_{vH}(t)) \geq a e^{S(J_{\rho_o})(t-t_2)} \tilde{\nu}, \quad \forall\, t \geq t_2.
$$

Since $S(J_{\rho_o}) > 0$, then the solution $\lim_{t\to\infty} I_{hH}(t) \to \infty, \lim_{t\to\infty} I_{vH}(t) \to \infty$ which is a contradiction, and hence $\lim_{t\to\infty} \text{Sup}\, \|\tau(t)P - E_0\| \geq \rho,\ \forall\, P \in \Omega_o$.

A.10 Proof of the Theorem 4.8

The Jacobian matrix of (11)–(18) at E_{01} is $J_1 = \begin{pmatrix} A^1_{4\times4} & B^1_{4\times4} \\ C^1_{4\times4} & D^1_{4\times4} \end{pmatrix}$, where

$$A^1_{4\times4} = \begin{pmatrix} -D & 0 & q & \eta \\ 0 & -A & 0 & 0 \\ 0 & \gamma_h & -B & 0 \\ \eta & 0 & 0 & -d_h \end{pmatrix}, \quad B^1_{4\times4} = \begin{pmatrix} 0 & 0 & 0 & -\beta_h \\ \theta & 0 & 0 & \beta_h \\ 0 & \eta & 0 & 0 \\ 0 & q & 0 & 0 \end{pmatrix},$$

$$C^1_{4\times4} = \begin{pmatrix} 0 & \theta & 0 & 0 \\ 0 & 0 & \eta & 0 \\ 0 & -C & 0 & 0 \\ 0 & C & 0 & 0 \end{pmatrix}, \quad D^1_{4\times4} = \begin{pmatrix} -A & 0 & 0 & 0 \\ \gamma_h & -B & 0 & 0 \\ 0 & 0 & -d_v & 0 \\ 0 & 0 & 0 & -d_v \end{pmatrix},$$

$A = (d_h + \gamma_h + \delta_h + \theta), B = (d_h + \eta + q), C = \frac{\phi d_h \beta_v (d_h+2\eta)}{\Lambda d_v (d_h+\eta)}$, and $D = (d_h + \eta)$. Let λ be eigenvalues of the matrix J_1, then the characteristic polynomial is

$$P(\lambda) = (d_h + \lambda)\,(d_v + \lambda)\,(d_h + 2\eta + \lambda)\left(d_h + \lambda + q\right)\left(d_h + 2\eta + \lambda + q\right) Q(\lambda),$$

where $Q(\lambda) = \lambda^3 + h_1\lambda^2 + h_2\lambda + h_3$,

$$h_1 = 2d_h + d_v + 2\,(\gamma_h + \delta_h + \theta)\,,$$

$$h_2 = \frac{\left(2 - R_1^2\right)\left(d_v\,(d_h + \gamma_h + \delta_h)\,(d_h + \gamma_h + \delta_h + 2\theta)\right)}{d_h + \gamma_h + \delta_h + \theta} + P_1,$$

$$h_3 = \left(1 - R_1^2\right) d_v\,(d_h + \gamma_h + \delta_h)\,(d_h + \gamma_h + \delta_h + 2\theta)\,,$$

$$P_1 = \frac{(\gamma_h + \delta_h)\left(2\theta^2 + \gamma_h\,(2\delta_h + 3\theta) + \gamma_h^2 + 3\theta\delta_h + \delta_h^2\right)}{d_h + \gamma_h + \delta_h + \theta} + \frac{d_h\left(2\theta^2 + 6\gamma_h\,(\delta_h + \theta) + 3\gamma_h^2 + 6\theta\delta_h + 3\delta_h^2\right) + 3d_h^2\,(\gamma_h + \delta_h + \theta) + d_h^3 + 2\theta^2 d_v}{d_h + \gamma_h + \delta_h + \theta}.$$

This implies that $\lambda = -d_h, -d_v, (-d_h + 2\eta), -(d_h + q), -(d_h + 2\eta + q)$ are five eigenvalues. The coefficients h_1 is positive and both $h_2 > 0, h_3 > 0$ if $R_1 < 1$. Also,

$$\begin{aligned} h_1h_2 - h_3 &= (2\,(d_h + \gamma_h + \delta_h + \theta) + d_v) \\ &\quad \times \left(\frac{\left(2 - R_1^2\right) d_v\,(d_h + \gamma_h + \delta_h)\,(d_h + \gamma_h + \delta_h + 2\theta)}{d_h + \gamma_h + \delta_h + \theta} + P_1\right) \\ &\quad - \left(1 - R_1^2\right) d_v\,(d_h + \gamma_h + \delta_h)\,(d_h + \gamma_h + \delta_h + 2\theta) \\ &= \left(3 - R_1^2\right) d_v\,(d_h + \gamma_h + \delta_h)\,(d_h + \gamma_h + \delta_h + 2\theta) \\ &\quad + 2P_1(d_h + \gamma_h + \delta_h + \theta) + P_2 > 0, \quad \text{if } R_1 < 1. \end{aligned}$$

where $P_2 = d_v(\frac{(2-R_1^2)d_v(d_h+\gamma_h+\delta_h)(d_h+\gamma_h+\delta_h+2\theta)}{d_h+\gamma_h+\delta_h+\theta} + P_1)$. Thus all the eigenvalues have negative real parts and hence E_{01} is locally asymptotically stable if $R_1 < 1$. If $R_1 > 1$, then h_0 and h_3 have opposite signs, which implies at least one λ to be positive. Hence, the disease-free equilibrium point E_{01} is unstable if $R_1 > 1$.

A.11 Proof of the Lemma 4.10

For any $(S_{hH}(0), I_{hH}(0), R_{hH}(0), S_{vH}(0), I_{vH}(0), S_{hM}(0), I_{hM}(0), R_{hM}(0)) \in \Omega_o$, we have from the first and fourth equations of the system (11)–(18)

$$S_{hH}(t) = e^{-\int_0^t B(s_1)\,\mathrm{d}s_1}\left[\int_0^t e^{\int_0^{s_2} B(s_1)\,\mathrm{d}s_1} A(s_2)\,\mathrm{d}s_2 + S_{hH}(0)\right],$$

$$S_{vH}(t) = e^{-\int_0^t F(s_1)\,ds_1}\left[\int_0^t e^{\int_0^{s_2} F(s_1)\,ds_1}\phi\,ds_2 + S_{vH}(0)\right],$$

where $A(t) := \Lambda + \eta S_{hM} + qR_{hH} > 0$, $B(t) := \frac{\beta_h I_{vH}}{N_{hH}} + \eta + d_h$, and $F(t) := \frac{\beta_v I_{hH}}{N_{hH}} + d_v$.

Again, the Jacobian J_0 corresponding to the second, seventh, and fourth equations of the system is

$$J_0 = \begin{pmatrix} \frac{-\beta_h I_{vH} S_{hH}}{N_{hH}^2} - (\theta + \delta_h + d_h + \gamma_h) & \theta & \frac{\beta_h S_{hH}}{N_{hH}} \\ \theta & -(\theta + \delta_h + d_h + \gamma_h) & 0 \\ \frac{\beta_v S_{vH}}{N_{hH}}\left(1 - \frac{I_{hH}}{N_{hH}}\right) & 0 & -d_v \end{pmatrix}.$$

Since J_0 is an irreducible matrix with non-negative off-diagonal elements then $S(J_0)$ is simple with an associated strongly positive eigenvector [56]. Hence the vector $(I_{hH}(t), I_{hM}(t), I_{vH}(t))$ is positive $\forall\, t > 0$. From the third, sixth, and eighth equations of the system (11)–(18), we get

$$R_{hH}(t) = e^{-\int_0^t D(s_1)\,ds_1}\left[\int_0^t e^{\int_0^{s_2} D(s_1)\,ds_1} C(s_2)\,ds_2 + R_{hH}(0)\right],$$

$$S_{hM}(t) = e^{-\int_0^t H(s_1)\,ds_1}\left[\int_0^t e^{\int_0^{s_2} H(s_1)\,ds_1} G(s_2)\,ds_2 + S_{hM}(0)\right],$$

$$R_{hM}(t) = e^{-\int_0^t D(s_1)\,ds_1}\left[\int_0^t e^{\int_0^{s_2} D(s_1)\,ds_1} L(s_2)\,ds_2 + R_{hM}(0)\right],$$

where $C(t) := \gamma_h I_{hH} + \eta R_{hM} > 0$, $D(t) := \eta + d_h + q$, $G(t) := \eta S_{hH} + qR_{hM} > 0$, and $H(t) := \eta + d_h + k$, and $L(t) := \gamma_h I_{hM} + \eta R_{hH} > 0$. This shows $S_{hH}(t), R_{hH}(t), S_{vH}(t), S_{hM}(t), R_{hM}(t) > 0, \forall\, t$. Hence the set Ω_o is positively invariant. Since Ω is positively invariant and $\partial\Omega_o$ is relatively closed in Ω_o, it gives $\partial\Omega_o$ is also positively invariant. Thus both Ω_o and $\partial\Omega_o$ are positively invariant under the flow induced by the system (11)–(18).

A.12 Proof of the Lemma 4.11

Since $P \in M_\partial$ then $\tau(t)P \in M_\partial$ for all $t \geq 0$ then $I_{vH}(t) = 0$ for all $t \geq 0$. Substituting $I_{vH}(t) = 0$ in (15), it follows that $I_{hH}(t) = 0$ for all $t \geq 0$. Again from (12), it follows that $I_{hM}(t) = 0$ for all $t \geq 0$. Now from (13) and (18),

$$\frac{dz}{dt} = \eta Z - \left(d_h + \eta + q\right) z, \quad \frac{dZ}{dt} = \eta z - \left(d_h + \eta + q\right) Z. \tag{A2}$$

Here, (A2) is a system of ordinary linear homogeneous differential equations with constant coefficients, which implies both $z(t), Z(t)$ tend to zero as t approaches to ∞. Also, from (11) and (16), it follows the system of linear non-homogeneous ordinary differential equations with constant coefficients

$$\frac{dx}{dt} = \Lambda + \eta X - (d_h + \eta)\, x, \quad \frac{dX}{dt} = \eta x - (d_h + \eta)\, X. \tag{A3}$$

implies that $x(t), X(t)$ converge to $\frac{\Lambda(d_h+\eta)}{d_h(d_h+2\eta)}$ and $\frac{\eta\Lambda}{2\eta d_h + d_h^2}$, respectively, as t approaches ∞. Also, $\lim_{t\to\infty} S_{vH}(t) = \frac{\phi}{d_v}$. Thus every forward orbit of $\tau(t)$ in M_∂ converges to E_{01}.

A.13 Proof of the Lemma 4.12

If possible suppose that there exists $P_o \in \Omega_o$, such that $\lim_{t\to\infty} \text{Sup}\, \|\tau(t)P_o - E_{01}\| < \rho$. Since $\lim_{t\to\infty} N_{hH}(t) \leq \frac{\Lambda}{d_h}, \lim_{t\to\infty} S_{hH}(t) = \frac{\Lambda(d_h+\eta)}{d_h(d_h+2\eta)}, \lim_{t\to\infty} S_{hM}(t) = \frac{\eta\Lambda}{2\eta d_h + d_h^2}$, and $\lim_{t\to\infty} S_{vH}(t) = \frac{\phi}{d_v}$, then there exists $t_2 > 0$ and a sufficiently small positive number ρ_o such that $N_{hH}(t) \leq \frac{\Lambda}{d_h} + \rho_o$,

$S_{hH}(t) \geq \frac{\Lambda(d_h+\eta)}{d_h(d_h+2\eta)} - \rho_o$, $S_{hM}(t) \geq \frac{\eta\Lambda}{2\eta d_h + d_h^2} - \rho_o$, and $S_{vH}(t) \geq \frac{\phi}{d_v} - \rho_o$. Here

$$\begin{aligned} kS_{hM} &= \frac{b'\alpha_{vh}I_{vA}S_{hM}}{N_{hA}} = \frac{b'\alpha_{vh}I_{vA}I_{hA}S_{hM}}{I_{hA}N_{hA}} \geq \frac{b'\alpha_{vh}I_{vA}I_{hA}S_{hM}}{M_1 N_{hA}}, \quad (|I_{hA}(t)| \leq M_1 \neq 0,\ \forall\, t) \\ &\approx k_1 I_{hA}S_{hM}, \quad \text{where } \frac{b'\alpha_{vh}I_{vA}}{N_{hA}M_1} \approx k_1, \text{Using Mean value theorem} \\ &\approx k_1 k_2 I_{hM}S_{hM} = k_3 I_{hM}S_{hM}, I_{hM}(t) \subset I_{hA}(t), \quad \forall\, t. \end{aligned}$$

Here $k = 0$ implies $k_1 \approx 0$ and hence $k_3 \approx 0$. Using these inequalities in Equations (12), (15), (17), it follows that

$$\begin{aligned} I'_{hH} &\geq \frac{\beta_h\left(\frac{\Lambda(d_h+\eta)}{d_h(d_h+2\eta)} - \rho_o\right)}{\frac{\Lambda}{d_h} + \rho_o} I_{vH} + \theta I_{hM} - (\theta + d_h + \delta_h + \gamma_h) I_{hH}, \\ I'_{vH} &\geq \frac{\beta_v\left(\frac{\phi}{d_v} - \rho_o\right)}{\left(\frac{\Lambda}{d_h} + \rho_o\right)} I_{hH} - d_v I_{vH}, \\ I'_{hM} &\geq k_3\left(\frac{\eta\Lambda}{2\eta d_h + d_h^2} - \rho_o\right) I_{hM} + \theta I_{hH} - (\theta + \delta_h + d_h + \gamma_h) I_{hM}, \quad \forall\, t \geq t_2. \end{aligned}$$

We now consider the following corresponding auxiliary equations

$$\begin{aligned} I'_{hH} &= \frac{\beta_h\left(\frac{\Lambda(d_h+\eta)}{d_h(d_h+2\eta)} - \rho_o\right)}{\frac{\Lambda}{d_h} + \rho_o} I_{vH} + \theta I_{hM} - (\theta + d_h + \delta_h + \gamma_h) I_{hH}, \\ I'_{vH} &= \frac{\beta_v\left(\frac{\phi}{d_v} - \rho_o\right)}{\left(\frac{\Lambda}{d_h} + \rho_o\right)} I_{hH} - d_v I_{vH}, \\ I'_{hM} &= k_3\left(\frac{\eta\Lambda}{2\eta d_h + d_h^2} - \rho_o\right) I_{hM} + \theta I_{hH} - (\theta + \delta_h + d_h + \gamma_h) I_{hM}, \quad \forall\, t \geq t_2. \end{aligned} \tag{A4}$$

Let $J_{1\rho_o}$ be the Jacobian matrix of the system (A4) at the disease-free equilibrium point E_{01}

$$J_{1\rho_o} = \begin{pmatrix} -(\theta + \delta_h + d_h + \gamma_h) & \frac{\beta_h\left(\frac{\Lambda(d_h+\eta)}{d_h(d_h+2\eta)} - \rho_o\right)}{\frac{\Lambda}{d_h} + \rho_o} & \theta \\ \frac{\beta_v\left(\frac{\phi}{d_v} - \rho_o\right)}{\left(\frac{\Lambda}{d_h} + \rho_o\right)} & -d_v & 0 \\ \theta & 0 & -(\theta + \delta_h + d_h + \gamma_h) \end{pmatrix}.$$

Since $R_1 > 1$ then from Lemma 4.9 $S(J_1) > 0$, then there exists a sufficiently small $\rho_o > 0$ such that $S(J_{1\rho_o}) > 0$. Here, $J_{1\rho_o}$ is irreducible and has non-negative off-diagonal elements, it follows that $S(J_{1\rho_o})$ is a simple and associates with strongly positive eigenvector $\tilde{v} \in \Re^3_+$ i.e.

$$(I_{hH}(t), I_{hM}(t), I_{vH}(t)) >> 0, \quad \forall\, t > t_2.$$

Then there is a positive number a such that $(I_{hH}(t), I_{hM}(t), I_{vH}(t)) \geq a\tilde{v}$.

Hence the solution of the system (A4) is

$$V(t) := ae^{S(J_{1\rho_o})(t-t_2)}\tilde{v}, \quad \forall\, t \geq t_2 \text{ with } V(t_2) := av.$$

It follows from [56, Theorem B.1] that

$$(I_{hH}(t), I_{hM}(t), I_{vH}(t)) \geq ae^{S(J_{1\rho_o})(t-t_2)}\tilde{v}, \quad \forall\, t \geq t_2.$$

Since $S(J_{1\rho_o}) > 0$, then the solution

$$\lim_{t\to\infty} I_{hH}(t) \to \infty, \quad \lim_{t\to\infty} I_{hM}(t) \to \infty, \quad \lim_{t\to\infty} I_{vH}(t) \to \infty.$$

This is a contradiction, and hence

$$\lim_{t\to\infty} \text{Sup } \|\tau(t)P - E_{01}\| \geq \rho, \quad \forall\, P \in \Omega_o.$$

A.14 Proof of the Theorem 4.14

The Jacobian matrix of (11)–(18) at E_{02} is $J_2 = \begin{pmatrix} A^2_{4\times4} & B^2_{4\times4} \\ C^2_{4\times4} & D^2_{4\times4} \end{pmatrix}$, where

$$A^2_{4\times4} = \begin{pmatrix} -a & 0 & q & 0 \\ 0 & -b & 0 & 0 \\ 0 & \gamma_h & -a & 0 \\ 0 & -\dfrac{K_1\phi\beta_v}{(P+Q_3)d_v} & 0 & -d_v \end{pmatrix}, \quad B^2_{4\times4} = \begin{pmatrix} -\dfrac{P\beta_h}{P+Q_3} & \eta & 0 & 0 \\ \dfrac{P\beta_h}{P+Q_3} & 0 & 0 & 0 \\ 0 & 0 & 0 & \eta \\ 0 & 0 & 0 & 0 \end{pmatrix},$$

$$C^2_{4\times4} = \begin{pmatrix} 0 & \dfrac{K_1\phi\beta_v}{(P+Q_3)d_v} & 0 & 0 \\ \eta & 0 & 0 & 0 \\ 0 & 0 & 0 & 0 \\ 0 & 0 & \eta & 0 \end{pmatrix}, \quad D^2_{4\times4} = \begin{pmatrix} -d_v & 0 & 0 & 0 \\ -d_h-\eta-k & 0 & q & \\ 0 & k & -b & 0 \\ 0 & 0 & \gamma_h & -a \end{pmatrix},$$

$a = d_h + \eta + q$ and $b = d_h + \gamma_h + \delta_h$. Let λ be eigenvalues of the matrix J_2, then the characteristic polynomial is,

$$P(\lambda) = (d_v + \lambda)Q(\lambda)R(\lambda),$$

where $Q(\lambda) = \lambda^2 + \lambda(d_h + d_v + \gamma_h + \delta_h) + (1 - R_2^2)d_v(d_h + \gamma_h + \delta_h)$, and $R(\lambda) = p_0\lambda^5 + p_1\lambda^4 + p_2\lambda^3 + p_3\lambda^2 + +p_4\lambda + p_5$. $\lambda = -d_v$ is one eigenvalue, and other eigenvalues are given by $Q(\lambda) = 0$ and $R(\lambda) = 0$. From $Q(\lambda) = 0$, the eigenvalues are

$$\lambda_2 = \frac{1}{2}\left(-\sqrt{(d_h + d_v + \gamma_h + \delta_h)^2 - 4\left(1 - R_2^2\right)d_v\,(d_h + \gamma_h + \delta_h)} - (d_h + d_v + \gamma_h + \delta_h)\right),$$

$$\lambda_3 = \frac{1}{2}\left(\sqrt{(d_h + d_v + \gamma_h + \delta_h)^2 - 4\left(1 - R_2^2\right)d_v\,(d_h + \gamma_h + \delta_h)} - (d_h + d_v + \gamma_h + \delta_h)\right).$$

Clearly, $\lambda_2 < 0$ and $\lambda_3 < 0$ if $R_2 < 1$. Furthermore, using Wolfram Mathematica, we showed $p_0, p_1, p_2, p_3, p_4, p_5$ are positive, $p_1p_2p_3 - p_3^2 - p_1^2p_4 > 0$, and $(p_1p_2p_3 - p_3^2 - p_1^2p_4)(p_1p_4 - p_5) > (p_1p_2 - p_3)^2p_5 + p_1p_5^2$ (see page 4–18 of Supplementary Material A). Then using the Routh Hurwitz theorem, we conclude that all the eigenvalues have negative real parts if $R_2 < 1$. Hence E_{02} is locally asymptotically stable if $R_2 < 1$ and unstable if $R_2 > 1$.

Nonlinear Anal. RWA 81 (2025) 104173

Contents lists available at ScienceDirect

Nonlinear Analysis: Real World Applications

journal homepage: www.elsevier.com/locate/nonrwa

Role of cross-border mobility on the backward bifurcation of malaria transmission model: Implications for malaria control in Nepal

Ramesh Gautam [a,h], Khagendra Adhikari [b,h], Anjana Pokharel [c,h], Kedar Nath Uprety [d,h], Naveen K. Vaidya [e,f,g,h,*]

[a] Ratna Rajya Laxmi Campus, Tribhuvan University, Kathmandu, Nepal
[b] Amrit Campus, Tribhuvan University, Kathmandu, Nepal
[c] Padma Kanya Multiple Campus, Tribhuvan University, Kathmandu, Nepal
[d] Central Department of Mathematics, Tribhuvan University, Kathmandu, Nepal
[e] Department of Mathematics and Statistics, San Diego State University, San Diego, CA, USA
[f] Computational Science Research Center, San Diego State University, San Diego, CA, USA
[g] Viral Information Institute, San Diego State University, San Diego, CA, USA
[h] Mathematical Biology Research Center, Kathmandu, Nepal

ARTICLE INFO

Keywords:
Backward bifurcation
Cross-border mobility
Global stability
Mathematical model
Malaria

ABSTRACT

The existence of backward bifurcation indicates an obstacle to disease eradication even when the basic reproduction number falls below unity. Bifurcation analysis allows us to identify causes for backward bifurcation, thereby helping to design a strategy to avoid such phenomena for disease eradication. In this study, we perform an in-depth bifurcation analysis of a malaria model incorporating cross-border mobility between two countries to explore mobility's role in backward bifurcation. Our analysis reveals that cross-border mobility can be a primary driving force for backward bifurcation in malaria dynamics. This novel result with cross-border mobility bringing backward bifurcation advances the traditional idea of disease-induced death being the primary driver of backward bifurcation. Using the malaria case in Nepal with cross-border mobility between Nepal–India, we validated analytical results by numerical simulations. Our model predicts that the disease-free equilibrium exists only if cross-border mobility or infection abroad are absent and malaria eradication is possible in Nepal. Otherwise, there is the coexistence of three endemic equilibria with a lower and higher stable epidemic level. Results on the bifurcation of our model may be helpful to control dynamics in order to maintain the malaria epidemic at a low level if it cannot be eradicated due to the entry of cases through cross-border mobility.

1. Introduction

Despite long-term efforts for global control and eradication, malaria is still one of the most prevalent vector-borne diseases worldwide and a major cause of illness and death in many developing countries [1–4]. Many low-malaria-endemic countries around the world are aiming to achieve malaria elimination. South-East Asian countries, such as Nepal, Bangladesh, Bhutan, Korea, India, Indonesia, Myanmar, Thailand, and Timor-Leste, have designed programs to eliminate malaria by 2030 [5]. However, most of these

* Corresponding author at: Department of Mathematics and Statistics, San Diego State University, San Diego, CA, USA.
E-mail address: nvaidya@sdsu.edu (N.K. Vaidya).

https://doi.org/10.1016/j.nonrwa.2024.104173
Received 8 September 2023; Received in revised form 22 June 2024; Accepted 26 June 2024
Available online 2 August 2024

countries, including Nepal, have faced a significant obstacle in achieving elimination goals primarily due to a higher percentage of imported malaria cases through cross-border mobility [6]. A meticulous analysis of the persistence of malaria is essential for a successful elimination plan. A bifurcation analysis of the malaria model serves as a valuable tool to identify ideal strategies for eliminating malaria from the country.

Mathematical models help describe infectious disease transmission and develop public health policies for control and prevention [7–10]. In disease dynamics, the basic reproduction number, R_0, has been widely considered a critical bifurcation parameter, providing conditions for disease persistence and elimination. If $R_0 < 1$, there is a disease-free equilibrium that is locally asymptotically stable, and the infection dies out. If $R_0 > 1$, there is a locally asymptotically stable endemic equilibrium, and infection persists. More precisely, as R_0 increases through 1, the endemic equilibrium appears, and there is an exchange of stability between the disease-free and endemic equilibrium, referred to as the forward bifurcation [11].

However, in some vector-borne disease models like malaria, even if $R_0 < 1$ disease may be endemic in the population; this phenomenon is known as backward bifurcation [11]. In this case, the classical requirement of the reproduction number being less than unity becomes only necessary but not sufficient for disease elimination [12,13]. Thus, in the case of vector-borne disease, the new threshold $R_0^* < 1$, often referred to as the transmission threshold, may be required to assert disease elimination. In such dynamics with a backward bifurcation, a bistability situation occurs when R_0 lies in the interval $\left(R_0^*, 1\right)$, where the system converges into either disease-free or endemic equilibrium, depending on initial conditions. The initial condition corresponding to the threshold for bistability, the breakpoint density, provides a prevalence level for malaria elimination when $R_0^* < R_0 < 1$. Thus, the backward bifurcation analysis is essential for adequately designing malaria control and elimination programs.

Several existing models of vector-borne diseases have possessed backward bifurcation, primarily due to disease-induced death [14–23]. Some other studies have also shown the possibility of backward bifurcation due to the impact of quarantine [24], income inequality among the susceptible human population [25], and vector biases [15] (biting preference of vector to infectious humans).

Since migration is one of the main obstacles to malaria elimination in many countries [26,27], a question naturally arises whether cross-border mobility has a role in backward bifurcation. Thus, studying the effects of cross-border mobility on backward bifurcation is crucial. While some studies [26–33] have considered the effects of host movement on vector-borne disease, we are unaware of any studies that address the backward bifurcation issue of the malaria model with cross-border mobility. In Gautam et al. [7], we developed a malaria model with cross-border mobility and performed basic stability analysis and simulations with malaria cases in Nepal. However, the previous study [7] lacks an analysis of a critical issue of backward bifurcation associated with different modes of cross-border mobility; the analysis of backward bifurcation can offer an essential condition for eradicating malaria.

In this study, we broaden the previous model by considering various cross-border mobilities and examine whether cross-border mobility can bring backward bifurcation, causing obstacles to malaria elimination even when the basic reproduction number is below unity. The novelty of our results constitutes the establishment of mobility conditions that can solely cause backward bifurcation, underscoring the need to consider cross-border mobility in devising malaria elimination strategies. We further extend our mobility-driven backward bifurcation techniques to the case where eradication is impossible due to cross-border mobility; in this case, our analysis allows us to identify mobility-related control strategies to maintain malaria endemic in a low burden level.

2. Model formulation and basic analysis

2.1. Malaria transmission model with cross-border mobility

To model malaria transmission with cross-border mobility, we consider the malaria-endemic country with a higher malaria burden as an abroad, where migrants from the home country live as workers. The home country is assumed to have a low malaria burden but is struggling to achieve the elimination goal. Both humans living in their home country (N_{hH}) and migrant workers living abroad (N_{hM}) are divided into susceptible (S_{hH}, S_{hM}), infectious (I_{hH}, I_{hM}), and recovered (R_{hH}, R_{hM}) groups. The mosquito population in the home country (N_{vH}) is divided into susceptible (S_{vH}) and infectious (I_{vH}) groups.

In the model, b, b' represent the per-capita mosquito biting rates, $\alpha_{vh}, \alpha'_{vh}$ represent the probabilities of malaria transmission from infectious mosquito to susceptible human in a single bite, and $\alpha_{hv}, \alpha'_{hv}$ represent the probabilities of malaria transmission from infectious human to susceptible mosquito in a single bite at home and abroad, respectively. q is the per-capita immunity loss rate of humans, and γ_h is the per-capita recovery rate of humans. Λ, ϕ are the recruitment rates of humans and mosquitoes, and d_h, δ_h, and d_v are the per-capita natural death rate, the disease-induced death rate of humans, and the natural death rate of mosquitoes, respectively. The per-capita cross-border mobility rate for susceptible and recovered individuals is assumed to be η. For the infected individuals, the cross-border mobility is altered by a factor $\omega \geq 0$, making the mobility rate for infected individuals $\omega\eta$.

Due to the complexity of tracking specific incidents abroad, we note that the incidence rate for migrants abroad $\frac{b'\alpha'_{vh}I_{vA}}{N_{hA}}$, where I_{vA} and N_{hA} are the total infectious mosquitoes and the total humans abroad, respectively, is approximated as follows [7]: $\frac{b'\alpha'_{vh}I_{vA}}{N_{hA}} \approx \frac{b'\alpha'_{vh}}{T}\int_0^T \frac{I_{vA}(t)}{N_{hA}(t)}dt \approx b'\alpha'_{vh}\frac{I_{vA}(t_0)}{N_{hA}(t_0)} = k$ for some $t_0 \in (0,T)$, and T is the final time of the dynamics (the mean value theorem of integral calculus [34]).

The schematic diagram of the model is shown in Fig. 1. The model system we consider is as follows:

$$S'_{hH} = \Lambda + \eta S_{hM} + qR_{hH} - \frac{b\alpha_{vh}I_{vH}}{N_{hH}}S_{hH} - (\eta + d_h)S_{hH}, \tag{1}$$

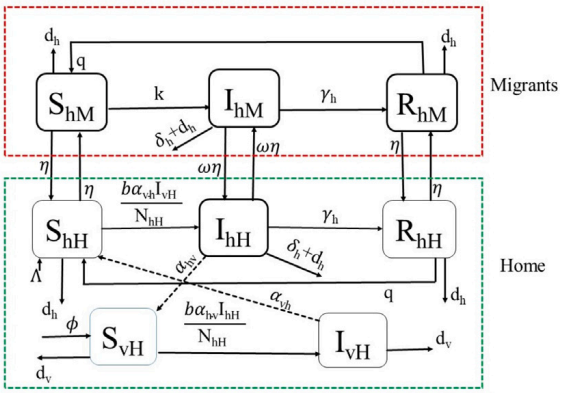

Fig. 1. Malaria transmission model with cross-border mobility. The upper SIRS model (within the red dashed box) captures the dynamics among migrant workers abroad, while the lower SI-SIRS model (within the green dashed box) represents the situation in the home country. The solid arrows indicate the movement of populations, while the dotted arrows illustrate the interactions between humans and mosquitoes. Subscripts H and M represent home and migrant, respectively, while subscripts h and v denote human and vector (mosquito), respectively. (For interpretation of the references to color in this figure legend, the reader is referred to the web version of this article.)

$$I'_{hH} = \frac{b\alpha_{vh} I_{vH}}{N_{hH}} S_{hH} + \omega\eta I_{hM} - (\omega\eta + d_h + \delta_h + \gamma_h) I_{hH}, \tag{2}$$

$$R'_{hH} = \gamma_h I_{hH} + \eta R_{hM} - (\eta + d_h + q) R_{hH}, \tag{3}$$

$$S'_{vH} = \phi - \frac{b\alpha_{hv} I_{hH}}{N_{hH}} S_{vH} - d_v S_{vH}, \tag{4}$$

$$I'_{vH} = \frac{b\alpha_{hv} I_{hH}}{N_{hH}} S_{vH} - d_v I_{vH}, \tag{5}$$

$$S'_{hM} = \eta S_{hH} + q R_{hM} - k S_{hM} - (d_h + \eta) S_{hM}, \tag{6}$$

$$I'_{hM} = k S_{hM} + \omega\eta I_{hH} - (\omega\eta + \delta_h + d_h + \gamma_h) I_{hM}, \tag{7}$$

$$R'_{hM} = \gamma_h I_{hM} + \eta R_{hH} - (\eta + d_h + q) R_{hM}. \tag{8}$$

For the simulations, we took the values of parameters given in Table 1, many of which were estimated from the model fitting to the malaria data of Nepal [7].

2.2. Basic properties of the model

For the system (1)–(8) to be biologically and epidemiologically meaningful, it is essential to demonstrate that all solutions with initially non-negative values always remain non-negative and bounded. For our model system (1)–(8), we can mathematically show that it is sufficient to assume non-negative initial conditions for all state variables to assert non-negative solutions. However, in reality, some humans and mosquitoes are expected to survive in the community. Therefore, to capture this reality, we present proof of positivity and boundedness of solutions with positive initial conditions for S_{hH} and S_{hM}.

Theorem 2.1 (*Positivity and Boundedness of Solutions*). *If* $S_{hH}(0) > 0,\ I_{hH}(0) \geq 0,\ R_{hH}(0) \geq 0,\ S_{vH}(0) > 0,\ I_{vH}(0) \geq 0,\ S_{hM}(0) > 0,\ I_{hM}(0) \geq 0,\ R_{hM}(0) \geq 0$*, then the solution*

$$\left(S_{hH},\ I_{hH},\ R_{hH},\ S_{vH},\ I_{vH},\ S_{hM},\ I_{hM},\ R_{hM}\right)$$

of the system (1)–(8) is always positive for all $t \geq 0$ *and eventually bounded.*

Proof. See Section 2 of Supplementary file. □

2.3. Equilibria condition

Equilibrium points represent steady states of the system, where disease prevalence remains constant over time. These points are applicable to identifying the conditions under which disease persists or is eliminated. The equilibria $\left(S^*_{hH},\ I^*_{hH},\ R^*_{hH},\ S^*_{vH},\ I^*_{vH},\ S^*_{hM},\ I^*_{hM},\ R^*_{hM}\right)$ of the system (1)–(8) can be expressed as

$$S^*_{hH} = \frac{P}{K_1 + K_2\,\lambda^*_h},\ I^*_{hH} = \frac{Q_1 + Q_2\lambda^*_h}{K_1 + K_2\,\lambda^*_h},\ R^*_{hH} = \frac{Q_3 + Q_4\lambda^*_h}{K_1 + K_2\,\lambda^*_h},$$

Table 1
Model parameters estimated from the malaria case data in Nepal.

Description	Parameters	Base value and unit	Reference
Probability of malaria transmission from an infectious mosquito to a susceptible human (per bite)	α_{vh}	0.0195	[35,36]
Probability of malaria transmission from an infectious human to a susceptible mosquito (per bite)	α_{hv}	0.63	[36–38]
Humans recruitment rate	Λ	287,460 yr^{-1}	[7]
Per capita recovery rate of humans	γ_h	1.85 yr^{-1}	[35,36]
Per capita natural birth and death rate of mosquitoes	d_v	27.9113 yr^{-1}	[35,36]
Per capita disease induced death rate of humans	δ_h	0.00171 yr^{-1}	[7]
Per capita natural death rate of humans	d_h	0.0149 yr^{-1}	[7]
Per capita mobility rate of healthy humans	η	0.04 yr^{-1}	Assumed
Mobility factor of infected humans	ω	25	Assumed
Per capita mobility rate of infectious humans	$\omega\eta$	1 yr^{-1}	Assumed
Per capita rate of Immunity loss of humans	q	4 yr^{-1}	[39]
Incidence rate in abroad	k	0.000105 yr^{-1}	[7]
Per capita biting rate of mosquitoes	b	43.75 yr^{-1}	[7]

$$
\begin{aligned}
&S^*_{hM} = \frac{S_1 + S_2\lambda^*_h}{K_1 + K_2\ \lambda^*_h},\ I^*_{hM} = \frac{T_1 + T_2\lambda^*_h}{K_1 + K_2\ \lambda^*_h},\ R^*_{hM} = \frac{U_1 + U_2\lambda^*_h}{K_1 + K_2\ \lambda^*_h},\\
&I^*_{vH} = \frac{\phi\beta_v(Q_1 + Q_2\lambda^*_h)}{d_v\left(\beta_v Q_1 + d_v P + Q_1 d_v + Q_3 d_v + (Q_2 d_v + Q_4 d_v + \beta_v Q_2)\lambda^*_h\right)},\\
&S^*_{vH} = \frac{\phi - I^*_{vH} d_v}{d_v},
\end{aligned}
\tag{9}
$$

where $\lambda^*_h = \beta_h \frac{I^*_{vH}}{N^*_{hH}}$, $\beta_h = b\alpha_{vh}$, $\beta_v = b\alpha_{hv}$, and P, K_1, K_2, Q_1, Q_2, Q_3, Q_4, S_1, S_2, T_1, T_2, U_1, and U_2 are non-negative (see Section 4 of Supplementary file). With some algebraic manipulation, the equilibria condition of the system (1)–(8) reduces to

$$
a_3\lambda^{*3}_h + a_2\lambda^{*2}_h + a_1\lambda^*_h + a_0 = 0, \tag{10}
$$

where,

$$
\begin{aligned}
&a_3 = Q_2Q_4d_v\beta_v + 2Q_2Q_4d_v^2 + Q_2^2d_v\beta_v + Q_2^2d_v^2 + Q_4^2d_v^2 > 0,\\
&a_2 = (p_1 - p_2\beta_h\beta_v),\\
&a_1 = (p_3 - p_4\beta_h\beta_v),\\
&a_0 = -K_1\eta^2\omega k\Lambda\left(d_h + q\right)\left(d_h + 2\eta + q\right)\phi\beta_h\beta_v < 0 \text{ and } p_1,\ p_2,\ p_3,\ p_4
\end{aligned}
$$

are non negative (see Section 5 of Supplementary file).

3. Model analysis

Using the model (1)–(8), we focus on the role of cross-border mobility in the bifurcations corresponding to the elimination or persistence of malaria. To explore this, we analyze two cases in detail: (I) $\eta = 0$ (absence of cross-border mobility); (II) $\eta \neq 0$ (presence of cross-border mobility).

3.1. Case-I: $\eta = 0$ (absence of cross-border mobility)

3.1.1. Equilibria

Since $\eta = 0$, we get a_0, Q_1, Q_3, S_1, T_1, and U_1 to be zero. Then, the disease-free equilibrium of the system (1)–(8) from Eq. (9) is

$$E^0 = \left(S^0_{hH},\ I^0_{hH},\ R^0_{hH},\ S^0_{vH},\ I^0_{vH},\ S^0_{hM},\ I^0_{hM},\ R^0_{hM}\right) = \left(\frac{\Lambda}{d_h},\ 0,\ 0,\ \frac{\phi}{d_v},\ 0,\ 0,\ 0,\ 0\right).$$

The basic reproduction number, derived using the next generation matrix method [40], is $R_0 = \sqrt{\dfrac{\phi d_h \beta_h \beta_v}{\Lambda(d_h+\delta_h+\gamma_h)d_v^2}}$. In this case, Eq. (10) gives

$$a_3 \lambda_h^{*2} + a_2 \lambda_h^* + a_1 = 0, \tag{11}$$

where, a_3, a_2, and a_1 are simplified to

$$\begin{aligned}
a_3 &= b_0 \Lambda d_v \left(d_h+\gamma_h+q\right)\left(\beta_v\left(d_h+q\right)+d_v\left(d_h+\gamma_h+q\right)\right) > 0,\\
a_2 &= \frac{b_0}{dh}\Lambda\left(G_0 - R_0^2\right) d_v^2 \left(d_h+q\right)\left(d_h+\gamma_h+\delta_h\right)\left(d_h\left(\gamma_h+\delta_h+q\right)+d_h^2+q\delta_h\right),\\
a_1 &= \Lambda\left(1-R_0^2\right) b_0\, d_v^2 \left(d_h+q\right)^2\left(d_h+\gamma_h+\delta_h\right)^2,\\
b_0 &= \left(d_h^2\left(\gamma_h+\delta_h+k+q\right)+d_h\left(\gamma_h(k+q)+\delta_h(k+q)+kq\right)+d_h^3+kq\delta_h\right)^2,
\end{aligned}$$

where $G_0 = \dfrac{d_h\left(\beta_v\left(d_h+q\right)+2d_v\left(d_h+\gamma_h+q\right)\right)}{d_v\left(d_h\left(\gamma_h+\delta_h+q\right)+d_h^2+q\delta_h\right)}$. Here $R_0 < 1$ if and only if $a_1 > 0$ and $R_0 < \sqrt{G_0}$ if and only if $a_2 > 0$. Let $\Delta(R_0) = a_2^2 - 4a_1a_3$. Then we have $\Delta(\sqrt{G_0}) = -4a_1a_3 < 0$ when $G_0 < 1$, and $\Delta(1) = a_2^2 > 0$. When $R_0 < 1$, by the intermediate value theorem for continuous function, there exists a unique $R_0^* \in \left(\sqrt{G_0}, 1\right)$ such that $\Delta(R_0^*) = 0$. Therefore, R_0^* is the value of $R_0 < 1$ such that the discriminant of the Eq. (11) is zero. Also, for $R_0 < 1$, $\Delta(R_0) > 0$ if and only if $R_0 > R_0^*$, and $\Delta(R_0) < 0$ if and only if $R_0 < R_0^*$ [14,17]. Now using $\Delta(R_0^*) = 0$, we obtain $R_0^* = \dfrac{\sqrt{B^2G - 2A + 2\sqrt{M^2 + B^2A(1-G0)}}}{B}$, where

$$\begin{aligned}
A &= d_h^2\left(d_h+q\right)^2\left(d_h+\gamma_h+\delta_h\right)^2\left(d_h+\gamma_h+q\right)\left(\beta_v\left(d_h+q\right)+d_v\left(d_h+\gamma_h+q\right)\right),\\
B^2 &= d_v\left(d_h+q\right)^2\left(d_h+\gamma_h+\delta_h\right)^2\left(d_h\left(\gamma_h+\delta_h+q\right)+d_h^2+q\delta_h\right)^2,\\
M &= d_h^2\left(d_h+q\right)^2\left(d_h+\gamma_h+\delta_h\right)^2\left(d_h+\gamma_h+q\right)\left(\beta_v\left(d_h+q\right)+d_v\left(d_h+\gamma_h+q\right)\right).
\end{aligned}$$

In Theorem 3.1, we present the general results about the existence of endemic equilibria.

Theorem 3.1. *Assume that $\eta = 0$ in (1)–(8), then the following statements hold.*

(i) For $R_0 > 1$, the system has unique endemic equilibrium;
(ii) For $R_0 = 1$, the system has unique endemic equilibrium when $a_2 < 0$ and no endemic equilibrium when $a_2 \geq 0$;
(iii) For $R_0^* < R_0 < 1$, the system has two distinct (upper and lower) endemic equilibria when $a_2 < 0$ and no endemic equilibrium when $a_2 \geq 0$;
(iv) For $R_0 = R_0^*$, the system has unique (coincident) endemic equilibria when $a_2 < 0$ and no endemic equilibrium when $a_2 \geq 0$;
(v) For $R_0 < R_0^*$, the system has no endemic equilibrium.

Proof. See Section 6 of Supplementary file. □

3.1.2. Bifurcation analysis

In this section, we discussed the local behavior of the disease-free and endemic equilibria using the Routh–Hurwitz Theorem and Castillo-Chavez and Song Theorem [41]. For the global stability of the disease-free equilibrium, we use the Krasovskii–LaSalle invariance Theorem [41].

Theorem 3.2 (*Local Stability of E^0*)**.** *Assume that $\eta = 0$, then the disease free equilibrium point E^0 of the system (1)–(8) is locally asymptotically stable if $R_0 < 1$, and unstable if $R_0 > 1$.*

Proof. See Section 7 of Supplementary file. □

Theorem 3.3 (*Forward and Backward Bifurcations*)**.** *Assume that $\eta = 0$, then the model possesses the forward bifurcation at $R_0 = 1$ when $0 \leq \delta_h \leq \delta_h^*$ and the backward bifurcation at $R_0 = 1$ when $\delta_h > \delta_h^*$, where*

$$\delta_h^* = \frac{d_h\left(d_h\beta_v + d_v\gamma_h + d_hd_v + qd_v + q\beta_v\right)}{d_v\left(d_h+q\right)}.$$

Proof. We apply the theorem by Castillo Chavez and Song [41] to derive the condition for forward and backward bifurcations. The system (1)–(8) of the model can be written as:

$$\frac{d\vec{x}}{dt} = \vec{f}(\vec{x}, \beta_h),\ \vec{f} : R^8 \times R \to R^8, \vec{f} \in C^2(R^8 \times R), \tag{12}$$

where $\vec{x} = \left(S_{hH},\ I_{hH},\ R_{hH},\ S_{vH},\ I_{vH},\ S_{hM},\ I_{hM},\ R_{hM}\right)$,

$\vec{f} = \left(f_1,\ f_2,\ f_3,\ f_4,\ f_5,\ f_6,\ f_7,\ f_8\right)$, and $\beta_h^* = \dfrac{\Lambda d_v^2\left(d_h+\gamma_h+\delta_h\right)}{\phi d_h \beta_v}$ corresponds to $R_0 = 1$ considered as one of the potential bifurcation parameters. Then, the Jacobian of the system at the bifurcation point $(E^0;\ \beta_h^*)$ is

$$J_0 = \begin{pmatrix} P_{5\times5} & 0_{5\times3} \\ 0_{3\times5} & Q_{3\times3} \end{pmatrix},$$

where

$$P = \begin{pmatrix} -d_h & 0 & q & 0 & -\dfrac{\Lambda d_v^2\left(d_h+\gamma_h+\delta_h\right)}{\phi d_h \beta_v} \\ 0 & -(d_h+\gamma_h+\delta_h) & 0 & 0 & \dfrac{\Lambda d_v^2\left(d_h+\gamma_h+\delta_h\right)}{\phi d_h \beta_v} \\ 0 & \gamma_h & -(d_h+q) & 0 & 0 \\ 0 & -\dfrac{\phi d_h \beta_v}{\Lambda d_v} & 0 & -d_v & 0 \\ 0 & \dfrac{\phi d_h \beta_v}{\Lambda d_v} & 0 & 0 & -d_v \end{pmatrix}$$

and

$$Q = \begin{pmatrix} -(d_h+k) & 0 & q \\ k & -(d_h+\gamma_h+\delta_h) & 0 \\ 0 & \gamma_h & -(d_h+q) \end{pmatrix}.$$

Five eigenvalues of the Jacobian J_0 are

$$\lambda = 0, -d_h, -d_v, -(d_h+q), -\left(d_h+d_v+\gamma_h+\delta_h\right),$$

and the rest three eigenvalues are given by the following characteristic polynomial equation of degree three.

$$\lambda^3 + M_2\lambda^2 + M_1\lambda + M_0 = 0, \tag{13}$$

where, $M_2 = 3d_h+\gamma_h+\delta_h+k+q$, $M_1 = 2d_h\gamma_h + 2d_h\delta_h + 2kd_h + 2qd_h + 3d_h^2 + k\gamma_h + k\delta_h + q\gamma_h + q\delta_h + kq$, $M_0 = d_h^2\gamma_h + d_h^2\delta_h + kd_h\gamma_h + kd_h\delta_h + kqd_h + kd_h^2 + qd_h\gamma_h + qd_h\delta_h + qd_h^2 + d_h^3 + kq\delta_h$. Here, $M_0,\ M_1,\ M_2,\ M_3$ all are positive and

$$\begin{aligned} M_1M_2 - M_0 =\ & 8d_h^2\left(\gamma_h+\delta_h+k+q\right) + 8d_h^3 + \gamma_h\left(2\delta_h(k+q) + k^2 + 3kq + q^2\right) \\ & + \gamma_h^2(k+q) + (k+q)\left(\delta_h+k\right)\left(\delta_h+q\right) + \\ & 2d_h\left(\gamma_h^2+\delta_h^2+\gamma_h\left(2\delta_h+3(k+q)\right) + 3\delta_h(k+q) + k^2 + 3kq + q^2\right) > 0. \end{aligned}$$

Thus, J_0 has one eigenvalue of zero, four negative, and the remaining three have negative real parts. Let $\vec{v} = \left(v_1,\ v_2,\ v_3,\ v_4,\ v_5,\ v_6,\ v_7,\ v_8\right)$ and $\vec{u} = \left(u_1,\ u_2,\ u_3,\ u_4,\ u_5,\ u_6,\ u_7,\ u_8\right)^T$ are the left and right eigenvectors of the zero eigenvalue of J_0, respectively. Solving the matrix equations $\vec{v}J_0 = 0$ and $J_0\vec{u} = 0$, we obtain the components of the eigenvectors $\vec{v}$ and $\vec{u}$ as $v_1 = v_3 = v_4 = 0$, $v_5 = \dfrac{\Lambda v_2 d_v\left(d_h+\gamma_h+\delta_h\right)}{\phi d_h \beta_v}$, $v_6 = v_7 = v_8 = 0$, $u_1 = -u_2\left(\dfrac{d_h+\gamma_h+\delta_h}{d_h} - \dfrac{q\gamma_h}{d_h\left(d_h+q\right)}\right)$, $u_3 = \dfrac{u_2\gamma_h}{d_h+q}$, $u_4 = -\dfrac{u_2\phi d_h\beta_v}{\Lambda d_v^2}$, $u_5 = \dfrac{u_2\phi d_h\beta_v}{\Lambda d_v^2}$, $u_6 = u_7 = u_8 = 0$, with v_2 and u_2 being free. The parameters a and b are obtained from the equation

$$a = \sum_{m,i,j=1}^{8} v_m u_i u_j \frac{\partial^2 f_m}{\partial x_i \partial x_j}(E_0),\ b = \sum_{m,i=1}^{8} v_m u_i \frac{\partial^2 f_m}{\partial x_i \partial \beta_h}(E_0), \tag{14}$$

where f_m be the mth component of $\vec{f}$. To compute the parameter b, we use Eq. (14) with $v_m = 0$ for $m = 1,\ 3,\ 4,\ 6,\ 7,\ 8$. Taking partial derivatives of f_2 and f_5 with respect to β_h, we get $\dfrac{\partial(f_2)}{\partial\beta_h} = \dfrac{x_1x_5}{x_1+x_2+x_3}$, $\dfrac{\partial(f_5)}{\partial\beta_h} = 0$, where, $f_2 = \beta_h\dfrac{x_1x_5}{x_1+x_2+x_3} - \left(d_h+\gamma_h+\delta_h\right)x_2$, $f_5 = \beta_v\dfrac{x_4x_2}{x_1+x_2+x_3} - x_5d_v$. Using $\vec{v}.\vec{u} = 1$, i.e., $v_2u_2 = \dfrac{d_v}{d_h+\gamma_h+\delta_h}$. Then, $b = \sum_{m,i=1}^{8} v_m u_i \dfrac{\partial^2 f_m}{\partial x_i\partial\beta_h}(E_0) = \sum_{i=1}^{8} v_2u_i\dfrac{\partial^2 f_2}{\partial x_i\partial\beta_h}(E_0) = \sum_{i=1}^{8} v_2u_i\dfrac{\partial}{\partial x_i}\left(\dfrac{x_1x_5}{x_1+x_2+x_3}\right)(E_0) = v_2u_5$
$= \dfrac{\phi d_h\beta_v}{(d_h+\gamma_h+\delta_h)\Lambda d_v} > 0$. Similarly, using Eq. (14),

$$a = v_2\left(u_1u_1\frac{\partial^2 f_2}{\partial x_1^2} + 2u_1u_2\frac{\partial^2 f_2}{\partial x_1\partial x_2} + 2u_1u_3\frac{\partial^2 f_2}{\partial x_1\partial x_3} + 2u_2u_3\frac{\partial^2 f_2}{\partial x_2\partial x_3} + u_2u_2\frac{\partial^2 f_2}{\partial x_2^2}\right) +$$

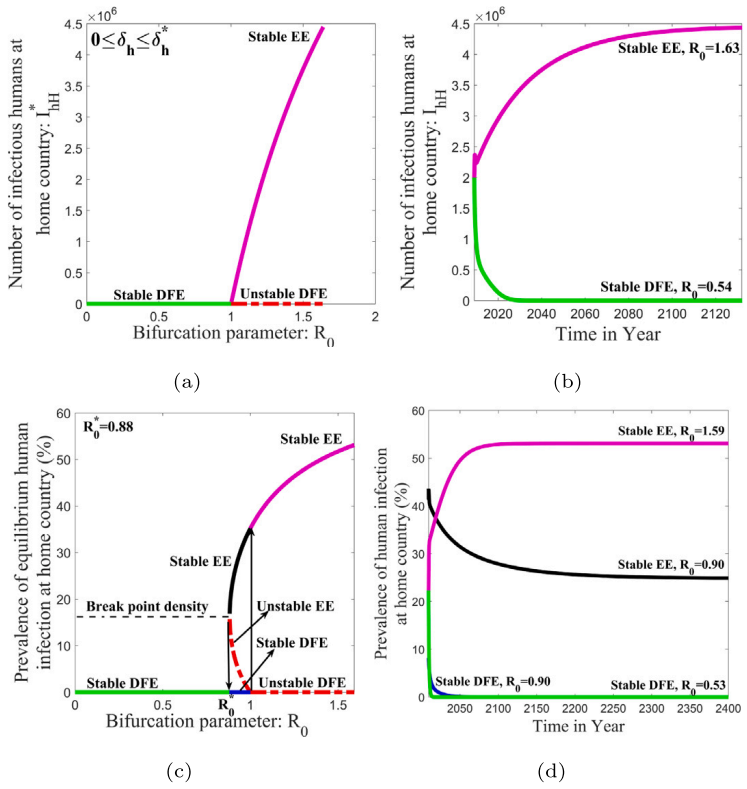

Fig. 2. Bifurcation diagrams and model solutions. (a) Forward bifurcation at $R_0 = 1$ when δ_h lies in $0 \le \delta_h \le \delta_h^*$ ($\delta_h^* = 0.029$). (b) Model solutions verifying (a), where model solution converges to the unique stable endemic equilibrium when $R_0 = 1.63$ ($R_0 > 1$) (end of the magenta curve) and converges to the stable disease-free equilibrium when $R_0 = 0.54$ ($R_0 < 1$) (end of the green curve), regardless of the initial conditions. (c) Backward bifurcation for $\delta_h = 0.11$ with $R_0^* = 0.88$. (d) Model solutions verifying (c), where model solution converge to the unique stable endemic equilibrium when $R_0 = 1.59$ ($R_0 > 1$) (end of the magenta curve) and for $R_0 = 0.53$ ($R_0 < R_0^* < 1$), model solution converges to the stable disease-free equilibrium (end of the green curve), regardless of the initial conditions. However, for $R_0 = 0.90$ ($R_0^* < R_0 < 1$), the model solution converge to the higher level endemic equilibrium (end of the black curve) when the initial prevalence is above the breakpoint density (horizontal dashed line), and the model solution converges to the disease-free equilibrium (end of the blue curve) when the initial prevalence is below the breakpoint density. (For interpretation of the references to color in this figure legend, the reader is referred to the web version of this article.)

$$
\begin{aligned}
&v_2\left(u_3u_3\frac{\partial^2 f_2}{\partial x_3^2}+2u_1u_5\frac{\partial^2 f_2}{\partial x_1\partial x_5}+2u_2u_5\frac{\partial^2 f_2}{\partial x_2\partial x_5}+2u_3u_5\frac{\partial^2 f_2}{\partial x_3\partial x_5}\right)+\\
&v_5\left(u_1u_1\frac{\partial^2 f_5}{\partial x_1^2}+2u_1u_2\frac{\partial^2 f_5}{\partial x_1\partial x_2}+2u_1u_3\frac{\partial^2 f_5}{\partial x_1\partial x_3}+2u_2u_3\frac{\partial^2 f_5}{\partial x_2\partial x_3}\right)+\\
&v_5\left(u_2u_2\frac{\partial^2 f_5}{\partial x_2^2}+u_3u_3\frac{\partial^2 f_5}{\partial x_3^2}+2u_1u_4\frac{\partial^2 f_5}{\partial x_1\partial x_4}+2u_2u_4\frac{\partial^2 f_5}{\partial x_2\partial x_4}+2u_4u_3\frac{\partial^2 f_5}{\partial x_4\partial x_3}\right).
\end{aligned}
\tag{15}
$$

After simplification, we get $a = \dfrac{2d_v\delta_h}{\Lambda} - \dfrac{2d_h\left(\beta_v\left(d_h+q\right)+d_v\left(d_h+\gamma_h+q\right)\right)}{\Lambda\left(d_h+q\right)}$. Here $a > 0$ if $\delta_h > \dfrac{d_h\left(d_h\beta_v+d_v\gamma_h+d_hd_v+qd_v+q\beta_v\right)}{d_v\left(d_h+q\right)} = \delta_h^*$. Thus the model possesses the backward bifurcation at $R_0 = 1$ when $\delta_h > \delta_h^*$ and forward bifurcation at $R_0 = 1$ when $0 \le \delta_h \le \delta_h^*$.

From the above result, in the absence of cross-border mobility of migrants between the home country and abroad ($\eta = 0$), if $0 \le \delta_h \le \delta_h^*$, malaria gets eliminated when $R_0 < 1$. However, if $\delta_h > \delta_h^*$, elimination is possible only when $R_0 < R_0^* < 1$. We also validated the above analytic results with the numerical solutions of the system (1)–(8) (Fig. 2).

3.1.3. Global stability and uniform persistence

Here we apply the Krasovskii–LaSalle Theorem [41] to establish the condition for the global stability of the disease-free equilibrium in the home country.

Theorem 3.4 (*Global Stability of E^0*). *For $\eta = 0$, the disease-free equilibrium E^0 of the system (1)–(5) is globally asymptotically stable when* $R_0^2 + \dfrac{\delta_h\phi\beta_h\beta_v}{\Lambda(d_h+\delta_h+\gamma_h)d_v^2} < 1$.

Proof. Let $p = \left(S_{hH}(t), I_{hH}(t), R_{hH}(t), S_{vH}(t), I_{vH}(t)\right)$, be any solution of the system (1)–(5), then $N_{vH}(t) \leq \frac{\phi}{d_v}$ and $N'_{hH} = \Lambda - d_h N_{hH} - \delta_h I_{hH} \geq \Lambda - (d_h + \delta_h) N_{hH}$. Then, $N_{hH}(t) \geq \frac{\Lambda}{d_h + \delta_h}$. We construct a Lyapunov function, $V\left(I_{hH}, I_{vH}\right) = \frac{d_v}{\beta_h} I_{hH} + I_{vH}$. Then, taking derivative with respect to t, we obtain

$$\begin{aligned}
V' &= \frac{d_v}{\beta_h} I'_{hH} + I'_{vH} \\
&= \frac{d_v I_{vH} S_{hH}}{N_{hH}} - \frac{d_v}{\beta_h}(d_h + \delta_h + \gamma_h) I_{hH} + \frac{\beta_v I_{hH} S_{vH}}{N_{hH}} - d_v I_{vH} \\
&= \left[\frac{\beta_v S_{vH}}{N_{hH}} - \frac{d_v}{\beta_h}(d_h + \delta_h + \gamma_h)\right] I_{hH} - \left[-\frac{d_v S_{hH}}{N_{hH}} + d_v\right] I_{vH} \\
&\leq \left[\frac{\beta_v \frac{\phi}{d_v}}{\frac{\Lambda}{d_h + \delta_h}} - \frac{d_v}{\beta_h}(d_h + \delta_h + \gamma_h)\right] I_{hH} \text{ (Since } S_{hH}(t) \leq N_{hH}(t)) \\
&= \left[R_0^2 + \frac{\delta_h \phi \beta_h \beta_v}{\Lambda(d_h + \delta_h + \gamma_h) d_v^2} - 1\right] I_{hH}.
\end{aligned}$$

This gives $V' \leq \left[\left(R_0^2 + \frac{\delta_h \phi \beta_h \beta_v}{\Lambda(d_h + \delta_h + \gamma_h) d_v^2} - 1\right)\right] I_{hH}$. Therefore, $V' \leq 0$ for all $p \geq 0$ when $R_0^2 + \frac{\delta_h \phi \beta_h \beta_v}{\Lambda(d_h + \delta_h + \gamma_h) d_v^2} < 1$.

Let $B = \{p : V' = 0\}$, then $B \subset \{p : I_{hH} = 0\}$. If $C \subset B$ is the largest invariant set of the system (1)–(5) and p is any solution of the system in C, then for all $t \in R$, p is defined and bounded. Again $C \subseteq \{p : I_{hH} = 0\}$, thus $I_{hH}(t) \equiv 0$. Moreover, from Eq. (3), $R_{hH} \equiv 0$. Also, from Eq. (5), $I_{vH} \equiv 0$ and finally, Eq. (1) gives $S_{hH} \equiv \frac{\Lambda}{d_h}$ and Eq. (4) gives $S_{vH} \equiv \frac{\phi}{d_v}$. Therefore, $p = (\frac{\Lambda}{d_h}, 0, 0, \frac{\phi}{d_v}, 0)$ and $C \equiv \{E^0\}$. Applying the Krasovskii–LaSalle theorem [41], the disease-free equilibrium E^0 is globally asymptotically stable and the disease eventually becomes extinct when $R_0^2 + \frac{\delta_h \phi \beta_h \beta_v}{\Lambda(d_h + \delta_h + \gamma_h) d_v^2} < 1$. □

It can be proved that the disease persists when $R_0 > 1$ [7]. We summarize the result showing uniform persistence in Theorem 3.5.

Theorem 3.5 (*Uniform Persistence*). *For $\eta = 0$, the decoupled system (1)–(5) is uniformly persistent with respect to $\left(\Omega_o, \partial\Omega_o\right)$ for $R_0 > 1$ in the sense that there is a positive constant $\sigma > 0$ such that every solution*

$$\left(S_{hH}, I_{hH}, R_{hH}, S_{vH}, I_{vH}\right)$$

of (1)–(5) with $\left(S_{hH}(0), I_{hH}(0), R_{hH}(0), S_{vH}(0), I_{vH}(0)\right) \in \Omega_o$ satisfies

$$\liminf I_{hH} \geq \sigma, \ \liminf I_{vH} \geq \sigma, \tag{16}$$

where,

$$\begin{aligned}
\Omega_o &= \{\left(S_{hH}, I_{hH}, R_{hH}, S_{vH}, I_{vH}\right) \in \mathfrak{R}_+^5 : I_{hH} > 0 \quad or \quad I_{vH} > 0\}, \\
\partial\Omega_o &= \{\left(S_{hH}, I_{hH}, R_{hH}, S_{vH}, I_{vH}\right) \in \mathfrak{R}_+^5 : I_{hH} = 0 \quad and \quad I_{vH} = 0\}, \\
\Omega &= \Omega_o \cup \partial\Omega_o = \mathfrak{R}_+^5.
\end{aligned}$$

3.2. Case-II: $\eta \neq 0$ (presence of cross-border mobility)

In the presence of cross-border mobility of the migrant workers ($\eta \neq 0$), the possibility of imported cases depends on malaria transmission abroad. Therefore, we perform our analysis for two subcases: (1) Case IIA (absence of transmission abroad, $\eta \neq 0,\ k = 0$) and (2) Case IIB (presence of transmission abroad, $\eta \neq 0,\ k \neq 0$).

3.2.1. Case- IIA ($\eta \neq 0,\ k = 0$)

- Equilibria

For $k = 0$, a_0, Q_1, Q_3, T_1, and U_1 are zero. Then, the disease-free equilibrium of the system (1)–(8) is derived from Eq. (9) as $E^{01} = \left(\frac{\Lambda\left(d_h + \eta\right)}{d_h\left(d_h + 2\eta\right)},\ 0,\ 0,\ \frac{\phi}{d_v},\ 0,\ \frac{\eta\Lambda}{2\eta d_h + d_h^2},\ 0,\ 0\right)$. The basic reproduction number, derived using the next-generation matrix method [40], is

$R_1 = \sqrt{\frac{\phi d_h \beta_h \beta_v \left(d_h + 2\eta\right)\left(d_h + \gamma_h + \delta_h + \omega\eta\right)}{\Lambda d_v^2 \left(d_h + \eta\right)\left(d_h + \gamma_h + \delta_h\right)\left(d_h + \gamma_h + \delta_h + 2\omega\eta\right)}}$. In this case, Eq. (10) reduce to

$$a_3 \lambda_h^{*2} + a_2 \lambda_h^* + a_1 = 0, \tag{17}$$

with a_3, a_2, and a_1 given by

$$
\begin{aligned}
a_3 &= \Lambda\left(Q_2+Q_4\right)d_v d_v\left(d_h+\eta\right)^2\left(\left(Q_2+Q_4\right)d_v+Q_2\beta_v\right)>0,\\
a_2 &= A_2\left(G_1-R_1^2\right),\\
A_2 &= \frac{\left(\Lambda d_v^2\left(d_h+\eta\right)\left(d_h+\gamma_h+\delta_h\right)\left(d_h+\gamma_h+\delta_h+2\eta\omega\right)\right)}{d_h\left(d_h+2\eta\right)\left(d_h+\gamma_h+\delta_h+\eta\omega\right)},\\
a_1 &= b_2\left(1-R_1^2\right),\\
b_2 &= \Lambda\left(d_v\left(d_h+\eta\right)\left(d_h+q\right)\left(d_h+\gamma_h+\delta_h\right)\left(d_h+2\eta+q\right)\left(d_h+\gamma_h+\delta_h+2\omega\eta\right)\right)^2,
\end{aligned}
$$

where $G_1=\dfrac{Pd_h\left(d_h+2\eta\right)\left(2\left(Q_2+Q_4\right)d_v+Q_2\beta_v\right)\left(d_h+\gamma_h+\delta_h+\eta\omega\right)}{\Lambda K_2 Q_2 d_v\left(d_h+\eta\right)\left(d_h+\gamma_h+\delta_h\right)\left(d_h+\gamma_h+\delta_h+2\eta\omega\right)}$. Here $R_1<1$ if and only if $a_1>0$ and $R_1<\sqrt{G_1}$ if and only if $a_2>0$. Let $\Delta(R_1)=a_2^2-4a_1a_3$. Then we have $\Delta(\sqrt{G_1})=-4a_1a_3<0$ when $R_1<1$, and $\Delta(1)=a_2^2>0$. It follows that when $R_1<1$, the intermediate value theorem for continuous function implies that there exists a unique $R_1^*\in\left(\sqrt{G_1},1\right)$ such that $\Delta(R_1^*)=0$. Therefore, R_1^* is the value of $R_1<1$ such that the discriminant of the Eq. (17) is zero. Also, for $R_1<1$, $\Delta(R_1)>0$ if and only if $R_1>R_1^*$, and $\Delta(R_1)<0$ if and only if $R_1<R_1^*$ [14,17]. Now using $\Delta(R_1^*)=0$, we obtain $R_1^*=\dfrac{\sqrt{A_2^2G_1-2a_3b_2+2\sqrt{a_3^2b_2^2+a_3A_2^2b_2\left(1-G_1\right)}}}{A_2}$. In Theorem 3.6, we present the general results about the existence of endemic equilibria.

Theorem 3.6. *Assume that $\eta\neq0$ and $k=0$ in the system (1)–(8), then the following statements hold.*

(i) For $R_1>1$, the system has unique endemic equilibrium;
(ii) For $R_1=1$, the system has unique endemic equilibrium when $a_2<0$ and no endemic equilibrium when $a_2\geq0$;
(iii) For $R_1^*<R_1<1$, the system has two (higher and lower) endemic equilibria when $a_2<0$ and no endemic equilibria when $a_2\geq0$;
(iv) For $R_1=R_1^*$, the system has unique (coincident) equilibria when $a_2<0$ and no endemic equilibria when $a_2\geq0$;
(v) For $R_1<R_1^*$, the system has no endemic equilibrium.

Proof is similar to Theorem 3.1.

- Bifurcation analysis (Case-IIA: $\eta\neq0,\ k=0$)

Theorem 3.7 (*Local Stability of E^{01}*). *Assume that $\eta\neq0, k=0$, the disease free equilibrium point E^{01} of the system (1)–(8) is locally asymptotically stable if $R_1<1$, and unstable if $R_1>1$.*

Proof. See Section 8 of Supplementary file. □

Again, we use the Castillo Chavez and Song Theorem [41] for the bifurcation analysis. We have already established in Theorem 3.3 the role of the disease-induced death rate in possessing the backward bifurcation. Since the primary focus of this study is to examine whether cross-border mobility alone can produce backward bifurcation phenomena, we consider the disease-induced death rate is zero and focus on cross-border mobility in the following sections.

Theorem 3.8 (*Forward and Backward Bifurcation*). *Assume that $\eta\neq0$ and $k=0$, then the model possesses the forward bifurcation when $0\leq\omega\leq\omega^*$ at $R_1=1$ and possesses the backward bifurcation when $\omega>\omega^*>1$ at $R_1=1$, where $\omega^*=\dfrac{\left(d_h+\gamma_h\right)A}{\eta\left(d_h+2\eta+q\right)B}$,*

$$
\begin{aligned}
A &= q^2d_h\beta_v+q^2d_hd_v+6\eta qd_h\beta_v+2qd_h^2\beta_v+2\eta qd_v\gamma_h+qd_hd_v\gamma_h+8\eta qd_hd_v+\\
&\quad 2qd_h^2d_v+4\eta^2d_h\beta_v+4\eta d_h^2\beta_v+d_h^3\beta_v+2\eta^2d_v\gamma_h+3\eta d_hd_v\gamma_h+d_h^2d_v\gamma_h+\\
&\quad 6\eta^2d_hd_v+5\eta d_h^2d_v+d_h^3d_v+3\eta q^2d_v+6\eta^2qd_v+2\eta q^2\beta_v+4\eta^2q\beta_v,\\
B &= qd_v\gamma_h-\left(qd_h\beta_v+2\eta d_h\beta_v+d_h^2\beta_v+2\eta d_v\gamma_h+2\eta d_hd_v+2\eta qd_v+2\eta q\beta_v\right).
\end{aligned}
$$

Proof. We apply the theorem by Castillo Chavez and Song [41] to derive the condition for forward and backward bifurcation. The value of β_h corresponding to $R_1=1$ is $\beta_{h1}^*=\dfrac{\Lambda d_v^2\left(d_h+\eta\right)\left(d_h+\gamma_h\right)\left(d_h+2\eta\omega+\gamma_h\right)}{\phi d_h\beta_v\left(d_h+2\eta\right)\left(d_h+\eta\omega+\gamma_h\right)}$ and E^{01} is the disease-free equilibrium. Then

the Jacobian of the system (1)–(8) at the bifurcation point $(E^{01};\ \beta^*_{h1})$ is $J_1 = [M,\ N]$, where

$$M = \begin{pmatrix} -(d_h+\eta) & 0 & q & 0 \\ 0 & -(d_h+\gamma_h+\omega\eta) & 0 & 0 \\ 0 & \gamma_h & -(d_h+\eta+q) & 0 \\ 0 & -\dfrac{\phi d_h\beta_v\left(d_h+2\eta\right)}{\Lambda d_v\left(d_h+\eta\right)} & 0 & -d_v \\ 0 & \dfrac{\phi d_h\beta_v\left(d_h+2\eta\right)}{\Lambda d_v\left(d_h+\eta\right)} & 0 & 0 \\ \eta & 0 & 0 & 0 \\ 0 & \eta\omega & 0 & 0 \\ 0 & 0 & \eta & 0 \end{pmatrix},$$

and

$$N = \begin{pmatrix} -\beta^*_{h1} & \eta & 0 & 0 \\ \beta^*_{h1} & 0 & \omega\eta & 0 \\ 0 & 0 & 0 & \eta \\ 0 & 0 & 0 & 0 \\ -d_v & 0 & 0 & 0 \\ 0 & -(d_h+\eta) & 0 & q \\ 0 & 0 & -(d_h+\gamma_h+\omega\eta) & 0 \\ 0 & 0 & \gamma_h & -(d_h+\eta+q) \end{pmatrix}.$$

Six eigenvalues of J_1 are $0,\ -d_h,\ -d_v,\ -(d_h+2\eta),\ -(d_h+q),\ -(d_h+2\eta+q)$, and the rest two eigenvalues are obtained from the quadratic equation,

$$(d_h+\gamma_h+\omega\eta)\lambda_1^2 + \left(d_h+\gamma_h+\omega\eta\right)\left(2d_h+d_v+2\gamma_h+2\omega\eta\right)\lambda_1 + B_3 = 0, \tag{18}$$

where, $B_3 = d_h\left(2d_v\left(\gamma_h+\omega\eta\right)+\omega^2\eta^2+3\gamma_h^2+6\gamma_h\omega\eta+\omega^2\eta^2\right) + d_h^2\left(d_v+3\gamma_h+3\omega\eta\right) + d_v\left(2\gamma_h\omega\eta+\gamma_h^2+2\omega^2\eta^2\right) + d_h^3 + \gamma_h\left(\gamma_h+\omega\eta\right)\left(\gamma_h+2\omega\eta\right)$. Since all the coefficients of the quadratic Eq. (18) are positive, then the remaining two eigenvalues of J_1 have also negative real parts. Let $\vec{v} = \left(v_1,\ v_2,\ v_3,\ v_4,\ v_5,\ v_6,\ v_7,\ v_8\right)$ and $\vec{u} = \left(u_1,\ u_2,\ u_3,\ u_4,\ u_5,\ u_6,\ u_7,\ u_8\right)^T$ are the left and right eigenvectors corresponding to the zero eigenvalue of the matrix J_1. Solving the matrix equations $\vec{v}J_1 = 0$ and $J_1\vec{u} = 0$, we get $v_1 = v_3 = v_4 = v_6 = v_8 = 0, v_5 = \dfrac{\Lambda v_2 d_v\left(d_h+\eta\right)\left(d_h+\gamma_h\right)\left(d_h+\gamma_h+2\omega\eta\right)}{\phi d_h\beta_v\left(d_h+2\eta\right)\left(d_h+\gamma_h+\omega\eta\right)},\ v_7 = \dfrac{\omega\eta v_2}{d_h+\gamma_h+\omega\eta},\quad u_1 = \dfrac{u_2(Q-R)}{U},$

$$u_3 = u_2\left(\frac{\omega\eta^2\gamma_h}{\left(d_h+q\right)\left(d_h+2\eta+q\right)\left(d_h+\gamma_h+\omega\eta\right)} + \frac{\gamma_h\left(d_h+\eta+q\right)}{\left(d_h+q\right)\left(d_h+2\eta+q\right)}\right),$$

$$u_4 = -\frac{u_2\phi d_h\beta_v\left(d_h+2\eta\right)}{\Lambda d_v^2\left(d_h+\eta\right)},\ u_5 = \frac{u_2\phi d_h\beta_v\left(d_h+2\eta\right)}{\Lambda d_v^2\left(d_h+\eta\right)},\ u_6 = \frac{u_2(S-T)}{U},$$

$$u_7 = \frac{\omega\eta u_2}{d_h+\gamma_h+\omega\eta},\ u_8 = \frac{u_2\gamma_h\left(\eta d_h+\omega\eta d_h+\omega\eta^2+\eta\gamma_h+\omega\eta^2+\omega\eta q\right)}{\left(d_h+q\right)\left(d_h+2\eta+q\right)\left(d_h+\gamma_h+\omega\eta\right)},$$

with $u_2,\ v_2$ free, where,

$$U = d_h\left(d_h+2\eta\right)\left(d_h+q\right)\left(d_h+2\eta+q\right)\left(d_h+\gamma_h+\omega\eta\right),$$
$$Q = q\gamma_h\left(d_h(2\eta+q)+d_h^2+\eta(2\eta+q)\right)\left(d_h+\gamma_h+\omega\eta\right)+q\omega\eta^2\gamma_h\left(2d_h+2\eta+q\right),$$
$$R = \left(d_h+\eta\right)\left(d_h+q\right)\left(d_h+\gamma_h\right)\left(d_h+2\eta+q\right)\left(d_h+\gamma_h+2\omega\eta\right),$$
$$S = \eta q\gamma_h\left(2d_h+2\eta+q\right)\left(d_h+\gamma_h+\omega\eta\right)+q\omega\eta\gamma_h\left(d_h(2\eta+q)+d_h^2+\eta(2\eta+q)\right),$$
$$T = \eta\left(d_h+q\right)\left(d_h+\gamma_h\right)\left(d_h+2\eta+q\right)\left(d_h+\gamma_h+2\omega\eta\right).$$

Here $\vec{v}.\vec{u} = 1$ implies

$v_2u_2 = \dfrac{d_v\left(d_h+\eta\omega+\gamma_h\right)^2}{\left(d_h+\gamma_h\right)\left(d_h+\eta\omega+\gamma_h\right)\left(d_h+2\eta\omega+\gamma_h\right)+d_v\left(d_h+\eta\omega+\gamma_h\right)^2+\eta^2\omega^2}$. For the computation of b, $f_2 = \beta_h\dfrac{x_1x_5}{x_1+x_2+x_3} - \left(d_h+\gamma_h\right)x_2, f_5 = \beta_v\dfrac{x_4x_2}{x_1+x_2+x_3} - x_5d_v, f_7 = \omega\eta x_2 - \left(d_h+\gamma_h+\omega\eta\right)x_7$. Then, taking the partial derivatives of f_2, f_5 and f_7 with respect to β_h, we get $\dfrac{\partial(f_2)}{\partial\beta_h} = \dfrac{x_1x_5}{x_1+x_2+x_3},\ \dfrac{\partial(f_5)}{\partial\beta_h} = \dfrac{\partial(f_7)}{\partial\beta_h} = 0$. Then, from Eq. (14), $b = \sum_{i=1}^{8} v_2u_i\dfrac{\partial^2 f_2}{\partial x_i\partial\beta_h}(E^{01}) = \sum_{i=1}^{8} v_2u_i\dfrac{\partial}{\partial x_i}\left(\dfrac{x_1x_5}{x_1+x_2+x_3}\right)(E^{01}) = v_2u_5 = v_2\dfrac{u_2\phi d_h\beta_v\left(d_h+2\eta\right)}{\Lambda d_v^2\left(d_h+\eta\right)} > 0$. For the computation of a, we use Eq. (15) at E^{01} with $\eta \neq 0$ and $k = 0$. After simplification, we get $a = \eta(\omega-1)d_h\gamma_h + \eta(\omega-1)d_h^2 - \dfrac{2\eta d_h\gamma_h\beta_v}{d_v} - \dfrac{d_h^2\gamma_h\beta_v}{d_v} - \dfrac{2\omega\eta^2d_h\beta_v}{d_v} - \dfrac{2\eta d_h^2\beta_v}{d_v} - \dfrac{\omega\eta d_h^2\beta_v}{d_v} - \dfrac{d_h^3\beta_v}{d_v} -$

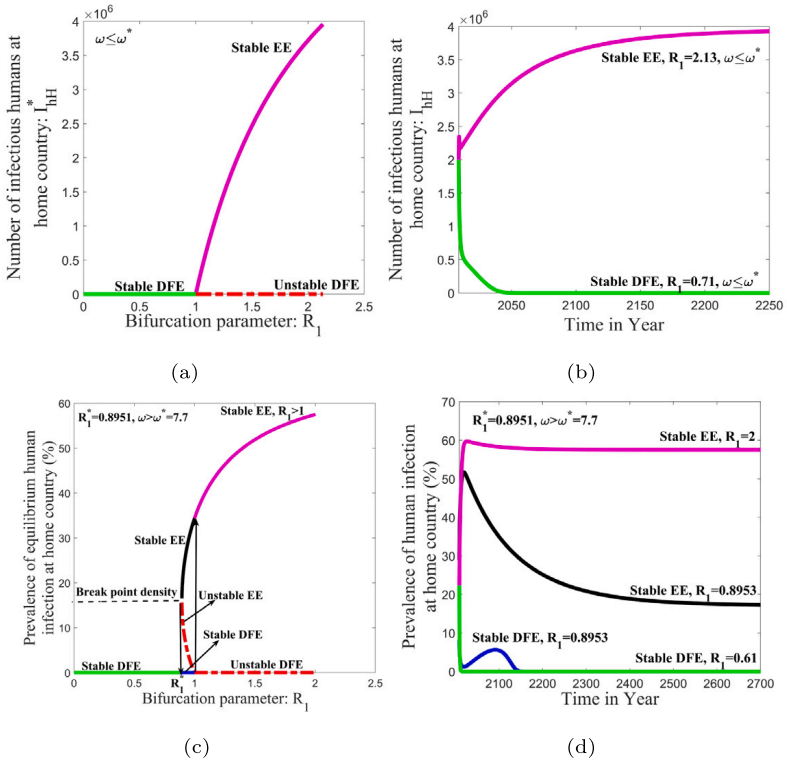

Fig. 3. Bifurcation diagrams and time series solutions for $\delta_h = 0$, $\omega^* = 7.7$. (a) Forward bifurcation at $R_1 = 1$ when $\omega \le \omega^*$ (here $\omega = 1$). (b) Model solutions verifying (a), where the model solution converges to the unique stable endemic equilibrium when $R_1 = 2.13$ ($R_1 > 1$) (end of the magenta curve) and converges to the stable disease-free equilibrium when $R_1 = 0.71$ ($R_1 < 1$) (end of the green curve), independent of initial conditions. (c) Backward bifurcation at $R_1 = 1$ with the transmission threshold $R_1^* = 0.8951, \omega > \omega^*$ (here $\omega = 25$). (d) Model solutions verifying (c); for $R_1 = 2(R_1 > 1)$, the model solution converges to the unique stable endemic equilibrium (end of the magenta curve), and for $R_1 = 0.61(R_1 < R_1^* < 1)$, the model solution converges to the unique stable disease-free equilibrium (end of the green curve), independent of initial conditions. However, for $R_1 = 0.8953(R_1^* < R_1 < 1)$, the model solution converges to the endemic equilibrium (end of the black curve) when the initial prevalence is above the breakpoint density (dashed line), and the model solution converges to the disease-free equilibrium (end of the blue curve) when the initial prevalence is below the breakpoint density. (For interpretation of the references to color in this figure legend, the reader is referred to the web version of this article.)

$\frac{d_h\left(d_h+2\eta\right)\left(\gamma_h\left(d_h+\gamma_h+\omega\eta\right)\left(d_h+\eta+q\right)+\left(d_h+q\right)\left(d_h+\gamma_h+\omega\eta\right)\left(d_h+2\eta+q\right)+\omega\eta^2\gamma_h\right)}{\left(d_h+q\right)\left(d_h+2\eta+q\right)}$. From the expression of a, it is clear that ω should necessarily be greater than 1 for backward bifurcation. Otherwise, a becomes negative, and the model possesses the forward bifurcation. Furthermore, $\omega > \omega^* > 1$ is sufficient for $a > 0$. Therefore, model possesses the forward bifurcation at $R_1 = 1$ for $\omega \le \omega^*$ and the backward bifurcation if $\omega > \omega^* > 1$, where $\omega^* = \frac{\left(d_h+\gamma_h\right)A}{\eta\left(d_h+2\eta+q\right)B}$. □

In the presence of cross-border mobility ($\eta \neq 0$) and the absence of malaria transmission abroad ($k = 0$), malaria elimination in the home country is possible for $\omega \le \omega^*$ and $R_1 < 1$. However, if $\omega > \omega^* > 1$, elimination of malaria is possible only when $R_1 < R_1^* < 1$. Taking the parameters given in Table 1, we validated the analytic results with the numerical solution of the system (1)–(8). The bifurcation diagrams and corresponding model solutions are shown in Fig. 3.

- Global stability and uniform persistence (Case-IIA: $\eta \neq 0,\ k = 0$)

We apply the Krasovskii–LaSalle Theorem [41] to establish the condition for the global stability of the disease-free equilibrium E^{01}.

Theorem 3.9 (*Global Stability of* E^{01})**.** *Assume that* $\eta \neq 0$ *and* $k = 0$*, then the disease-free equilibrium* E^{01} *of the system* (1)–(8) *is globally asymptotically stable when* $R_1^2 + M < 1$*,where* $M = \frac{\beta_v\beta_h\delta_h(d_h+2\eta)(d_h+\gamma_h+\delta_h+\omega\eta)\phi}{d_v^2\Lambda(d_h+\eta)(d_h+\gamma_h+\delta_h)(d_h+\gamma_h+\delta_h+2\omega\eta)} + \frac{\omega\eta}{(d_h+\gamma_h+\delta_h+2\omega\eta)}$.

Proof. Let $s = \left(S_{hH}(t), I_{hH}(t), R_{hH}(t), S_{vH}(t), I_{vH}(t), S_{hM}(t), I_{hM}(t), R_{hM}(t)\right)$ be any solution of the system (1)–(8), then $N_{vH}(t) \le \frac{\phi}{d_v}$. Again, $N_{hH} = S_{hH} + I_{hH} + R_{hH}$, and $N_{hM} = S_{hM} + I_{hM} + R_{hM}$, then $N'_{hH} + N'_{hM} = \Lambda - d_h(N_{hH} + N_{hM}) - \delta_h(I_{hH} + I_{hM}) \ge \Lambda - (d_h + \delta_h)(N_{hH} + N_{hM})$. It follows that $N_{hH} + N_{hM} \ge \frac{\Lambda}{d_h+\delta_h}$. Since the solutions $N_{hH}(t)$ and $N_{hM}(t)$ are general and

should satisfy the disease-free equilibrium as well, we get $N_{hH}(t) \geq \left(\frac{\Lambda(\eta+d_h)}{(d_h+\delta_h)(d_h+2\eta)}\right)$. Here, we construct a Lyapunov function $V_1\left(I_{hH}, I_{vH}, I_{hM}\right) = \frac{d_v}{\beta_h} I_{hH} + I_{vH} + \frac{d_v}{\beta_h} I_{hM}$. Now, taking the derivative of V_1 with respect to t,

$$
\begin{aligned}
V_1' &= \frac{d_v}{\beta_h} I_{hH}' + I_{vH}' + \frac{d_v}{\beta_h} I_{hM}' \\
&= \frac{d_v I_{vH} S_{hH}}{N_{hH}} + \frac{d_v}{\beta_h}\omega\eta I_{hM} - \frac{d_v}{\beta_h}(\omega\eta + d_h + \delta_h + \gamma_h) I_{hH} + \\
&\frac{\beta_v I_{hH} S_{vH}}{N_{hH}} - d_v I_{vH} + z\omega\eta I_{hM} - \frac{d_v}{\beta_h}(\omega\eta + d_h + \delta_h + \gamma_h) I_{hM} \\
&= \left[\frac{d_v}{\beta_h}\omega\eta + \frac{\beta_v S_{vH}}{N_{hH}} - \frac{d_v}{\beta_h}(\omega\eta + d_h + \delta_h + \gamma_h)\right] I_{hH} - \left[-\frac{d_v S_{hH}}{N_{hH}} + d_v\right] I_{vH} + \\
&\left[\frac{d_v}{\beta_h}\omega\eta - \frac{d_v}{\beta_h}(\omega\eta + d_h + \delta_h + \gamma_h)\right] I_{hM} \\
&\leq \left[\frac{\frac{\phi}{d_v}\beta_h\beta_v}{\left(\frac{\Lambda(\eta+d_h)}{(d_h+\delta_h)(d_h+2\eta)}\right) d_v(d_h+\delta_h+\gamma_h)} - 1\right] I_{hH} \\
&= \left[\frac{\beta_v\beta_h(d_h+\delta_h)(d_h+2\eta)\phi}{d_v^2\Lambda(d_h+\eta)(d_h+\gamma_h+\delta_h)} - 1\right] I_{hH},
\end{aligned}
$$

After some algebraic manipulations, we get $V_1' < 0$ when $R_1^2 + M < 1$. Therefore, V_1 is a Lyapunov function when $R_1^2 + M < 1$. Let $s = (S_{hH}, I_{hH}, R_{hH}, I_{vH}, S_{hM}, I_{hM}, R_{hM})$ be any solution of the system (1)–(8) and $D = \{s : V_1' = 0\}$, then $D \subset \{s : I_{hH} = 0\}$. If $F \subset D$ is the largest invariant set of the system (1)–(8) and s is any solution of the system (1)–(8) in F, then for all $t \in R$, s is defined and bounded. Again $F \subseteq \{s : I_{hH} = 0\}$, thus $I_{hH} \equiv 0$. Then from Eq. (7), $I_{hM} \equiv 0$. Also, from Eq. (5) $I_{vH} \equiv 0$ and from Eq. (4) $S_{vH} \equiv \frac{\phi}{d_v}$. Now, the system (1)–(8) for the rest four compartments reduce to

$$R_{hH}' = \eta R_{hM} - (\eta + d_h + q) R_{hH}, R_{hM}' = \eta R_{hH} - (\eta + d_h + q) R_{hM}, \tag{19}$$

$$S_{hH}' = \Lambda + \eta S_{hM} + q R_{hH} - (\eta + d_h) S_{hH}, S_{hM}' = \eta S_{hH} + q R_{hM} - (\eta + d_h) S_{hM}. \tag{20}$$

From Eq. (19), we get $(R_{hH} + R_{hM})' = -(d_h + q)(R_{hH} + R_{hM})$. It follows that $R_{hH} \equiv 0$ and $R_{hM} \equiv 0$. Again, from Eq. (20), we get $(S_{hH} + S_{hM})' = \Lambda - d_h(S_{hH} + S_{hM})$. It follows that $S_{hH} + S_{hM} \equiv \frac{\Lambda}{d_h}$. Now, substituting $S_{hM} = \frac{\Lambda}{d_h} - S_{hH}$ in Eq. (1), we get $S_{hH} \equiv \frac{\Lambda\left(d_h+\eta\right)}{d_h\left(d_h+2\eta\right)}$ and then $S_{hM} \equiv \frac{\eta\Lambda}{2\eta d_h + d_h^2}$. Thus, $s = \left(\frac{\Lambda\left(d_h+\eta\right)}{d_h\left(d_h+2\eta\right)}, 0, 0, \frac{\phi}{d_v}, \frac{\eta\Lambda}{2\eta d_h + d_h^2}, 0, 0\right)$ and $F \equiv \{E^{01}\}$. Then, applying Krasovskii–LaSalle Theorem [41], the disease-free equilibrium E^{01} is globally asymptotically stable when $R_1^2 + M < 1$. □

In the presence of mobility and absence of malaria transmission abroad, malaria elimination is possible only when the mobility factor of infectious migrants ω is less than the threshold ω^* when $R_1 < 1$. It can be proved that the disease persists when $R_1 > 1$ [7]. The result for persistence is summarized in Theorem 3.10.

Theorem 3.10 (*Uniform Persistence*). *If $R_1 > 1$, then the system (1)–(8) is uniformly persistent with respect to $\left(\Omega_o, \partial\Omega_o\right)$ in the sense that there is a positive constant $\sigma > 0$ such that every solution*

$$\left(S_{hH}, I_{hH}, R_{hH}, S_{vH}, I_{vH}, S_{hM}, I_{hM}, R_{hM}\right)$$

with $\left(S_{hH}(0), I_{hH}(0), R_{hH}(0), S_{vH}(0), I_{vH}(0), S_{hM}(0), I_{hM}(0), R_{hM}(0)\right) \in \Omega_o$ satisfies $\liminf I_{hH} \geq \sigma$, $\liminf I_{vH} \geq \sigma$, $\liminf I_{hM} \geq \sigma$, *where*

$$\Omega_o = \{\left(S_{hH}, I_{hH}, R_{hH}, S_{vH}, I_{vH}, S_{hM}, I_{hM}, R_{hM}\right) \in \mathfrak{R}_+^8 : I_{hH} > 0 \text{or } I_{vH} > 0 \text{ or } I_{hM} > 0\},$$
$$\partial\Omega_o = \{\left(S_{hH}, I_{hH}, R_{hH}, S_{vH}, I_{vH}, S_{hM}, I_{hM}, R_{hM}\right) \in \mathfrak{R}_+^8 : I_{hH} = 0,\ I_{vH} = 0,\ I_{hM} = 0\}.$$

- Sensitivity of backward bifurcation phenomenon (Case-IIA: $\eta \neq 0,\ k = 0$)

As established in Theorem 3.8, the cross-border mobility factor ω can bring the backward bifurcation, resulting in a threshold $R_1^* < 1$ such that malaria eradication requires $R_1 < R_1^* < 1$. In Fig. 4, we present the sensitivity of these backward bifurcation phenomena (i.e., the sensitivity of R_1^*) to the cross-border mobility rate (η), the immunity loss rate of human (q), human recovery rate (γ_h), and mosquito death rate (d_v).

If the mobility rate (η) is reduced to 0.013, 0.01, and 0.005 from its base value ($\eta = 0.04$), then the elimination threshold R_1^* increases towards 1 with its values 0.8975, 0.9169, and 0.9776, respectively (Fig. 4, 1st row). With this trend, the threshold R_1^*

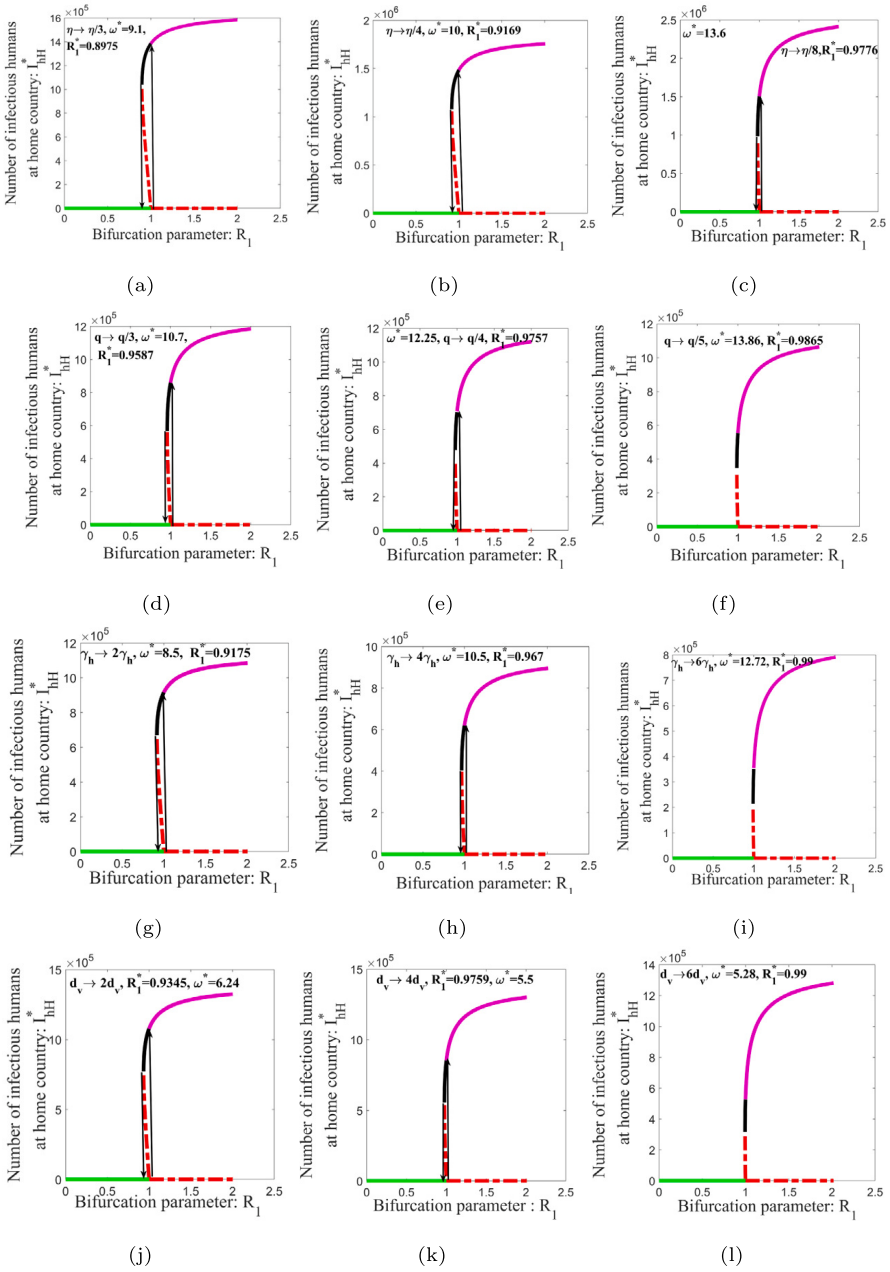

Fig. 4. Sensitivity of the backward bifurcation threshold R_1^*. (a), (b), and (c) are for the reduction of the mobility rate (η) from its base value of 0.04 to 0.013, 0.01, and 0.005, respectively. (d), (e), and (f) are for the reduction of immunity loss rate q from its base value of 4 to 1.33, 1, and 0.8, respectively. (g), (h), and (i) are for the increment of human recovery rate γ_h from its base value of 1.85 to 3.7, 7.4 and 11.1, respectively. (j), (k), and (l) are for the increment of mosquito death rate d_v from its base value of 27 to 54, 108 and 162, respectively.

approaches one when $\eta \to 0$, transforming the backward bifurcation into a forward bifurcation at $\eta = 0$. This result is consistent with Theorem 3.3, which shows forward bifurcation for $\eta = 0,\ \delta_h = 0$. The reduction of the immunity loss rate (q) to 1.33 (loss of immunity in nine months), 1 (loss of immunity in one year), and 0.8 (loss of immunity for 15 months) from the base value ($q = 4$), the threshold R_1^* increases to 0.9587, 0.9757, and 0.9865, respectively (Fig. 4, 2nd row).

Making the human recovery rate double (three-month recovery time), four-fold (45 days recovery time), and six-fold (27 days recovery time) from its base value $\gamma_h = 1.85$ per year (6.45 months recovery time) increases the thresholds R_1^* to 0.9175, 0.967, and 0.99, respectively (Fig. 4, 3rd row). Similarly, making the mosquito mortality rate double, four-fold, and six-fold of its base value ($d_v = 27$) increases the threshold R_1^* to 0.9345, 0.9759, and 0.99, respectively (Fig. 4, 4th row). From the 2nd, 3rd, and 4th rows of Fig. 4, it is clear that in the presence of cross-border mobility and the absence of malaria transmission abroad ($\eta \neq 0, k = 0$), an

increase in the parameters q, γ_h, or d_v increases the threshold R_1^* converging to 1 and transferring the backward bifurcation into the forward bifurcation.

3.2.2. Case-IIB: $\eta \neq 0,\ k \neq 0$

• Equilibria

Note that there is no disease-free equilibria in the presence of mobility and infection abroad ($\eta \neq 0,\ k \neq 0$). Here, the product of the roots of Eq. (10) is $\frac{-a_0}{a_3} > 0$, then Eq. (10) has either three positive roots or one positive root with two negative or a complex pair and corresponding endemic equilibria can be obtained from Eq. (9). We consider two sub cases: three endemic equilibria (Case-IIB1) and one endemic equilibrium (Case-IIB2). Eq. (10) is transformed into

$$t^3 + pt + q = 0, \tag{21}$$

where $\lambda_h^* = t - \frac{a_2}{3a_3}$, $p = \frac{3a_3a_1 - a_2^2}{3a_3^2}$, $q = \frac{2a_2^3 - 9a_3a_2a_1 + 27a_3^2a_0}{27a_3^3}$ and the discriminant D of Eq. (21) is $-(4p^3 + 27q^2)$ [42–44]. For the Case-IIB1, $D \geq 0$ (i.e. $p \leq 0$) together with $a_2 < 0$ and $a_1 > 0$ (Descart's rule of sign [45]), i.e.,

$$\frac{p_1}{p_2\alpha_{hv}\alpha_{vh}} < b^2 < \frac{p_3}{p_4\alpha_{hv}\alpha_{vh}}. \tag{22}$$

If $D = 0$ and $p = 0$, then $q = 0$. In this case, Eq. (21) has triple roots and hence Eq. (10) has triple positive roots $\lambda_h^* = \frac{-a_2}{3a_3}$. Again, if $D \geq 0$ and $p < 0$ then trigonometric identity

$$4\cos^3\theta - 3\cos\theta - \cos3\theta = 0 \tag{23}$$

can be used to obtain three real roots of Eq. (21) (double root with one simple root or three distinct roots). Let $t = A\cos\theta$, then Eq. (21) becomes

$$A^3\cos^3\theta + pA\cos\theta + q = 0. \tag{24}$$

Now, consider the trigonometric identity

$$4\cos^3\theta - 3\cos\theta - \cos3\theta = 0. \tag{25}$$

Comparing Eq. (24) with Eq. (25), we get $\frac{4}{A^3} = \frac{-3}{Ap} = \frac{-\cos3\theta}{q}$. It follows that $A = 2\sqrt{\frac{-p}{3}}$ and $\cos3\theta = \frac{3q}{Ap} = \cos\phi$, where $\theta = \frac{2n\pi \pm \phi}{3}$, and $\phi = \cos^{-1}\left(\frac{9q}{2p\sqrt{-3p}}\right) \in [0, \pi]$. Using the periodicity and even property of the cosine function, $n = 0,\ 1,\ 2$, we get three values of θ and then three values of t and hence λ_h^* are $2\sqrt{\frac{-p}{3}}\cos\left(\frac{\phi}{3}\right) - \frac{a_2}{3a_3}$, $2\sqrt{\frac{-p}{3}}\cos\left(\frac{2\pi+\phi}{3}\right) - \frac{a_2}{3a_3}$, $2\sqrt{\frac{-p}{3}}\cos\left(\frac{4\pi+\phi}{3}\right) - \frac{a_2}{3a_3}$, where $\phi = \cos^{-1}\left(\frac{9q}{2p\sqrt{-3p}}\right) \in [0, \pi]$. In particular, if $\phi = 0$, then two of λ_h^* are equal. Now for Case-IIB2, there are two possibilities. (1) One positive λ_h^* exists with two negatives if $D \geq 0$, $p < 0$ together with $a_2 = 0,\ a_1 < 0$, or $a_2 > 0,\ a_1 = 0,$ or $a_2 > 0,\ a_1 < 0$ (Descart's rule of sign [45]). The value of t and corresponding endemic equilibrium can be obtained using the trigonometric identity [42–44] as discussed in Case-IIB1. (2) One positive λ_h^* exists with complex pair when $D < 0$. In this case, if $p = 0$, then $t = (-q)^{\frac{1}{3}}$ and $\lambda_h^* = (-q)^{\frac{1}{3}} - \frac{a_2}{3a_3}$. If $p \neq 0$ then the real root t can be obtained by using the sine or cosine hyperbolic identities according to $p > 0$ or $p < 0$. In each case, corresponding endemic equilibria can be obtained from Eq. (9).

• Bifurcation Analysis (Case-IIB: $\eta \neq 0,\ k \neq 0$)

As revealed in Eq. (22), mosquito biting rate b plays a vital role in the existence of three endemic equilibria when $D \geq 0$. Therefore, we took b as a bifurcation parameter. Note that there is no disease-free equilibrium or reproduction number to establish the threshold criteria. This causes the stability analysis of endemic equilibria to be mathematically untractable. Thus, we numerically demonstrated the possibility of one and three endemic equilibria and their stability. We also estimated the approximate threshold value of the mosquito biting rate (b) for the low endemic level, bi-stability, and high malaria endemic level in the home country of Nepal (Fig. 5).

• Sensitivity of threshold for malaria burden (Case-IIB: $\eta \neq 0,\ k \neq 0$)

In this section, we estimated the impacts of cross-border mobility rate (η), incidence rate abroad (k), mobility factor of infectious migrants (ω), loss of immunity rate (q), increase of mosquito death rate (d_v), and increase of human recovery rate (γ_h) on the threshold (b^*) to maintain lower endemic level, bi-stability, and the higher endemic level of malaria in Nepal (Figs. 6 and 7).

If the mobility rate (η) is reduced to 0.013, 0.01, and 0.005 from its base value ($\eta = 0.04$), malaria can be maintained at a lower endemic level in the home country when the biting rate is less than threshold 72.67 (0.19 bites per day), 75 (0.20 bites per day), and 82 (0.22 bites per day), respectively (Fig. 6, 1st row). Here, the range of bistability decreases as η decreases, and eventually, the region vanishes for $\eta \to 0$, giving the smooth transition from the lower endemic level to the higher endemic level. However, the

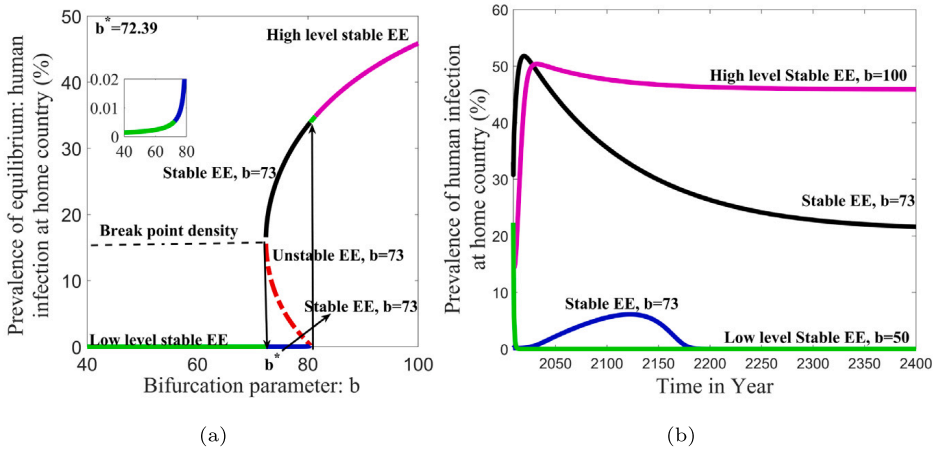

Fig. 5. Bifurcation diagram and model solutions with $\delta_h = 0$. (a) Backward bifurcations showing the intervals of b for the existence of lower-level stable endemic equilibrium, bi-stability, and the existence of higher-level stable endemic equilibrium. The lower green section represents one stable endemic equilibrium, with a complex pair representing the lower level of stable endemic equilibrium of malaria in the home country that exists when $b < 72.39$. The upper green section (one endemic equilibrium with a complex pair) and the magenta section (one endemic equilibrium with two negative solutions), respectively, represent the higher level stable endemic equilibrium of malaria in the home country that exists when $b > 80$. The three endemic equilibria in bistability region ($72.39 < b < 80$) are represented by the blue, dotted red, and black lines. (b) Model solutions verifying the backward bifurcation (a), where the model solution converges to a higher level stable endemic equilibrium when $b = 100(b > 80)$ (end of the magenta curve) and converges to a lower level stable endemic equilibrium when $b = 50(b < b^*)$ (end of the green curve), regardless of the initial conditions. For $72.39 < b < 80$, bi-stability (ends of the black and blue curves) occurs, i.e., the solution converges to a higher endemic level or lower endemic level depending on the prevalence above or below the breakpoint density, respectively. (For interpretation of the references to color in this figure legend, the reader is referred to the web version of this article.)

Table 2
Summary of bifurcation analysis of malaria model with cross-border mobility. DFE: disease-free equilibrium, EE: endemic equilibrium, CB: cross-border, FB: forward bifurcation, BB: backward bifurcation, and GS: global stability.

Bifurcation Analysis of malaria model with cross-border mobility		
Case-I ($\eta = 0$)	Case-IIA ($\eta \neq 0,\ k = 0$)	Case-IIB ($\eta \neq 0,\ k \neq 0$)
Absence of CB mobility	CB Mobility and protection	CB Mobility without protection
DFE exist	DFE exist	No DFE
FB if $0 \leq \delta_h \leq \delta_h^*$	FB if $\omega \leq \omega^*,\ \delta_h = 0$	One or three EE
BB if $\delta_h > \delta_h^*$	BB if $\omega > \omega^* > 1,\ \delta_h = 0$	Low-high, bi-stability
Elimination: $R_0 < R_0^*$	Elimination: $R_1 < R_1^*$	Endemic
GS, E^0: $R_0 < 1, \delta_h = 0$	GS, E^{01} : $R_1 < 1, \delta_h = 0, \omega = 0$	Endemic

reduction of incidence rate abroad (k) to 0.000035, 0.000026, and 0.000013 from its base value ($k = 0.000105$) has a negligible impact on the threshold for malaria endemic level (Fig. 6, 2nd row). Similarly, reducing the infectious migrants' mobility factor ω to 8.33 from its base value ($\omega = 25$) changes convergence to a higher endemic level to a lower endemic level, and further reduction to 6.25 and 3.15 allow the malaria epidemic to maintain at an even lower level in the home country (Fig. 6, 3rd row).

With the reduction of the immunity loss rate (q) to 1.33 (loss of immunity in nine months), 1 (loss of immunity in one-year), and 0.5 (loss of immunity in two years) from its base value $q = 4$ (loss of immunity in three months), the malaria epidemic can be maintained at a lower level in the home country Nepal when the biting rate is less than 77 (0.21 bites per day), 79 (0.21 bites per day), and 82 (0.22 bites per day), respectively (Fig. 7, 1st row). Making the human recovery rate double (three-month recovery time), four-fold (45 days recovery time), and eight-fold (24 days recovery time) of its base value $\gamma_h = 1.85$ per year (about 6 months recovery time), the malaria epidemic can be maintained at a lower level with the controlled biting rate below 100 (0.27 bites per day), 142 (0.38 bites per day), and 1500 (4.1 bites per day), respectively (Fig. 7, 2rd row). Similarly, when the biting rate remains below 213 (0.58 bites per day), 632 (1.7 bites per day), and 1500 (4.1 bites per day), making the mosquito mortality rate double (7 days life), four-fold (3.5 days life), and eight-fold (1.5 days life), respectively, of its base value ($d_v = 27$) helps maintain the malaria epidemic at a lower level (Fig. 7, 3rd row). Here, decreasing q, increasing γ_h, or increasing d_v eventually provides a curve with smooth transitioning from lower to higher epidemic level (see Table 2).

4. Discussion

Malaria is a major public health challenge worldwide, with millions of cases reported annually, leading to a significant burden of illness and death [14]. Despite the efforts of many countries to eliminate malaria, cases are rising in many places, primarily due to the mobility of migrant workers [46]. This indicates that local malaria control and intervention programs focused locally alone may not be enough to achieve the elimination goal. Therefore, a thorough analysis of why many countries with a long history of low malaria burdens struggle to achieve their elimination plan is necessary. We implemented an in-depth bifurcation analysis

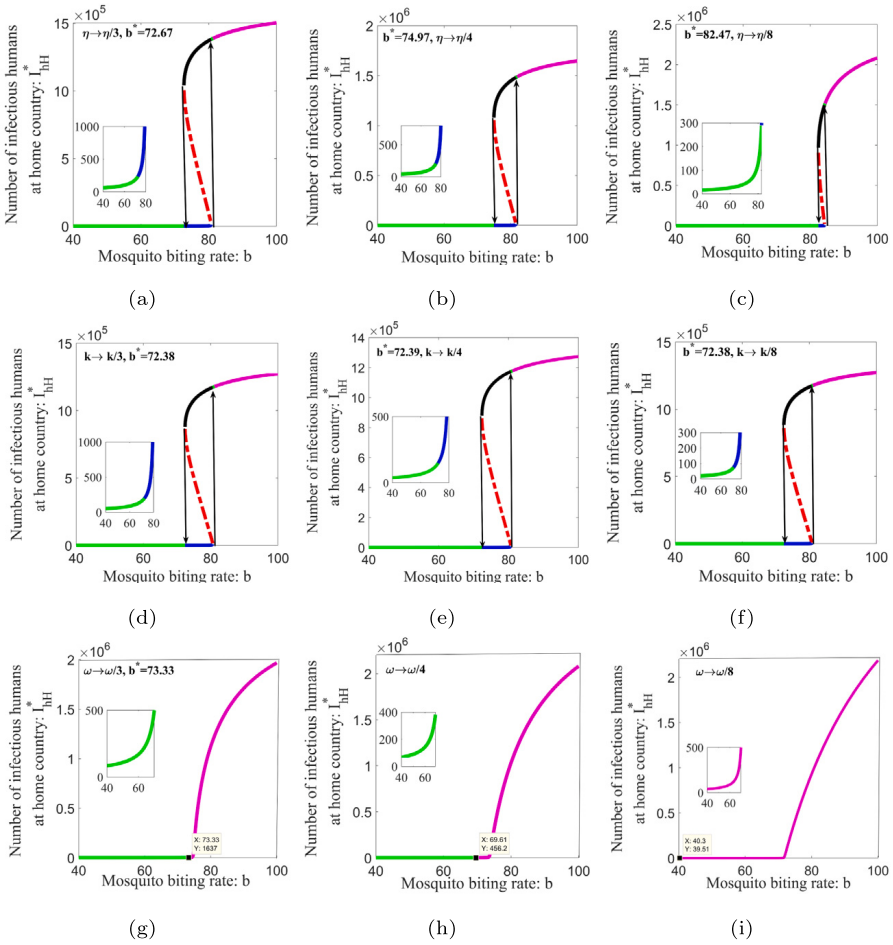

Fig. 6. The sensitivity of threshold (b^*) for malaria burden to migration-related parameters with $\delta_h = 0$. (a), (b), and (c) are the successive reduction in mobility rate (η) to 0.013, 0.01 and 0.005, respectively, from its base value ($\eta = 0.02$). (d), (e), and (f) are the successive reduction in incidence rate abroad (k) to 0.000035, 0.000026 and 0.000013, respectively, from its base value ($k = 0.000105$). (g), (h), and (i) are the successive reduction in the mobility factor of infectious migrants (ω) to 8.33, 6.25, and 3.12, respectively, from its base value ($\omega = 25$).

to evaluate the role of mobility in hindering the achievement of malaria elimination goals. Our ultimate focus is on the existence of a backward bifurcation, an interesting phenomenon in which the disease cannot be eliminated by simply reducing the basic reproduction number R_0 below unity; instead, another critical threshold R_0^* is required for the elimination of the disease.

Using the malaria model with cross-border mobility developed in our earlier study [7], we performed the bifurcation analysis, exploring two critical cases: the absence and presence of cross-border mobility. The condition for forward and backward bifurcation of our model in the lack of cross-border mobility is consistent with the results obtained for some other malaria models [14–16,19–22]. Specifically, the disease-induced death rate (δ_h) is a primary driver for backward bifurcation. However, our advanced model with cross-border mobility establishes that mobility can be a vital factor responsible for backward bifurcation even without the disease's death. Our results underscoring mobility as a critical factor for backward bifurcation, even in the absence of disease death, significantly contributes to vector-borne diseases, providing a valuable tool to design mobility-focused controls for disease eradication.

Through our bifurcation analysis, we have established a mobility threshold ω^* of infectious migrants, such that the backward bifurcation does not occur in the absence of malaria transmission abroad ($\eta \neq 0, k = 0$) (Section 3.1.2) when the mobility factor of infectious migrants is below the threshold ($\omega \leq \omega^*$). Note that the mobility of infectious migrants can be reduced through the strict border screening implemented with collaboration between the home country and abroad, and our result on the threshold can help to identify the level of border screening required to avoid backward bifurcation. In this case, we also established a critical threshold R_1^* corresponding to a condition for eradicating disease (Theorem 3.6). In the presence of malaria transmission abroad, our models show that malaria elimination is only possible in the home country unless cross-border mobility is allowed. In the presence of cross-border mobility, two epidemic levels (lower and higher) are possible, as revealed by numerical simulations of our model. We have conducted detailed simulations to identify threshold conditions, depending on various parameters, that help us maintain the epidemic at a lower level. In particular, the mosquito biting rate, which may vary with location, season, and mosquito type, as a bifurcation and control parameter, is one of the determinant factors of whether the epidemic stays at the lower or higher level. It

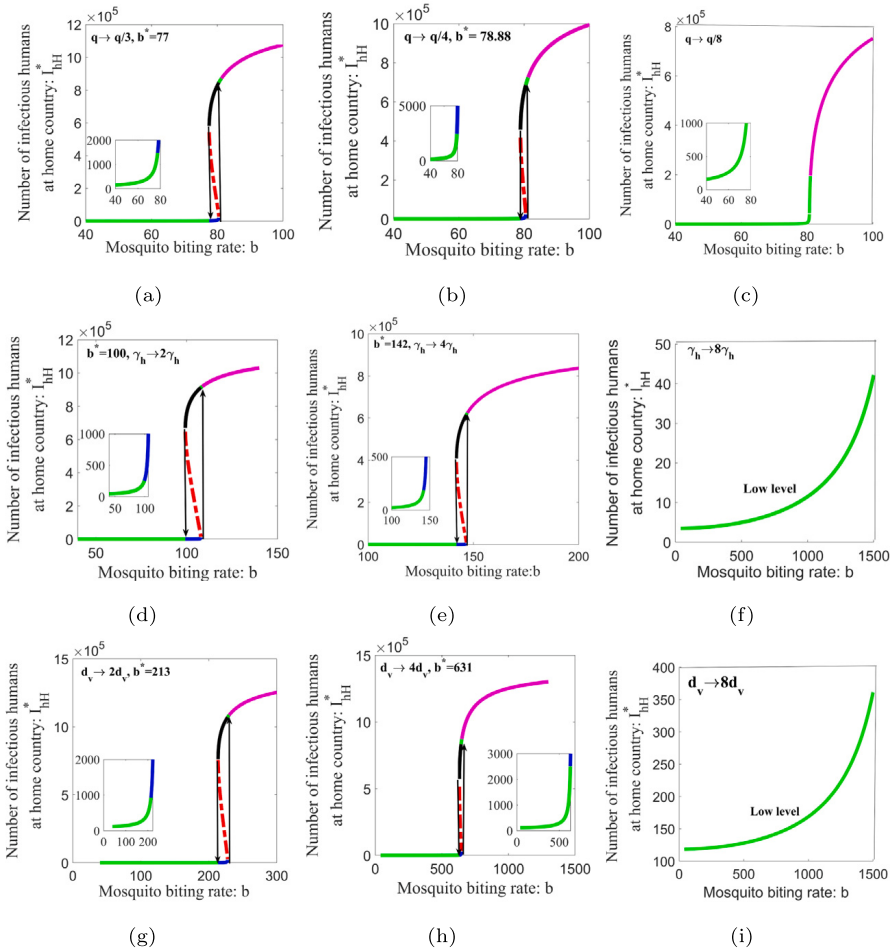

Fig. 7. The sensitivity of threshold for malaria burden to humans and mosquito parameters for $\delta_h = 0$. (a), (b), (c) are the impact of the reduction of the immunity loss rate to 1.33, 1 and 0.5, respectively, of its base value (q=4). (d), (e), (f) are the impact of two-fold, four-fold, and eight-fold of the recovery rate, respectively, of its base value ($\gamma_h = 1.85$). (g), (h), (i) are the impact of a two-fold, four-fold, and eight-fold increase in the mosquito death rate, respectively, from its base value ($d_v = 27$ i.e.13.5 days lifetime of a mosquito).

is worth noting that the current status of malaria in Nepal, as predicted by our model with current parameters of Nepal (Table 1), is at the low endemic level but struggles to achieve the elimination goal due to cross-border mobility.

We acknowledge some limitations of our study. We were not able to prove the global stability of the endemic equilibrium for $R_0 > 1$ and $R_1 > 1$ analytically. Instead, we showed persistence for $R_0 > 1$ and $R_1 > 1$ in our previous study [7]. We could not provide analytical proof of the stability of one or three endemic equilibria when there is a presence of mobility and infection abroad. However, taking the wide range of parameters, we numerically demonstrated the stability of lower and upper endemic equilibria and the instability of the middle endemic equilibrium. Furthermore, our model approximated the incidence rate abroad, keeping the mosquito's role in the disease spread abroad constant. Analysis of the model with the entire transmission dynamics through mosquitoes abroad as in the home country would provide broad opportunities for model analysis and produce more advanced results.

In summary, we studied in detail how backward bifurcation arises due to the cross-border mobility of migrant workers in the malaria dynamics model. Our central result on the role of mobility in backward bifurcation provides a novel insight into the cross-border mobility rate impacting the persistence and eradication of malaria in the home country. Our results may aid in developing effective malaria elimination strategies for countries like Nepal with low local malaria transmission but vulnerable to obstacles to eradication due to the cross-border mobility across other high epidemic countries.

CRediT authorship contribution statement

Ramesh Gautam: Formal analysis, Investigation, Methodology, Numerical simulation, Writing – original draft. **Khagendra Adhikari:** Formal analysis, Writing – review & editing. **Anjana Pokharel:** Formal analysis, Writing – review & editing. **Kedar Nath Uprety:** Formal analysis, Supervision, Writing – review & editing. **Naveen K. Vaidya:** Conceptualization, Formal analysis, Supervision, Writing – review & editing.

Declaration of competing interest

The authors declare that they have no known competing financial interests or personal relationships that could have appeared to influence the work reported in this paper.

Acknowledgments

This research is supported by the GRAID (Graduate Research Assistantships in Developing Countries) awards from the International Mathematical Union (IMU). RG acknowledges the University Grants Commission (UGC) Nepal for Ph.D. Fellowship 2021. KA acknowledges the Nepal Academy of Science and Technology (NAST) for Ph.D. Fellowship. The work of NKV was supported by grants DMS-1951793 and DEB-2030479 from the National Science Foundation of USA and UGP award from San Diego State University. We are grateful to the anonymous referees for their valuable suggestions, which have significantly improved the quality of our paper.

Appendix A. Supplementary data

Supplementary material related to this article can be found online at https://doi.org/10.1016/j.nonrwa.2024.104173.

References

[1] H. Alhassan, N. Shidali, S. Manga, K. Abdullahi, K. Hamid, Co-infection profile of *Salmonella typhi* and Malaria parasite in Sokoto-Nigeria, Global J. Sci. Eng. Technol. 2 (201) (2012) 13–20.
[2] P. Prasanna, Coinfection of Typhoid and Malaria, J. Med. Lab. Diagn. 2 (3) (2011) 22–26.
[3] A.O. Ekesiobi, M.C. Igbodika, O.O. Njoku, Co-infection of Malaria and Typhoid fever in a tropical community, Animal Res. Int. 5 (3) (2008).
[4] J.M. Mutua, F.-B. Wang, N.K. Vaidya, Modeling Malaria and Typhoid fever co-infection dynamics, Math. Biosci. 264 (2015) 128–144.
[5] World Health Organization, Eliminating Malaria by 2030 – south-east Asia region member states reaffirm commitment, 2017, URL https://www.who.int/southeastasia/activities/eliminating-malaria-by-2030-south-east-asia-region-member-states-reaffirm-commitment.
[6] World Health Organization, Countries in WHO south-east Asia region renew commitment to eliminate Malaria by 2030, 2022, URL (https://www.who.int/southeastasia/news/detail/05-05-2022-countries-in-who-south-east-asia-region-renew-commitment-to-eliminate-malaria-by-2030).
[7] R. Gautam, A. Pokharel, K. Adhikari, K.N. Uprety, N.K. Vaidya, Modeling Malaria transmission in Nepal: impact of imported cases through cross-border mobility, J. Biol. Dyn. 16 (1) (2022) 528–564, PMID: 35833562.
[8] K. Adhikari, R. Gautam, A. Pokharel, M. Dhimal, K.N. Uprety, N.K. Vaidya, Insight into Delta variant dominated second wave of COVID-19 in Nepal, Epidemics 41 (2022) 100642.
[9] K. Adhikari, R. Gautam, A. Pokharel, K.N. Uprety, N.K. Vaidya, Transmission dynamics of COVID-19 in Nepal: Mathematical model uncovering effective controls, J. Theoret. Biol. 521 (2021) 110680.
[10] A. Pokharel, K. Adhikari, R. Gautam, K.N. Uprety, N.K. Vaidya, Modeling transmission dynamics of measles in Nepal and its control with monitored vaccination program, Math. Biosci. Eng. 19 (8) (2022).
[11] F. Brauer, Backward bifurcations in simple vaccination models, J. Math. Anal. Appl. 298 (2) (2004) 418–431.
[12] A.B. Gumel, Causes of backward bifurcations in some epidemiological models, J. Math. Anal. Appl. 395 (1) (2012) 355–365.
[13] X. Fenga, Z. Tenga, K. Wangb, F. Zhangc, Backward bifurcation and global stability in an epidemic model with treatment and vaccination, Discrete Contin. Dyn. Syst. Ser. B 19 (4) (2014).
[14] Y. Xing, Z. Guo, J. Liu, Backward bifurcation in a Malaria transmission model, J. Biol. Dyn. 14 (1) (2020) 368–388, PMID: 32462991.
[15] N. Chitnis, J.M. Cushing, J. Hyman, Bifurcation analysis of a mathematical model for Malaria transmission, SIAM J. Appl. Math. 67 (1) (2006) 24–45.
[16] H. Wan, J.-A. Cui, A model for the transmission of Malaria, Discrete Contin. Dyn. Syst. Ser. B 11 (2) (2009) 479.
[17] X. Feng, S. Ruan, Z. Teng, K. Wang, Stability and backward bifurcation in a Malaria transmission model with applications to the control of Malaria in China, Math. Biosci. 266 (2015) 52–64.
[18] M. Tilahun, Backward bifurcation in SIRS Malaria model, 2017, arXiv: Populations and Evolution.
[19] J. Wang, X.-Z. Li, S. Bhattacharya, The backward bifurcation of a model for Malaria infection, Int. J. Biomath. 11 (02) (2018) 1850018.
[20] B. Buonomo, C. Vargas-De-León, Stability and bifurcation analysis of a vector-bias model of Malaria transmission, Math. Biosci. 242 (1) (2013) 59–67.
[21] R. kamel Naji, A.a. Adnan Thirthar, Stability and bifurcation of an SIS epidemic model with saturated incidence rate and treatment function, Iran. J. Math. Sci. Inf. 15 (2) (2020) 129–146.
[22] A. Sha, S. Samanta, M. Martcheva, J. Chattopadhyay, Backward bifurcation, oscillations and chaos in an eco-epidemiological model with fear effect, J. Biol. Dyn. 13 (1) (2019) 301–327.
[23] J. Mohammed-Awel, R. Zhao, E. Numfor, S. Lenhart, Management strategies in a Malaria model combining human and transmission-blocking vaccines, Discrete Contin. Dyn. Syst. Ser. B 22 (3) (2017) 977.
[24] X. Jin, S. Jin, D. Gao, Mathematical analysis of the Ross–Macdonald model with quarantine, Bull. Math. Biol. 82 (4) (2020) 1–26.
[25] S.I. Bala, B. Gimba, Modeling the impacts of income inequality on Malaria transmission dynamics, Int. J. Eng. Res. Appl. 12 (2) (2022) 31–46.
[26] J. Tumwiine, J. Mugisha, L. Luboobi, A host-vector model for Malaria with infective immigrants, J. Math. Anal. Appl. 361 (1) (2010) 139–149.
[27] P. Martens, L. Hall, Malaria on the move: human population movement and Malaria transmission, Emerg. Infect. Diseases 6 (2) (2000) 103.
[28] M.A. Acevedo, O. Prosper, K. Lopiano, N. Ruktanonchai, T.T. Caughlin, M. Martcheva, C.W. Osenberg, D.L. Smith, Spatial heterogeneity, host movement and mosquito-borne disease transmission, PLoS One 10 (6) (2015) e0127552.
[29] D. Gao, S. Ruan, A multipatch Malaria model with logistic growth populations, SIAM J. Appl. Math. 72 (3) (2012) 819–841.
[30] S. Kim, A. Tridane, D.E. Chang, Human migrations and mosquito-borne diseases in Africa, Math. Popul. Stud. 23 (2) (2016) 123–146.
[31] C. Cosner, J.C. Beier, R.S. Cantrell, D. Impoinvil, L. Kapitanski, M.D. Potts, A. Troyo, S. Ruan, The effects of human movement on the persistence of vector-borne diseases, J. Theoret. Biol. 258 (4) (2009) 550–560.
[32] C. Cosner, Models for the effects of host movement in vector-borne disease systems, Math. Biosci. 270 (2015) 192–197.
[33] A.Y. Mukhtar, J.B. Munyakazi, R. Ouifki, Assessing the role of human mobility on Malaria transmission, Math. Biosci. 320 (2020) 108304.
[34] Wikipedia, Mean value thorem — Wikipedia, the free encyclopedia, 2023, https://en.wikipedia.org/wiki/Mean_value_theorem. (Online; Accessed 3 September 2023).
[35] L.J. Abu-Raddad, P. Patnaik, J.G. Kublin, Dual infection with HIV and Malaria fuels the spread of both diseases in Sub-Saharan Africa, Science 314 (5805) (2006) 1603–1606, URL http://www.jstor.org/stable/20032992.

[36] F. Chamchod, N. F. Britton, Analysis of a vector-bias model on Malaria transmission, Bull. Math. Biol. 73 (3) (2011) 639–657, http://dx.doi.org/10.1007/s11538-010-9545-0.
[37] J.L. Aron, Mathematical modelling of immunity to Malaria, Math. Biosci. 90 (1) (1988) 385–396.
[38] C. Castillo-Chavez, B. Song, Dynamical model of tuberculiosis and their application, Math. Biosci. Eng. 1 (2) (2004) 361–404.
[39] N. Chitnis, J.M. Hyman, J.M. Cushing, Determining important parameters in the spread of Malaria through the sensitivity analysis of a mathematical model, 70, 2008, pp. 1272–1296.
[40] P. Van den Driessche, Reproduction numbers of infectious disease models, Infect. Dis. Model. 2 (3) (2017) 288–303.
[41] M. Martcheva, An Introduction to Mathematical Epidemiology, vol. 61, Springer, 2015.
[42] Wikipedia, Cubic equation — Wikipedia, the free encyclopedia, 2023, https://en.wikipedia.org/wiki/Cubic_equation. (Online; Accessed 14 April 2023).
[43] R. Nickalls, Viete, descartes and the cubic equation, Math. Gazette 90 (518) (2006) 203–208.
[44] I. Zucker, 92.34 The cubic equation-a new look at the irreducible case, Math. Gazette 92 (524) (2008) 264–268.
[45] A. Eigenwillig, On multiple roots in Descartes' rule and their distance to roots of higher derivatives, J. Comput. Appl. Math. 200 (1) (2007) 226–230.
[46] WHO, World Malaria Report, 2021, Report, WHO, 2021.